Ecole Doctorale Sciences Marines et Halieutiques
Université de Toliara

THÈSE DE DOCTORAT

2025

ANALYSE DIACHRONIQUE DES COMMUNAUTÉS BENTHIQUES DES RÉCIFS DE TOLIARA, MADAGASCAR : PERSPECTIVES PASSÉES, PRÉSENTES ET FUTURES À PARTIR DE L'IMAGERIE SATELLITAIRE ET IDENTIFICATION DES ZONES CORALLIENNES RÉSILIENTES

Aina Le Don NOMENISOA

MINISTERE DE L'ENSEIGNEMENT SUPERIEUR ET DE LA RECHERCHE SCIENTIFIQUE
UNIVERSITE DE TOLIARA

INSTITUT HALIEUTIQUE ET DES SCIENCES MARINES

ECOLE DOCTORALE : SCIENCES MARINES ET HALIEUTIQUES

THESE

Pour l'obtention du diplôme de

DOCTORAT EN SCIENCES MARINES ET HALIEUTIQUES

OPTION : Gestion de Ressources Marines

Analyse diachronique des communautés benthiques des récifs de Toliara, Madagascar : perspectives passées, présentes et futures à partir de l'imagerie satellitaire et identification des zones coralliennes résilientes

Thèse présentée en vue de l'obtention du grade de Docteur en Sciences

Par

Aina Le Don NOMENISOA

Soutenu publiquement le 29 Avril 2025, devant le jury composé de:

Président :	Professeur Titulaire Eulalie Ranaivoson
Directeur de Thèse :	Professeur Titulaire Igor Eeckhaut
Co-Directeur de Thèse :	Professeur Gildas Todinanahary
Rapporteur interne :	Professeur Thierry Lavitra
Rapporteur externe :	Professeur Emerite Gérard Lasserre
Examinateurs :	Professeur Lala Ranaivomanana
	Professeur Angelot Jamal Mahafina

Remerciements

« Ma thèse de Doctorat a reçu la prime HERA Doctoral Thesis Award », me disait Prof. Todinanahary Gildas. « Cette prime de 22 000 Euros m'a été offerte par la Fondation Belge pour la Génération Future, avec un financement du programme Aether. Je te la donne en totalité pour que tu en fasses quelque chose d'intéressant en préparant la tienne », ajoutait-il avec un sourire amusé. Je n'en revenais pas. Comment devrais-je vous exprimer suffisamment ma gratitude ? Cette bourse m'a non seulement permis de débuter ma thèse mais m'a également ouvert la porte pour décrocher d'autres financements. En plus de me l'avoir confié, vous avez accepté d'être mon promoteur de thèse. Merci également pour vos conseils avisés et votre accompagnement, tant pour ma thèse que sur le plan professionnel, où j'ai pu établir un solide réseau à Madagascar et à l'international.

Je suis profondément reconnaissant envers le Professeur Igor Eeckhaut, chef du Service du Laboratoire BOMB (Laboratoire des Organismes Marins et Biomimétisme) en Belgique, pour m'avoir accueilli au sein de son laboratoire et pour m'avoir encadré. Je vous remercie tout particulièrement pour votre patience et surtout pour le temps que vous avez généreusement consacré à m'enseigner les techniques de la rédaction scientifique et à m'aider à mieux communiquer mes concepts techniques à un large public. Vos conseils, vos critiques constructives et vos corrections minutieuses ont enrichi ce travail, tout comme vos encouragements inestimables tout au long de ces quatre années de recherche.

Comment pourrais-je vous oublier Professeur Jamal Mahafina et Dr. Jaonalison Henitsoa pour votre soutien dans l'acquisition des équipements hors de prix dans le cadre du projet MASMA. Ces équipements m'ont permis de traiter mes images satellitaires tels le progamme Ecognition Developer. Je remercie également le Dr. Faustinato Behivoke pour le projet de mise en place de récifs artificiels à Sarodrano (projet VALDECOR) ainsi que nos longs échanges très constructifs concernant l'effort de pêche à Toliara.

Ce travail n'aurait pas eu la même qualité sans l'apport de Professeur Eulalie Ranaivoson, Professeur Igor Eeckhaut, Professeur Thierry Lavitra, Professeur Gérard Lasserre, Pofesseur Lala Ranaivomanana, Professeur Jamal Mahafina et Professeur Gildas Todinanahary d'avoir accepté de faire partie de mon jury et pour toutes les discussions qui m'ont permis d'améliorer la qualité scientifique de mon travail. Je vous en remercie infiniment.

Cette thèse n'aurait pas pu voir le jour sans le soutien financier du projet Aether, de la fondation pour les générations futures, du projet MASMA/WIOMSA, de l'Académie Belge de Recherche Supérieur (ARES-CCD) et du projet MarCOSIO du programme GMES & Africa à qui j'exprime toute mon entière gratitude.

Je remercie aussi les étudiants à l'IH.SM qui m'ont accompagné dans la collecte des données sur le terrain : Hubert, Toky, Laza, Saverio, Israel, Najoro, Sarah, Misandratra, Amoros, et Michel. Ensemble, nous avons mis en place plus de 40 transects de 500 mètres, parcourant ainsi plus de 20 kilomètres à la nage. Nous avons expérimenté différentes techniques de collecte de données sans jamais être sûrs du résultat, et avons adapté des équipements sophistiqués et coûteux avec les moyens limités à notre disposition. À chaque moment de doute, lorsque je pensais que nous n'y arriverions jamais, vous m'avez toujours rappelé que je finissais par trouver des solutions. Qui aurait pu croire que cette aventure ouvrirait la voie à la cartographie des habitats marins à l'échelle de Madagascar ? Nous explorerons bientôt plus de 1000 kilomètres de la côte Malagasy, de Toliara à Antsiranana, et de Mahajanga à l'Ile Sainte Marie. Merci pour votre persévérance et votre confiance. D'autres étudiants m'ont rejoint également dont Béatrice, Nahim, Princia et tant d'autres. La liste est très longue, je ne peux pas tous les citer ici, mais soyez rassurés de toute ma gratitude.

A mes amis du laboratoire BOMBs ainsi que les doctorants de l'IH.SM avec qui j'ai partagé une expérience inoubliable en tant que thésard. Merci beaucoup pour les échanges, merci beaucoup pour les écoutes.

J'adresse un remerciement très spécial à ma femme, Nomeniarivelo (Noumé) et à mes enfants. Merci pour votre soutien infaillible, merci d'avoir tenu bon pour mes longues périodes d'absence. En vous, j'ai puisé ma force, surtout lorsque les sentiments de doute et de faiblesse allaient m'envahir. Je suis entièrement reconnaissant envers ma famille, notamment mes parents pour le soutien moral, les encouragements et les longues prières qui m'ont toujours accompagnées dans les périodes les plus difficiles. Je remercie infiniment chacun d'entre vous pour vos soutiens que vous avez manifestés sous différentes formes durant mes longues années d'études.

A la mémoire de Papa qui a tellement souhaité voir l'aboutissement de cette Thèse mais a dû nous quitter trop tôt. Puisse ton âme reposer en paix Papa Nomenisoa Rembolakely.

Table des matières

Liste des figures

Liste des tableaux

Résumé

L'étude de la dynamique des récifs coralliens par la cartographie de l'habitat, la détection des changements et l'évaluation de la résilience permet de mieux comprendre la santé des récifs et les stratégies de conservation. L'image satellite Sentinel-2 a été utilisée pour étudier la composition benthique et géomorphologique du Grand Récif de Toliara (GRT) et ses récifs coralliens avoisinants afin de fournir des données spatiales précises pour la gestion. L'étude a combiné des photo transects géoréférencées issus des données in-situ avec une analyse d'images orientée-objets (OBIA) et des algorithmes d'apprentissage automatique appliqué sur une image Sentinel-2. Le classificateur k-Nearest Neighbors (k-NN) a obtenu la plus grande précision (83 %), surpassant les algorithmes Bayes (79 %), Decision Trees (68 %), Random Trees (67 %) et Support Vector Machines (42 %). L'analyse a permis de délimiter les zones d'habitat : herbiers marins (21 km²), sable (73 km²), gravats (21 km²), coraux (10 km²) et algues (6 km²). L'étude souligne l'importance de la sélection des algorithmes et de l'intégration des données locales, démontrant l'efficacité de l'OBIA avec l'imagerie Sentinel-2 pour surveiller la santé des récifs et guider les pratiques durables. Cette étude analyse aussi l'évolution temporelle de la couverture corallienne benthique de 2015 à 2024 en intégrant l'imagerie Sentinel-2, un réseau de neurones convolutif (CNN) pour détecter les changements et un modèle d'automates cellulaires (CA) pour des projections jusqu'à 2034. Les données de terrain de 2021 et 2024 ont validé les résultats, révèlant une diminution de la superficie des algues/coraux de 2 200 à 1 500 ha et des herbiers marins de 2 000 à 1 700 ha, et une augmentation des débris de 1 700 à 2 400 ha entre 2015 et 2024. Le modèle CA prévoit une perte supplémentaire d'environ 150 ha d'herbiers marins et 110 ha d'algues/coraux d'ici 2034 si ces tendances persistent. Cette dégradation remet en question l'objectif 30x30 en matière de biodiversité (30 % de protection d'ici 2030), nécessitant des stratégies inclusives avec la participation des communautés locales et des ajustements politiques pour freiner la perte d'habitats. L'application de cette recherche à l'amélioration des pratiques de gestion a été réalisée à l'aide d'un cadre d'évaluation multicritères (MCE) avec le processus d'analyse hiérarchique (AHP) et une combinaison linéaire pondérée (WLC), afin d'évaluer la résilience des récifs coralliens pour soutenir la petite pêche. La cartographie de la résilience des coraux était basée sur sept facteurs : l'abondance des coraux, la structure, l'activité des herbivores, la profondeur, la pression de pêche, le stress thermique et la turbidité. Six scénarios ont donné la priorité à la biodiversité (scénarios 1 et 2), aux impacts locaux (scénarios 3 et 4) ou aux facteurs de stress mondiaux (scénarios 5 et 6).

Les cartes de résilience ont classé les zones en quatre catégories : faible, moyenne, élevée ou très élevée. Le scénario 2 (axé sur la biodiversité) a identifié 2 770 ha de résilience moyenne à très élevée, en mettant l'accent sur la complexité structurelle. Le scénario 4 (focalisation locale) a réduit les zones de faible résilience à 250 ha, tandis que le scénario 6 (focalisation globale) a montré 820 ha de très haute résilience. Les zones de haute résilience sont apparues le long du front de récif, et la pente externe, les zones profondes et sablonneuses étant moins résilientes. Cette approche guide la conservation en identifiant les zones à protéger et à restaurer. Cette recherche fournit une méthodologie standardisée pour la cartographie des récifs coralliens au niveau local, la détection de changement permet de suivre la dégradation et prédit les tendances d'évolution, et l'évaluation de la résilience informe la conservation ciblée. Ces efforts soutiennent les objectifs de biodiversité et aident les communautés de pêcheurs face aux menaces telles que le changement climatique et la surpêche, présentant un modèle reproductible pour la conservation mondiale des récifs.

Mots clés : *Télédétection, Récif corallien, Sentinel-2A, OBIA, Détection de changement, Evaluation multicritère*

Abstract

Addressing coral reefs dynamics through habitat mapping, temporal change detection, and resilience assessment offers insights into reef health and conservation strategies. The satellite image Sentinel-2 was used to investigates benthic and geomorphic composition of the Great Reef of Toliara (GRT) and its surrounding coral reefs to provide precise spatial data for management. The study combined georeferenced photo transects from fieldwork with Object-Based Image Analysis (OBIA) and machine learning algorithms applied on a Sentinel-2 image. The k-Nearest Neighbors (k-NN) classifier achieved the highest accuracy (83%), outperforming Bayes (79%), Decision Trees (68%), Random Trees (67%), and Support Vector Machines (42%). The analysis delineated habitat areas: seagrass (21 km^2), sand (73 km^2), rubble (21 km^2), coral (10 km^2), and algae (6 km^2). The study highlights the importance of algorithm selection and local data integration, demonstrating OBIA's efficacy with Sentinel-2 imagery for monitoring reef health and guiding sustainable practices. This study analyzes also the temporal evolution of benthic coral coverage from 2015 to 2024 by integrating Sentinel-2A imagery, a convolutional neural network (CNN) for change detection, and a cellular automata (CA) model for projections up to 2034. Field data from 2021 and 2024 validated the results, showing a decrease in algae/coral area from 2200 to 1500 ha and seagrass area from 2000 to 1700 ha, alongside an increase in debris from 1700 to 2400 ha between 2015 and 2024. The CA model predicts an additional loss of approximately 150 ha of seagrass and 110 ha of algae/coral by 2034 if the trends persist. This degradation challenges the 30x30 biodiversity goal (30% protection by 2030), requiring inclusive strategies with local community involvement and policy adjustments to curb habitat loss. The application of this research in improving management practices was performed using a Multi-Criteria Evaluation (MCE) framework with the Analytical Hierarchy Process (AHP) and a Weighted Linear Combination (WLC), in order to assess coral reef resilience to support small-scale fishing communities. The mapped resilience was based on seven factors: Coral Abundance, Framework, Herbivorous activity, Depth, Fish Pressure, Temperature Stress, and Turbidity. Six scenarios prioritized biodiversity (Scenarios 1–2), local impacts (Scenarios 3–4), or global stressors (Scenarios 5–6). Resilience maps categorized areas as Low, Medium, High, or Very High. Scenario 2 (biodiversity-focused) identified 2770 ha of Medium to Very High resilience, emphasizing structural complexity. Scenario 4 (local-focused) reduced low-resilience areas to 250 ha, while Scenario 6 (global-focused) showed 820 ha of Very High resilience. High-resilience zones appeared along the reef front, and the external slope, with deep and sandy areas less resilient. This approach guides conservation by pinpointing protection and restoration areas. This research provides a standardized methodology to map coral reefs at local scale, the change detection study tracks degradation and forecasts trends, and the resilience assessment informs targeted conservation. These efforts support biodiversity goals and sustain fishing communities amid threats like climate change and overfishing, presenting a replicable model for global reef conservation.

Keywords : *Remote sensing, Coral reef, Sentinel-2A, OBIA, Change detection, Multicriteria Evaluation*

Chapitre 1 : Introduction Générale

Chapitre 1 : Introduction générale

1.1. Formation, types et subdivision des récifs coralliens

Le terme « coraux » désigne communément des organismes benthiques appartenant à l'embranchement des Cnidaires, et plus spécifiquement à la classe des Anthozoaires (Todinanahary, 2016) . Ces organismes sont répartis en deux sous-classes principales : les Octocoralliaires (incluant notamment les coraux mous) et les Hexacoralliaires, au sein desquels on retrouve l'ordre des Scléractiniaires. Les coraux scléractiniaires sont généralement coloniaux, et leur unité de base est le polype, un petit organisme qui joue un rôle essentiel dans la formation du squelette calcaire. Les récifs coralliens sont des écosystèmes marins complexes, construits au fil du temps par l'accumulation des squelettes de ces coraux dits hermatypiques, c'est-à-dire capables de former des structures récifales. Ces formations solides sont constituées à la fois par les restes calcifiés de coraux morts et par les apports de matière calcaire produits par les algues corallines (Todinanahary, 2016). Le terme « corail hermatypique » désigne ainsi les espèces de scléractiniaires qui participent activement à la construction des récifs. Les récifs coralliens se développent dans les zones où les conditions environnementales sont favorables à la croissance des coraux hermatypiques. Ils se trouvent généralement dans des eaux peu profondes, jusqu'à environ 30 mètres de profondeur, afin de permettre à la lumière d'atteindre les coraux et leurs algues symbiotiques, telles les zooxanthelles. En outre, la température doit être comprise entre 18 et 34°C tout au long de l'année. L'eau doit être contenir suffisamment de carbonate de calcium pour soutenir le processus de calcification, tout en demeurant oligotrophe, car une concentration élevée en nutriments, tels que les nitrates, peut nuire à cette calcification (Erez et al., 2011). A l'échelle mondiale, ces conditions sont généralement réunies dans les régions situées 30° de latitude nord et 30° de latitude sud (Figure I.1).

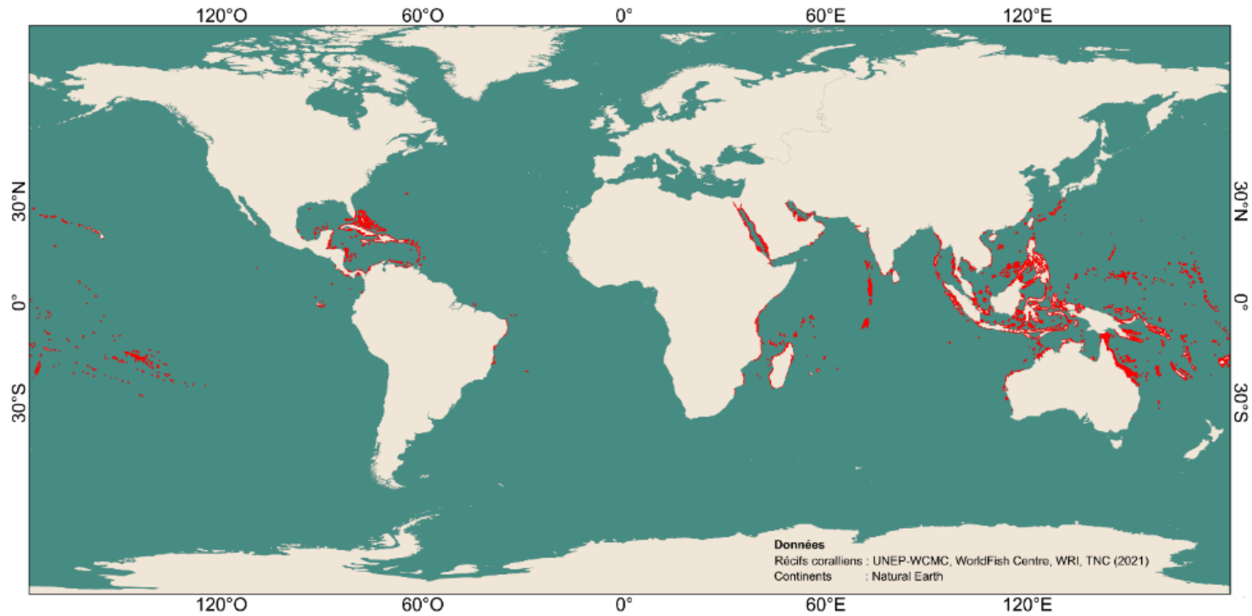

Fig.I. 1. Distribution géographique des récifs coralliens. Les zones en rouge indiquent les emplacements des récifs coralliens, basés sur les données de l'UNEP-WCMC, WorldFish Centre, WRI, et TNC (2021). Les continents sont représentés selon les données de Natural Earth.

Il existe plusieurs types de récifs coralliens dont les principaux sont les atolls, les récifs barrières, les récifs frangeants, et les bancs coralliens (Veron, 2000). Un récif frangeant est un récif corallien formé contre une terre émergée, non récifale, ou contre un récif émergé, directement accolé à la côte ou juste séparée d'elle par un chenal étroit. Un banc corallien est un vaste édifice récifal, généralement de haute mer, de forme quelconque. Il peut être émergé ou non. Un récif barrière est un ensemble de récifs coralliens entourant une terre non récifale dont il est séparé par un lagon ayant le plus souvent une profondeur de quelques dizaines de mètres et une largeur de l'ordre du kilomètre. Battistini et al. (1975) définissent un atoll comme un ensemble récifal de haute mer, émergé à marée haute, sans roche volcanique affleurante, le plus souvent de forme annulaire avec un lagon central (Figure I. 2).

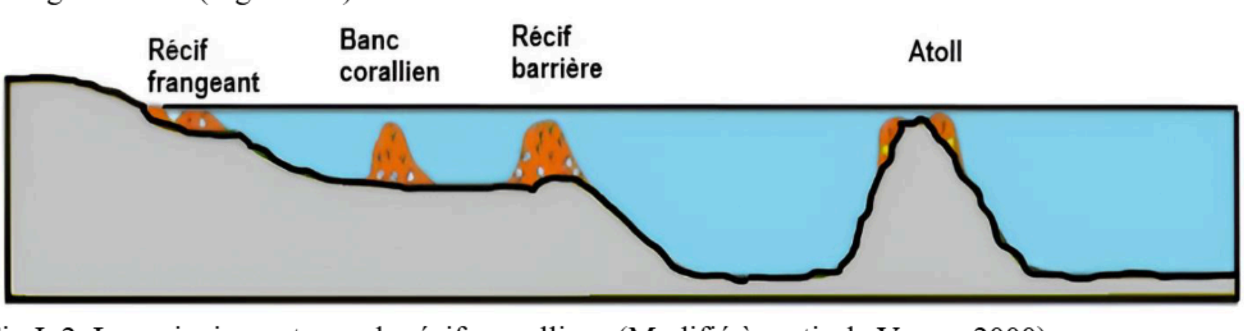

Fig.I. 2. Les principaux types de récifs coralliens (Modifié à partir de Veron, 2000)

Dans ces différents types de récifs coralliens, il existe différentes zonations géomorphologiques. La géomorphologie récifale fait référence aux zones récifales de quelques dizaines à quelques centaines de mètres correspondant aux parties d'un récif caractérisé par des structures benthiques et des types de substrats façonnés par une combinaison de facteurs tels que la profondeur de l'eau, l'énergie des vagues et l'intensité des courants (Phinn et al. 2012). Ces zones ont tendance à évoluer plus lentement dans le temps. Madagascar rassemble 86 unités géomorphologiques récifales (Andréfouët et al., 2009). Les principales unités géomorphologiques utilisés dans cette étude incluent : récifs internes, lagon, platier récifal, bassins fermés, crête récifale, front récifal et pente récifale, selon les définitions proposées par (Battistini et al., 1975). Un lagon est une dépression naturelle de profondeur et de taille variables, généralement située derrière une barrière récifale ou complètement entourée par des structures récifales. Les vasques, quant à elles, sont de petites dépressions ou cuvettes peu profondes situées à l'intérieur de la structure récifale, sur le platier. La pente récifale constitue la partie submergée du récif, inclinée vers le large, avec des pentes de degré variable. Elle est composée de formations coralliennes et de dépôts sédimentaires principalement d'origine biogénique. Le front récifal marque la bordure externe du platier à marée basse, en particulier lors des marées de vives-eaux. Le platier récifal est une plateforme horizontale au sommet de la structure récifale, atteignant souvent ou excédant le niveau de la mer. Il peut présenter des accumulations de matériaux et des incisions en surface. La crête récifale est principalement composée d'éléments grossiers et se situe à l'avant du platier, prenant différentes formes telles que des dômes, des bourrelets ou des amas rocheux. Les récifs internes sont situés à l'intérieur du lagon, souvent séparés de l'océan ouvert par une barrière récifale. Ils présentent des tailles et des formes variées et sont généralement entourés par des eaux peu profondes du lagon. Ces récifs internes comprennent des formations coralliennes lagonaires, dont certaines affleurent à la surface, ainsi que de plus grands récifs lagonaires (formations coralliennes substantielles situées dans le lagon), partiellement émergées ou submergées. Ces formations plus vastes présentent souvent des zonations distinctes, similaires à celles observées sur les platiers récifaux.

Les zones de communautés benthiques (généralement d'un à quelques dizaines de mètres) font référence aux habitats présentes dans les zones géomorphologiques. Elles désignent des ensembles plus localisés, où coexistent différentes associations de coraux, d'algues, de débris et de sable. Ces zones sont généralement plus sensibles aux variations environnementales (Phinn et al. 2012). Madagascar abrite une grande diversité de coraux constructeurs de récifs, surpassant les autres pays de l'océan Indien occidental (Cooke, 2012). Le Grand Récif de Toliara (GRT), présente une composition corallienne variée en fonction de sa zonation géomorphologique, comprenant 112 espèces réparties sur 61 genres (Pichon, 1978). La pente externe est dominée par des familles comme *Agariciidae, Pectiniidae*, *Mussidae*, *Oculinidae* et *Faviidae*, ainsi que par les genres *Acropora*, *Porites* et *Montipora* (Pichon, 1972). Les platiers récifaux abritent principalement *Acropora*, *Pocillopora*, *Favia*, *Favites* et *Goniastrea*, tandis que les récifs internes sont caractérisés par des bourrelets formés par la prolifération d'*Acropora* branchus. La grande vasque du GRT maintient une forte diversité, principalement composée d'*Acropora* (Bruggemann et al., 2012). La plus grande diversité générique se trouve au niveau de la pente externe, suivies des bancs coralliens puis des platiers internes (Razakandrainy, 2018). Des études récentes montrent une diminution de la diversité corallienne au niveau du GRT. Pichon (1978) recensait 61 genres au GRT contre 43 genres en 2021 (Botosoamananto et al., 2021). La dégradation des récifs, particulièrement au GRT, résulte de multiples pressions : cyclones, apports terrigènes, surpêche et augmentation de la température de l'eau (Bruggemann et al., 2012). Les genres *Acropora* et *Pocillopora*, sont plus sensibles au stress thermique contrairement à *Porites* et *Diploastrea*, qui se montrent plus résistants (Randrianarivo, 2023). Cependant, les genres *Acropora*, *Pocillopora*, *Seriatopora* et *Stylophora* sont privilégiés pour la restauration et la transplantation récifale. Ils sont également prisés en aquariophilie (Todinanahary, 2016; Botosoamananto et al., 2021).

1.2. Les besoins en cartographie pour le suivi des récifs coralliens

Les récifs coralliens jouent un rôle important en protégeant les côtes des tempêtes, en servant de nurseries pour les poissons et en fournissant divers avantages socio-économiques liés au tourisme, aux loisirs, à la protection des côtes, à la pêche et aux services de biodiversité (Eakin et al., 2010). Ils présentent ainsi des services éco-sociologiques d'une grande valeur (l'Organisation des Nations Unies-ONU a estimé la valeur des récifs coralliens entre 100 000 et 600 000 $/ha) (Nicet et al., 2016). Toutefois, ces écosystèmes sont confrontés à plusieurs menaces, tant au niveau mondial que local, principalement en raison du changement climatique et des activités humaines (Xu et Zhao, 2014). L'homme endommage les récifs depuis qu'il a commencé à interagir avec ceux-ci (McClanahan et al. 2012), mais ce n'est que depuis une quarantaine d'années que des impacts tels que la surpêche, la pollution et le changement climatique ont précipité leur effondrement à l'échelle mondiale (Bellwood et al. 2004). Les tendances récentes indiquent qu'entre 70 et 90 % des récifs coralliens mondiaux sont menacés d'extinction dans un avenir proche (Foo et Asner, 2019), une situation qui s'applique également aux récifs de Madagascar (van Hooidonk et al., 2016). Une intervention ciblée peut inverser cette disparition grâce à des outils allant des aires marines protégées à la restauration des récifs, mais pour être efficace, il est nécessaire de comprendre leur rôle dans les écosystèmes marins (Purkis et al., 2019). Pour surveiller efficacement les récifs coralliens, les stratégies doivent tenir compte des dimensions spatiales et temporelles. Il s'agit notamment de suivre la répartition des espèces dans l'environnement benthique et leurs substrats associés sur de longues périodes, en tirant parti de la technologie satellitaire disponible depuis des décennies (Nurlidiasari et Budiman, 2010). Au fil du temps, la complexité des écosystèmes des récifs coralliens a suscité un grand intérêt scientifique et a conduit au développement de nouvelles technologies et approches pour les observer. En outre, lorsque l'on veut une vue d'ensemble sur l'évolution de l'environnement sous-marin, celui-ci est plus difficile à étudier que l'environnement terrestre. La majorité des travaux sur la distribution spatiale des récifs coralliens ont été réalisés soit à partir d'analyse d'images satellites, soit à partir de navires de surface, ce qui nécessite une vue aérienne de l'habitat benthique, et/ou par des plongeurs. Les cartes d'habitats constituent un outil précieux, car elles permettent de : i) fournir des informations essentielles à la planification spatiale et stratégique (gestion des activités, aménagement littoral; délimitation optimale d'Aires Marines Protégées, ...) ; ii) soutenir une utilisation durable des ressources benthiques ; iii) aider à mettre en œuvre une approche écosystémique de la gestion de l'environnement marin ; iv) améliorer les bilans de l'état de l'environnement, en particulier en inscrivant les résultats des stations de surveillance dans un contexte géographique plus vaste ; v) aider à cibler les efforts de surveillance (Nicet et al., 2016). À Madagascar, les estimations de la couverture récifale varient selon les sources, ce qui complique le choix d'une base de référence fiable pour la mise en œuvre de mesures de gestion. Les données disponibles indiquent des superficies de 3100km^2 (UNEP-WCMC, WorldFish Centre, WRI, TNC, 2021), 3949 km^2 (Lyons,2024), et 5076km^2 (Andréfouët et al., 2009). Si les données globales peuvent servir de point de départ pour estimer la répartition potentielle des récifs coralliens, elles ne devraient pas être utilisées comme unique référence pour les décisions liées à leur gestion ou à leur restauration. Il est donc essentiel de privilégier la collecte de données locales et le traitement d'images satellites à l'échelle nationale afin d'obtenir des évaluations plus précises. L'imagerie satellite en libre accès, comme Sentinel-2, combinée à des moyens logistiques de base pour les relevés de terrain, permet d'atteindre une précision suffisante pour cartographier la géomorphologie récifale et les habitats benthiques.

1.3. Développement historique de la technologie de la télédétection en milieu récifal

1.3.1. Vue d'ensemble des instruments de télédétection pour les récifs coralliens

Au sens large, la télédétection est une méthode d'observation d'un objet sans contact physique direct avec celui-ci (Green et al., 2000). Depuis les années 1970, diverses techniques de télédétection ont été utilisées dans le monde entier pour cartographier les récifs coralliens et déterminer leur état de santé. Ces méthodes ont beaucoup évolué, de même que les capteurs utilisés pour cartographier ces habitats. L'amélioration des capacités de stockage des données, l'augmentation de la vitesse de connexion pour le téléchargement de fichiers d'images volumineux et l'amélioration des performances générales des ordinateurs ont facilité la cartographie détaillée des caractéristiques spécifiques des récifs coralliens. Il existe deux méthodes d'acquisition de données en télédétection: active et passive (Hochberg, 2011). Un système de télédétection passif enregistre simplement l'énergie ambiante, généralement celle du soleil, réfléchie par une surface (ce qui équivaut à la photographie à la lumière du jour). Les imageurs multispectraux et hyperspectraux sont des exemples de systèmes passifs. Les imageurs multispectraux enregistrent un petit nombre de bandes de longueurs d'onde spécifiques (généralement de 3 à 10), tandis que les imageurs hyperspectraux vont plus loin, capturant des centaines de bandes de longueurs d'onde très étroites sur un large spectre. Les images Landsat et Sentinel peuvent être classée dans cette catégorie. Une bande spectrale est une sorte de filtre utilisé par un capteur d'un satellite pour enregistrer des plages de longeurs d'onde de la lumière. Chaque bande capte un type particulier de la lumière, comme le bleu, le vert, l'infrarouge etc. Un exemple est donné en Annexe 2 pour illustrer les bandes spectrales d'une image Sentinel-2A. Dans la télédétection active, un signal sur une longueur d'onde particulière est transmis et le capteur enregistre la réflexion. Un exemple de télédétection active pertinente pour les récifs coralliens est le LIDAR (LIght Detection And Ranging, ci-après dénommé « lidar ») (Green et al., 2000). Avec le lidar, le capteur émet une impulsion laser très courte et mesure très précisément le temps nécessaire pour que l'impulsion se réfléchisse sur la surface du récif et revienne au capteur. La distance jusqu'à l'objet est (essentiellement) égale à la moitié du temps de trajet multiplié par la vitesse de la lumière. Ces systèmes peuvent générer des données bathymétriques très détaillées sur les récifs coralliens jusqu'à des profondeurs de ~40 m, en fonction de la clarté de l'eau. Ces données peuvent être intégrées dans une procédure de classification des fonds marins (Hochberg, 2011). Depuis le début de l'année 2010, l'utilisation des données lidar pour la cartographie des récifs est en augmentation, mais l'utilisation de l'imagerie satellitaire multispectrale et hyperspectrale est beaucoup plus répandue. L'objectif de l'étude ainsi que la précision recherchée détermine le type et le choix des capteurs à utiliser (Figure I.3). Des exemples de résolutions obtenues à partir de différentes techniques de télédétection sont présentées en Annexe 5.

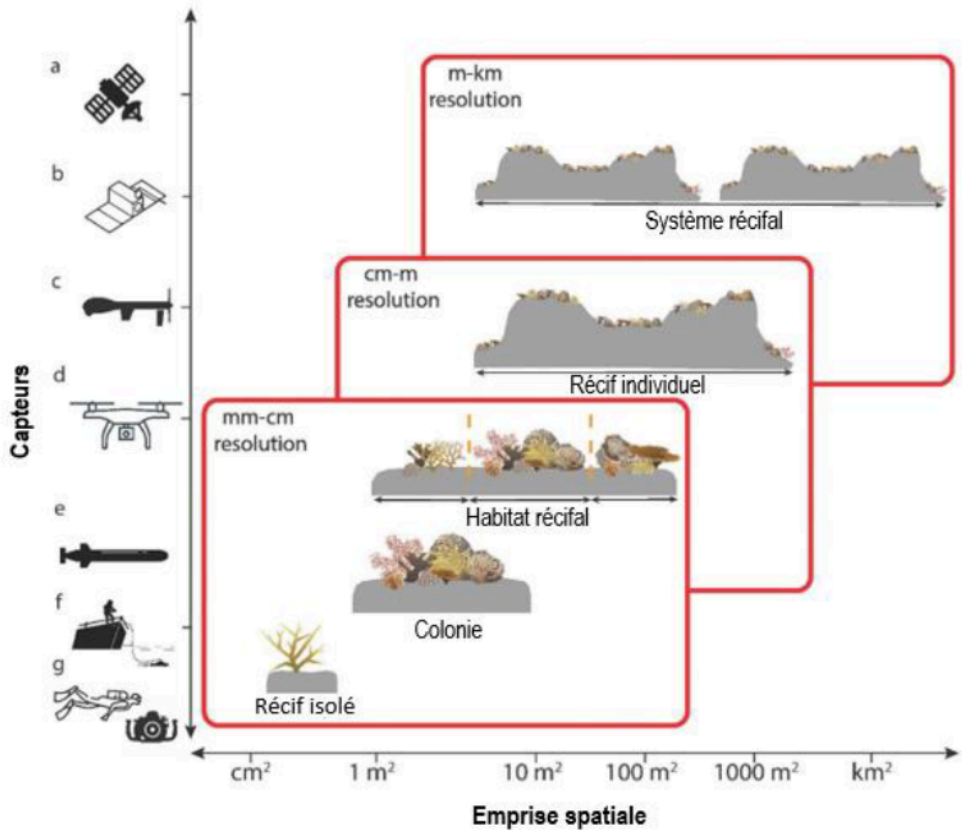

Fig.I. 3. Différences d'emprise spatiale et de résolution spatiale entre les technologies et les approches utilisées dans la recherche sur les écosystèmes des récifs coralliens. Plus précisément, les différences entre les plateformes de télédétection satellitaires et aériennes (c'est-à-dire a-satellite, b-avion, c-véhicules aériens sans pilote, et d-drones) ; et les plateformes de télédétection dans l'eau, y compris : e-véhicules sous-marins autonomes, f-drones sous-marins, et g-systèmes de caméra opérés par des plongeurs. (Modifiée à partir de Lutzenkirchen et al, 2024).

Diverses technologies sont adoptées dans le monde entier pour étudier les écosystèmes coralliens, notamment les véhicules sous-marins autonomes (AUV), les véhicules télécommandés (ROV), les véhicules aériens sans pilote (UAV), les petits bateaux, les avions, la photographie sous-marine, les drones et les satellites (Figure I.3). Ces outils utilisent une variété d'approches telles que les systèmes multispectraux, hyperspectraux, infrarouges thermiques, lidars et sonars pour capturer des données (Green et al., 2000). La disponibilité et l'utilité de ces approches se sont rapidement accrues depuis les années 1990, et elles offrent aujourd'hui une gamme d'options en différente résolution spatiale. Cette dernière fait référence à la taille de pixel de l’image. Une résolution spatiale faible, telle celle de l'imagerie AVHRR (1000 m) présente moins de détails et une netteté réduite. Une haute résolution spatiale, telle que celle de l’imagerie QuickBird (2.5m) permet une représentation beaucoup plus précise (Figure I.4). L’emprise spatiale fait référence à la zone géographique que le capteur du satellite peut couvrir en une seule prise. Il existe des compromis entre l'emprise spatiale, la résolution spatiale et le coût des données dans les différentes technologies et approches (Hedley et al., 2016). Une résolution plus fine fournit des informations plus détaillées, mais réduit généralement l'emprise spatiale qui peut être couverte (Figure I.4). Cela signifie qu'à mesure que la résolution augmente, la capacité à surveiller de plus grandes zones diminue, car il faut plus de temps et de ressources pour obtenir une couverture à haute résolution sur de grandes zones. Inversement, une zone plus étendue peut être surveillée plus rapidement, mais avec des images moins détaillées. Le coût des données peut également augmenter à mesure que la résolution spatiale devient plus fine. Il est donc important de tenir compte de ces compromis lors du choix de la méthode, des images ou des instruments appropriés.

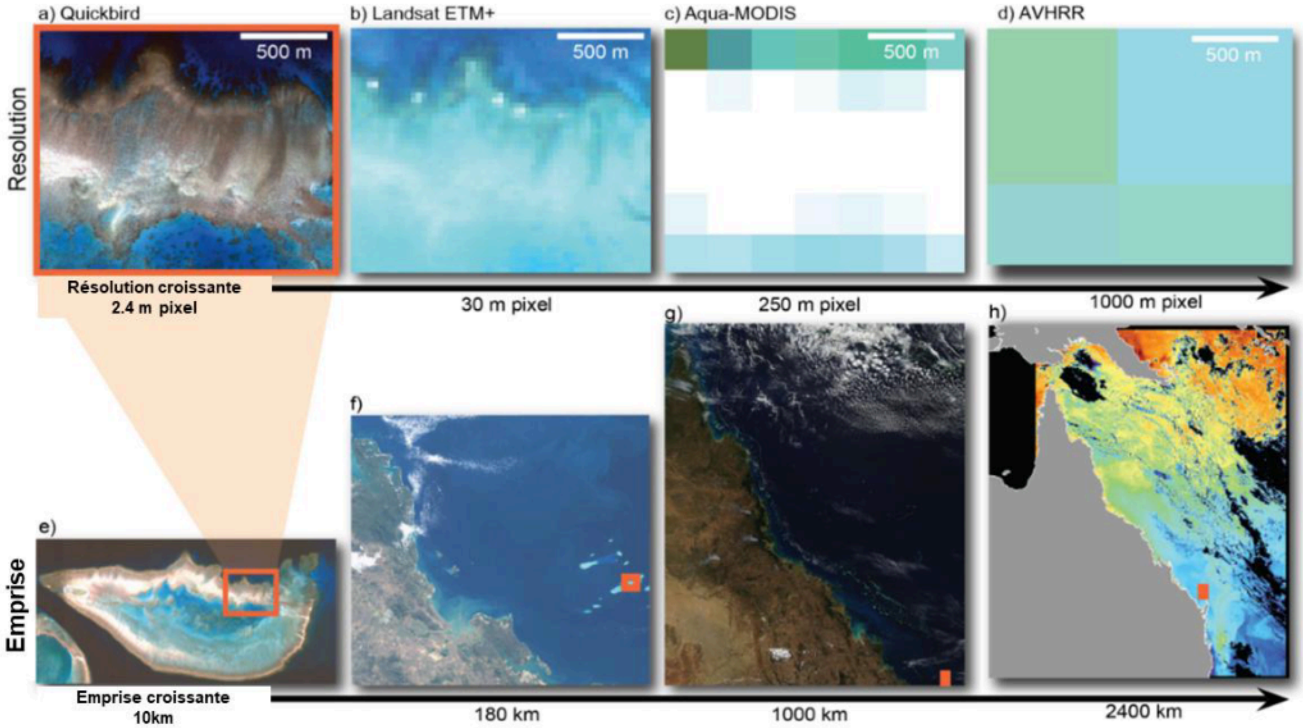

Fig.I. 4. Différentes dimensions spatiales des données de télédétection pour une image de Heron Reef, en Australie.. Les images (a-d) montrent les effets de tailles de pixels progressivement plus grandes pour une section de 1,5 km de long de Heron Reef, dans le sud de la Grande Barrière de corail, en Australie ; les images (e-g) montrent différentes étendues d'image ; en commençant par Heron Reef et en passant à l'ensemble de la Grande Barrière de corail (h) ; l'imagerie des radiomètres perfectionnés à très haute résolution (AVHRR) fournit des informations à l'échelle océanographique (Modifiée à partir de Hedley et al., 2016)

1.3.2. Évolution de la cartographie des récifs coralliens par télédétection

La télédétection par satellite des récifs coralliens a commencé au début des années 1970 avec le lancement de Landsat 1 (Smith et al. 1975). Les premières études menées dans les années 1970 et 1980 s'appuyaient sur les images des capteurs embarqués à bord des satellites Landsat et SPOT (Satellite pour l'Observation de la Terre) (Hochberg, 2011). Ces images étaient multispectrales (deux ou trois bandes d'ondes dans le spectre visible), à large bande (chaque bande d'onde ayant une largeur de 60 à 100 nm) et avaient une résolution spatiale modérée (20 à 30 m). Bien que la taille des pixels de 20 à 30 m de ces capteurs ait été considérée comme une haute résolution pour l'époque et qu'elle ait permis de donner un aperçu des caractéristiques du fond marin, les résultats obtenus à partir de ces données étaient insuffisantes pour capturer l'hétérogénéité d'un environnement récifal typique tel qu'il serait perçu *in situ* (Purkis et al., 2019). Les nombres restreints de bandes spectrales larges, combinés à une résolution spatiale modérée, l'absence d'algorithmes adaptées pour compenser les effets confondants de l'atmosphère, de la surface de la mer et de la colonne d'eau, représentait un défi majeur (Nguyen et al., 2021) et a ainsi limité la plupart des études à la simple détection des zones récifales et à la délimitation de leur géomorphologie (Platier récifal, Pentes externe, Lagon, etc.) (Kuchler, 1986). C'est dans ce contexte qu'a été réalisée la première cartographie globale des récifs coralliens à partir de données de télédétection, aboutissant à la publication de l'Atlas mondial des récifs coralliens publié par le Centre mondial de surveillance de la conservation du Programme des Nations unies pour l'environnement (WCMC-UNEP) (Spalding et al., 2001). Celle-ci a fondé les bases du Millennium Coral Reef Mapping Project (MCRMP), lancée en 2004 (Andréfouët et al., 2006). Ce projet a analysé plus de 1600 images satellite Landsat 7 ETM+ (Enhanced Thematic Mapper Plus) à l'échelle mondiale. Ces images, d'une résolution spatiale 30 m x 30 m comprennent quatre bandes spectrales adaptées à la cartographie des habitats récifaux. Des techniques de photo-interprétation (cartographie manuelle) ont été utilisées pour cartographier les systèmes récifaux des principales régions récifales du monde en utilisant une typologie cohérente et applicable à l'échelle globale regroupant 800 classes (Andréfouët et al., 2006). Avec sa résolution de 30m, certes relativement grossière, le satellite Landsat permet néanmoins une cartographie à grande échelle des structures géomorphologiques majeures, et de différencier bien qu'il ne permette pas de distinguer les communautés benthiques (Corail, Herbier, Débris, Sable) au niveau des récifs avec un niveau de détail plus fin. Les années 1990 ont vu l'avènement de l'imagerie hyperspectrale à partir de plates-formes aéroportées. Les plates-formes aéroportées volaient à proximité des récifs, les images obtenues ont une résolution spatiale plus élevée (0,5-20 m, en fonction de l'altitude de vol). Les années 2000 ont été marquées la mise à disposition du public d'images satellitaires commerciales provenant d'IKONOS et de Quickbird, en fournissant une résolution spatiale qui était bien meilleure que celle de Landsat (2,4-4 m) (Hamylton, 2017). En général, l'imagerie satellitaire commerciale permettait de distinguer entre cinq et neuf classes benthiques avec une précision de 50 à 80 %, selon les études. Pour la première fois, les satellites ont offert des vues détaillées et relativement abordables des récifs coralliens, alors qu'auparavant, de telles observations n'étaient accessibles qu'au prix de relevés aériens coûteux. Cette avancée a suscité un intérêt croissant au sein des communautés scientifiques et des gestionnaires des récifs, qui ont commencé à utiliser ces images comme cartes de références pour les études sur le terrain, et à produire leurs propres analyses à partir de la télédétection (Hochberg, 2011). Les progrès les plus récents dans l'imagerie satellitaire ont été progressifs, notamment grâce à la série de satellites WorldView, lancée à partir de 2007. Ces satellites offrent une résolution spatiale comprises entre 1 et 2 m, soit une amélioration deux ordres de grandeur par rapport aux capteurs Landsat ou SPOT de la génération précédente. Au-delà de l'amélioration de la résolution spatiale, le programme WorldView fournit des données dans huit bandes spectrales, dont cinq pénètrent dans l'eau, permettant une meilleure différentiation des types de fond marins et une estimation d'une bathymétrie plus précise. La cartographie des récifs coralliens a considérablement progressé depuis la mise à disposition gratuite des images Landsat en 2008. Avant 2008, une image Landsat MSS (Multispectral Scanner) coûtait entre 20 USD (1972-1978) et 200 USD (1979-1982), tandis que le prix d'une image Landsat Thematic Mapper s'élevait à 3000 à 4000 USD (1983-1998). Pour une image ETM+ (Enhanced Thematic Mapper Plus), le coût était de 600 USD (1999-2008) (Zhu et al., 2019) . L'accès libre aux images Sentinel-2, fourni par l'Agence spatiale européenne (ESA), a encore accéléré ces avancées. Sentinel-2 offre une résolution spectrale améliorée et une taille de pixel de 10 mètres, soit trois fois plus fine que celle des images Landsat. Bien que les capteurs orbitaux actuels puissent imager la Terre avec des résolutions spatiales et spectrales autrefois accessibles uniquement par avion, ce n'est que récemment que les projets de cartographie récifale ont commencé à adopter une approche régionale et mondiale, plutôt que de se limiter à des récifs isolés ou à de petites collections de récifs situés dans des zones spécifiques. Cette approche locale initiale s'explique par :

i) les contraintes informatiques : le traitement des ensembles de données couvrant de larges régions ou le monde entier est exigeant en ressources et compliqué par les grandes variations environnementales, telles que les marées, les vagues et la clarté de l'eau,

ii) le manque de financements : les projets de cartographie récifale mondiale ont historiquement souffert d'un soutien financier limité.

Un petit nombre de programmes de cartographie des récifs ont néanmoins fait franchir le pas vers des cartographies régionales adaptés aux initiatives de planification de l'espace marin (Purkis et al., 2019). A ce jour, deux programmes majeurs de cartographie des récifs ont été réalisés à l'échelle régionale, avec une résolution spatiale de l'ordre du mètre. Le premier programme à avoir fourni des cartes détaillées des récifs coralliens avec une résolution de l'ordre du mètre à l'échelle régionale est le KSLOF-GRE (Khaled bin Sultan Living Oceans Foundation – Global Reef

Expedition) (Purkis et al., 2019). Le second programme de cette catégorie est l'Allen Coral Atlas (www.allencoralatlas.com), lancé en 2020. Financé par le cofondateur de Microsoft et philanthrope Paul Allen, ce projet ambitieux vise à offrir un accès libre et mondial aux données sur les récifs coralliens. Ce programme utilise des images satellites à haute résolution de 5 mètres (taille de pixel de 5 mètres carrés), dont la licence commerciale a été accordée par Planet Labs (Lyons et al., 2024). Cela met en évidence le coût important associé à l'obtention de ces images, malgré l'engagement d'Allen Coral Atlas d'offrir ses données gratuitement. Le projet vise à produire des cartes de zonation géomorphologique et d'habitat benthique à l'échelle mondiale. Les méthodes utilisées sont basées sur les travaux de Roelfsema et al. (2018) dans la Grande Barrière de Corail. Toutes ces données sont accessibles via le portail web du projet www.allencoralatlas.com (Purkis et al., 2019). La NASA (National Aeronotic and Space Administration) développe également une initiative appelée NeMO-Net (www.nemonet.info), qui, comme l'Allen Coral Atlas, vise à cartographier les récifs coralliens mondiaux, mais à l'échelle du centimètre. NeMO-Net et l'Allen Coral Atlas s'appuient tous deux sur des données de « vérités-terrain » de grande qualité pour améliorer leur précision. La facilité d'utilisation et la précision de ces cartes sont directement liées à la disponibilité et à la qualité des données de terrain utilisées pour entrainer leurs algorithmes. Bien que ces initiatives en soient encore à leurs débuts, elles sont très prometteuses pour l'avenir et devraient s'améliorer au fur et à mesure de leur évolution.

1.3.3. Evolution des techniques de cartographie des récifs coralliens

L'interprétation visuelle des photographies aériennes est le premier moyen par lequel des données de télédétection ont été utilisées pour la cartographie des récifs. Elle consiste à regrouper des caractéristiques des récifs en différentes classes (pente récifale, crête récifale, lagon, etc.) basées sur des observations de terrain détaillées et des connaissances d'experts, et se sont appuyées sur une vaste connaissance concernant le développement et l'écologie des récifs (Kennedy et al., 2021). L'utilisation de photographies aériennes pour la cartographie des récifs coralliens s'est d'abord appuyée sur des images collectées lors de vastes investigations aériennes entreprises par l'armée pendant la Seconde Guerre mondiale (Teichert, 1995). Plus tard, ces images ont été appuyées par tout un ensemble de données écologiques et géologiques (tels les carottages, les relevés bathymétriques, les données écologiques benthiques). Le lancement du programme Landsat dans les années 1970 a permis d'obtenir un flux constant d'images mondiales, générant une énorme quantité de données au fil du temps. Cette abondance d'informations a rendu de plus en plus difficile de se fier uniquement à l'interprétation visuelle et à la délimitation manuelle des caractéristiques des images. Pour surmonter cette difficulté, la classification automatique d'images a émergé, visant à améliorer la reconnaissance des caractéristiques du substrat. Cette approche repose sur le calcul informatique de la similarité entre les pixels d'une image. Les pixels présentant des caractéristiques similaires sont regroupés dans une même classe, tandis que ceux qui diffèrent sont affectés à des classes distinctes. Le résultat est une classification des pixels en groupes définis par l'utilisateur, constituant ainsi la légende de la carte (Figure I.5). Cette approche offre les avantages d'une vitesse de traitement accrue, d'une répétabilité constante et la possibilité de couvrir de zones étendues. Selon les objectifs et les catégories d'habitats à extraire de ces images, différentes images satellites et différentes méthodes ont été adoptées au fil des années (Tableau I.1).

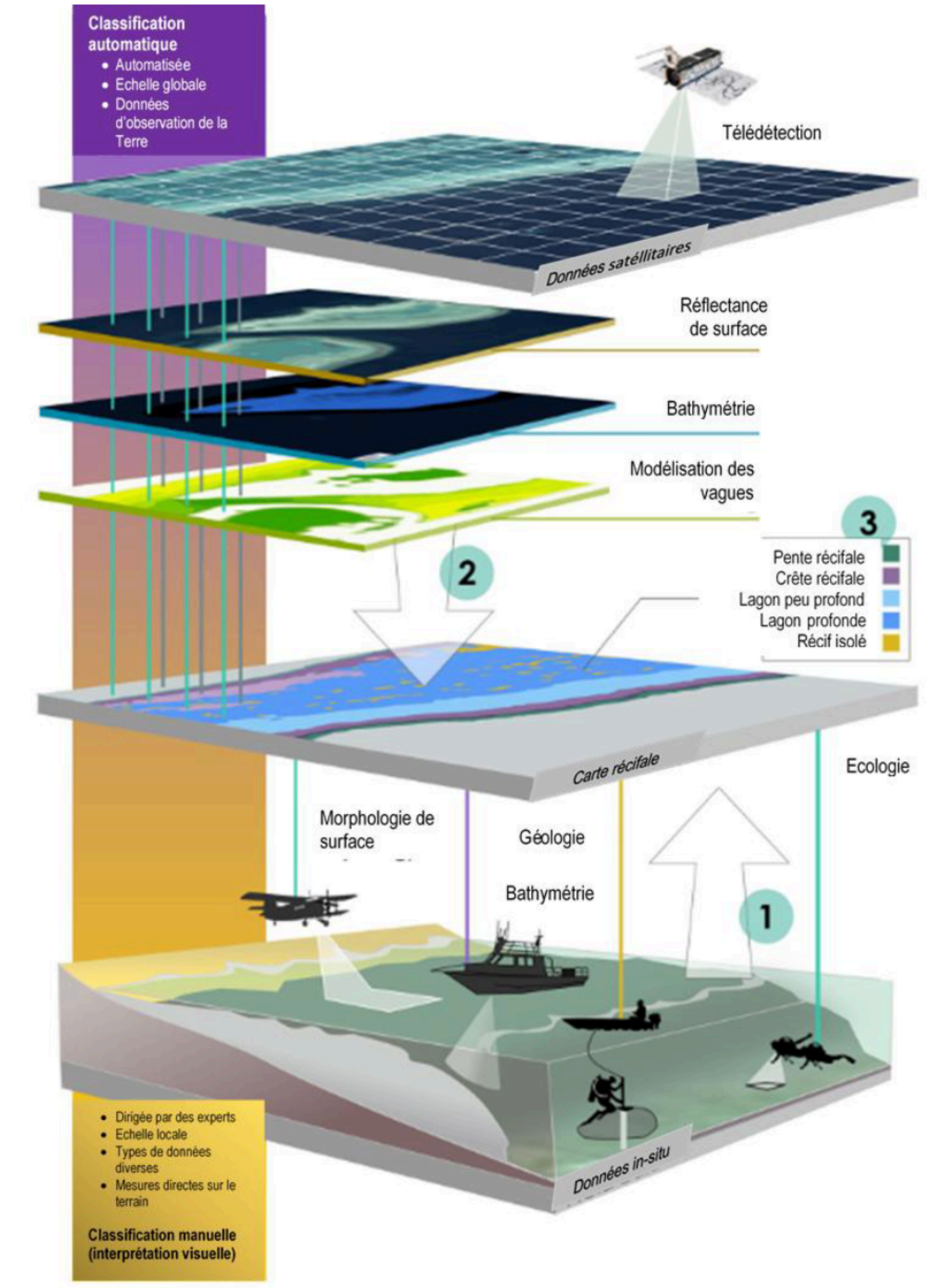

Fig.I. 5. Différentes échelles (globale ou locale) et approches scientifiques (mesures directes sur le terrain ou observations à distance par satellite). (Modifiée à partir de Kennedy et al., 2021)

L'interprétation des images de télédétection est souvent difficile à cause de la présence de nuages qui masquent les caractéristiques intéressantes, l'absorption et la diffusion de la lumière dans l'atmosphère, la profondeur limitée de pénétration de la lumière dans la colonne d'eau, la variation de la qualité de l'eau sur une même scène d'image et la rétrodiffusion de la lumière causant des reflets du soleil à la surface de la mer. Il est donc nécessaire de prétraiter les images de télédétection afin d'éliminer autant que possible ces artefacts avant de les interpréter en termes de fond marin. Lyzenga (1978, 1981) a démontré le potentiel de la télédétection dans la surveillance des récifs coralliens en utilisant des informations dans différentes bandes spectrales provenant d'avions et d'images Landsat. Son travail a consisté à cartographier la bathymétrie des eaux peu profondes et le type de substrat, ainsi qu'à corriger la colonne d'eau. Cette méthode a fourni des informations cruciales sur la distribution spatiale des récifs coralliens et de leurs habitats, ce qui a permis des avancées significatives dans la cartographie des récifs coralliens et l'étude des environnements benthiques associés. Une série de techniques de prétraitement, y compris la correction de l'atmosphère, de la colonne d'eau et des reflets, ont été mises au point pour améliorer la précision avec laquelle les environnements de récifs coralliens peuvent être cartographiés à partir d'images de télédétection aéroportées et satellitaires (Mumby et al., 2004), (Hamylton, 2017). Une technologie émergente appelée Fluid lensing a récemment été développée, visant à améliorer la correction de la colonne d'eau (Figure I.6). Cette technologie est capable de produire des images en 3 dimensions à travers les vagues océaniques et sans distorsion à des résolutions spatiales inférieures au centimètre (Chirayath et Instrella, 2019). La cartographie des récifs coralliens en est à la fois à son stade naissant et à un moment tournant de son évolution. Les technologies utilisées pour cartographier ces habitats à l'échelle mondiale et à des résolutions plus élevées ont considérablement progressé, grâce à la disponibilité croissante de données de vérité terrain, d'images satellite et d'algorithmes de classification facilement accessibles.

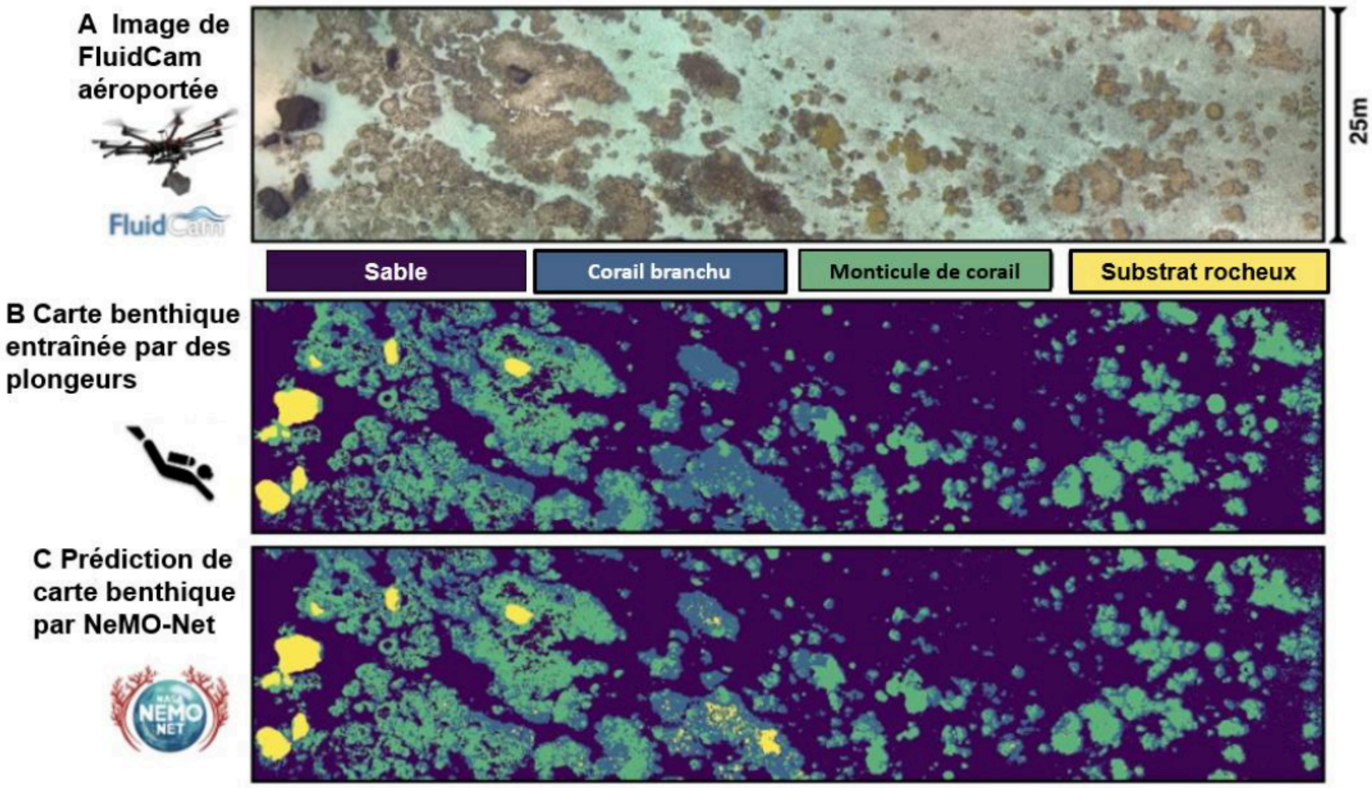

Fig.I. 6. Produit de carte benthique à l'échelle centimétrique de NeMO-net à partir de FluidCam (Modifié à partir de Chirayath et Instrella, 2019). Produit de carte benthique à l'échelle centimétrique de NeMO-net à partir de FluidCam (Modifié à partir de Chirayath et Instrella, 2019). Précision de prédiction de NeMO-Net = 94.4% sur 4 classes benthiques en utilisant un entraînement avec 0.2% de données échantillonéées aléatoirement

Tab.I. 1. Images satellites et méthodes utilisées dans la cartographie récifale. Synthèse des études sur la classification des habitats benthiques et la zonation géomorphologique des récifs coralliens. Les données incluent la référence, la localisation, l'image utilisée, les objectifs, l'année d'acquisition de l'image, les méthodes appliquées, et la typologie des classifications.

Reference	**Localisation**	**Image utilisée**	**Objectifs**	**Année d'acquisition de l'image**	**Méthodes**	**Typologie**
(Ahmad and Neil, 1994)	Heron Reef, Australia	Landsat	Habitat Benthique et Zonation géomorphologique	1990	MicroBIAN	Zonation géomorphologique : Eau libre, Eau profonde, Hauts-fonds récifaux, Lagon profond, Lagon profond avec récifs isolés, Lagon peu profond, Pente récifale, Bordure récifale Classification des images benthiques : Coraux, Coraux et sable, Sable, Plage de sable, Plage rocheux, Vagues déferlantes, Île Heron
(S. Andréfouët et al., 2006)	Couverture globale	Landsat	Zonation géomorphologique	1999-2003	Segmentation and photo-interpretation techniques	966 classes géomorphologiques aux niveaux des principaux complexes récifaux (par exemple, atolls, récifs barrières, etc.) et de leurs sous-complexes (par exemple, bordure d'atoll, lagon d'atoll, etc.)

(Hedley et al., 2018)	Couverture globale	Landsat, Sentinel-2	Bathymétrie, Habitat Benthique et Zonation géomorphologique	2015-2016	OBIA	Benthique : Blanchi, Corail/Algues, Roche, Débris coralliens, Sable, Petit récif, Récifs en patchs, Eau profonde, Pente profonde, Lagon profond, Plateau Géomorphologie : Crête récifale, Platier externe, Platier interne, Lagon peu profond, Pentes, Pentes profondes, Plateau, Lagon profond, Récifs en patchs, Petits récifs, Eau profonde
(Joyce et al., 2004)	Capricorn Bunker Reefs, Southern Great Barrier Reef, Australia	Landsat	Habitat benthique	2001	Unsupervised ISODATA	Sable, Corail, Substrat rocheux, Débrix, Macroalgue
(B. Lyons et al., 2020)	Heron reef, Cairn-to-Cooktown, Great Barrier Reef (Australia), South West Pacific	World View, Landsat, Sentinel-2, Planet Dove	Zonation géomorphologique et habitat benthique	2014-2019	Segmentation and Random Forest	Zonation géomorphologique : Profond, Turbide, Lagon peu profond, Platier interne, Platier externe, Bordure récifale, Platier terrestre, Pente abritée, Pente exposée, Plateau, Lagon complexe ouvert, Récif isolé, Petit récif Classification benthique des images : Sable, Débris coralliens,

						Roche, Corail/Algues, Algues, Corail, Vase, Mangrove, Herbiers marins
(Lyons et al., 2024)	Couverture globale	Sentinel 2 et Planet Dove CubeSat	Zonation géomorphologique et habitat benthique	2018-2020	Random Forest	Zonage géomorphologique : Pente récifale, Pente récifale abritée, Crête récifale, Platier externe, Platier interne, Plateau, Pente arrière-récifale, Lagon peu profond, Lagon profond Classe benthique : Corail/Algues, Herbiers marins, Nappes microalgales, Roche, Débris coralliens, Sables
(Poursanidis et al., 2020)	QuirimbasNational Park, Mozambique	Sentinel-2	Habitat benthique	2019-2020	DT, RF, SVM	Substrat mou, Substrat dur, Vegetation, Eau profonde
(Velloth et al., 2014)	Agatti and Flat Islands, India	Hyperion	Habitat benthique	2003, 2008	k-means	Géomorphologie : Crête récifale, pente récifale, lagon intermédiaire, nappe de sable, lagon profond, lagon peu profond, récif submergé, platier récifal, piscine peu profonde, platier récifal, platier récifal exposé avec algues, plage de sable

(Wicaksono, 2016)	Kemujan Island (Indonesia)	World View	Habitat benthique	2012	Principal Component Analysis, Independent Component Analysis	Algues+corail, Algues+débris, Algues+sable, Algues+herbiers marins, Macroalgues, Débris d'algues, Débris, Sable+algues, Sable+débris, Sable+herbiers marins, Sable, Corail+débris, Corail+sable, Récifs coralliens, Corail+algues, Herbiers marins+algues, Herbiers marins+sable
(Xu et al., 2021)	Northern Great Barrier Reef, Australia	Sentinel-2	Detection du blanchissement corallien	2015-2016	SVM	Coraux blanchis, Corail sain, Algues, Sable

1.4. Objectifs de la thèse

L'objectif de cette thèse est de caractériser les écosystèmes coralliens à Madagascar, en se focalisant sur le Grand Récif de Toliara (GRT) et les récifs avoisinants en tirant parti des données de télédétection, des observations sur le terrain et des techniques analytiques avancées afin de soutenir des stratégies de conservation et des pratiques de gestion. Cette approche est particulièrement adaptée aux pays en développement, où les contraintes budgétaires limitent souvent l'accès à des ressources et des technologies coûteuses.

Cette thèse de doctorat est présentée en six chapitres. Le chapitre 1 décrit les différentes méthodes de cartographie satellitaires existantes. Il se poursuit par la méthodologie générale entreprise au cours de ce travail (Chapitre 2). Les trois chapitres suivants décrivent le corps de la présente recherche (Chapitre 3 à Chapitre 5) et ils se terminent par une discussion générale (Chapitre 6) replaçant notre travail dans un contexte général.

Chapitre 3: Télédétection des habitats des récifs coralliens à Madagascar à l'aide d'images satellite Sentinel-2

La technique adoptée dans ce chapitre se distingue par son caractère hybride, intégrant des techniques de terrain (phototransects géoréférencées) et des outils avancés de télédétection (Analyse Orientée Objet ou OBIA, correction de la colonne d'eau avec l'algorithme de Lyzenga). Cette combinaison est originale dans le contexte de Madagascar, où les études précédentes se sont souvent limitées à des relevés manuels ou à des analyses satellitaires ou des données de validation sur le terrain sont très ponctuelles et peu suffisantes. L'utilisation d'un GPS flottant dans un boîtier étanche, synchronisé avec des plongeurs, pour géoréférencer les photos sous-marines est une solution ingénieuse et peu coûteuse, adaptée aux contraintes logistiques locales. L'objectif du présent chapitre est d'analyser la couverture benthique existant sur le Grand Récif de Toliara (GRT) et les systèmes récifaux avoisinant la ville de Toliara à Madagascar, en utilisant l'analyse OBIA sur les images satellite Sentinel-2A couplée à la collecte de données sur le terrain. L'étude vise à fournir une base de référence des communautés benthiques récifales dans la région de Toliara afin de permettre aux scientifiques marins de mieux documenter les changements dans le système et aux décideurs de surveiller sa santé et de le gérer pour une durabilité à long terme.

Chapitre 4 : Détection des changements de la couverture corallienne benthique à Toliara, Madagascar : Tendances passées, présentes et futures

Ce chapitre utilise une série d'images satellite Sentinel-2A entre 2015-2024, appuyées par des photos sous-marins collectées sur le terrain en 2021 et 2024, pour analyser la dégradation des récifs coralliens à l'échelle locale. En appliquant des techniques avancées de reconnaissance d'objets, telles que les réseaux de neurones convolutionnels (CNN), nous avons pu reconstruire les changements historiques du Grand récif de Toliara et les systèmes récifaux avoisinants, notamment caractériser les changements significatifs dans la couverture des récifs coralliens entre 2015 et 2024. De plus, l'application de modèles prédictifs comme le Cellular Automata (CA) via l'extension MOLUSCE (Modules for Land Use Change Evaluation) pour prédire les changements jusqu'en 2035 est rare dans les études récifales, sachant que MOLUSCE est majoritairement utilisé dans le domaine terrestre. L'objectif est d'identifier les zones de récifs coralliens stables et celles qui se dégradent rapidement, ces dernières indiquant probablement les niveaux les plus élevés de stress environnemental et anthropique.

Chapitre 5 : Évaluation de la résilience des récifs coralliens par télédétection et approche sur le terrain pour l'aide à la décision pour les communautés de pêcheurs

Ce chapitre présente une évaluation de la résilience des récifs coralliens par une évaluation multicritères (MCE) basée sur le processus hiérarchique analytique (AHP) et la combinaison linéaire pondérée (WLC). Cette approche évalue sept facteurs (abondance des coraux, structure, herbivores, profondeur, effort de pêche, stress thermique, turbidité) selon six scénarios de conservation adaptés aux priorités locales et mondiales. Contrairement aux études précédentes qui utilisaient un nombre variable de facteurs sans contextualisation spatiale explicite, ce chapitre propose des cartes détaillées de résilience (en hectares) pour identifier les zones à protéger ou à restaurer, en particulier au niveau des communautés des petits pêcheurs.

Le Chapitre 6 est consacré à la Discussion. Il traite de l'importance d'une approche intégrée pour la recherche et la conservation des récifs coralliens, analyse l'évolution des systèmes récifaux de Toliara entre 1960 et 2030, explore la gestion fondée sur la résilience à travers différents scénarios de conservation, et se termine par une réflexion sur les perspectives futures.

Chapitre 2: Méthodologie Générale

Chapitre 2: Méthodologie Générale

2.1. Zone d'étude

Cette étude se concentre sur la baie de Toliara, dans le sud de Madagascar, une région marquée par la présence du Grand Récif de Toliara (GRT), un récif barrière de 19 kilomètres de long situé entre 43.614°E/-23.355°S et 43.690°E/-23.502°S (Figure II.1). De plus, les systèmes récifaux de Sarodrano et d'Ankilibe, s'étendant de 43.714°E/-23.504°S à 43.743°E/-23.547°S, constituent une partie intégrante de la zone d'intérêt (Figure II.1). Le choix de ces sites a été guidé par trois principaux facteurs : (1) l'accessibilité, facilitant les opérations logistiques ; (2) la variabilité écologique, englobant à la fois des zones récifales dégradées et saines pour mieux évaluer les stress locaux ; et (3) la complexité écologique, due à la combinaison unique de récifs barrières, frangeants et en banc coralliens au sein de ce système récifal.

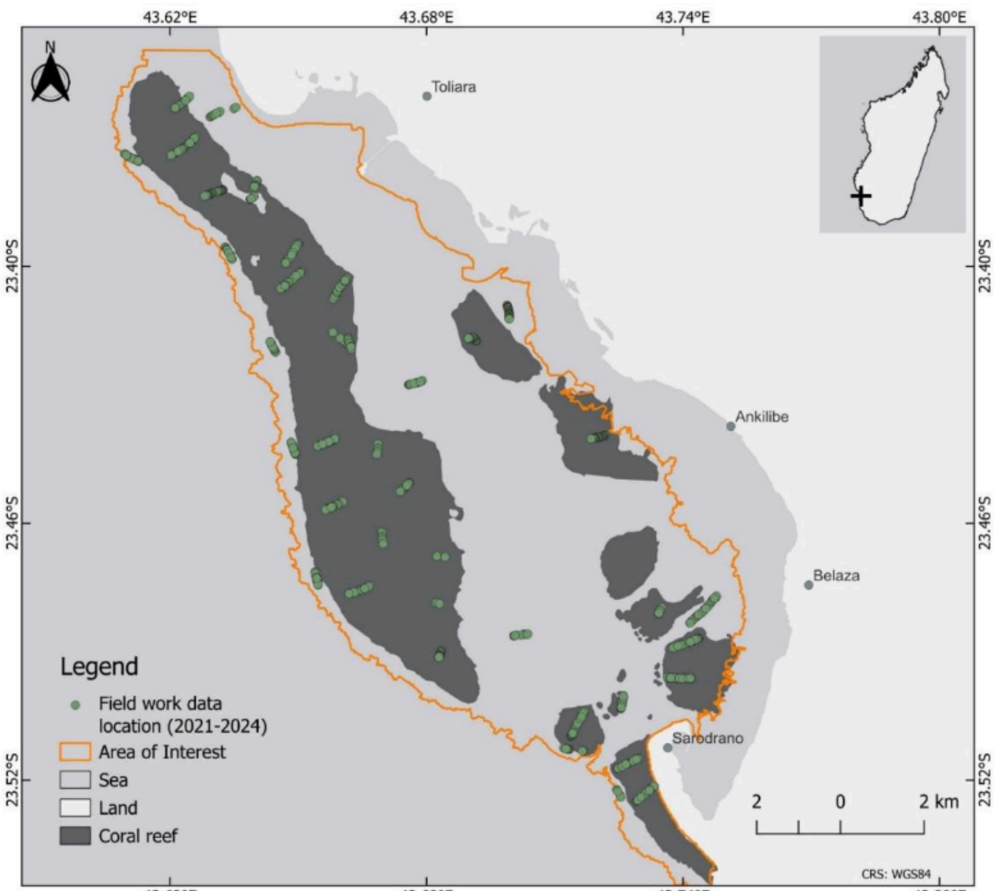

Fig.II. 1. Zone d'étude et localisation des trajectoires des photo transects

2.2. Approche méthodologique

La méthodologie générale de cette thèse aborde la combinaison des images satellites Sentinel-2A à des données sur le terrain pour la conservation des récifs coralliens. Le Chapitre 3 établit une méthodologie de standardisation de la cartographie des habitats benthique à l'échelle locale en combinant les données *in-situ* avec l'image satellite Sentinel-2A. Le chapitre 4 évalue les tendances temporelles de 2015 à 2024 et prédit jusqu'en 2035 avec les modèles de réseaux de neuronnes convolutifs (CNN) (Raphael et al., 2020) et du Cellular Automata lequel est intégré dans l'extension MOLUSCE (Modules for Land Use Change Evaluation) du logiciel QGIS (Alam et al., 2021). Le chapitre 5 se concentre sur la résilience et propose plusieurs scénarios de conservation avec l'analyse multi-critère (MCE) (Carver, 1991; Voogd, 1983). Le chapitre 3 se concentre sur le développement d'une méthodologie standardisée pour cartographier les habitats des récifs coralliens à Madagascar, en ciblant spécifiquement le Grand Récif de Toliara (GRT) et les récifs d'Ankilibe et Sarodrano, à l'aide d'images Sentinel-2A gratuites de l'Agence spatiale européenne (ESA). À Madagascar, les ensembles de données existants, comme ceux de l'UNEP-WCMC et de l'Allen Coral Atlas, souffrent de mises à jour irrégulières et d'une précision incohérente. Cela nécessite une approche adaptée et économique pour un suivi complet. L'étude utilise les images Sentinel-2A d'une résolution spatiale de 10 mètres (taille de pixel de 10 mètres carrés), acquise le 21 août 2021, avec des données de terrain provenant de 30 transects à moins de 20 mètres de profondeur. Le travail sur le terrain impliquait deux plongeurs : l'un prenant 250 photos benthiques par transect (4187 au total) tous les 3 à 5 mètres, guidé par une boussole, tandis qu'un autre gérait un GPS en surface dans un boitier étanche flottant pour pouvoir géoréférencer les photos ultérieurement (Figure II.2). La durée de la prise de phototransects couvrait environ 30minutes, ce qui représentait une distance d'environ 500m. Cependant dans les zones à fortes courants, le temps passé sous l'eau était réduit entrainant par conséquent une diminution proportionnelle de la longueur des transects. L'équipement de base pour la collecte de photos sous-marines géoréférencées comprend une planche flottante, une boussole, un GPS, une corde, un boîtier étanche (pour protéger le GPS), un appareil photo submersible et une montre (pour estimer la longueur moyenne des transects) (Annexe 3).

Fig.II. 2. Collecte de photos sous-marines géoréférencées

Les photos ont été liées à leur coordonnées GPS respectives avec le logiciel GPS Photo Manager (Roelfsema et al., 2019). La couverture benthique a été extraite de ces photos avec le logiciel Coral Point Count with Excel (CPCe) (Kohler et Gill, 2006). À partir des 4187 photos, 1243 points de contrôle ont été dérivés — 75 % ont été utilisé pour le calibrage du modèle de classification et 25% pour la validation. Le prétraitement des images satellites incluait une correction atmosphérique à l'aide de l'extension sen2cor du programme Sentinel Application Plateform (SNAP) (Louis et al., 2016) et une correction de la colonne d'eau, suivant l' algorithme de Lyzenga (Lyzenga, 1978). L'analyse orientée-objet (OBIA) dans eCognition Developer 10.3 (Trimble Germany GmbH, 2022) a segmenté et classifié les images en zones géomorphologique (récifs internes, lagon, platier récifal, vasques, crête récifal, front récifal, pente récifal) et catégories benthiques (coraux, algues, sables, herbiers, débris), validées par les données de terrain.

Le chapitre 4 examine les changements temporels de la couverture benthique des coraux à Toliara, Madagascar, en utilisant des images Sentinel-2A et des modélisations pour analyser les changements de la couverture benthique et prédire les tendances jusqu'en 2035. Cette étude prolonge les travaux historiques réalisés par Andréfouët et al. (2013), qui analysaient cinquante ans de changements dans le GRT. Cette étude introduit une approche de modélisation à l'aide des modèles CNN et Cellular Automata, permettant d'analyser les changements de la couverture benthique des récifs coralliens entre 2015 et 2024, et d'estimer les dynamiques potentielles de la couverture benthique à l'horizon 2035. Le travail sur le terrain a eu lieu en 2021 (4187 phototransects) et 2024 (2578 phototransects), avec la même méthode à deux plongeurs mentionnée dans le Chapitre 3 : l'un prenant des photos du substrat tous les 3 à 5 mètres, l'autre gérant un GPS en surface. Tous ces phototransects ont été annoté manuellement au programme CPCe et ont ainsi généré au total 6 765 fichiers au format Excel, dont un exemple est donné en Annexe 1. 4405 données similaires ont été collectés au niveau des récifs coralliens dans l'AMP Salary à 80 km au Nord de Toliara. Ces données servent de validation terrain pour les analyses d'images satellitaires, mais également aux études de répartition de la couverture benthique. Elles peuvent également servir pour entrainer d'autres algorithmes de classification automatique d'images. Dix images Sentinel-2A de 2015 à 2024, choisies dans des périodes similaires, un faible couvert nuageux, et des conditions de marée uniformes, ont été prétraitées avec une correction atmosphérique (niveau 2A) et masquées pour exclure les zones non concernées. Les bandes 2, 3, 4 et 8 de chaque image Sentinel-2A (Annexe 2) ont été sélectionnées en raison de leur résolution spatiale élevée et de leur pertinence pour la cartographie des habitats marins. À ces bandes ont été ajoutés deux autres bandes dérivées : l'indice de végétation normalisé (NDVI) (Sentinel Hub, 2025a) et l'indice de végétation amélioré (EVI) (Sentinel Hub, 2025b), afin d'enrichir le contexte spectral de l'image et de mieux caractériser les habitats benthiques. Ces deux indices sont largement utilisés en télédétection pour évaluer la densité et la vigueur de la végétation verte. Un modèle réseau de neurones convolutif (CNN) a donc été appliqué sur cette nouvelle empilement d'image (Bande 2, Bande 3, Bande 4, Bande 8, NDVI, EVI) pour classifier la couverture benthique avec le logiciel eCognition Developer 10.3. Les CNN sont largement appliqués dans les technologies de reconnaissance faciale (Raphael et al., 2020). La reconnaissance faciale est une série de plusieurs étapes liées, commençant par l'analyse de l'image et la recherche de tous les visages, en se concentrant sur chacun d'eux et en comprenant que même si un visage est tourné dans une direction étrange ou dans un mauvais éclairage, il s'agit toujours de la même personne. Les CNN commencent par identifier des caractéristiques simples et petites telles que des lignes et des cercles. Ils les transforment ensuite en caractéristiques plus complexes telles que des yeux et des nez. Enfin, ils regroupent ces caractéristiques pour former des visages complets (Figure.II.3).

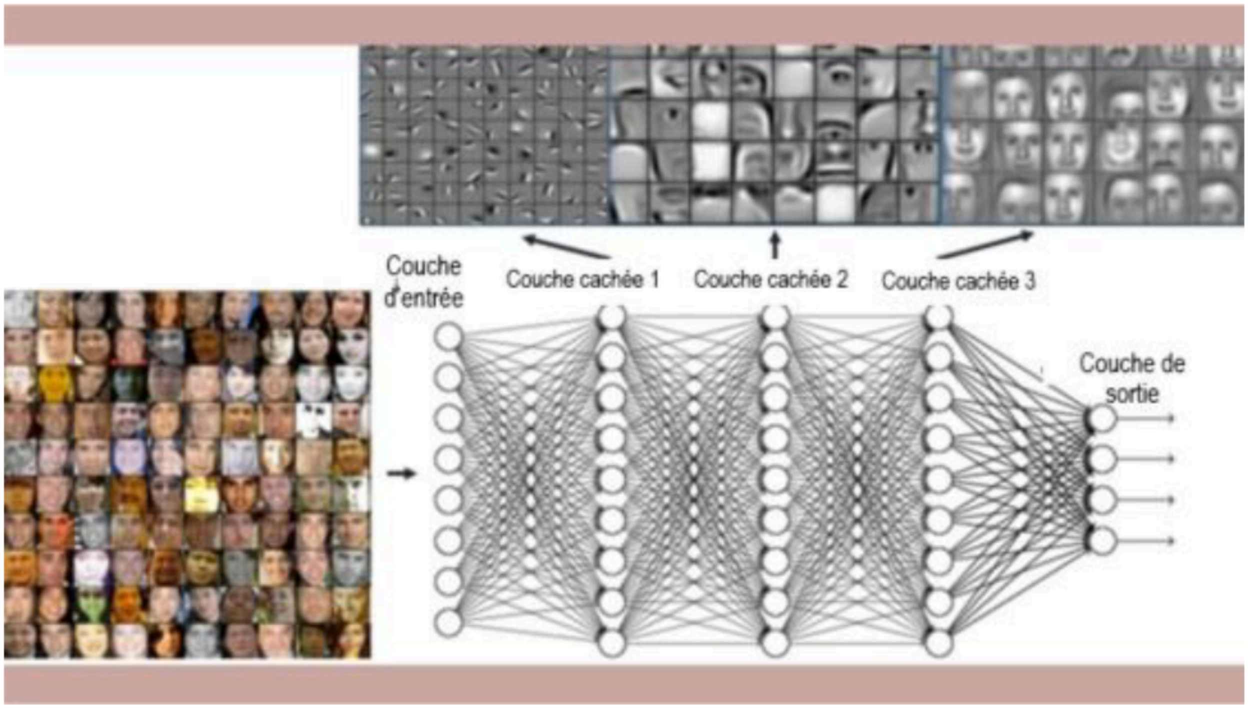

Fig.II. 3. Les réseaux de neurones profonds apprennent des représentations hiérarchiques des caractéristiques. Modifiée à partir de Raphael et al., (2020)

Nous avons utilisé ici les mêmes principes pour évaluer les changements au niveau du GRT entre 2015-2021. Généralement les CNN appliquent des convolutions ou des filtres à une image. Chaque filtre peut répondre à différentes caractéristiques de l'image (Raphael et al., 2020). Les filtres des premières couches du réseau ont tendance à sélectionner les propriétés de bas niveau de l'image d'entrée, y compris la fréquence spatiale, les bords et la couleur. À mesure que nous empilons des couches convolutives supplémentaires, des filtres plus complexes commencent à évoluer. Dans le chapitre 4, le CNN a été optimisé par ajustement itératif des paramètres (Annexe 4). Les données de sortie du CNN ont alimenté l'OBIA pour la segmentation et la classification, validées avec 75 % des données d'entraînement et 25 % des données validation en 2021, et entièrement évaluées avec toutes les données collectées sur le terrain en 2024. La haute précision de la classification sur les images de 2024 a justifié son application sur toute la série temporelle depuis 2015. L'analyse de détection des changements et les prévisions sur 10 ans ont utilisé le modèle Cellular Automata de l'extension MOLUSCE (Modules for Land Use Change Evaluation) dans le logiciel QGIS, intégrant l'effort de pêche (Behivoke et al., 2021), le stress thermique (MODIS Aqua, 2002-2022) et la turbidité (Atlas Coral Atlas) comme facteurs.

Le chapitre 5 développe un cadre basé sur la résilience pour évaluer la santé des récifs coralliens dans la baie de Toliara (Sarodrano, Ankilibe, GRT). Cette étude utilise une Analyse Multi-Critère (MCE - Multi Criteria Evaluation) avec le processus hiérarchique analytique (AHP - Analytical Hierachy Process) et la combinaison linéaire pondérée (WLC) pour cartographier la résilience selon sept facteurs : Abondance de coraux, Abondance de Cadre (Substrat dur, favorable au recrutement coralliens), Zones d'attraction des herbivores (ZAH), Indice de profondeur invariant de Sentinel-2A, Effort de pêche, Stress thermique et Turbidité. La donnée de couverture benthique dans le chapitre 3 a été ici réutilisée. Les facteurs considérés dans cette analyse ont été obtenus de façon suivante :

- « Abondance de coraux » et Abondance de Cadre obtenus à partir des résultats de la classification de la couverture benthique dans le chapitre 3 et les traitements des phototransects au CPCe (Annexe 3) ;
- « Indice de profondeur invariant » calculé à partir de la correction de la colonne d'eau sur l'image Sentinel-2A (Lyzenga, 1978) ;
- « Zone d'attraction des herbivores - ZAH » obtenus à partir des résultats de la classification de la couverture benthique dans le chapitre 3 et des traitements des données de phototransects au CPCe (Annexe 3) ;
- « Effort de pêche » via des pirogues suivies par GPS (Behivoke et al., 2021) ;
- « Turbidité » de l'Allen Coral Atlas (moyenne des fichiers comprises entre 2019-2024) ;
- « Stress thermique » en Degree Heating Weeks (DHW) ou Température de la semaine la plus chaude (calculé à partir des données satellites MODIS Aqua entre 2002-2022 selon la méthodologie proposée par Liu et al. (2014)

Les facteurs ont été standardisés sur une échelle de 0 à 1 avec la logique floue dans le logiciel TerrSet LiberaGIS (Clark Center for Geospatial Analytics-ClarkCGA, 2024), utilisant des fonctions sigmoïdes (décroissantes pour les facteurs de stress, croissantes pour les facteurs positifs). L'AHP a attribué des poids via des comparaisons par paires dans huit scénarios regroupés en priorités de biodiversité (Abondance de coraux), impacts locaux (par exemple, Effort de pêche) et stress globaux (par exemple, Stress thermique). Les ratios de cohérence (<0,1) ont validé les matrices, et le WLC a calculé des indices de résilience, reclassés en cinq niveaux (non résilient à très élevé) et cartographiés dans QGIS. Les résultats ont quantifié les zones de résilience en hectares, identifiant les zones à haute et à faible résilience.

Chapitre 3 : Télédétection des habitats coralliens à Madagascar à l'aide d'imageries Satellitaires accessibles au publique tels Sentinel-2


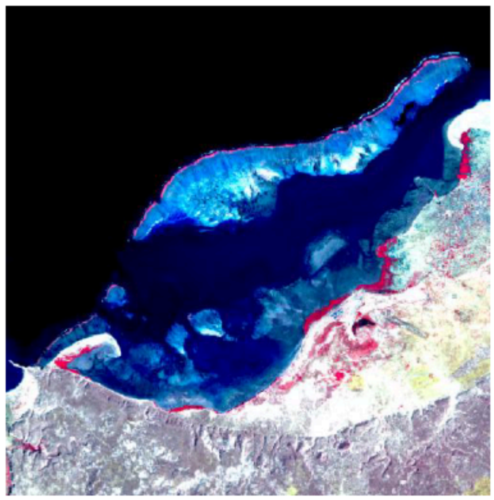
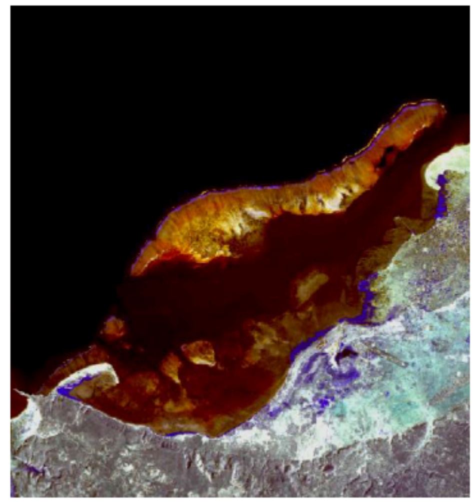

Article publié:

Nomenisoa A.L., Todinanahary G, Edwin HZ, Razakarisoa T, Israel JB, Raseta S, Jaonalison H, Mahafina J, Eeckhaut I, 2024 - Remote sensing of coral reef habitats in Madagascar using Sentinel-2 satellite images. Western Indian Ocean Journal of Marine Science 23(2): 41-56 [doi:10.4314/wiojms.v23i2.4]

Chapitre 3 : Remote sensing of coral reef habitats in Madagascar using publicly-available Sentinel-2 satellite images

Abstract

The study addresses the need for precise spatial data in coral reef management by using Sentinel-2 satellite imagery for coral reef mapping. Focused on the Great Reef of Toliara in Madagascar, it aims to establish standardized methodologies for data collection and processing to monitor reef health and guide sustainable management practices. Fieldwork conducted between March and December 2021 used georeferenced photoquadrats to assess benthic structure. The satellite image classification was based on the Object-Based Image Analysis and machine learning algorithms, with k-NN achieving the highest overall accuracy at 83%, followed by the Bayes classifier, DT, RT, and SVM, with overall accuracy of 79%, 68%, 67%, and 42% respectively. The analysis identified distinct surface areas occupied by seagrass (21 km^2), sand (73 km^2), rubble (21 km^2), coral (10 km^2), and algae (6km^2). Comparative assessment with the Allen Coral Atlas underscored the importance of aligning satellite image analysis with *in-situ* data. The study emphasizes the role of selecting appropriate classifier algorithms for precise mapping and stresses the importance of local data collection for accurate habitat mapping. It also showcases the successful application of OBIA with satellite imagery and field data for coral reef mapping, providing insights into habitat health and spatial changes essential for effective conservation.

***Keywords**: Remote sensing, coral reef, Madagascar, Sentinel-2, OBIA, Machine learning algorithms*

3.1. Introduction

Coral reefs protect shorelines against storms, serve as fish nurseries, and provide socio-economic benefits when associated with tourism and recreation, shoreline protection, fisheries, and biodiversity services (Eakin et al., 2010). However, these ecosystems face significant threats on both global and local scales, primarily due to climate change and anthropogenic pressures (Xu and Zhao, 2014). Nearly half of the world coral reefs have been destroyed or badly damaged in the last 30 years (Wilkinson, 2008). Current trends suggest that between 70 % to 90 % of global coral reefs are at risk of extinction within the foreseeable future (Foo and Asner, 2019), a fate that extends to the reefs of Madagascar as well (Van Hooidonk et al., 2016). Effective management and conservation efforts requires comprehensive monitoring strategies that encompass both spatial and temporal dimensions, focusing on the distribution of species on the benthos as well as their associated substrates (Nurlidiasari, 2004). Such measures require a reliable method that can efficiently process continuous data into manageable spatial units (Kennedy et al., 2021). The European Space Agency (ESA) has made Sentinel-2 images freely available since 2015 (ESA's Sentinel-2 team, 2015) offering a 10 m spatial resolution (pixel size), which significantly enhances the utility of these images for coral reef mapping. Remote sensed mapping of coral reefs is particularly important for developing countries, where 80 % of the world's coral reefs occur (UNEP-WCMC, WorldFish Centre, WRI, TNC, 2021). Therefore, it is critical to determine the efficacy of mapping using freely available satellite images from Sentinel-2 (Hedley et al., 2012, 2018; Wouthuyzen et al., 2019; Yunus et al., 2019). To achieve comprehensive mapping of coral reefs, it is crucial to derive maps of geomorphic zones and benthic communities at various scales (Phinn et al. 2012). Numerous initiatives have been undertaken globally to map coral reefs and understand their distribution, including coral reefs from Madagascar. However, existing datasets, such as those from the United Nations Environment Program-World Conservation Monitoring Centre (UNEP-WCMC) and the Allen Coral Reef Atlas, have limitations such as irregular updates, and unstable accuracy, hindering their applicability in dynamic monitoring. Although efforts to study coral reefs from Madagascar have provided valuable insights, further studies are necessary to fully comprehend these ecosystems and their changing habitats. Efficient and cost-effective methods using remote sensing data are needed to delineate comprehensive reef coverage, geomorphic zoning, and benthic composition in Madagascar. Despite numerous studies on mapping coral reefs, variations in processing schemes, data characterization, and classification methods pose challenges, emphasizing the necessity for a tailored methodology. Therefore, there is a need for a comprehensive methodology tailored to coral reefs from Madagascar, encompassing standardized fieldwork data collection and image processing workflows. This study focuses on the barrier reef in Toliara, commonly known as the 'Grand Récif de Toliara' (GRT), and the reefs of Ankilibe and Sarodrano, where local coral reef geomorphology has been conducted (Pichon, 1972; Battistini et al., 1975; Andréfouët et al., 2013), and several studies focusing on the bio-ecology of coral reefs have been realized (Botosoamananto et al., 2021; Razakandrainy, 2018; Todinanahary, 2016). Undertaking a comprehensive study at the scale of the Toliara region is essential for coral reefs of Madagascar, necessitating standardized methodologies for future data collection and processing. The primary aim of this research was to develop a methodology for coral reef mapping in Madagascar, using freely accessible satellite imagery and advanced remote sensing techniques. Specifically, the study aimed to assess geomorphic zonation and benthic coverage along the barrier reef and fringing reefs of Toliara, using Object-Based Image Analysis (OBIA) applied to Sentinel-2 satellite data, alongside fieldwork data acquisition. This study seeks to establish a foundational understanding of nearshore benthic communities in Madagascar, serving as a vital resource for marine scientists to effectively track ecosystem changes. Furthermore, it aims to furnish policymakers with essential data for monitoring the health of these reefs and formulating sustainable management strategies over the long term.

3.2. Materials and methods

3.2.1. Study area, field data collection and processing

The study was carried out within the Bay of Toliara, and was focused on the fringing reef of Sarodrano, the fringing reef of Ankilibe, and the barrier reef of Toliara (Figure III.1). The selection of these sites was based on several factors: (1) accessibility, (2) ecological variability, encompassing both degraded and healthy areas to facilitate the discernment of local stressors, and (3) ecological complexity, given the co-existence of a barrier reef, a fringing reef, and patch reefs within the same coral reef system. Fieldwork was conducted between March and December 2021, during low spring tides to optimize the time available for in-water surveying. It consisted of collecting georeferenced photoquadrats (in-water images) along transect lines (Figure III.1).

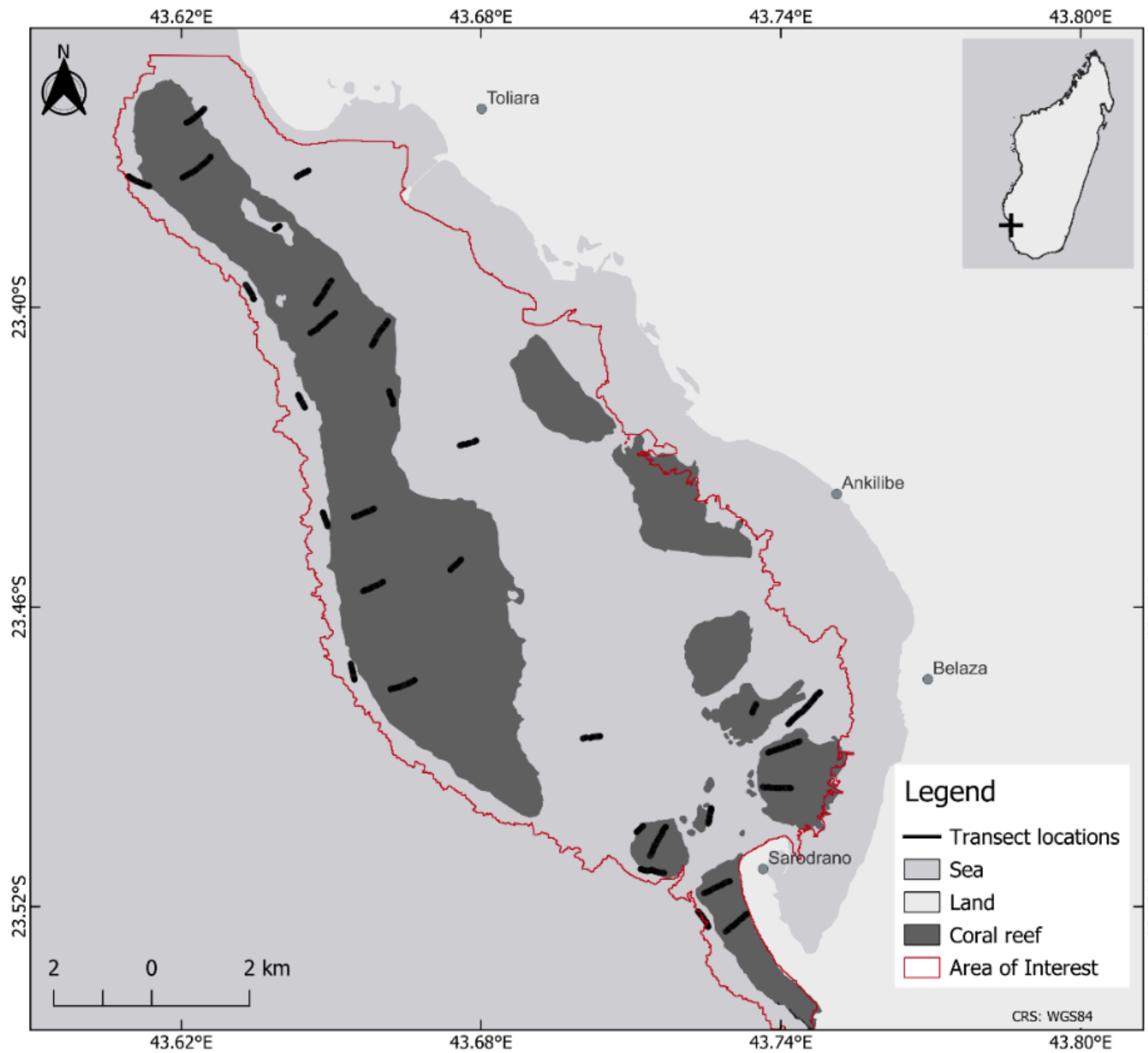

Fig.III. 1.Study area showing the placement of transect lines. The red line outlines the area of interest, indicating the boundary for satellite image clipping. The map distinguishes between land, sea, coral reef, and key areas of interest, with transect locations marked by black lines.

Due to the limitation of GPS signal penetration underwater, the GPS device was secured in a floating airtight bag at the surface. This device was programmed to record new geographic positions every second. Specifically, one diver captured benthic images every 3-5 meters, guided by a compass to maintain course, while a second diver at the surface maneuvered the GPS-containing bag, moving in synchronization with the diver below (Figure III.2). Each dive averaged 30 minutes, covering approximately 500 meters of transect where current conditions allowed; however, in instances of stronger currents, transects were shortened accordingly. Initial and final GPS coordinates of each transect were logged on a diving slate to facilitate subsequent GPS data integration. Approximately 250 photos were collected per transect, totaling 4187 photos across the 30 transects. Ground-truthing data collection was confined to depths shallower than 20 meters. Subsequently, the photos were linked to GPS data to assign specific geographic positions to each photoquadrat using the software GPS Photo Manager (Roelfsema et al., 2019). This integration facilitated the visualization of photos and associated benthic attributes within a Geographic Information System (GIS) interface. All the GIS operations in this study were performed using the QGIS software, version 3.34.

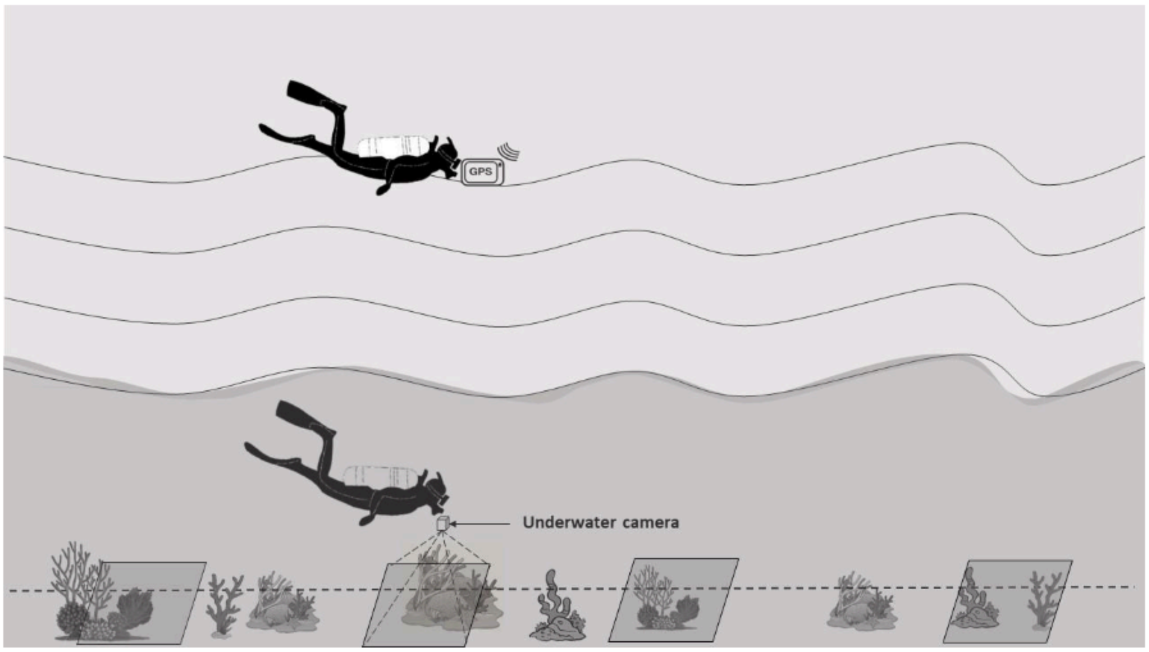

Fig.III. 2. Method of photoquadrats data collection. A surface diver uses a GPS to record the geographical coordinates of the transect path. Simultaneously, a second diver takes photographs of the benthic substrate using an underwater camera. The camera is set to collect images covering a surface of 1m x 1m size. These images will be later linked with the GPS data in order to enable subsequent analysis of the composition and coverage of the benthic communities.

3.2.2. Assessment of benthic cover from geotagged photos

Benthic cover within the transect lines was obtained from each geotagged photo by analyzing photoquadrats using the Coral Point Count with Excel extension (CPCe) software (Kohler and Gill, 2006). A total of 49 stratified points were distributed on each photo and the substrates corresponding to these points were identified using a predefined code name "CPCe benthic codes 41 Madagascar" provided with the software (Figure III.3). Based on their knowledge and the 41

CPCe benthic codes, the users attributed specific classes to each of the 49 stratified points. This number of stratified points per photoquadrat was sufficient to identify down to the level of benthic habitat classes. The benthic cover of the photoquadrat was then automatically estimated by the software as a function of the number of points occupied by each category of substrate. Once the analysis was finished, the software exported the data in an Excel file.

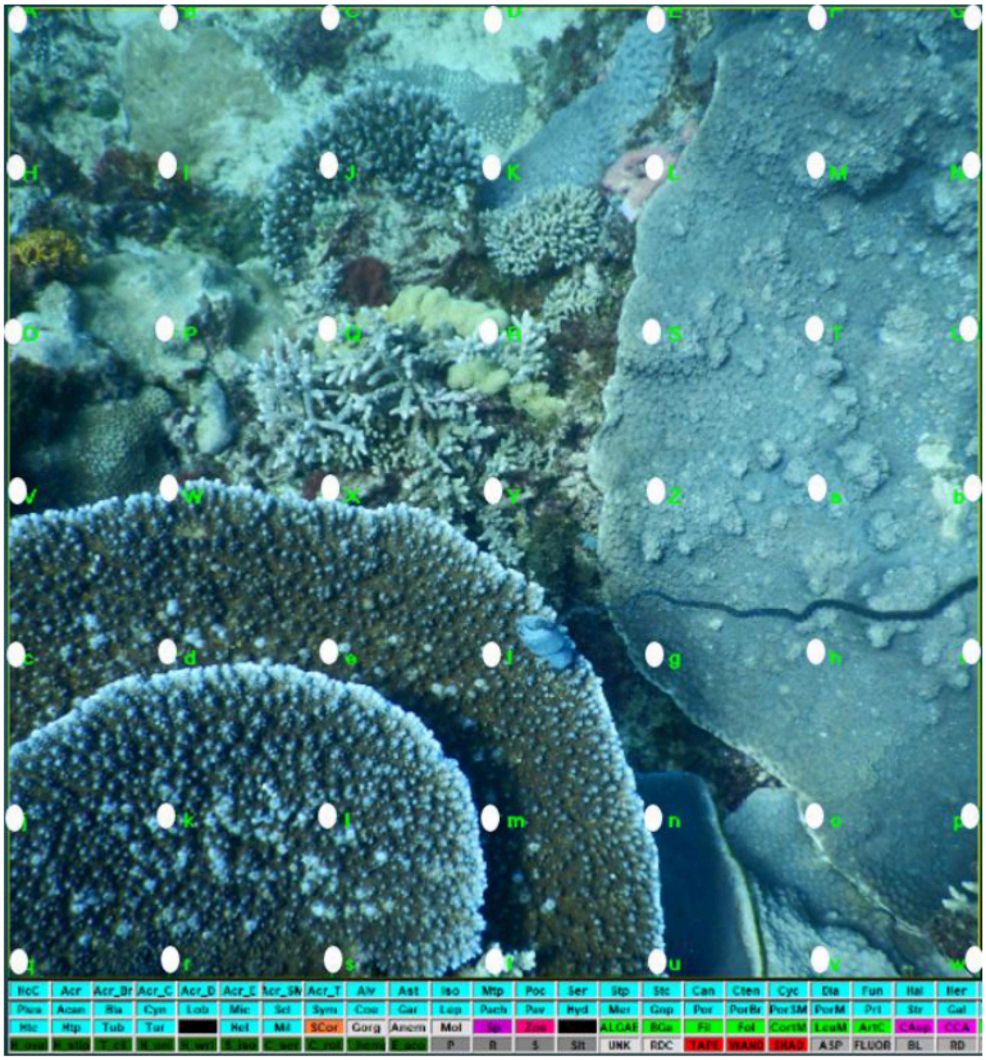

Fig.III. 3. 49 stratified points (7 points per lines) on CPCE. The image displays a benthic photoquadrat (1m x1m size) analyzed using the Coral Point Count with Excel extensions (CPCE) software. A total of 49 points are systematically overlaid in a 7×7 grid to facilitate consistent assessment of benthic cover. Each point is manually identified and classified according to the benthic category beneath it.

3.2.3. Conversion of the CPCE data into calibration and validation sample points

The data points produced by the CPCe software spans a 1x1 meter area, whereas the pixel size of a Sentinel-2 image measures 10 meters by 10 meters. To ensure comparability between CPCe data points and Sentinel-2 pixels, the 41 benthic CPCe codes were refined into five classes: Coral (i.e., live corals), Algae, Rubbles, Sand, and Seagrass. These data points were the overlaid onto Sentinel-2 image layer. A new sample was then manually created and assigned a pixel category based on the predominant benthic cover depicted in the CPCe data pie chart (Figure III.4). From the 4187 photos, 1243 control points were derived, where 75 % were used for calibrating the machine learning algorithms to classify the satellite image, while the remaining 25 % served as validation points to assess their accuracy.

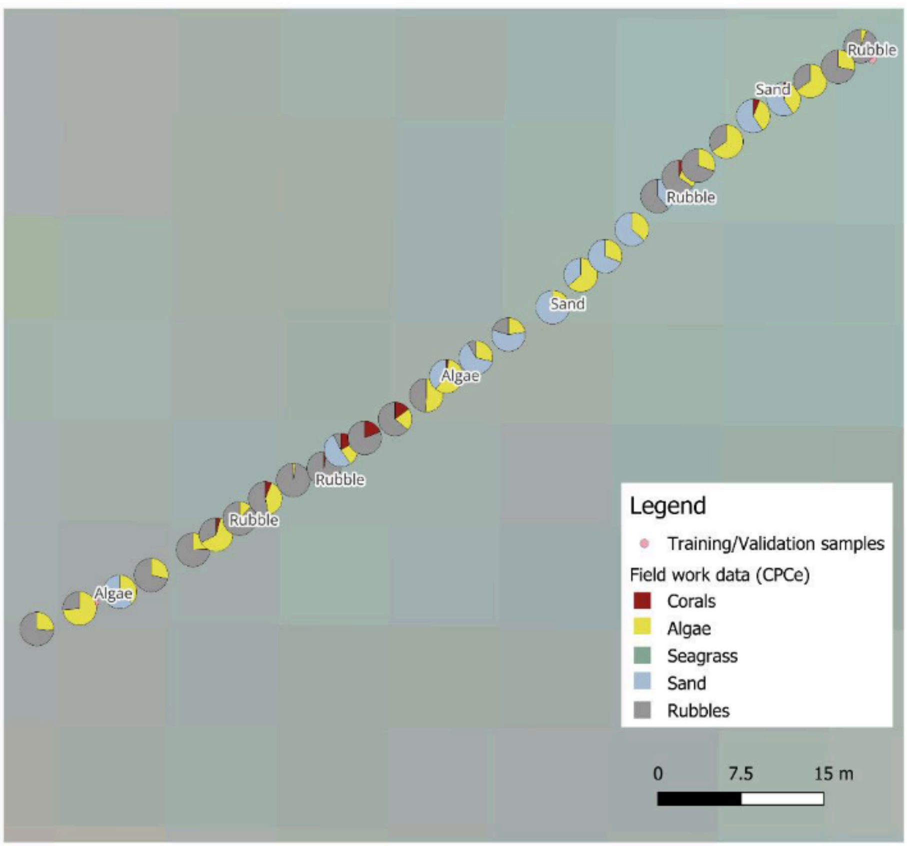

Fig.III. 4. Example of a transect line composed by field work data. The spatial distribution of field data collected using the CPCE method is overlaid on a classified habitat map. Each pie chart represents the relative benthic cover (corals, algae, seagrass, sand, and rubble) at individual photoquadrat locations.

3.2.4. Satellite image processing

3.2.4.1. Pre-processing

Sentinel-2A data were accessed from the Copernicus server (https://scihub.copernicus.eu/dhus/#/home). The Sentinel-2A image collected on 21-08-2021 was used in this study (Tableau III.1). The Sentinel-2 satellite was launched in 2015 and offers 10 m spatial resolution for the visible and the Near Infra-Red (NIR) bands (ESA's Sentinel-2 team, 2015). The most appropriate images for coral reef habitat mapping are those that contain the least cloud cover and sun glint and are acquired during the spring low tide period. This last requirement is crucial in the analyses as the characterization of the benthos is complicated especially when they are submerged in the water column. The raw downloaded Sentinel-2 image was first corrected for the effect of the atmosphere. For this correction, the sen2cor atmospheric Correction Processor algorithm was used from the SNAP software or Sentinel Application Platform (Louis et al., 2016). This approach consisted of transforming the Level-1C image (surface reflectance measured at the top of the atmosphere) into Level-2A (bottom-of-atmosphere reflectance). Next, as the benthos was submerged underwater, the water column effect needed to be corrected. The water column correction algorithm of Lyzenga (1981) was used for this purpose. This was processed using the sen2coral module of the SNAP software. As a result, three bands of the depth invariant index (DII) were generated, each composed of different combinations of spectral bands (Tableau 2): blue and green (DII_ B2B3), blue and red (DII_B2B4), and green and red (DII_B3B4). Additionally, the Normalized Difference Vegetation Index (NDVI) was computed (Zoffoli et al., 2020). These newly generated layers were added to the atmospheric corrected image for the geomorphic and benthic image classification.

Tab.III. 1. Sentinel-2 image specification used in this study

Name	**Sentinel-2A**			
Correction level	Level 1C			
Date of acquisition	21-08-2021			
Radiometric resolution	12 bit/pixel			
Swath width	290 km at nadir			
Multispectral Bands	Band number	Spectral Bands	Central wavelength (nm)	Spatial resolution (m)
	1	Coastal Aerosol	442.7	60
	2	Blue	492.7	10
	3	Green	559.8	10
	4	Red	664.6	10
	5	Vegetation Red Edge	704.1	20
	6	Vegetation Red-Edge	740.5	20
	7	Vegetation Red-Edge	782.8	20
	8	Near Infra-Red (NIR)	832.8	10
	8A	Narrow NIR	864.7	20
	9	Water vapor	945.1	60
	10	Short Wave Infra-Red (SWIR)-Cirrus	1373.5	60
	11	Short Wave Infra-Red (SWIR)	1613.7	20
	12	Short Wave Infra-Red (SWIR)	2202.4	20

3.2.4.2. Image classification

Coral reef habitat classification serves as an important tool for surveying and understanding these marine ecosystems. The process involves leveraging raw input data—such as videos or images—captured from coral sites (Nguyen et al., 2021). Through this data, distinctive features of the seabed, referred to as classes, are extracted and categorized, including corals, sands, rubbles, seagrass, etc. To undertake this mapping, there are two approaches used: manual extraction of features, which offers high accuracy but is laborious and time-intensive, or the use of machine-learning algorithms for rapid processing and replicability, albeit with a potential risk of misclassification. While manual methods ensure precision, the advent of machine learning presents an efficient alternative, albeit with a need for careful validation and refinement to minimize errors in classification. For this, the OBIA method (Object-Based Image Analysis) was applied using eCognition Developer Software version 10.3 (Trimble Germany GmbH, 2022). This approach consists of grouping similar pixels (form, colour, texture, etc.) into segments (Figure III.5), and then attributing classes to those segments (Hedley et al., 2016).

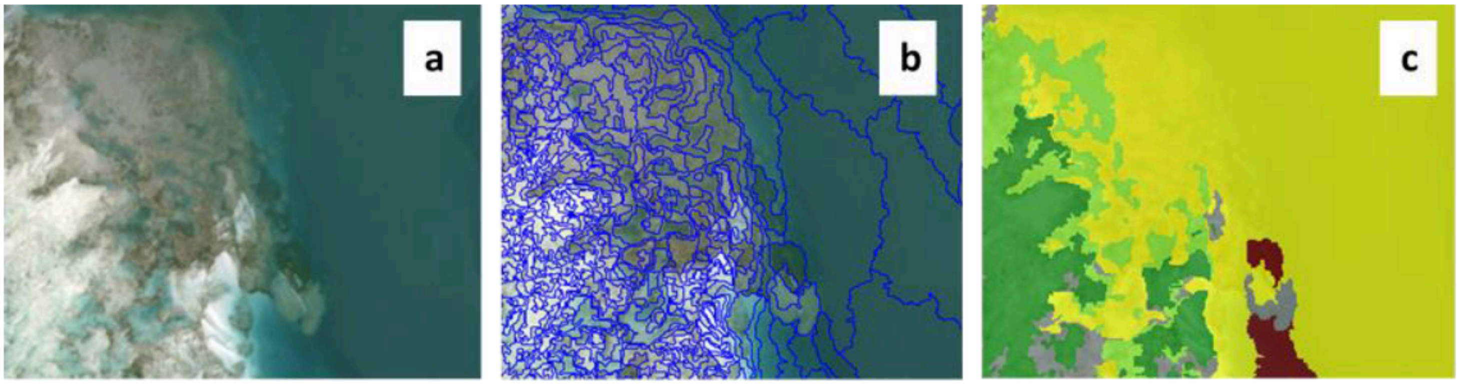

Fig.III. 5. Object Based image analysis (OBIA) process. a) Acquired image, b) Image segmentation, c) Image classification

Geomorphic zonation

The concept of geomorphic zonation in coral reefs involves identifying features that are relatively stable over time. In this study, the extraction of several key geomorphic features was focused on, including Internal Reefs, Lagoon, Reef Flat, Enclosed Basins, Reef Crest, Reef Front, and Reef Slope, following the definitions provided by Battistini et al. (1975). A lagoon is a naturally occurring depression with varying depths and sizes, typically found either behind a barrier reef or completely enclosed by reef structures. Enclosed basins, on the other hand, are smaller, shallower depressions or pools nestled within the reef structure on the reef flat. The reef slope constitutes the submerged front portion of a reef, sloping seaward with differing inclinations. It comprises coral formations and sedimentary deposits primarily of biogenic origin. The reef front delineates the outer edge of the reef flat at low tide, particularly during spring tides. Meanwhile, the reef flat is a horizontally oriented platform atop a reef structure, often reaching or surpassing sea level. It may exhibit material accumulations and surface incisions. The reef crest is primarily composed of coarse elements and is situated on the anterior part of the reef flat, manifesting in various shapes such as domes, ramparts, or scattered accumulations. Internal reefs are positioned within a lagoon, frequently separated from the open ocean by a barrier reef. They exhibit diverse sizes and shapes and are typically surrounded by shallow lagoon waters. These internal reefs consist of lagoonal coral patches, some of which extend to the surface and larger lagoon reefs, which are substantial coral formations within the lagoon, either partially exposed or submerged. These larger formations often display distinctive zoning patterns akin to those observed on reef flats. After the image segmentation, these features were extracted by the visual photo-interpretation method using the built-in manual classification tools within the Ecognition Developer software.

Benthic image classification

For this purpose, the processed satellite image comprised: (i) the 10-meter resolution spectral bands from Sentinel-2 images (Table 1) which were atmospherically corrected, (ii) the calculated depth invariant bottom indexes (DII_B2B3, DII_B2B4, DII_B3B4), and (iii) the NDVI layer. Several satellite imageries, classification techniques, typologies and machine learning algorithms have been globally adopted to gather data on benthic coverage of coral reefs (Burns et al., 2022). However, determining the most effective approach presents challenges due to inconsistencies in various factors, including the spectral and spatial resolutions of satellite images, methodologies for in situ reference data collection, the diversity and quantity of benthic classes mapped, and protocols for accuracy assessment. In this study, five prominent machine learning classifiers commonly employed in mapping coral reef benthic habitats were assessed with the goal of identifying the best performer tailored to environmental conditions, fieldwork data characteristics, and the particular benthic classes under study. These findings will inform future investigations, guiding parameter choices, and streamlining classification processes, minimizing trial-and-error efforts. The five machine learning classifiers were: Support Vector Machine (SVM). This assigns class labels to segmented objects by determining an optimal hyperplane, guided by feature vectors extracted from objects' attributes such as spectral values, texture, and spatial relationships. This hyperplane maximizes the margin between classes while minimizing misclassifications, with a focus on support vectors to define the boundary effectively (Mountrakis et al., 2011). Decision Tree (DT). The DT algorithm recursively partitions the dataset into subsets based on feature conditions, constructing a tree where each internal node represents a feature test and each leaf node denotes a class label. It employs a divide-and-conquer approach to classify instances, following a path from the root to a leaf node determined by feature conditions (Dietterich, 2000). Random Trees (RT). This is a combination of multiple tree-based classifiers to produce a single classification, an ensemble of decision trees, where each single tree contributes a vote for the assignment of the most popular class to the input data (Xie and Niculescu, 2021). k-Nearest

Neighbour (k-NN). The k-NN algorithm classifies segmented objects based on the class most represented by their k nearest neighbours. K is a user-defined parameter that is the number of nearest neighbouring objects that are included in the majority voting process (Burns et al., 2022). The Bayesian algorithm assigns classes to segmented objects by calculating the probability of each class given the object's features. It uses Bayes' theorem to compute the conditional probability of each class, incorporating prior knowledge and assuming feature independence to make informed decisions (Lewis, 1998). The flow chart of the image processing is provided in Figure III.6.

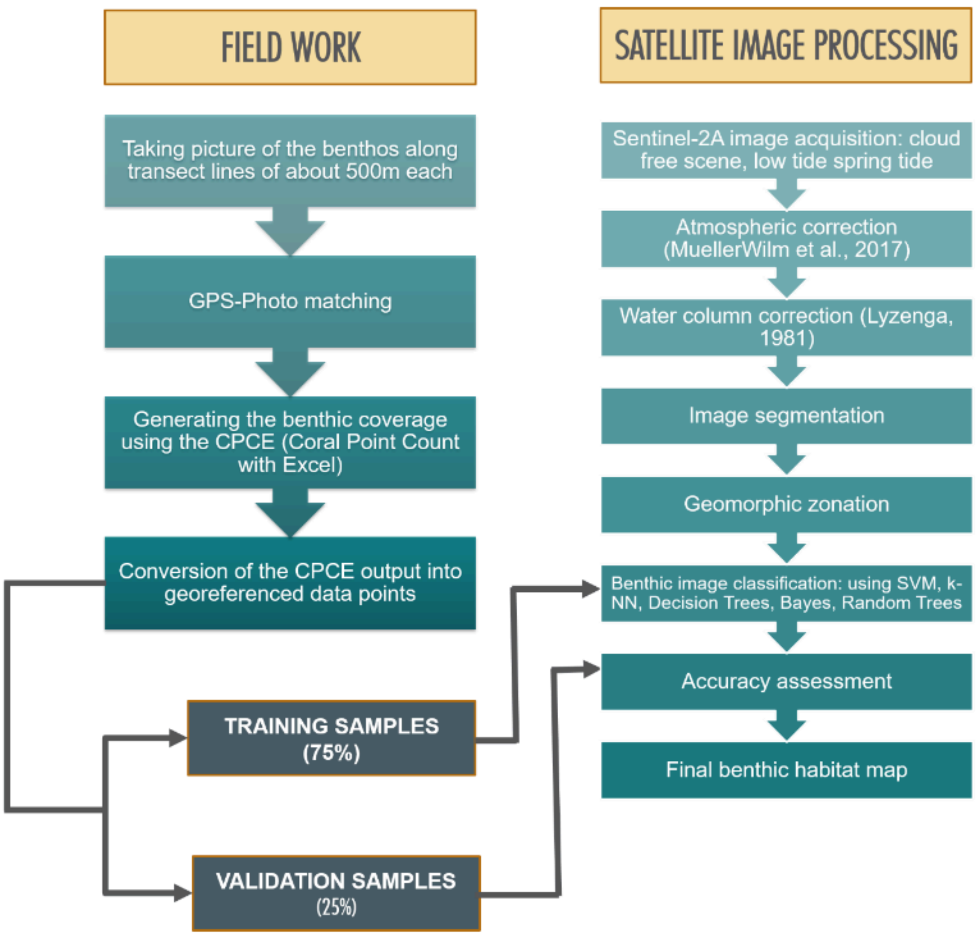

Fig.III. 6. Image processing workflow. The left panel outlines field work steps including photo acquisition, GPS matching, and benthic coverage assessment using CPCE (Coral Point Count with Excel), culminating in the generation of georeferenced data points. The right panel outlines satellite image processing using Sentinel-2A data. 75% of the samples are used to train the machine learning classifiers (SVM, k-NN, Decision Trees, Bayes, and Random Trees) in order to generate a benthic image classification, while the remaining 25% are used to assess the accuracy of the classification and for post-classification.

Benthic class description

The coral class (Figure III.7a) refers to a category with a hard underlying framework that is typically composed of coral-derived limestone, although non-carbonate materials can also be present. This class includes living corals. The rubble class (Figure III.7b) pertains to any area featuring loose, cylindrical to irregularly shaped fragments of bedrock or clasts of corals, bivalves, and coralline algae. This category encompasses limestone reef matrix and underlying areas of coral sand cemented together. The macroalgae class (Figure III.7c) is composed of large, multicellular marine plants that typically thrive in shallow waters surrounding coral reefs. Macroalgae are often observed on top of dead corals, in areas with clear water and abundant sunlight. The seagrass class (Figure III.7d) pertains to a soft-bottomed environment that is mainly characterized by the prevalence of a single or a combination of different species of seagrass. This classification also encompasses sparser or spatially confined seagrass as long as it forms the dominant benthic class. The sand class (Figure III.7e) pertains to soft-bottomed reef regions where fine unconsolidated granular material prevails. This granular material is finer than coral rubble but coarser than mud and thickly overlays any underlying bedrock. Sparse algae, scattered rocks, or small, isolated coral heads may also occur in the sand class. This class also encapsulates areas that are covered by a layer of fine-grained sediment that is mostly composed of organic matter and inorganic particles.

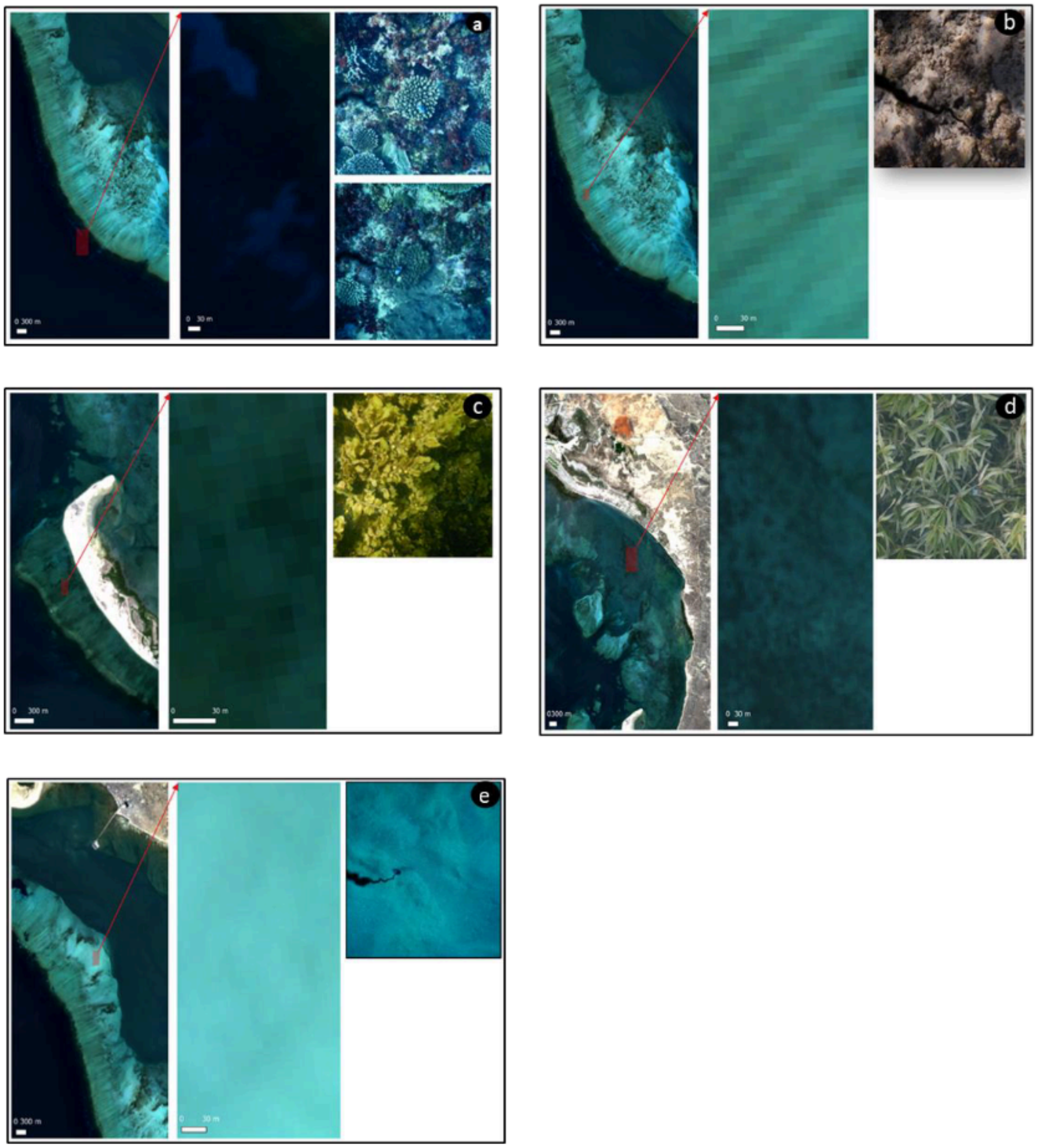

Fig.III. 7. Examples of benthic classes across multiple scales: 300m, 30m, and 1m Above the Substrate. (a) Coral, (b) Rubbles, (c) Algae, (d) Seagrass, (e) Sand

3.2.5. Accuracy assessment of the benthic habitat mapping

The validity, or usefulness, of any interpretation or classification map may be determined with an accuracy assessment that compares the created map with the field work data (Yamano, 2013). Accuracy assessment is commonly derived using an error matrix (also called confusion matrix), which tabulates the level of agreement between the thematic class at a location in the image-based map and the same location in the reference data (Yamano, 2013). The accuracy of each mapping category is described by the individual class accuracies, or according to the user's accuracy (UA) and producer's accuracies (PA) and Overall accuracy (OA), which are all derived from the error matrix. This is generated by using the built-in accuracy assessment tool in the eCognition Developer software. These metrics adhere to the definitions provided by Congalton and Green (2008). OA focuses on assessing the general performance of a classification algorithm across all classes in a dataset. It provides a holistic measure of the classifier's accuracy by considering all classes simultaneously. PA represents the proportion of correctly classified pixels or features for a specific class in relation to the total number of pixels or features that belong to that class on the ground. It focuses on how accurately the algorithm identifies and maps the pixels or features that truly belong to a specific class on the ground. UA represents the proportion of correctly classified pixels or features for a specific class in relation to the total number of pixels or features classified as that class by the classifier. It focuses on how accurately the algorithm assigns pixels or features to a particular class, regardless of whether they truly belong to that class or not. Five classifier algorithms (SVM, DT, RT, Bayes, k-NN) were executed on the image and their accuracy evaluated. Using the classifier algorithm that demonstrated the highest overall accuracy, the benthic classification outcome was refined by merging similar classes and eliminating small misclassified objects, thus improving the clarity and coherence of the final result.

3.2.6. Accuracy assessment of the Allen Coral Atlas

To assess the effectiveness of the benthic cover results for the reefs surrounding Toliara, a comparison with vector data from the Allen Coral Reef Atlas (ACA) (https://allencoralatlas.org) was conducted, acquired in August 2021. This data was cropped to match the scale of the current study, enabling meaningful comparisons. The ACA has the great advantage that it covers reefs around the world, so it is easy to refer to this atlas for a first approximation of benthic coverage of coastal and reef habitats (Allen Coral Atlas, 2020). Andréfouët (2008) mentioned the necessity of alignment of the extent of the ground truth data with the spatial resolution of the sensors. For a meaningful multi-sensor comparison accompanied by objective accuracy assessment, it is imperative that ground truth observations and typology align with the spatial resolution of the sensors. Given this, the raw CPCe data from this study, derived from 1 m x 1 m photoquadrat (with new pictures captured every 3-5 meters), offers a suitable basis for evaluating the accuracy of the ACA data rather than the readapted training and validation data (Figure 10) that was used to match with the pixel size of the Sentinel-2 image. The ACA data is sourced from Planet Dove satellite images, a commercial satellite that provides a spatial resolution of 3-5meters (Safyan, 2020). The benthic cover of the reefs of the ACA was composed by 6 categories: “Coral/Algae”, “Microalgal Mats”, “Rock”, “Rubble”, “Sand”, and “Seagrass”. To facilitate this comparison, the field work dataset was reorganized to mirror the typology of the ACA for the accuracy assessment. Specifically, classes such as “Coral” were changed to “Coral/Algae” and “Algae” to “Coral/Algae” in order to align with the ACA data. Classes such as “Rock” and “Microalgal mats” were also removed, as they were absent in the typology of raw data from the current study. However, classes like “Seagrass”, “Sand”, and “Rubbles” remained unaltered to maintain consistency across datasets.

3.3. Results

3.3.1. Accuracy of the image classifications

The overall accuracies of the classifier algorithms used for classifying benthic habitats of coral reefs in Toliara are depicted in Figure III.14. The k-NN algorithm showed the highest Overall Accuracy (OA) at 83 %, followed by the Bayes classifier, DT, RT, and SVM, with OA values of 79 %, 68 %, 67 %, and 42 % respectively. Tableau III.2 provides an analysis of classifier performance in categorizing various benthic habitat samples. It highlights the challenges faced by the Support Vector Machine (SVM) algorithm in accurately classifying Algae and Seagrass samples, with low values of Producer’s Accuracy (PA) and User’s Accuracy (UA). Other classifiers, such as Naive Bayes, DT, k-NN, RT, showed more robust performance. Naive Bayes and DT achieved high PA values for Rubble and Seagrass, respectively, while k-NN demonstrated effectiveness in identifying Coral and Algae habitats. RF performed well in classifying Algae and Sand but struggled with Seagrass. In contrast, SVM struggled with Algae and Seagrass classification, with notably low PA values across multiple classes and variable UA values.

Tab.III. 2. Confusion matrix of the five classifiers algorithms from the present study. OA is the Overall Accuracy. PA is the Producer's Accuracy and UA is the User's Accuracy. Marked in grey are the cells where map and reference data classifications correspond.

Classifier Algorithm	User Class \ Sample	Algae	Coral	Rubble	Sand	Seagrass
Bayes OA = 79%	Algae	9	0	0	0	0
	Coral	0	6	0	0	0
	Rubble	2	0	23	5	3
	Sand	1	0	1	20	2
	Seagrass	0	0	2	6	23
	PA	0,75	1	0,88	0,65	0,82
	UA	1	1	0,70	0,83	0,74
DT OA = 68%	User Class \ Sample	Algae	Coral	Rubble	Sand	Seagrass
	Algae	9	0	2	1	5
	Coral	0	6	0	0	0
	Rubble	0	0	22	7	9
	Sand	3	0	1	23	4
	Seagrass	0	0	1	0	10
	PA	0,75	1	0,85	0,74	0,36
	UA	0,53	1	0,58	0,74	0,91
KNN OA = 83%	User Class \ Sample	Algae	Coral	Rubble	Sand	Seagrass
	Algae	11	0	2	2	2
	Coral	0	6	0	0	0
	Rubble	0	0	19	1	1
	Sand	1	0	4	28	3
	Seagrass	0	0	1	0	22
	PA	0,92	1	0,73	0,90	0,79
	UA	0,65	1	0,90	0,78	0,96
RT OA = 67%	User Class \ Sample	Algae	Coral	Rubble	Sand	Seagrass
	Algae	10	0	3	2	3
	Coral	0	6	0	0	0
	Rubble	0	0	16	6	6
	Sand	2	0	4	23	5
	Seagrass	0	0	3	0	14
	PA	0,83	1	0,62	0,74	0,50
	UA	0,56	1	0,57	0,68	0,82
SVM OA = 42%	User Class \ Sample	Algae	Coral	Rubble	Sand	Seagrass
	Algae	0	0	0	0	0
	Coral	3	6	0	2	0
	Rubble	4	0	12	1	0
	Sand	4	0	2	9	12
	Seagrass	1	0	12	19	16
	PA	0	1	0,46	0,29	0,57
	UA	undefined	0,55	0,71	0,33	0,33

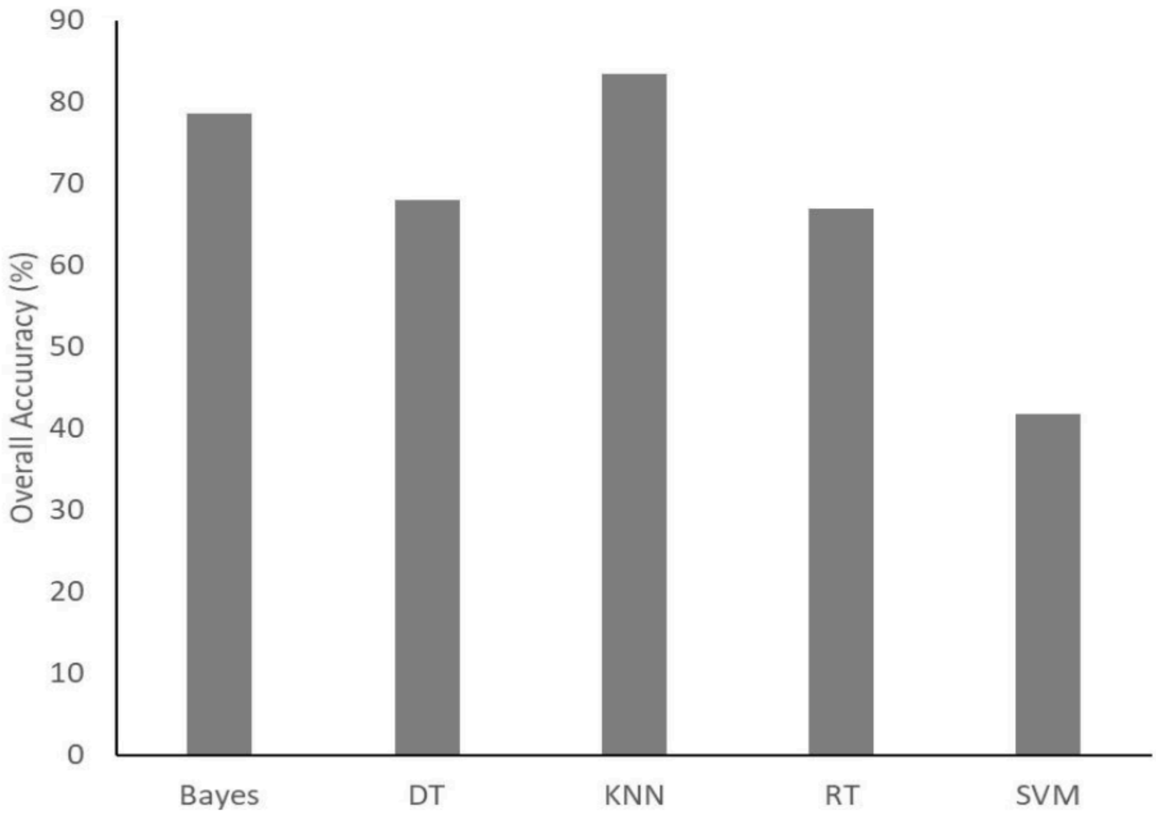

Fig.III. 8. Overall accuracies of the classifiers algorithms used for benthic image classification

Compared to other classifiers evaluated in this study (Figure III.8), SVM exhibited lower OA, UA and PA for most habitat classes, indicating its potentially unsuitability for benthic habitat mapping applications under the given data calibration types and benthic environment. Figure III.9 depicts various outputs of benthic habitat classification, highlighting the variability in results despite employing identical calibration data and image pre-processing techniques. This shows the importance of selecting the appropriate classifier algorithm, as it profoundly impacts the outcomes of benthic coverage assessment and the precise evaluation of each benthic habitat's surface area. In reference to ACA, Tableau III.3 presents the outcome of the accuracy assessment for its benthic coverage data.

Tab.III. 3. Confusion matrix of the benthic coverage of the Allen Coral Atlas

Overall Accuracy = 50%	Coral/Algae	Rubble	Sand	Seagrass
Coral/Algae	596	35	155	54
Rubble	181	617	408	281
Sand	2	53	180	15
Seagrass	206	140	103	241
User accuracy (%)	0.6	0.7	0.2	0.4
Producer accuracy (%)	0.7	0.4	0.7	0.3

Compared with the 4187 CPCe data, the ACA achieves an overall accuracy of 50 %, failing to meet the 60 % minimum standard outlined in Yamano (2013). Additionally, a very low overall accuracy (OA) and user accuracy (UA) was noticed across all classes, particularly for rubbles and seagrass habitats.

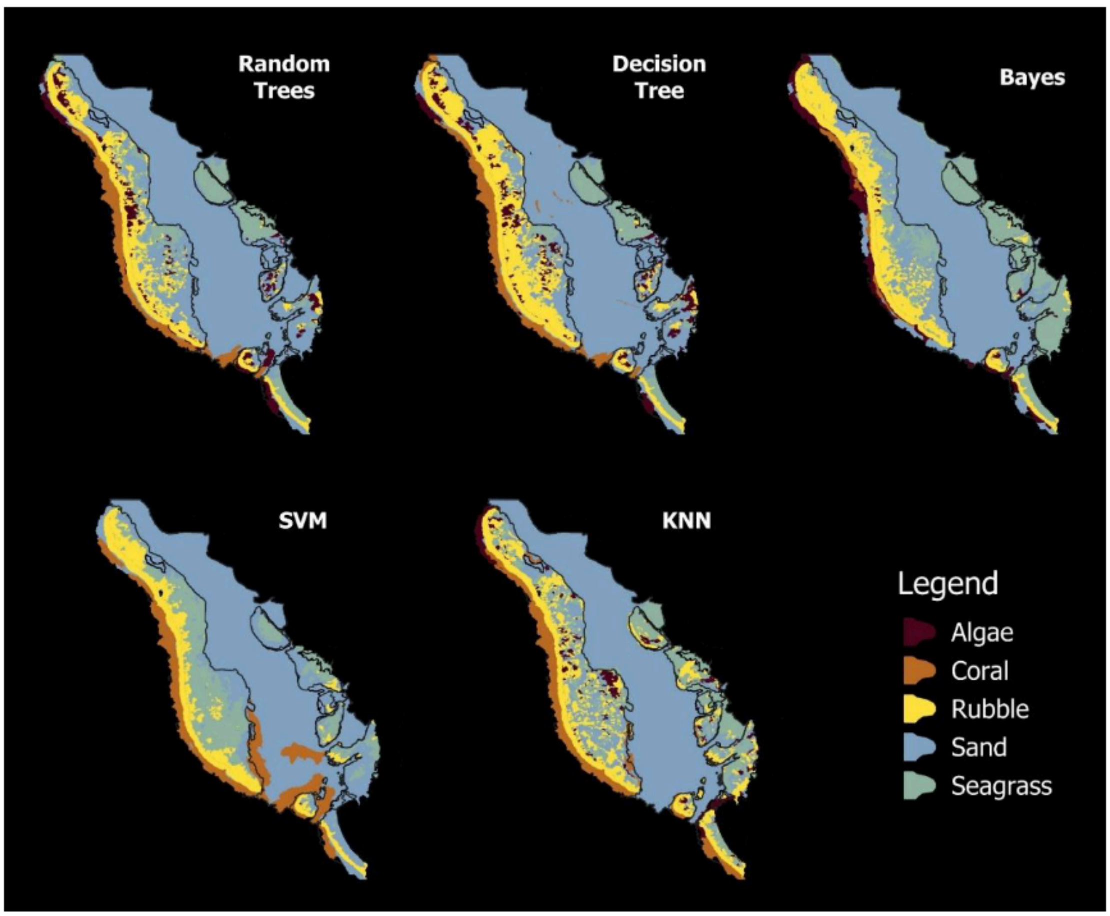

Fig.III. 9. Outputs of the classifiers machine learning algorithms to map benthic coverage of Toliara's coral reefs

3.3.2. Benthic coverage extent of the reefs of Toliara

The benthic coverage of the Toliara reefs was evaluated by using the k-NN classifier, which demonstrated the highest accuracy compared to the four other algorithms. Each habitat type is categorized based on its location within the reef system (Figure III.10). The internal reefs, along with their associated habitats, primarily span the area between Ankilibe and Sarodrano, as illustrated in Fig. 12c. The surface area measurements are presented for five benthic classes: Rubble (21 km^2), Coral (10 km^2), Algae (6 km^2), Seagrass (22 km^2), and Sand (73 km^2). Internal reefs exhibit substantial surface area coverage, particularly for Seagrass (8 km^2) and Rubble (4 km^2). Coral and Algae also contribute significantly to the internal reef ecosystem, with surface areas of 0.4 km^2 and 1.46 km^2 respectively. The Lagoon habitat features smaller surface areas compared to internal reefs. Notably, Sand is the predominant substrate in the lagoon, covering a substantial area of 57 km2. Unlike Rubble (0.4 km^2), Coral (0.3 km^2) and Algae (0.5 km^2) that represent less significant surface coverage, Seagrass emerges as the next dominant feature in this habitat type, spanning an area of 5 km^2 indicating its importance as a habitat within the lagoon environment. Reef flat habitats showcase considerable surface area coverage, particularly for Seagrass (8 km2) and Rubble (11 km^2) and Sand (12 km^2). Enclosed basin habitats exhibit relatively smaller surface area coverage compared to other habitat types. Sand dominates this habitat type, covering 0.2 km^2, while Coral (0.04 km^2), Algae (0.004 km^2) and Seagrass (0.006 km^2) habitats exhibit minor surface area coverage. Both Reef Crest and Reef Front habitats exhibit minimal surface area coverage for all habitat classes, indicating their relatively limited extent within the reef system. These habitats are predominantly composed of Rubble which both represents about 3 km^2. Reef slope habitats demonstrate unique characteristics with significant surface area coverage for Coral (8 km^2). Algae (1 km^2) and Sand (0.5 km^2) classes also exhibit notable coverage, while Seagrass (0.017 km^2) and Rubble classes are present in smaller amounts.

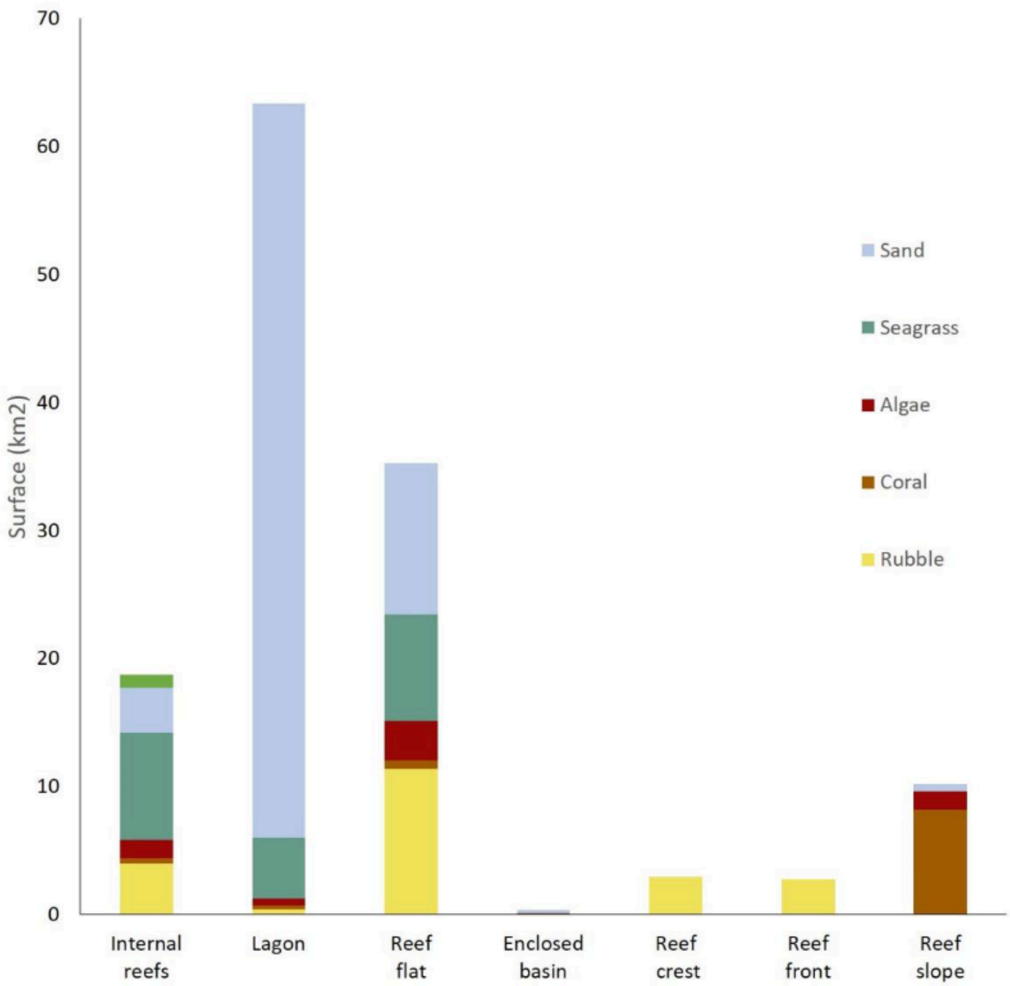

Fig.III. 10. Surface of coral benthic cover per reef geomorphology

3.4. Discussion

3.4.1. Evaluating global coral reef mapping initiatives

Recent initiatives aimed at enhancing global coral reef mapping, such as the Allen Coral Atlas (Allen Coral Atlas, 2020) and the Global Distribution of Coral Reefs (UNEP-WCMC, WorldFish Centre, WRI, TNC, 2021) provide publicly accessible datasets facilitating easy access to information on coral reef geomorphology and benthic coverage. However, caution is warranted when using such data for national coral reef management strategies, restoration programmes, or economic valuations of these ecosystems. A comparison of the coral reef data generated by the UNEP-WCMC, the ACA geomorphology and the present study is provided in Figure III.11. A total surface of 162 km^2 for the total extent of coral reef systems surrounding Toliara was calculated in the present study, while ACA provides a total of 126.8 km^2 and the UNEP-WCMC coral reef data totaled 61.1 km^2. It is also worth noting that this later dataset misses the fringing reef of Sarodrano (Figure III.11a) which is present in both Figure III.11b and Figure Figure III.11c. Figure III.11b also shows that the enclosed basin, locally known as "Grande Vasque" is erroneously interpreted as reef slope.

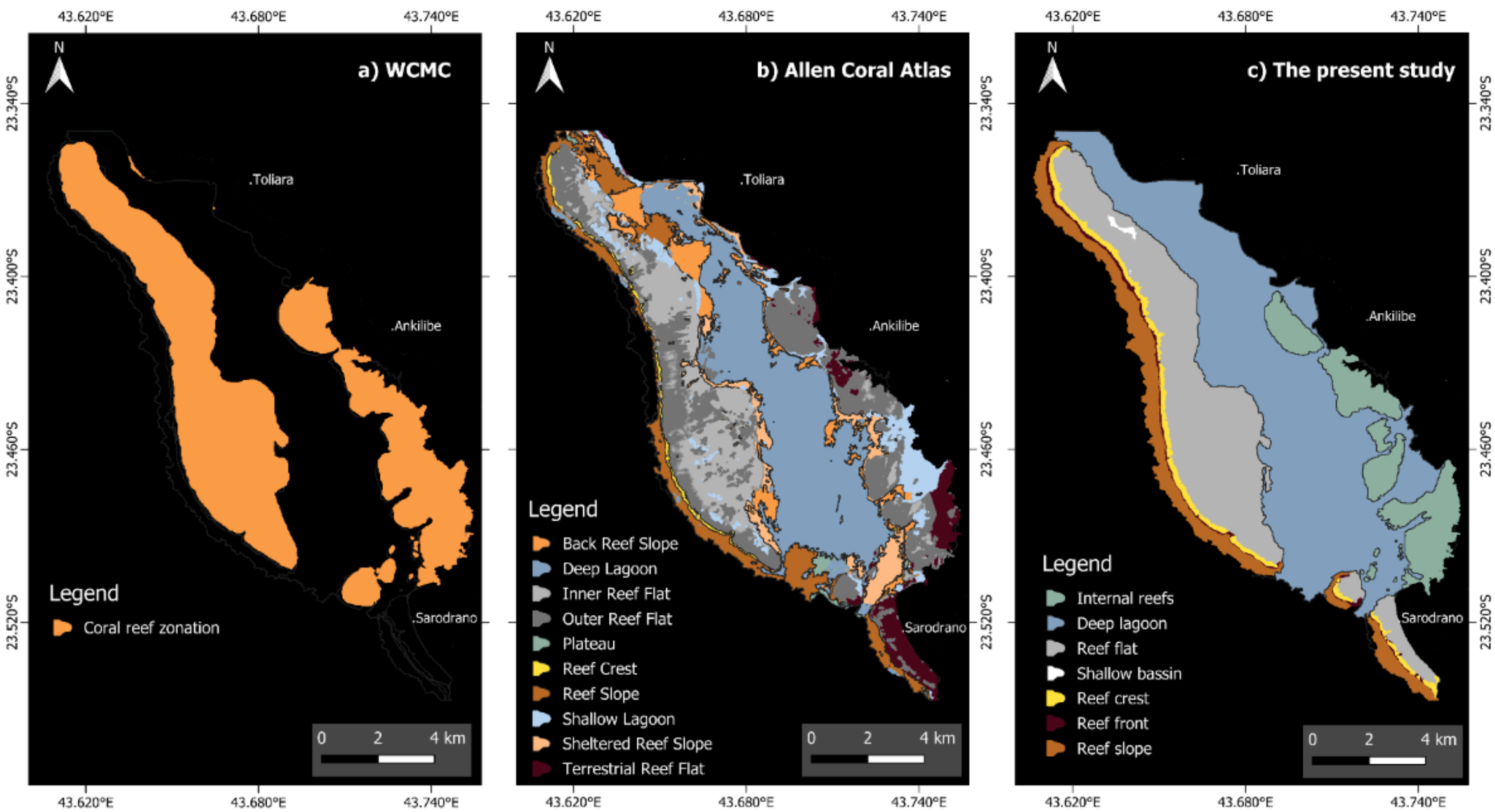

Fig.III. 11. Comparison between the available data of coral reef geomorphology in Toliara

Figure III.11 b also showcases several hard reef structures within the lagoon which are misrepresented as reef slopes where it is clearly just a deep lagoon. Furthermore, concerning the benthic coverage of the coral reef system in Toliara, the current analysis reveals surface areas occupied by seagrass, sand, rubble, coral, and algae, amounting to 21 km^2, 73 km^2, 21 km^2, 10 km^2, and 6 km^2 respectively. Had marine scientists or policymakers used the ACA dataset, their calculations would have shown 22 km^2 for seagrass, and 48 km^2 for sand, 21 km^2 for Coral/ Algae, and 28 km^2 for Rubble. The findings from the present study align with those reported by

Botosoamananto et al., (2021), who conducted localized surveys within this coral reef system. The outer reef slope is predominantly characterized by robust hard corals, as highlighted, with the highest concentration of macroalgae observed in its northern section. Additionally, the authors noted substantial hard coral coverage within the reef patches of Sarodrano and the southern segment of the inner slope of the "Grand Récif de Toliara" (GRT). They also observed a significant presence of rubble on the reef flats as illustrated in (Figure III.12) a phenomenon documented by Bruggemann et al., (2012) and Andréfouët et al., (2013). These studies describe this particular section of the barrier reef, marked by an accumulation of dead coral and rubble on the reef flat.

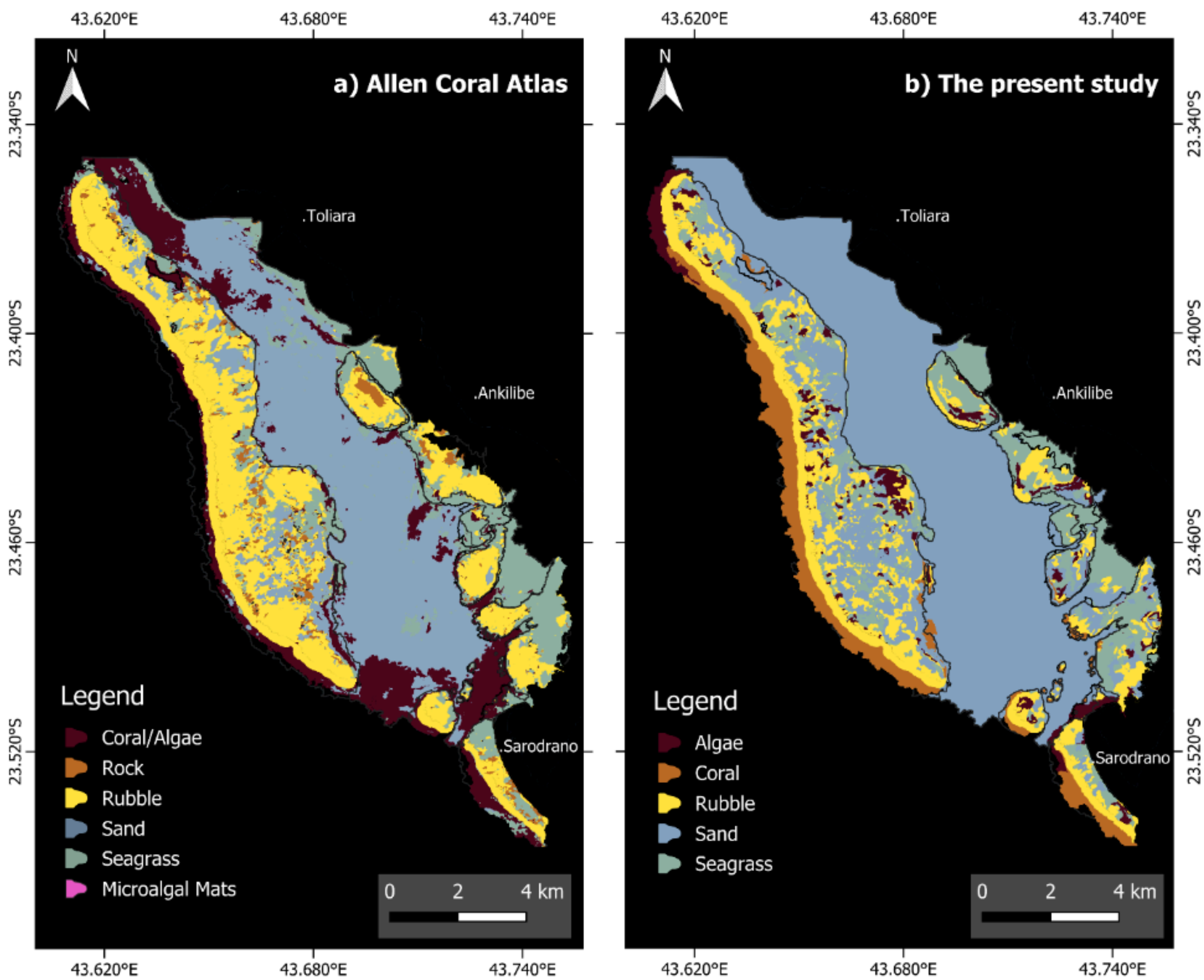

Fig.III. 12. Comparison of benthic coverage provided by the ACA data and our present study

3.4.2. Insight and considerations to enhance coral reef mapping

Assessment of benthic cover of coral reefs requires special attention, as variations in methodology can lead to inconsistencies in coral reef mapping and classification. The total surface area of coral reefs in Madagascar has been reported differently across studies, with (UNEP-WCMC, WorldFish Centre, WRI, TNC, 2021) reporting a total surface area of about 3,100 km^2 and the Allen Coral Atlas (Allen Coral Atlas, 2020) showing a total of 5,076 km^2 for the coral reefs of Madagascar. These variations do not indicate changes in coral reef extent but rather the different methodologies used to assess them. Coral reefs are complex and diverse ecosystems, with different species, morphology, and spatial arrangement depending on local environmental conditions. Inaccurate coral reef mapping and classification can have serious consequences for conservation efforts, leading to misinformed policy and management decisions. Overestimating coral cover can lead to inappropriate land-use decisions such as coastal development or tourism which can result in coral reef degradation and loss. Conversely, underestimating coral cover can result in inadequate protection or management measures, putting these important ecosystems at risk. Therefore, when using remote sensing techniques, a consistent and standardized methodology for assessing marine habitats is essential for accurate and effective conservation and management. Validation and calibration of these techniques using in-situ data are necessary to ensure their accuracy and reliability. Overall, remote sensing can be a powerful tool for marine habitat assessment but it must be used with caution and care to avoid the negative consequences of methodology diversity. This study of the Toliara coral reef system underscores the significance of integrating multiple fieldwork datasets into the model training process, resulting in a notably enhanced mapping accuracy. This emphasizes the crucial role of in situ data collection in refining remote sensing techniques for more precise benthic habitat mapping. Across the globe, various classification algorithms are used for coral reef classification, with their effectiveness contingent upon regional characteristics, available field data, and the spectral and temporal resolution of satellite imagery. While SVM, k-NN, and RT algorithms are prevalent in object-based coral reef benthic mapping publications (Burns et al., 2022), studies such as those by Mountrakis et al., (2011) indicate that SVM often yields higher accuracy values compared to other techniques. However, the current research reveals that in this specific context, the k-NN algorithm outperforms SVM in terms of accuracy. This highlights the importance of selecting the most suitable algorithm tailored to local conditions when mapping coral habitats. Moreover, the performance of classification algorithms is subject to variations in image quality and resolution, training data set size, class types, and algorithm-specific parameter tuning. Hence, it is imperative to identify the most effective approach for this region based on these factors.

Conclusion

This study highlights the successful application of the OBIA method in conjunction with in-situ data to map coral reefs at local scales, using freely available high-resolution satellite images from Sentinel-2. This approach provides a replicable methodology for coral reef mapping projects using the same types of image and field data and lays the foundation to assess long term changes in coral reef habitats, spatial observations of coral reef resilience, evaluation of seagrass distribution, and assessment of habitat health for herbivorous fishes. The use of georeferenced photographs not only establishes a formal linkage between the image and field data but also presents a valuable opportunity for informing stakeholders, managers, and other interested parties on the capabilities of satellite imaging for mapping and measuring reef features. Over 4,000 georeferenced photographs were used as reference data to produce a highly accurate map of the 18 km-long barrier reef of Toliara and the nearby reef systems. The efficacy of this mapping approach relies on both the quantity and quality of fieldwork data used to train the classifier algorithms for identifying features within satellite images. The greater the availability of comprehensive field data, the higher the accuracy of the resultant map. This explains why the ACA does not perform optimally in areas with limited field data. While global data may offer an initial reference for evaluating the extent or likelihood of coral reef occurrence, solely depending on such information for decision-making concerning coral reef management or restoration programs entails considerable risks. Therefore, nations should prioritize local data collection and national-level satellite image processing to ensure precise assessments. This study illustrates that, even with freely available satellite imagery such as Sentinel-2 and basic logistical resources for field work data collection, sufficient accuracy can be attained to produce maps of coral reef geomorphology and benthic habitats.

Chapitre 4

Détection de changement de la couverture corallienne benthique à Toliara, Madagascar : Tendances passées, présentes et futures

Ce chapitre sera soumis pour publication: Aina Le Don Nomenisoa, Gildas Todinanahary, Behivoke Faustinato, Mandimbilaza Tsiresimiary, Mitondrasoa Yves Amoros, Michel Ratsizafy, Toky Razakarisoa, Henitsoa Jaonalison, Jamal Mahafina, Igor Eeckhaut. Change Detection of Benthic Coral Cover in Toliara, Madagascar: Past, Present, and Future Trends. *Journal of Marine Conservation.* (En cours de publication)

Chapitre 4: Change Detection of Benthic Coral Cover in Toliara, Madagascar: Past, Present, and Future Trends

Abstract

This study analyzes coral reef changes in the Great Reef of Toliara (GRT), Madagascar, from 2015 to 2024 using Sentinel-2A satellite imagery, a Convolutional Neural Network (CNN) model, and the Cellular Automata model for change detection and prediction. Field data from 2021 and 2024 validated classification accuracy. Findings revealed significant habitat shifts: coral/algae declined from 2200 to 1500 ha, and seagrass from 2000 to 1700 ha, while rubble increased from 1700 to 2400 ha. Annual losses averaged 84 ha for coral/algae and 33 hectares for seagrass, whereas sand and rubble increased by 48 and 86 ha per year, respectively. Projections for 2034 indicate continued degradation, with coral/algae and seagrass shrinking by 1400 and 1500 ha, replaced by sand and rubble due to persistent stressors. However, the transformation will not be uniform across the reef system as the model reveals that the northern and central parts of the GRT will see the most pronounced changes. The GRT's situation showcases the challenges of meeting the 30x30 biodiversity conservation goal, which aims for 30% protection of the planet's land and oceans by 2030. The continued degradation of the GRT could indicate a failure to meet these targets unless there is significant intervention. Achieving this goal in areas like Toliara involves inclusive strategies that engage local communities, integrate sustainable economic activities, and adjust policies to foster conservation.

Keywords: *Coral reef, Remote Sensing, Change detection analysis, CNN, Madagascar, Sentinel-2*

4.1. Introduction

Coral reefs are among the most biologically diverse and economically valuable ecosystems, providing essential services such as habitat for marine life, shoreline protection, and support for fisheries (Eakin et al., 2010). However, these ecosystems face several threats, both natural and human-induced, including pollution, overfishing, coastal development, hurricanes, global warming, coral bleaching, and ocean acidification. Over recent decades, there has been a marked degradation of coral reefs worldwide, prompting significant concern and necessitating urgent conservation efforts (Hughes et al., 2017). The resilience and response of coral reef communities to these stressors are inherently variable, influenced by both their environmental context and historical exposure to disturbances (Bajjouk et al., 2019). This variability underscores the need for comprehensive monitoring strategies that can capture the temporal dynamics of reef health, accounting for both natural fluctuations and human impacts. Traditional monitoring techniques like Line or Point Intercept Transects (LIT, PIT) and Quadrats offer valuable insights but are constrained by their spatial scale, often missing the broader heterogeneities and long-term geomorphological changes critical for understanding reef dynamics (Bajjouk et al., 2019). In contrast, remote sensing technology presents a viable solution for monitoring coral reefs over larger spatial and temporal scales. It allows for frequent, broad, and accessible data collection which is essential for understanding decadal changes in reef ecosystems. Change detection analysis is particularly important as it allows comparing remote sensing images that are acquired over the same geographic area, but at different times, and then identifying the changed regions (Fang et al., 2019). Change detection has been effectively applied in coral reef studies using various satellite platforms like IKONOS (Palandro et al., 2003, D. Elvidge et al., 2004), Quickbird (Kabiri et al., 2013, Zhou et al. (2018), Ampou et al. (2018), and Worldview (Andréfouët et al., 2013, Zhou et al., 2018, Ampou et al., 2018). Moreover, predictive modeling has emerged as a tool within geospatial studies, particularly for anticipating ecosystem transformations. Two models are used in the present study: a CNN model (Convolutional Neural Network) is used for image classification and a Cellular Automata (CA) model for change detection analyses and future prediction. CNNs, which are composed of multi-layered artificial neural networks, have been widely adopted for image classification and recognition tasks since the early 2000s. Initially applied to tasks like traffic sign and face recognition, CNNs have since expanded to more complex fields, including forest monitoring, and recently, coral reef mapping (Raphael et al., 2020).

Spatio-temporal models like the Cellular Automata (CA) model are frequently used to simulate changes in land use and environmental conditions due to their flexibility in handling spatial and temporal dynamics (Alam et al., 2021). The CA model's adaptability makes it suitable for predicting future scenarios in coral reef environments, similar to its applications in land-use change in terrestrial settings. The MOLUSCE (Modules for Land Use Change Evaluation) plugin within QGIS, which incorporates a CA model has become an important tool for land-use and land-cover change (LULC) analysis (NEXTgis, 2017). The CA model integrated within MOLUSCE program has demonstrated its utility in predicting future benthic patterns, aiding in marine environmental management and planning. This study builds upon the historical analyses by Andréfouët et al. (2015) by integrating both remote sensing data and field observations to track changes in the GRT reef system over the past decade. It specifically illustrates the effectiveness of using freely accessible Sentinel-2 satellite imagery alongside on-site data collection to document the dynamics of coral reef systems. Additionally, the study introduces predictive modeling using the MOLUSCE program to classify changes of benthic coverage of coral reefs from 2015 to 2024 and attempts to forecast potential changes up to the year 2035. By examining past trends and predicting future scenarios, this research aims to enhance our understanding of coral reef dynamics and inform more effective management and conservation strategies.

4.2. Materials and Methods

4.2.1. Study area and field work data collection

This study focuses on the Bay of Toliara in the southwest of Madagascar, a region distinguished by the presence of the Great Reef of Toliara (GRT), a 18-kilometer-long barrier reef located between 43.614°E/-23.355°S and 43.690°E/-23.502°S. Additionally, the reef systems of Sarodrano and Ankilibe, spanning 43.714°E/-23.504°S to 43.743°E/-23.547°S, form an integral part of the area of interest (Figure II.1). The selection of these sites was guided by three key factors: (1) accessibility, facilitating logistical operations; (2) ecological variability, encompassing both degraded and healthy reef areas to better assess local stressors; and (3) ecological complexity, given the unique combination of barrier, fringing, and patch reefs within this coral reef system. Fieldwork was conducted over two periods, from March to December 2021 and in January 2024. Data collection involved capturing georeferenced photoquadrats (underwater images) along transect lines. It consisted of two divers, one taking benthic photos every 3-5 meters, guided by a compass to maintain course, while another at the surface moving synchronically with the first diver holding a GPS device that is secured in a floating airtight bag as GPS signal do not penetrate underwater. Each dive averaged 30 minutes, covering approximately 500 meters of transect where current conditions allowed; however, in instances of stronger currents, transects were shortened accordingly. Initial and final GPS coordinates of each transect were logged on a diving slate to facilitate subsequent GPS data integration. Approximately 250 photos were collected per transect, totaling 4187 photos for 2021 and 2578 photos for 2024. Ground-truthing data collection was confined to depths shallower than 20 meters. Detailed descriptions of the processing of underwater photos with their GPS integration can be found in Nomenisoa et al. (2024)[1].

4.2.2. Satellite data acquisition and preprocessing

The study used 10 Sentinel-2A images acquired between 2015 and 2024, accessed from the Copernicus server (https://scihub.copernicus.eu/dhus/#/home). These images were selected based on specific criteria to ensure consistency in environmental factors. The criteria required that the images be captured using the same platform (Sentinel-2A), acquired during similar time periods, exhibit minimal cloud cover, and be obtained under uniform tidal conditions Tableau IV.1. All images were downloaded at Level-2A, a processing level that incorporates atmospheric correction. This correction ensures uniformity across the images by converting Top-of-Atmosphere (TOA) reflectance (Level-1C) into Bottom-of-Atmosphere (BOA) reflectance, by removing atmospheric effects such as aerosols, water vapor, and ozone interference (Delwart, 2015). This correction ensures that all the images are comparable and representative of surface conditions with reduced atmospheric distortions. Image masking involves concealing parts of images that are irrelevant to the analysis by Convolutional Neural Network (CNN) algorithms, such as land areas or regions outside the designated Area of Interest (Figure II.1). For the time series analysis, each image consisted of six layers: Bands 2, 3 4, 8, NDVI and EVI after applying the mask. Sentinel -2A Bands 2, 3, 4 and 8 (Annexe 2) were selected due to their high spatial resolution and their relevance for mapping marine habitats. In addition to these bands, two derived indices were included: the Normalized Difference Vegetation Index (NDVI) (Sentinel Hub, 2025a) and the Enhanced Vegetation Index (EVI) (Sentinel Hub, 2025b). These indices enriched the spectral context of the

[1] Chapitre 3

imagery, providing better characterization of benthic habitats. NDVI and EVI are widely used in remote sensing to assess the density and vigor of green vegetation. To enhance the contextual information within the images, both the NDVI and EVI were computed and integrated into each image (Trimble Germany GmbH, 2022). These indices help in categorizing the underwater vegetation such as seagrass, providing additional insights for the analysis.

Tab.IV. 1. References of the downloaded Sentinel-2A images

Image reference	Date and time	Time	Tide coefficient
S2A_MSIL2A_20151022T071142_N0204_R020_T38KLV	22-10-2015	07:11:42 UTC	0.8m
S2A_MSIL2A_20160906T071212_N0500_R020_T38KLV	06-09-2016	07:12:12 UTC	0.6m
S2A_MSIL2A_20170911T071211_N0500_R020_T38KLV	11-09-2017	07:12:11 UTC	0.8m
S2A_MSIL2A_20180926T071201_N0500_R020_T38KLV	26-09-2018	07:12:01 UTC	0.8m
S2A_MSIL2A_20190921T071211_N0500_R020_T38KLV	21-09-2019	07:12:11 UTC	0.8 m
S2A_MSIL2A_20200925T071211_N0500_R020_T38KLV	15-10-2020	07:12:11 UTC	0.8 m
S2A_MSIL2A_20210920T071201_N0500_R020_T38KLV	20-09-2021	07:12:01 UTC	0.6 m
S2A_MSIL2A_20221025T071211_N0400_R020_T38KLV	25-10-2022	07:12:11 UTC	0.8 m
S2A_MSIL2A_20230930T071211_N0509_R020_T38KLV	30-09-2023	07:12:11 UTC	0.8 m
S2A_MSIL2A_20240904T071211_N0511_R020_T38KLV	04-09-2024	07:12:11 UTC	0.8m

Nomenclature of the downloaded images:

- **S2A** : Satellite Sentinel-2A.
- **MSI** : The Multispectral Instrument onboard the Sentinel-2 satellite
- **L2A** : It specifies the processing Level of the data product, meaning that the that the data has been atmospherically corrected to provide Bottom-Of-Atmosphere (BOA) reflectance.
- **20151022T071142** : Date and time acquisition: October 22, 2015, at 07:11:42 UTC.
- **N0204**: Processing Baseline which is at the version 02.04 of the software
- **R020** : Relative orbit Number. Sentinel-2 satellites follow a sun-synchronous orbit with a 10-day repeat cycle (5 days when combined with both satellites). R020 indicates the specific orbit within this cycle when the data was captured.
- **T38KLV** : Location of the image. It corresponds to the tile identifier showing the specific geographic tile within the UTM (Universal Transverse Mercator) zone 38 coordinate system.

4.2.3. Benthic class description

The benthic classes utilized in this study are based on the comprehensive descriptions provided by Nomenisoa et al., (2024)[2]. The “Rubble” class pertains to any area featuring loose, cylindrical to irregularly shaped fragments of bedrock or clasts of corals, bivalves, and coralline algae. This category encompasses limestone reef matrix and underlying areas of coral sand cemented together. The “Seagrass” class pertains to a soft-bottomed environment that is mainly characterized by the prevalence of a single species of seagrass or a combination of different species. This classification also encompasses sparser or spatially confined seagrass as long as it forms the dominant benthic class. The “Sand” class pertains to soft-bottomed reef regions where fine unconsolidated granular material prevails. This granular material is finer than coral rubble but coarser than mud and thickly overlays any underlying bedrock. This class also encapsulates areas that are covered by a layer of fine-grained sediment that is mostly composed of organic matter and inorganic particles. “Coral class” refers to a category with a hard underlying framework that is typically composed of coral-derived limestone, although non-carbonate materials can also be present. This class includes living corals. The “Algae” class is composed of large, multicellular marine plants that typically thrive in shallow waters surrounding coral reefs. In this study, the “Macroalgae” and “Coral” classes have been combined into a single class termed “Coral/algae”. We chose to combine these two classes due to the model's limitations in distinguishing them effectively.

4.2.4. General architecture of a CNN model

A CNN is a type of deep learning model specifically designed for image classification tasks, drawing inspiration from the structure of biological multilayer neural networks (Trimble Germany GmbH, 2022). The model developed in this study uses the integrated algorithms of Convolutional Neural Network (CNN) creation architecture within Trimble eCognition Developer v.10. (Trimble Germany GmbH, 2022), which is based on the Google TenserFlow library, a widely used deep learning framework. CNNs consist of filter layers that can learn hierarchically: low-level features are learned in the first layers, more high-level features are learned in the last layers (Sefrin et al., 2020).

[2] Chapter 2

It is a sequence of layers that transform input data into useful classifications or predictions (Figure 20). A fully description of the CNN architecture is provided by Thamarai and Aruna (2023). The process starts with the input layer, which receives the 2021 stacked Sentinel-2A data. The data then passes through convolutional layers, where kernels (small matrices) slide across the input to extract key features like edges, textures, or patterns. This results in feature maps, which highlight important patterns in the image. Next, pooling layers reduce the spatial dimensions of the feature maps, focusing on the most significant features while lowering computational complexity. Max pooling is commonly used, selecting the maximum value from a local area of the feature map. After feature extraction, the CNN moves to fully connected layers, where the feature maps are flattened and linked to a dense layer of neurons. These neurons work together to make the final prediction or classification, such as identifying seagrass, coral, algae, sand, or rubble. The output layer gives the model's final result of the model (Figure IV.1).

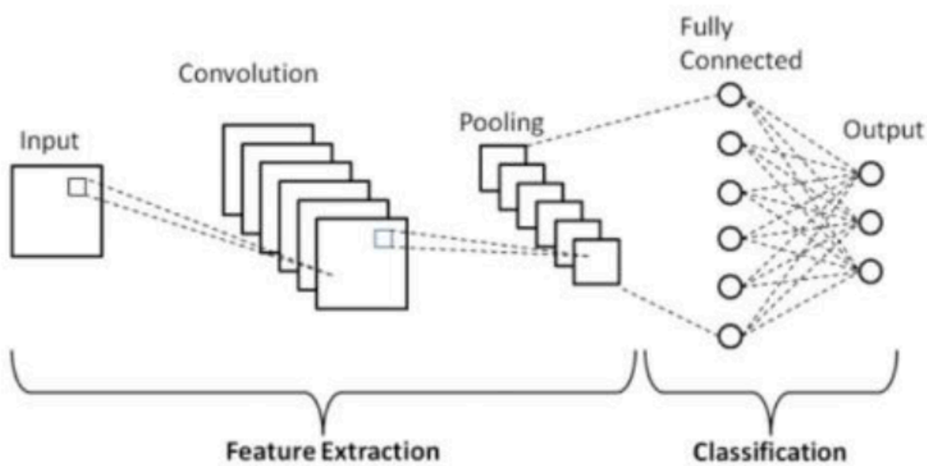

Fig.IV. 1. Typical convolution neural network architecture (Thamarai and Aruna, 2023)

4.2.4.1. Generation of labeled sample patches for CNN Model

A labeled image sample for CNN is called sample patch in Ecognition Developer, which is a small, fixed-size sub-region or window extracted from the original image (Burns et al., 2022) (Figure IV.2). It consists of one or several image layers. In this study, a training sample patch is composed by six layers (Band2, Band3, Band4, Band8, NDVI and EVI), made up one sample. It determines the spatial extent of features analyzed at a time. The size of the sample patch depends on the context we need. After a visual assessment of the results and accuracy assessment, the sample patch size of 32x32 was chosen in this study. A full set of the parameters used to build this model is provided in Annexe 4. Deep learning such as CNN requires several labeled samples to generate good results. We can increase the number of samples by rotating the sample patches. First, we create labeled samples, then we rotate them from 0 to 330° which will augment our sample patches. In this studies, 80000 labeled sample patches were generated for the model to improve its performance.

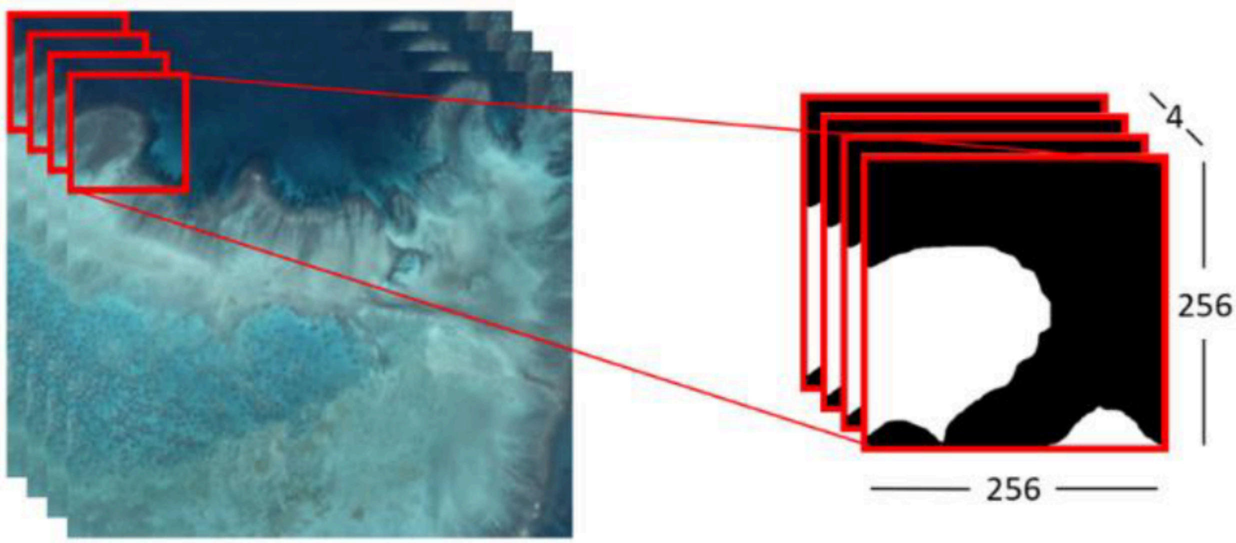

Fig.IV. 2. Example of a 256x256x4 training samples representing the class 'Coral' (white) used as input to a CNN. (Burns et al., 2022). The values 256x256 represent height and width in pixels while 4 represents the depth/number of bands in the satellite image. The 256x256x4 sample is first extracted from the satellite image on the next. Next, all 'coral' pixels (white) are created in order to assign the value of 0 to all non-coral pixels (black) from the training sample.

4.2.4.2. Creation and training of the CNN model

Building the model requires configuring various parameters, including the number of hidden layers, kernel size, number of feature maps, max pooling, etc. These parameters significantly influence both the accuracy and effectiveness of the model, as detailed in Annexe 4. Consequently, optimizing these values (a process often referred to as parameter tuning) is typically essential to enhance the model's performance (Arnold et al., 2024). To find the optimal value for each parameter, we used an iterative process where we ran the model multiple times, evaluating the accuracy of the CNN output for different parameter settings. After each run, we adjusted the parameters and reassessed performance until no further improvement could be observed. We repeated this process for each parameter listed in Annexe 4, training and analyzing the model's performance across various configurations. We generated multiple variants of the CNN model for the 2021 image, using the parameters specified in Annexe 4. The performance of these models was evaluated through both visual interpretation and accuracy assessment calculations. The model variant that demonstrated the highest performance was then applied to data from 2024 to assess model transferability, with accuracy assessments conducted on 2024 imagery. Given its superior performance on the 2024 data, this model was then used to generate benthic habitat maps for the rest of the years.

4.2.5. Image classification using Object Based Image Analysis (OBIA)

After applying the developed CNN model, fully connected layers in the form of heatmaps were generated. Each heatmap layer provided outputs that corresponded to a specific benthic class: sand, seagrass, coral, algae, and rubble. The heatmaps assigned a value to each predicted benthic class, where a value close to 1 indicated a higher likelihood of the class, while a value near 0 represented a lower likelihood. The four generated heatmap layers corresponded to the four benthic classes considered in this study. The heatmap was used here as the input features to perform the Object Based Image Analysis (OBIA). The OBIA consist of grouping similar pixels into segments and then attributing classes to those segments (Hedley et al., 2016). Here, the heatmaps were used as the input features to perform the OBIA. The segmentation consists of affecting different values for parameters such as scale parameters, shape and compactness which values were set as 47, 0.1 and 0.7 respectively based on trial-and-error.

4.2.5.1. Accuracy assessment

The accuracy assessment consists of comparing the classification map with the field work data (Yamano, 2013). This was performed using an error matrix (also known as a confusion matrix), which measures the agreement between the thematic benthic class as resulted by the model and the corresponding class in the reference data at the same location (Yamano, 2013). Metrics such as Overall Accuracy (OA), User Accuracy (UA), and Producer Accuracy (PA) were used. Overall Accuracy (OA) represents the overall performance of the model by calculating the ratio of correctly classified pixels to the total number of pixels across all benthic classes. Producer Accuracy (PA) evaluates how effectively the CNN model identifies and maps pixels or features that truly belong to a specific class on the ground. User Accuracy (UA) measures how accurately the CNN model assigns pixels or features to a specific class, regardless of whether they truly belong to that class. For the 2021 imagery, 75% of the field data were used to train the CNN model, while the remaining 25% were used for validation to assess the model's accuracy. To evaluate the model's temporal transferability, validation was conducted using the full set of ground-truth data collected in 2024, comprising 2,578 reference points. Since the CNN model achieved higher accuracy when applied to the 2024 Sentinel-2A imagery, the model was extended to classify the entire Sentinel-2A time series from 2015 to 2024. This decision was based on the assumption that the model's performance remains consistent across the time series.

4.2.5.2. Change detection analyses

The change detection analysis and the 10-year prediction assessment were conducted using the MOLUSCE (Model for Land Use Change Simulation) plugin in QGIS (Amgoth et al., 2022). This process required trend data spanning from 2015 to 2024, along with key factors influencing future trends. To inform the model, we used: i) fishing effort data that were derived from Behivoke et al. (2021). ii)Temperature stress data that was generated based on temperature data acquired from 8-days MODIS Aqua (https://oceancolor.gsfc.nasa.gov/) between 2002-2022, and calculated as Degree of Heating Week from (Mumby et al., 2004) and turbidity data that was acquired from the Allen Coral Atlas (Allen Coral Atlas, 2020). All these datasets were standardized in terms of size and format (same coordinate systems, same extent) using the QGIS software to ensure compatibility before being processed through the MOLUSCE program (Figure IV.3).

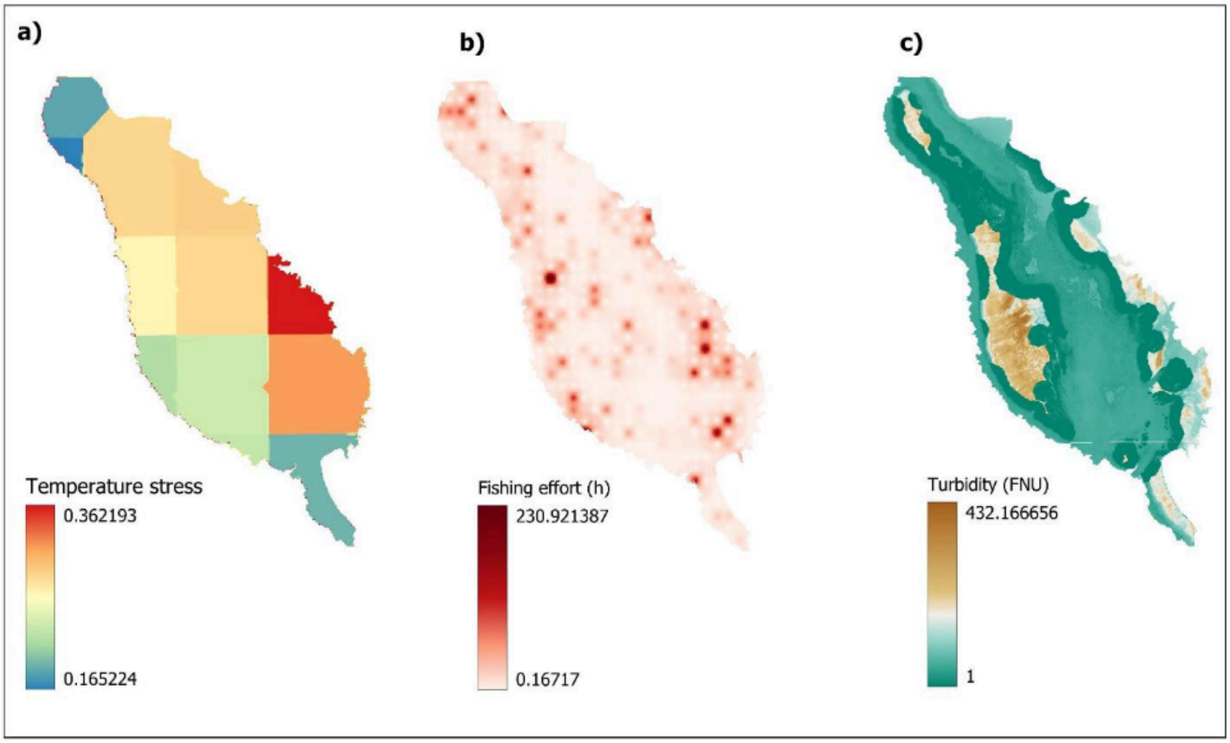

Fig.IV. 3. Variables used for the 10 years prediction

4.3. Results

4.3.1. Spatio-temporal change of benthic coverage from 2015-2024

The image classifications for 2021 and 2024 show a high overall accuracy 82% for 2021 and 81% for 2024 (Tableau IV.2). It also shows that the CNN model accurately classified the Seagrass, the sand, the coral/algae and the rubble classes with Producer's Accuracy (PA) and User's Accuracy (UA) higher than 70%.

Tab.IV. 2. Confusion matrices for the 2015-2024 images

Years	**User Class \ Sample**	**Seagrass**	**Sand**	**Coral/algae**	**Rubble**	**Sum**
2021	Seagrass	32	5	1	0	38
	Sand	2	26	1	3	32
	Coral/algae	1	1	26	3	31
	Rubble	3	2	1	21	27
	Sum	38	34	29	27	
	Producer's Accuracy (PA)	0.84	0.76	0.90	0.78	
	User's Accuracy (UA)	0.84	0.81	0.84	0.78	
	Overall Accuracy (OA)	0.82				
2024	User Class \ Sample	Seagrass	Sand	Coral/algae	Rubble	Sum
	Seagrass	13	2	0	1	16
	Sand	6	20	0	6	28
	Coral/algae	0	2	19	0	21
	Rubble	2	2	2	30	36
	Sum	17	26	21	37	
	Producer's Accuracy (PA)	0.76	0.77	0.90	0.81	
	User's Accuracy (UA)	0.81	0.71	0.90	0.83	
	Overall Accuracy (OA)	0.81				

As the CNN model demonstrated high accuracy for data from 2024, we extended its application to analyze the spatio-temporal changes in benthic coverage from 2015 to 2024. While year-to-year changes may appear subtle (Figure IV.4), the cumulative shifts over the ten-year period reveal significant transformations in the benthic environment (Figure IV.5). In 2015, the initial conditions showed a notable presence of "coral/algae," predominantly concentrated along the reef flat and scattered across central areas. It's important to highlight that the reef flat of the GRT and the fringing reef at Sarodrano is largely dominated by algae rather than coral. Conversely, the outer reef primarily consists of living coral.

While the outer reef remained relatively stable, a clear decline in coral/algae coverage was observed over the years. Tableau IV.3 reveals a consistent reduction in coral/algae from 2200 ha in 2015 to 1500 ha by 2024. Seagrass beds exhibited a concerning trend of diminishing coverage; in 2015, a significant seagrass patch was present in the center part of the GRT, which progressively decreased, resulting in a much less pronounced coverage by 2024. According to Tableau IV.3, seagrass coverage declined from 2000 ha in 2015 to 1700 ha in 2024. An increase in rubble was notably observed on the reef flat, spreading inward over time.

Tab.IV. *3.* Evolution (in Ha) of benthic habitats in the GRTTableau IV.3 also indicates that rubble coverage increased from 1700 ha in 2015 to a peak of 2400 ha in 2024. Sand, however, remained the most extensive habitat, with coverage that was relatively stable, fluctuating slightly between 7000 and 7500 ha, maintaining its position as the dominant benthic class.

Tab.IV. 3. Evolution (in Ha) of benthic habitats in the GRT

Benthic class	**2015**	**2016**	**2017**	**2018**	**2019**	**2020**	**2021**	**2022**	**2023**	**2024**	**2034**
Coral/algae	2248	2196	2092	1968	1662	1726	1735	1683	1629	1540	1424
Rubble	1714	1794	2030	2216	2137	2085	2106	2264	2226	2391	2679
Sand	7046	7134	7132	7084	7518	7504	7519	7365	7524	7444	7467
Seagrass	2064	1956	1832	1822	1766	1777	1731	1776	1707	1690	1538

Despite its stability, there were subtle shifts in its distribution over the period. Between 2015 and 2024, Coral/algae and seagrass habitats have lost 710 ha and 375 ha respectively, while the extents of rubble and sand have increased by 675 ha and 420 ha respectively (Figure IV.6). This shows that while annual changes might not be immediately apparent, significant trends in benthic habitat changes become evident over a decade-long observation period.

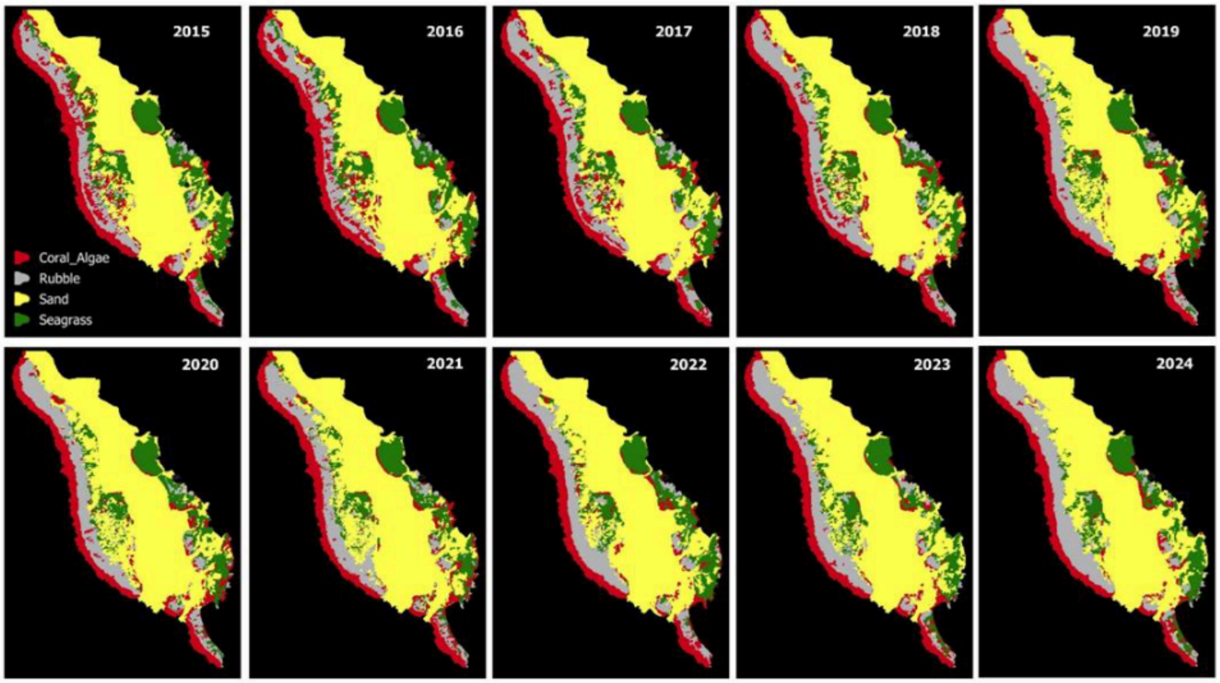

Fig.IV. 4. Benthic image classification between 2015-2024

Predictions suggest that coral/algae and seagrass habitats will lose about only 110 ha and 150 ha respectively between 2024-2034. Besides, the extents of sand and rubble will increase only by 23 ha and 290 ha respectively between 2024-2034.

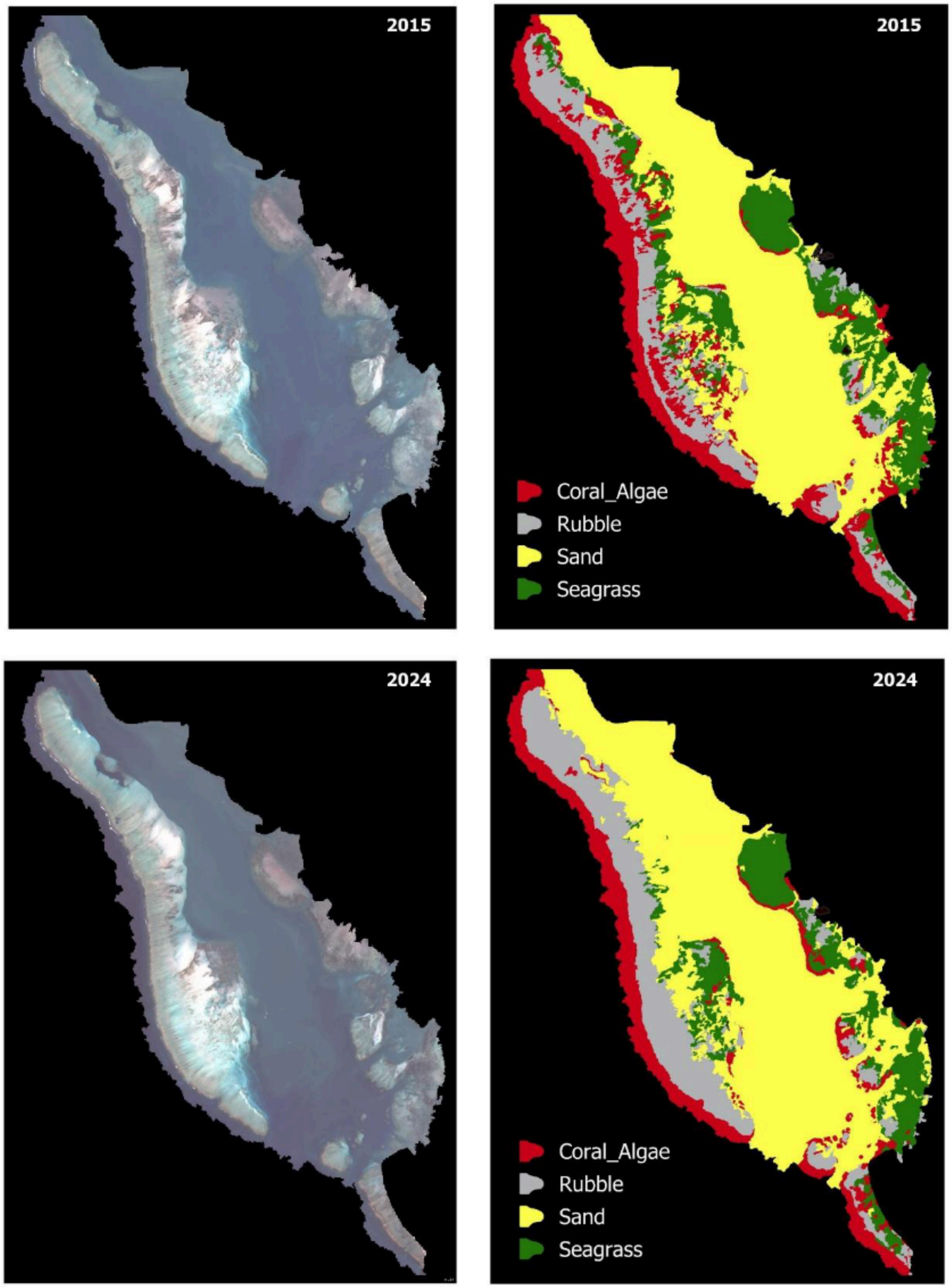

Fig.IV. 5. Benthic changes between 2015-2024

By calculating the difference between two consecutive years and calculating the average, we found that the reef systems in Toliara are losing seagrass of about 33 ha/year, the Coral/algae cover is losing a surface of about 84 ha/year. Sand grows by approximately 48 ha/year and Rubble grows by 86 ha/year. Tableau IV.4 showcases the transition probabilities of different benthic habitat classes (Coral/algae, Rubble, Sand, Seagrass) from one class to another over between 2015-2024. Each row represents the state of the benthic coverage in 2015, and each column represents the state in 2024. Sand is the most stable class (91.9% persistence), meaning little change is occurring. Rubble also has high persistence (78.0%), indicating that once coral degrades into rubble, it rarely transitions back. Coral/algae and Seagrass have a moderate persistence (54.1% and 55.3% respectively), meaning nearly half of the Coral/algae and Seagrass covers are changing. The most significant transition from Coral/algae is to Rubble at 26.3%, with a notable shift to Sand at 13.5%, while only 6% transition to seagrass. Once transformed into Rubble, there's a low change (6.4%) of it recovering back to Coral/algae. Instead, Rubble has a slightly higher likelihood of transitioning to Seagrass (8.3%) or Sand (7.2%). Seagrass has a considerable transition rate to Sand at 26.5%. The recovery of Coral/algae from Seagrass is minimal, at just 4.8%.

Tab.IV. 4. Transition probability matrix of benthic coverage between 2015-2024

	Coral/algae	**Rubble**	**Sand**	**Seagrass**
Coral/algae	0.54	0.26	0.14	0.06
Rubble	0.06	0.78	0.07	0.08
Sand	0.02	0.03	0.92	0.04
Seagrass	0.05	0.13	0.27	0.55

3.3.2. Prediction of the benthic cover between 2024-2034

Based on predictors such as temperature stress, fishing effort, and turbidity, CA models reveals that the benthic cover in the GRT over the past ten years indicates a significant shift. If these stressors continue to increase, Coral/algae cover is expected to decrease approximately by 1400 ha, and seagrass cover by around 1500 ha (Tableau IV.3). The resulting ecosystem in the Bay of Toliara is predicted to be predominantly composed of sand and rubble, with sand expected to remain relatively stable at about 7400 ha, while rubble increases by approximately 2700 ha. However, the transformation will not be uniform across the reef system; the northern and central parts of the GRT will see the most pronounced changes. However, there will be localized increases in seagrass in areas like Ankilibe and Belaza, contrasted by significant decreases on the reef flat of the GRT. The outer reefs are expected to be less affected, but the reef flat of Sarodrano is projected to transition into an area dominated by Coral/algae cover. The reason for these less pronounced changes in the 2024-2034 projections could be attributed to the limited variables considered in these forecasts (Figure IV.7). The projections are based solely on three key factors: temperature stress, fishing effort, and turbidity. Other potential influences like pollution, ocean acidification, or changes in species interactions might not be fully captured in these models, possibly leading to a more pronounced estimate of future changes. Over the last decade, environmental degradation has markedly worsened, with forecasts predicting a continued decline by 2034. The transition from coral to algal dominance has quickened, with a loss of 700 ha of coral between 2015 and 2024, expected to slow to a reduction of 100 Ha from 2024 to 2034 (Figure IV.6). Likewise, seagrass coverage is anticipated to decline by another 100 ha in the next decade, down from 400 ha lost in the previous one. Changes in sand coverage are projected to be minimal, with an increase of only 23 ha. Conversely, rubble has seen an increase of 280 ha, though this growth is less than what was observed in the preceding decade.

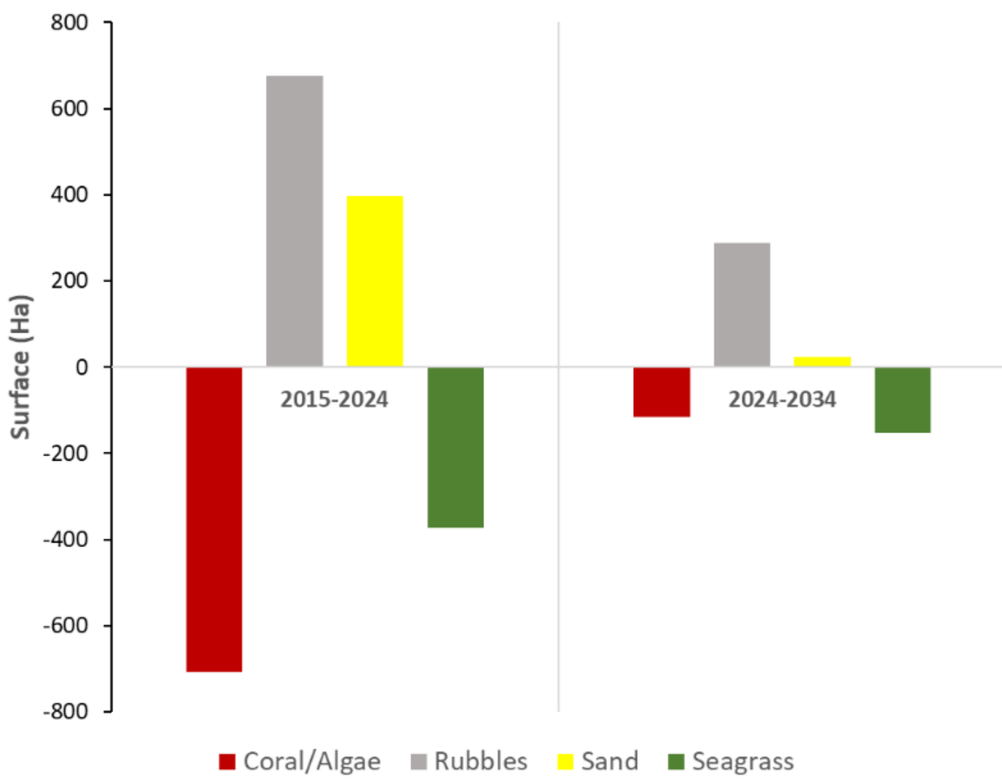

Fig.IV. 6. Gained and lost surfaces of benthic habitats in the GRT between 2015-2024 and 2015-2034

3.4. Discussion

3.4.1. Image classification

Our study involved classifying images from 2021 using a Convolutional Neural Network (CNN) algorithm, enhanced by field work data. Initially, we achieved an overall accuracy (OA) of 78%. When the model was applied to the 2024 image, however, this accuracy decreased to 65%, which was lower compared to other classifiers like k-NN (83%), Bayes (79%), Decision Trees (68%), Random Trees (67%), and SVM (42%) as cited in Chapter 3 for the same area. To address this decline in accuracy, we adjusted our CNN model by reducing the number of classes, merging 'Coral' and 'Algae' into a single category. Although coral and algae are ecologically distinct, this compromise was necessary to improve temporal generalization. As a result, the merged class should be interpreted with caution. This resulted in improved accuracies of 84% for the 2021 images and 81% for the 2024 images, without the need for new training data for the latter year. The 2024 in-situ data was solely used for validation. Despite the initial lower performance, we favored CNNs over other classifiers due to their ability to apply models trained on one dataset to different temporal images without retraining, which is crucial for time series analysis. This adaptability is supported by studies like (Boston et al., 2023) and (Pelletier et al., 2019) which highlight CNNs' prowess in temporal data classification. Although deep learning in time series analysis is more established in terrestrial research, its application in coral reef mapping is relatively new. Initial findings indicate that CNNs could enhance accuracy and scalability over conventional methods (Raphael et al., 2020; Li et al., 2020; Burns et al., 2022). However, the performance of CNNs heavily depends on adequate in situ data for training and meticulous hyper-parameter tuning (Alzubaidi et al., 2021). Our parameter selection, as outlined in Table 1, could potentially be optimized for different geographical contexts. Mapping coral benthic composition over time presents unique challenges due to variable conditions like atmospheric effects, water clarity, and depth, which differ across multi-temporal satellite images (Burns et al., 2022). Besides, the classification categories chosen for mapping vary widely among studies, influenced by image type, resolution, location, and research goals (Joyce et al., 2004). The selection of habitat classes for extraction varies among researchers, influenced by factors such as the satellite imagery's type, spatial or spectral resolution, the specific location, and the objectives of the habitat mapping. For instance Joyce et al., (2004) chose five benthic classes—Sand, Rock, Rubble, Fleshy algae, and Coral—to ensure compatibility with reef check protocols. In contrast, the World Conservation

Monitoring Centre (UNEP-WCMC, 2010) simplified their approach by using just one class to map global reef extent. The Millennium Coral Reef Mapping (MCRMP) adopted an expansive classification globally with 966 different classes (Andréfouët et al., 2006), while the Allen Coral Atlas used 15 classes for their mapping efforts (Lyons et al., 2024). Other studies have tailored their classifications based on local conditions, available imagery, and specific research goals. Our approach builds on the work of Andréfouët et al. (2013), who used aerial photos from the 1960s and commercial satellite images like Quickbird, alongside Landsat imagery, to study changes over fifty years. By contrast, we used freely available Sentinel-2 images since 2015 to assess and predict changes in the Great Reef of Toliara for the next decade, offering a cost-effective and scalable method for ongoing reef monitoring. This research not only advances methodological approaches but also provides crucial data for understanding and predicting changes in coral reef ecosystems, particularly in Madagascar.

3.4.2. Benthic coverage changes in the GRT and its neighboring reef system

The Great Reef of Toliara (GRT) has been documented to undergo significant degradation since the late 1960s. Pichon (1978) noted that the reef flat was predominantly covered by living corals at that time. However, subsequent studies have captured a narrative of decline. Ranaivomanana, (2006) initially reported the degradation of the GRT, which was later quantified by Bruggeman et al. (2012) who confirmed an ongoing degradation rate. Expanding on this, Andréfouet et al. (2013) conducted a comprehensive study detailing a fifty-year change, revealing a progressive degradation with a significant loss of coral communities. They specifically noted a reduction in coral strip habitats from 0.70 km² to 0.2 km² on the reef flat. Multiple factors contribute to this degradation. The primary environmental stressor identified is hypersedimentation, with significant sediment inputs from the Fiherena (36 million tons/year) and Onilahy (84 million tons/year) rivers (Payet et al., 2011), (Rakotondralambo, 2008). Additional stressors include erosive wave actions, algal overgrowth, urban pollution, fish gleaning, human extraction of coral blocks, and an abundance of coral predators like *Acanthaster planci* (Ranaivomanana, 2006). Bruggemann et al., (2012) highlighted high turbidity, while Ramahatratra (2014) pointed to the decline in herbivorous fish biomass, both significantly impacting the reef's health. Randrianandrasana (2019) added temperature stress to the list of major drivers of degradation, with Andréfouet (2013) noting the exacerbating effects of cyclones and population growth. Despite the grim outlook at Figure IV.7, Botosoamananto et al. (2021) propose an optimistic scenario where rigorous and immediate conservation efforts could maintain the GRT's capacity to support local communities. They assert that the coral assemblages still possess maintenance capabilities sufficient for sustainability, provided that local disturbances are effectively managed. While the degradation of the GRT is well-documented and expected to worsen, strategic conservation measures could potentially mitigate further decline and preserve this ecosystem.

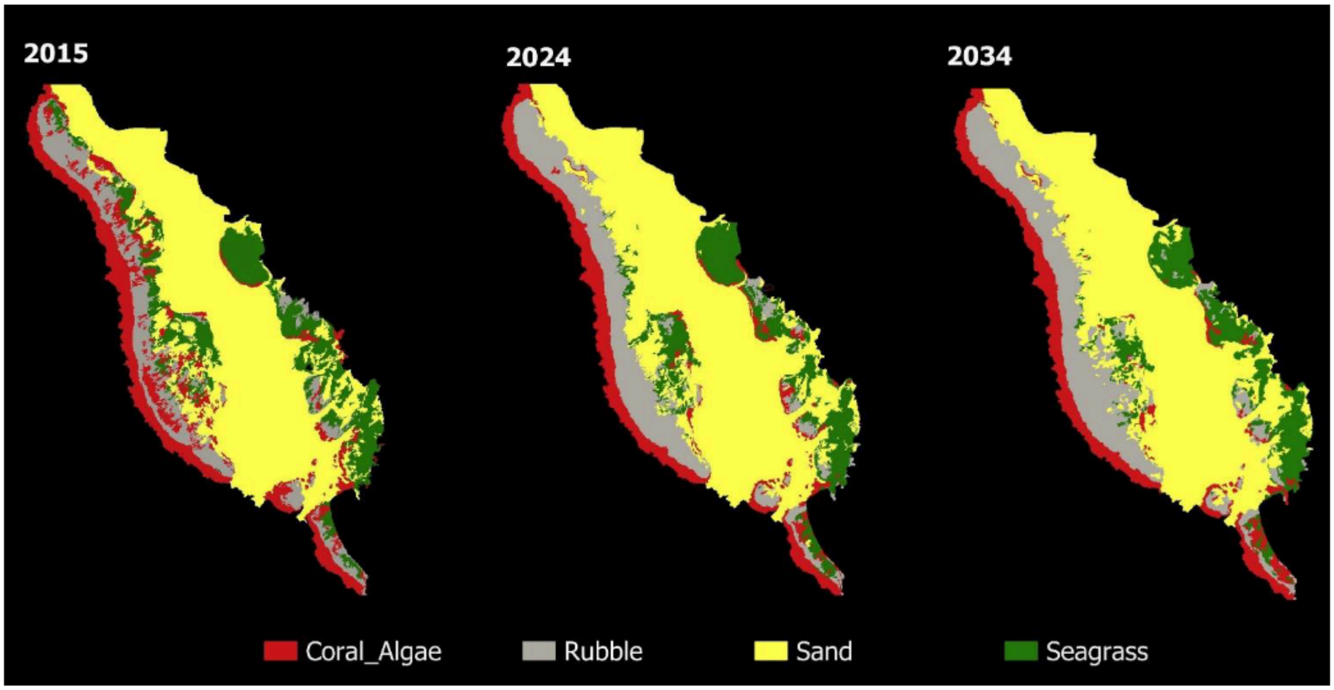

Fig.IV. 7. Benthic change of the benthic coverage of the GRT and prediction for the next 10 years

Conclusion

Understanding the degradation of coral reefs like the Great Reef of Toliara (GRT) and its surrounding reef systems requires a holistic view that considers multiple variables simultaneously. Individually, metrics such as benthic coverage, turbidity, temperature stress, and fishing pressures provide limited insight. However, when these are analyzed over time and in combination, they reveal a more comprehensive narrative of change, including the speed of degradation, transition probabilities of benthic classes, and even future predictions. This latter could be enhanced by integrating additional variables and exploring their interrelationships, which would facilitate a multi-criteria analysis for identifying priority areas for conservation, restoration, and educational initiatives. This study demonstrates the effectiveness of the MOLUSCE program in detecting changes in coral reef benthic cover, despite its original design for terrestrial applications. The degradation of the GRT and its surrounding reefs is driven by both global and local threats, such as El Niño, coral bleaching, ocean acidification, hypersedimentation, pollution, and fishing pressures. Managing this complex phenomenon cannot solely rely on addressing either global or local factors in isolation. For instance, focusing only on fishing restrictions might not yield the desired conservation outcomes if not complemented by strategies addressing broader climate impacts. Effective solutions must therefore integrate various approaches, considering all major variables. Current efforts include the establishment of coral mesocosms by the CORRECT (Coral Reef Research, Education and Conservation Team) (Todinanahary et al., 2024), which serve not only as research tools but also as reserves for coral transplantation post-bleaching events. Coral transplantation (Todinanahary, 2016) and restoration programs (Behivoke et al., 2022) have shown promise, yet these must be supported by policies that regulate herbivorous fish catches, manage riverine sediment input, and enhance local and international collaborations, particularly in addressing climate change. Since the 1960s, population growth and the increasing frequency and intensity of cyclones (e.g., Fundi in 2015, Batsirai, Emnati, Jasmine in 2022, Freddy in 2023, and Dikeledi in 2025) have further complicated the scenario for coral reefs. The sedimentation from rivers like Fiherena and Onilahy has visually increased (Payet et al., 2011), (Rakotondralambo, 2008), highlighting the need for proactive measures in erosion and sediment control. The question now shifts from how much the reefs will change to how we can halt or slow this degradation. There isn't a singular solution; instead, it requires coordinated efforts across local, national, and international levels, encompassing research, policy, community education, and engineering solutions to manage sediment and erosion. The GRT's situation underlines the challenges of meeting the 30x30 biodiversity conservation goal, which aims for 30% protection of the planet's land and oceans by 2030. The continued degradation of the GRT could indicate a failure to meet these targets unless there is significant intervention. Achieving this goal in areas like Toliara involves inclusive strategies that engage local communities, integrate sustainable economic activities, and adjust policies to foster conservation. This case could serve as a catalyst for policy reform and increased funding for marine conservation, emphasizing the need for international cooperation. Coral reefs are globally interconnected, underlining the necessity for shared responsibility in knowledge, technology, and financial resource allocation to ensure their preservation.

Chapitre 5

Cartographie des zones potentielles à la gestion basée sur la résilience dans les communautés de petits pêcheurs à l'aide de la télédétection et des données de terrain.

Aina Le Don Nomenisoa, Gildas Todinanahary, Edwin Zafimampiravo Hubert, Behivoke Faustinato, Mandimbilaza Tsiresimiary, Mitondrasoa Yves Amoros, Michel Ratsizafy, Toky Razakarisoa, Henitsoa Jaonalison, Jamal Mahafina, Igor Eeckhaut. Assessing Coral Reef Resilience through Remote Sensing and field based approach for Decision Support in Small-Scale Fishing Communities. *Perspectives in Ocean, Marine and Coastal Governance: Coastal resilience, access and livelihoods* (En cours)

Chapitre 5: Mapping support areas for resilience based management in small scale fishing communities using remote sensing and field data

Abstract:

Coral reefs play roles for marine biodiversity and small-scale fishing communities. However, they face escalating threats from climate change, overfishing, and habitat degradation. This study uses a Multi-Criteria Evaluation (MCE) framework, integrating the Analytical Hierarchy Process (AHP) and Weighted Linear Combination (WLC), to assess coral reef resilience and inform conservation strategies. Using remote sensing data from Sentinel-2 imagery and field observations, we mapped resilience across a reef system, focusing on seven key factors: “Coral Abundance”, “Framework”, “Herbivorous Attractive Areas (HAA)”, “Depth”, “Fishing Pressure”, “Temperature Stress”, and “Turbidity”. Six scenarios were developed to reflect diverse priorities: biodiversity (Scenarios 1–2), local impacts (Scenarios 3–4), and global stressors (Scenarios 5–6). Results reveal that biodiversity-focused scenarios, emphasizing Coral Abundance and Framework (Scenario 2), yield the largest resilient area (2770 ha of Medium to Very High resilience), highlighting the role of structural complexity. Local scenarios prioritizing Fishing Pressure and Depth (Scenario 4) reduce low-resilience areas (250 ha), enhancing resilience through manageable factors. Global scenarios addressing Temperature Stress and Turbidity (Scenario 6) show strong very high resilience (820 ha), underscoring climate-focused strategies. High-resilience zones consistently appear along the reef front and external slope of the GRT, adjacent the enclosed basin “Grande Vasque”, as well as those of Nosy Tafara and the fringing reefs of Sarodrano. These findings guide conservation by identifying areas for protection (High/Very High resilience) and restoration (Medium resilience), tailored to scenario priorities. The study demonstrates the efficacy of combining AHP with geospatial tools for spatially explicit resilience assessments, offering a scalable approach for reef management. Future research should incorporate dynamic models, validate maps with long-term data, and engage local stakeholders to enhance community-driven conservation. This framework supports sustainable management of coral reefs, balancing ecological health with the needs of small-scale fishing communities in a changing climate.

Keywords: *Remote sensing, Satellite, Coral reef, Resilience based management, Madagascar, GIS*

4.1. Introduction

Coral reefs are among the most productive and biodiverse marine ecosystems (Wilkinson, 2008). These habitats help prevent floods and safeguard beaches and coastlines from erosion. The UN estimates an economic value ranging from $100,000 to $600,000/ha for coral reefs when social and economic benefits are combined (Nicet et al., 2016). Due to climate change and the impacts of human activities, these ecosystems are threatened at a global and local level (Xu and Zhao, 2014). Nearly half of the world's coral reefs have already been destroyed or severely damaged in the past 30 years (Wilkinson, 2008). 70 to 90% of the world's coral reefs are at risk of extinction (Foo and Asner, 2019) in the coming decades including those in Madagascar (Van Hooidonk et al., 2016). Several actions are being taken worldwide to understand and protect these ecosystems. Resilience-based management (RBM) has emerged as a promising approach to safeguard coral reefs by prioritizing areas that can resist and recover from disturbances, ensuring the continued provision of ecosystem services under changing conditions (Mcleod et al., 2019). It is defined as using knowledge of current and future drivers (ecological or anthropogenic) influencing ecosystem function (e.g., coral disease outbreaks; changes in land-use, trade, or fishing practices) to prioritize, implement, and adapt management actions that sustain ecosystems and human well-being. The main goal of RBM is to identify and prioritize management actions that enhance system resilience (e.g., by protecting processes and species that support a system's capacity to withstand and recover from disturbance). However, a key challenge in implementing such strategies is the lack of spatially explicit tools that can identify resilient reef areas and guide targeted conservation actions. While previous studies have assessed coral reef resilience using varying numbers of factors, from 1 factor (Ramahatratra, 2014) to 126 factors (Lam, 2017), they often lack the flexibility to adapt to diverse management priorities and provide actionable spatial insights for local stakeholders. This study addresses these gaps by developing a Multi-Criteria Evaluation (MCE) framework that integrates the Analytical Hierarchy Process (AHP) and Weighted Linear Combination (WLC) to assess coral reef resilience in a spatially explicit manner. Using Sentinel-2 imagery and field data, we evaluate seven factors such as Coral Abundance, Framework, Herbivorous Attractive Areas (HAA), Depth, Fishing Pressure, Temperature Stress, and Turbidity across six scenarios reflecting biodiversity, local, and global priorities. This study aims to advance resilience-based management, ensuring the long-term sustainability of coral reefs and the communities that depend on them in the face of ongoing environmental challenges. The specific objectives are to: i) map resilience levels and quantify their surface areas in hectares, ii) identify high-resilience areas for protection and medium-resilience areas for restoration, and iii) provide practical, scenario-based strategies to support small-scale fishing communities.

4.2. Materials and methods

4.2.1. Study Area

The study was conducted in the Toliara Bay, specifically within the coral reef systems of Sarodrano (a fringing reef), Ankilibe, and the Great Toliara Reef (a barrier reef). The selection of these sites was based on several factors: i) accessibility, ii) ecological variability, encompassing both degraded and healthy areas to facilitate the discernment of local stressors, and iii) ecological complexity, given the co-existence of a barrier reef, a fringing reef, and patch reefs within the same coral reef system (Figure V.1)

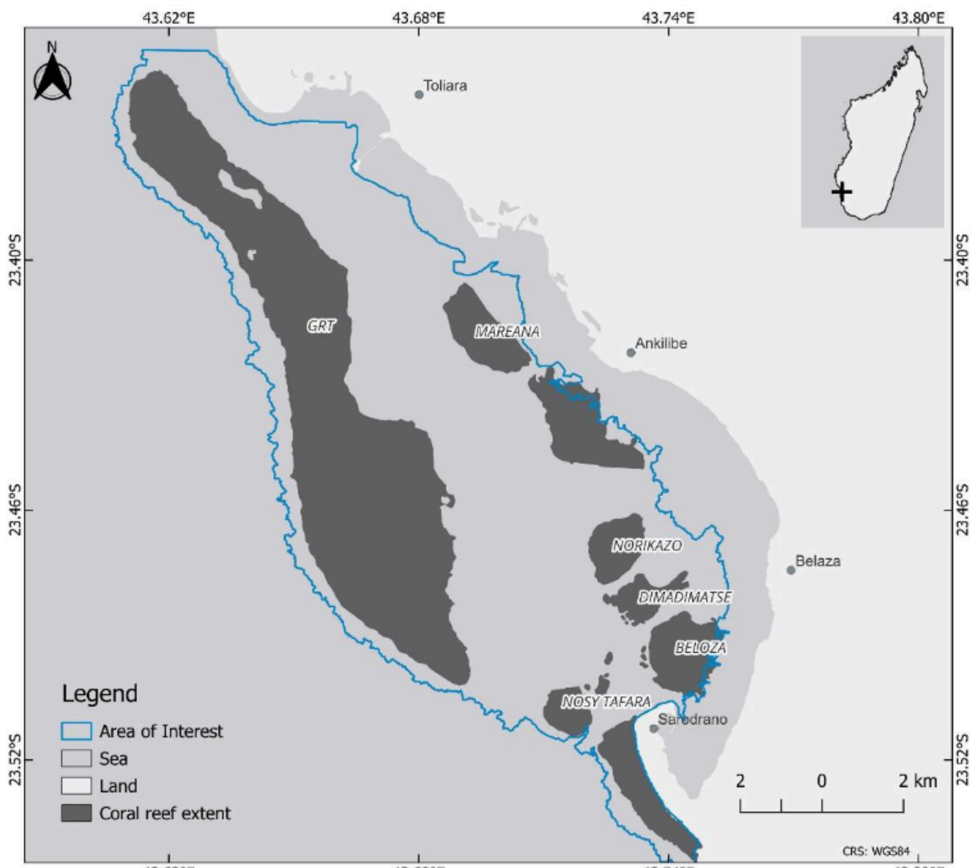

Fig.V. 1. Study area and local names of main coral reefs in Toliara. The blue line outlines the area of interest, indicating the boundary for satellite image clipping. The map distinguishes between land, sea, coral reef, and key areas of interest as well as the local name of the corresponding coral reefs.

4.2.2. Choice of Resilience Indices

Coral reef resilience is defined as the capacity of a reef ecosystem to resist or recover to its original state following disturbance (Randrianarivo et al., 2023). The present study assesses potential resilience areas by evaluating them against ecological, seascape, and anthropogenic indicators, in accordance with Resilience-Based Management principles (Maynard et al., 2015). We evaluate the resilience of coral reefs using seven key factors, organized into two categories. Landscape factors, including the abundance of live corals, framework abundance, the herbivorous fish attractive area (HAA), and water depth variability positively contribute to reef health. In contrast, stress factors, such as fishing pressure, turbidity, and temperature-related stress exert a negative influence on coral reefs. These factors were selected based on their proven significance in prior research, notably the studies by Rowlands et al., (2012) as well as their feasibility and relevance to our specific study area.

4.2.3. Data Collection

Benthic coverage

Benthic coverage was obtained from the processing of Sentinel-2A image accessed on 21-08-2021 from the Copernicus server (https://scihub.copernicus.eu/dhus/#/home), and a field work data collected between March and December 2021. Field work data collection consisted of two or three divers, one or two are taking benthic photos every 3-5 meters, guided by a compass to maintain course, while another at the surface moving synchronically with the first diver holding a GPS device that is secured in a floating airtight bag as GPS signal do not penetrate underwater. Each dive averaged 30 minutes, covering approximately 500 meters of transect where current conditions allowed; however, in instances of stronger currents, transects were shortened accordingly. Initial and final GPS coordinates of each transect were logged on a diving slate to facilitate subsequent GPS data integration. Approximately 250 photos were collected per transect, totaling 4187 photos. Ground-truthing data collection was confined to depths shallower than 20 meters. Detailed descriptions of the Sentinel-2A image processing to derive benthic coverage data can be found in Nomenisoa et al., (2024)[3].

[3] Chapter 3

Live coral abundance

Coral abundance is a direct measure of ecosystem robustness, making it a fundamental factor for assessing resilience and the reef's capacity to rebound from stress. Abundant coral populations indicate a system capable of withstanding and recovering from disturbances (Randrianarivo et al., 2024). Coral presence areas were identified based on benthic cover data provided by Nomenisoa et al. (2024). "Live coral abundance" was then estimated by interpolating "living coral" data points from the example of excel files generated by the CPCe (Annexe 1) across these areas using the Universal Kriging method, as described by Knudby et al. (2013).

Framework abundance

In this study, "Framework" refers to hard substrata (such as "living coral" and "rubble") based on the extents defined by Nomenisoa et al. (2024). These structures provide essential surfaces for coral larvae to settle and grow. Framework presence areas were first identified using benthic cover data from Nomenisoa et al. (2024). Subsequently, framework abundance was estimated by interpolating "living coral" and "rubble" data points from the Excel file (Annexe 1) across these areas, using the Universal Kriging method as described by Knudby et al. (2013). A stable and suitable framework enhances coral recruitment by offering attachment points and shelter, which are critical for rebuilding coral populations after disturbances like bleaching or storms (Wilson et al., 2006). Adequate hard substratum ensures successful coral recruitment, which sustains coral abundance and ecosystem function over time, making it essential for assessing how reefs recover and maintain stability.

Depth invariant index

Variations in depth influence the types of corals present and their resilience to stressors such as temperature shifts or sedimentation, making it a key structural factor. Depth affects light availability and temperature stability. These conditions shape coral growth patterns and their ability to cope with environmental changes. Deeper waters experience more stable temperatures and are less prone to the rapid warming events that cause bleaching in shallow reefs. Surface waters absorb more heat from solar radiation, while deeper areas benefit from thermal buffering, reducing the likelihood of exceeding corals' thermal tolerance thresholds (Lesser et al., 2018). The depth invariant index was retrieved from the Sentinel-2A image based on the water column correction technique from (Lyzenga, 1978). It is called "depth invariant" because it minimizes the influence of water depth on seafloor reflectance, aiming to isolate bottom type characteristics. This was useful for the benthic habitat mapping as shown in Chapter 3. The Depth Invariant Index (DII) does not directly measure water depth but can provide a rough indication of relative depth variations, suggesting areas where water is deeper or shallower based on reflectance patterns. In the absence of comprehensive bathymetric data during the preparation of this study, we applied this metric as a proxy to estimate depth trends across Toliara Bay, including the Great Reef of Toliara (GRT), Ankilibe reefs, and Sarodrano fringing reef.

Herbivorous Attractive Areas (HAA)

Initially, we quantified herbivorous fish biomass at selected sampling sites. However, we later determined that these data were not suitable, as they did not reliably reflect the actual presence of herbivorous fish in the surveyed areas. Fish are mobile, and each location was surveyed only once, making the resulting data unrepresentative of true fish biomass. Accurately capturing spatial patterns of fish biomass would require a long-term, multi-site survey, which was beyond our logistical capacity. As an alternative, we used "Herbivore Attractive Areas" (HAA) as a proxy for fish biomass data. In this study, HAA refers to areas within the reef ecosystem dominated by a mix of "seagrass", "algae", and "living coral" based on the extents defined by Nomenisoa et al. (2024). HAA presence areas were first identified using benthic cover data from Nomenisoa et al. (2024). Subsequently, HAA abundance was estimated by interpolating "living coral" and "seagrass" and "algae" data points from the Excel file (Annexe 1) across these areas, using the Universal Kriging method as described by Knudby et al. (2013). These habitats are indicators of presence of herbivorous organisms such as fish and invertebrate that dominate these zones. The herbivorous organisms within these areas enhance this resilience by controlling algal growth, preventing algae from overtaking coral surfaces maintain an ecological balance crucial for long-term reef health, ensuring corals remain competitive and capable of rebounding from disturbances (Mumby et al., 2006). However, we acknowledge the limitations of using HAA as a proxy. The presence of algae, for instance, does not always indicate herbivore activity as algae often colonize dead coral surfaces, which may not support herbivorous populations. Moreover, seagrass beds, while ecologically important, do not provide suitable substrate for coral recovery. These caveats were considered in our interpretation of the HAA data.

Fishing effort

Fishing effort refers to the intensity and methods of fishing activities within a coral reef ecosystem. Excessive or unsustainable fishing effort can deplete populations of key species, such as herbivorous fish that graze on algae. Without these herbivores, algae can overgrow, outcompeting corals for space and light, which weakens the reef's ability to recover from disturbances like bleaching or storms. Overfishing, particularly of herbivores, disrupts ecological balance and reduces coral recovery potential.(Bellwood et al., 2004; Hughes et al., 2010). Fishing effort is a critical human-induced stressor that directly affects reef resilience. By altering fish populations and ecosystem dynamics, it undermines the reef's capacity to maintain balance and recover from environmental challenges. Including fishing effort in the assessment ensures that management strategies can address this controllable factor to enhance reef health and stability. The spatial variability of the fishing efforts is retrieved from GPS trackers that are embarked onboard fishing pirogues. These GPS data are readily available for the small fishing villages around Toliara (Behivoke et al., 2021). The gridded data used in this study combine one year of monitoring all fishing practices in Toliara Bay, including beach seine, gillnet, handline, speargun, and mosquito trawl net.

Water turbidity

Turbidity reduces light penetration essential for photosynthesis by zooxanthellae within corals. High turbidity limits coral energy production, impairing growth and survival, especially under additional stressors. Turbidity from runoff or from very long raining seasons reduces the light available for photosynthesis by macroscopic and turf algae and endosymbiotic zooxanthellae within the tissues of corals (Rogers, 1990). By influencing the energy available to corals, turbidity is a vital factor in determining resilience to challenges like bleaching or disease. In this study, turbidity data reflect suspended particles in the water column that cause cloudiness from natural processes or human activities. These data represent the average annual turbidity value per pixel from 2019 to 2024, downloaded from Allen Coral Atlas (2020).

Thermal stress index

Rising sea temperatures are a major cause of coral bleaching, where corals expel their symbiotic algae (zooxanthellae), leading to weakened health and reduced recovery capacity. Prolonged or severe thermal stress can result in coral mortality. As a primary environmental stressor linked to climate change, thermal stress directly affects coral health and is critical for assessing how reefs might withstand future warming scenarios (Baker et al. 2008). Daily sea surface temperature (SST) data are obtained from MODIS Aqua satellite observations using the 11–12 micron channels, spanning June 2002 to June 2022. These data are publicly accessible at https://oceancolor.gsfc.nasa.gov/. Thermal stress is quantified as Degree Heating Weeks (DHW), calculated from the SST data following the methodology outlined by Liu et al. (2014). From June 2002 to June 2022, SST data were aggregated into 12-week (84-day) periods in order to calculate the DHW as shown in Liu et al. (2014). In this study, the thermal stress index represents the mean of DHW across all SST data collected over the 20-year period.

4.2.4. Standardization of Factors

After obtaining the results for all studied factors, we standardized them to enable comparison across variable with different units and scales (*i.e* they have different maximum values). The standardization ensures weighting across factors, despite their differing units or scales. This process transforms the data to a 0-1 range, aligning with the principles of fuzzy logic, as described by Zarin et al., (2021). In the TerrSet LiberaGIS software (Clark Center for Geospatial Analytics-Clark CGA, 2024), this approach involves applying membership functions. So, we select a decreasing sigmoidal function for negative factors (*e.g.,* thermal stress) and an increasing sigmoidal function for positive factors (*e.g.,* coral abundance) (Clark Center for Geospatial Analytics-Clark CGA, 2024).

4.2.5. Multicriteria Evaluation

Multi-Criteria Evaluation (MCE) also known as Multi-Criteria Decision Making (MCDM) emerged in the 1960’s as a decision-making framework to tackle complex problems involving multiple, often conflicting criteria (Zeleny, 1975). MCE gained popularity in the 1980’s as computational advancements enabled broader applications (Zeleny, 1975), and has extensively applied beyond marine contexts, ranging from business and supply chain management (Kahraman et al., 2003), to urban planning (Mosadeghi et al., 2015), and even in healthcare (Özkan, 2013) among several other applications. The MCE framework is designed to evaluate several criteria to meet a specific objective (Voogd, 1983; Carver, 1991). Criteria is divided into two categories: constraints and factors. Constraints define areas where the model refers as non-resilient areas, unsuitable for coral restoration, or transplantation programs. These areas include regions dominated by sand, deep water, or any regions outside of the area of interest (Figure 28-h). Sand presence areas were first identified using benthic cover data from Nomenisoa et al. (2024). Factors, on the other hand, are criteria that either positively or negatively influence coral reef resilience. In this study, factors such as Live coral abundance, Framework abundance, Depth invariant index, HAA, positively influence coral reef resilience when their value increase. Conversely, fishing effort, water turbidity and thermal stress negatively impact resilience when their value increase. The core of the evaluation process involves the Analytical Hierarchy Process (AHP), a structured decision-making technique developed by Saaty (1977) to determine the relative importance of each factor. The process starts by defining the objective, which consists of identifying resilient reefs suitable for protection and restoration programs in this study, guiding the prioritization of factors. Pairwise comparisons are then conducted between all factors to assess their relative importance in achieving this objective. These comparisons are made on a 9-point continuous scale, ranging from 1/9 (indicating one factor of very low importance) to 9 (indicating factors of very high importance), with intermediate values like 1/3, 1, and 3 representing moderate differences or equality (Tableau V.1).

Tab.V. 1. The continuous rating scale

Scale	1/9	1/7	1/5	1/3	1	3	5	7	9
Attribute	Extremely	Very strongly	Strongly	Moderately	Equally	Moderately	Strongly	Very strongly	Exremely
	Less important					More important			

A square pairwise comparison matrix is elaborated, where rows and columns represent the seven factors (Fishing Pressure, Thermal stress, Turbidity, Coral Abundance, Depth, Framework, HAA). The diagonal entries of the matrix are always 1, as each factor is equally important to itself, and reciprocity is enforced to maintain logical consistency: if for example, a Factor A is three times more important than a Factor B, then Factor B must be one-third as important as Factor A. (*e.g.*, If "Thermal Stress" is suggested as strongly more important than "Depth" for resilience, a value of 5 is assigned. If "Depth" is strongly more important, the reciprocal 1/5 is used). The pairwise comparison matrices are built using expert knowledge and scenario-specific priorities. Six scenarios are developed to reflect diverse conservation priorities, each represented by a unique matrix. These scenarios were categorized into three thematic groups: biodiversity-focused scenario, local impact scenarios, and global environmental stressor scenarios. The biodiversity scenarios include Scenario 1, which prioritizes "Coral abundance" and "HAA" while designating "Fishing Pressure" as the least important factor. This reflects a focus on ecological health and natural recovery processes. Scenario 2 prioritizes "Coral Abundance" and "Framework", treating "Thermal stress" as the least significant factor, showcasing the role of structural complexity and living coral cover in resilience. The local impact scenarios address factors influenced by human activity and habitat conditions at the local level. This includes Scenario 3 that prioritizes "Coral Abundance" and "Depth", with "Thermal stress" considered as least important, suggesting that resilience depends on coral health and water depth rather than climate stress. Scenario 4 focuses on "Fishing Pressure" and "Depth", with "Turbidity" assigned the lowest priority indicating concern for fishing pressure and local habitat stability in clear-water environments. Scenario 5 prioritizes "Fishing Pressure" and "Thermal stress", with "Framework" considered the least important. This approach combines the effects of local fishing activities with climate-related stress, placing less emphasis on the reef's structural features. Scenario 6 focuses on "Thermal stress" and "Turbidity", with "Framework" as the least significant factor, suggesting a resilience against warming and sediment stress in a global context.

4.2.6. Validation of matrices

To ensure the reliability of these matrices, their consistency is evaluated using the Consistency Ratio (CR), a metric that indicates the likelihood that the matrix ratings were randomly generated. The step-by-step method for the calculation of the CR is provided in Taherdoost (2017). A CR lower than 0.1 means that the values were likely adjusted to avoid logical contradiction. If the CR exceeds 0.1, the matrix is revised through iterative refinement, adjusting inconsistent judgments, such as ensuring that if "Thermal stress" is assigned a higher weight compared to "HAA", and "HAA" is assigned a higher weight compared to "Turbidity", then the weight of "Thermal stress" must be proportionally higher than "Turbidity's weight". This is repeated until CR is lower than

0,1. Once the matrices are validated, factor weights are derived using AHP. Each matrix column is normalized by dividing its entries by the column sum, and the average of each row in the normalized matrix yields the weight for the corresponding factor. These weights, which sum to 1, represent the relative importance of each factor in determining coral reef resilience. The weights are then applied in a Weighted Linear Combination (WLC) model to compute a resilience index, ranging from 0 to 1, for each pixel in the study area in order to map the scenarios. The resilience indices are then reclassified into five categories: non-resilient (index = 0), low, medium, high, very high. The MCE and the WLC computation are performed using geospatial software like TerrSet liberaGIS 20.0.1 (Clark Center for Geospatial Analytics-ClarkCGA, 2024). The QGIS software was used for geospatial data handling and visualization.

4.3. Results

4.3.1. Spatial variability of the resilience factors

Positive factors (Figure V.2.a-d) such as “Coral Abundance”, “Framework”, “HAA”, and “Depth Invariant Index” highlight areas of ecological strength, while negative factors (Figure V.2.e–g) such as “Thermal Stress”, “Fishing Effort”, and “Turbidity” identify stressors that undermine resilience. For these positive factors, a higher value (closer to 1) indicates areas where the conditions strongly enhance resilience. In contrast, negative factors (Figure V.2.e-g), lower values (closer to 0) indicate greater stress and thus lower the resilience. For example, elevated thermal stress values reflect intense heat exposure, increasing risks of coral bleaching, which lower the resilience (values close to 0), while higher values (near 1) mark areas with minimal heat stress, better suited for coral resilience. “Live corals” are clearly visible in Figure 28-a, particularly at the beginning of the outer slope. They are also present at deeper parts of the outer slope; however, this resilience study is limited to a maximum depth shallower than 20 meters as allowed by our satellite image processing to derive benthic coverage. The northern outer slope of the GRT hosts fewer live corals, though certain areas along the slope reach a maximum normalized abundance of 1 (especially prominent in the central section). The Sarodrano fringing reef and the internal reefs, particularly in Mareana, Nosy Tafara, and a few locations, also show a presence of live coral. Hard substrates, which are essential for coral larvae attachment, are abundant along the outer slope of the GRT, as well as within the fringing reef of Sarodrano, face oriented toward the outer slope. In contrast, the southern tip of the GRT is characterized by soft substrate. Hard substrate zones are also found around Nosy Tafara, the Sarodrano fringing reef, Belaza, and Ankilibe. The "HAA" (defined by the presence of live coral, encrusting algae on coral, and marine phanerogams) is more spatially dispersed across the GRT. Live coral and encrusting algae are primarily located at the beginning of the outer slope, while phanerogam areas are concentrated on the reef flat near the inner slope. Seagrass beds are also present within internal reef areas closer to the shore. In terms of depth suitability, the most favorable areas are found along the outer slope of the GRT and along a northern section of the inner slope. Additional suitable zones are located within the lagoon, surrounding patch reefs, and along the Sarodrano fringing reef. "Thermal stress" appears to be less severe in three areas: the northwest GRT, a central-west section of the reef, and the Sarodrano fringing reef. In contrast, the eastern parts of the reef and the lagoon experience higher levels of thermal stress. "Fishing pressure" is concentrated in distinct patches, many of which are located on the reef flat of the GRT, with others dispersed throughout the lagoon. Finally, "Turbidity" is notably high in two areas on the reef flat, while it remains relatively low on the outer slope and in the lagoon. The constraint map (Figure V.2.h) ensures that the analysis is limited to areas that are potentially suitable for coral growth. Regions where conditions are most favorable for coral resilience include the western zone of the GRT, particularly the outer slope and the western portion of the reef flat, as well as the internal reefs within the lagoon and the Sarodrano fringing reef. When combined in the WLC model with scenario-specific weights (e.g., from Scenarios 1–6), these standardized factors produce resilience maps that guide conservation efforts, such as prioritizing restoration or mitigating stressors in vulnerable areas.

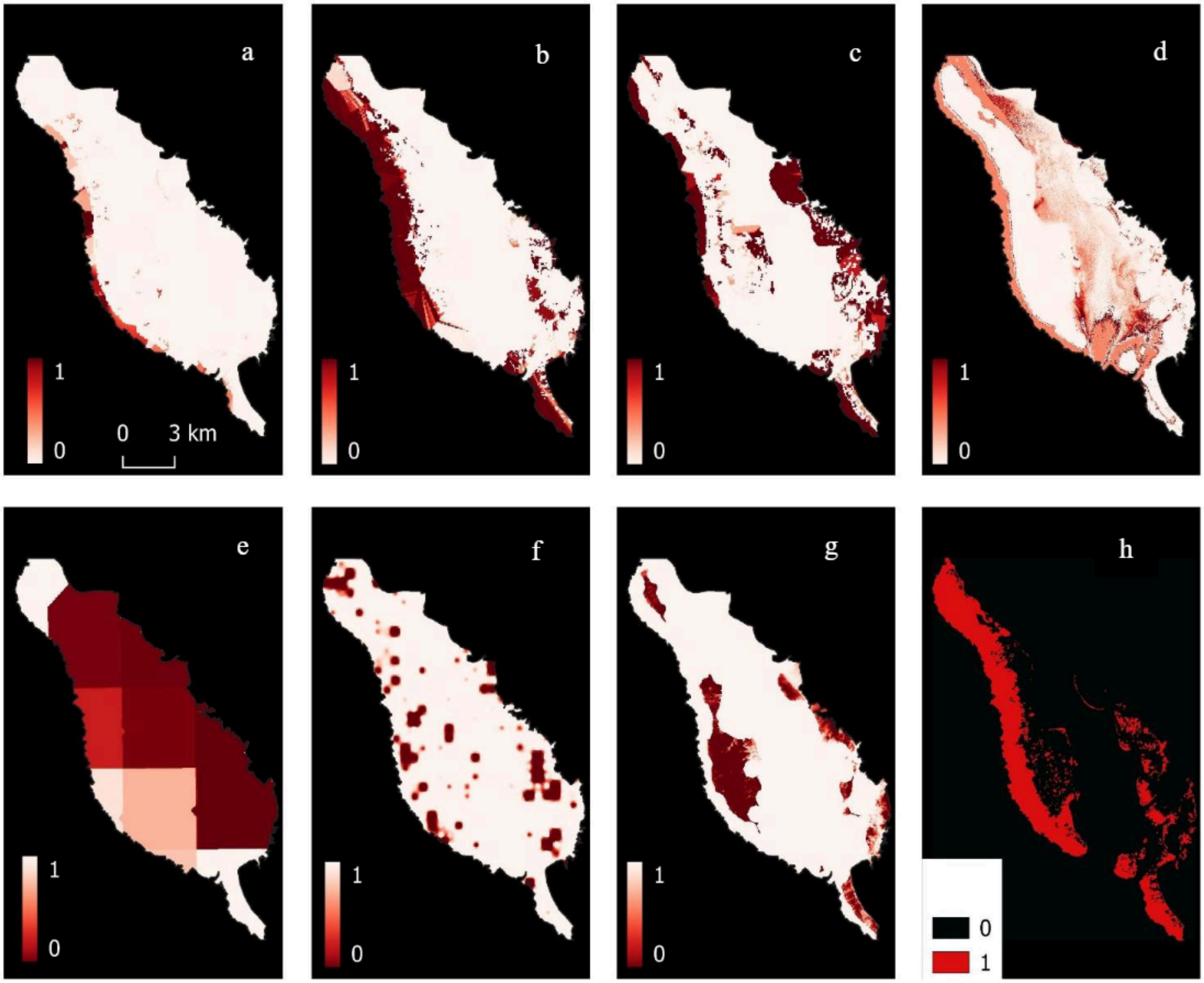

Fig.V. 2. Standardized factors. - a-abundance of living coral, b-framework abundance, c- herbivorous attractive areas, d-depth invariant index, e-Thermal stress, f-fishing effort, g-turbidity, h- constraint. For these positive factors (Figure 28 a-d), a higher value (closer to 1) indicates areas where the conditions strongly enhance resilience. In contrast, negative factors (Figure 28 e-g), lower values (closer to 0) indicate greater stress and thus lower the resilience. Constraints define areas where the model refers as non-resilient areas (black areas), unsuitable for coral restoration, or transplantation programs. These areas include regions dominated by sand, deep water, or any regions outside of the area of interest.

4.3.2. Conservation scenarios

First, during scenario construction (Annexe 6), an iterative process was conducted to validate the logical weighting of factors (see Materials and Methods). Consistency ratios (CR) were maintained below 0.1 across all scenarios, ensuring the reliability of the AHP-derived weights. Tableau V.2 presents the factor weights and corresponding CR values for each scenario.

Tab.V. 2. Factor weights and consistency ratio across scenarios (sc. = scenario)

Scenario	Biodiversity		Local effects		Global stressors	
Factor weight	Sc.1	Sc. 2	Sc.3	Sc. 4	Sc.5	Sc. 6
Fishing Pressure	0.03	0.1	0.12	0.26	0.29	0.12
Thermal Stress	0.15	0.03	0.03	0.09	0.29	0.29
Turbidity	0.15	0.05	0.09	0.03	0.1	0.29
Coral Abundance	0.27	0.27	0.33	0.15	0.16	0.06
Depth	0.09	0.15	0.33	0.26	0.05	0.1
Framework	0.05	0.27	0.05	0.09	0.02	0.03
HAA	0.27	0.13	0.08	0.15	0.09	0.12
Corresponding Consistency ratio for each scenario	0.01	0.01	0.01	0.02	0.01	0.01

4.3.2.1. Biodiversity Scenarios

These scenarios prioritize factors tied to biodiversity: “Coral Abundance” (abundance of reef-building species), “HAA” (Herbivorous attractive areas), and “Framework” (structural habitat supporting biodiversity). Scenario 1 emphasizes ecological health and resilience through biodiversity. “Coral abundance” and “HAA” are given the highest score compared to Fishing Pressure (Annexe 6.1). Fishing Pressure (overfishing) is deprioritized, suggesting that human exploitation is less critical than natural ecosystem processes in this context. High “Coral Abundance” ensures a diverse, living reef capable of withstanding stress, while “HAA” attract herbivorous that can control algae, preventing overgrowth and supporting coral recovery. Reefs here would thrive in areas with low fishing impact and strong herbivore populations and high coral abundance. Scenario 2 prioritizes focuses on biodiversity through living corals (Coral Abundance) and the physical structure they create (Framework), which supports diverse marine life (Annexe 6.2). “Thermal stress” is downplayed, implying resilience is driven by structural and biological integrity rather than climate-related stressors. These reefs might be in stable climates or deep waters less affected by warming, where habitat complexity is key. The biodiversity-focused scenarios both highlight areas of high and very high resilience along the outer reef slope of the Grand Toliara Reef (GRT), adjacent to the enclosed basin known as “*Grande Vasque*” as well as around Nosy Tafara and the Sarodrano fringing reef (Figure V.3). In Scenario 1, the “Fishing Pressure” factor was assigned a minimal weight, reducing its influence on the analysis. As a result, other stress-related factors, namely “Thermal Stress” (0.15), “Turbidity” (0.15), and “Depth” (0.09), had a more pronounced impact, as shown in Tableau 10. This explains the low resilience observed in areas with high thermal stress, such as the reef flat, fringing reefs, and shallow internal reefs in Belaza and Ankilibe. In Scenario 2, high to very high resilience is again observed along the outer slope, the Sarodrano fringing reef, and in the internal reefs of Belaza and Ankilibe. In this scenario, the “Thermal Stress” factor was assigned minimal weight, which reduced its influence. Instead, factors like “HAA” (0.13), “Depth” (0.15), and “Fishing Pressure” (0.10) played a more significant role in the multi-criteria evaluation (MCE) as shown in Tableau V.2. As a result, areas on the reef flat generally show “medium resilience”, while “low resilience” is found in the northern and southern sections of the GRT, as well as in some internal reef zones.

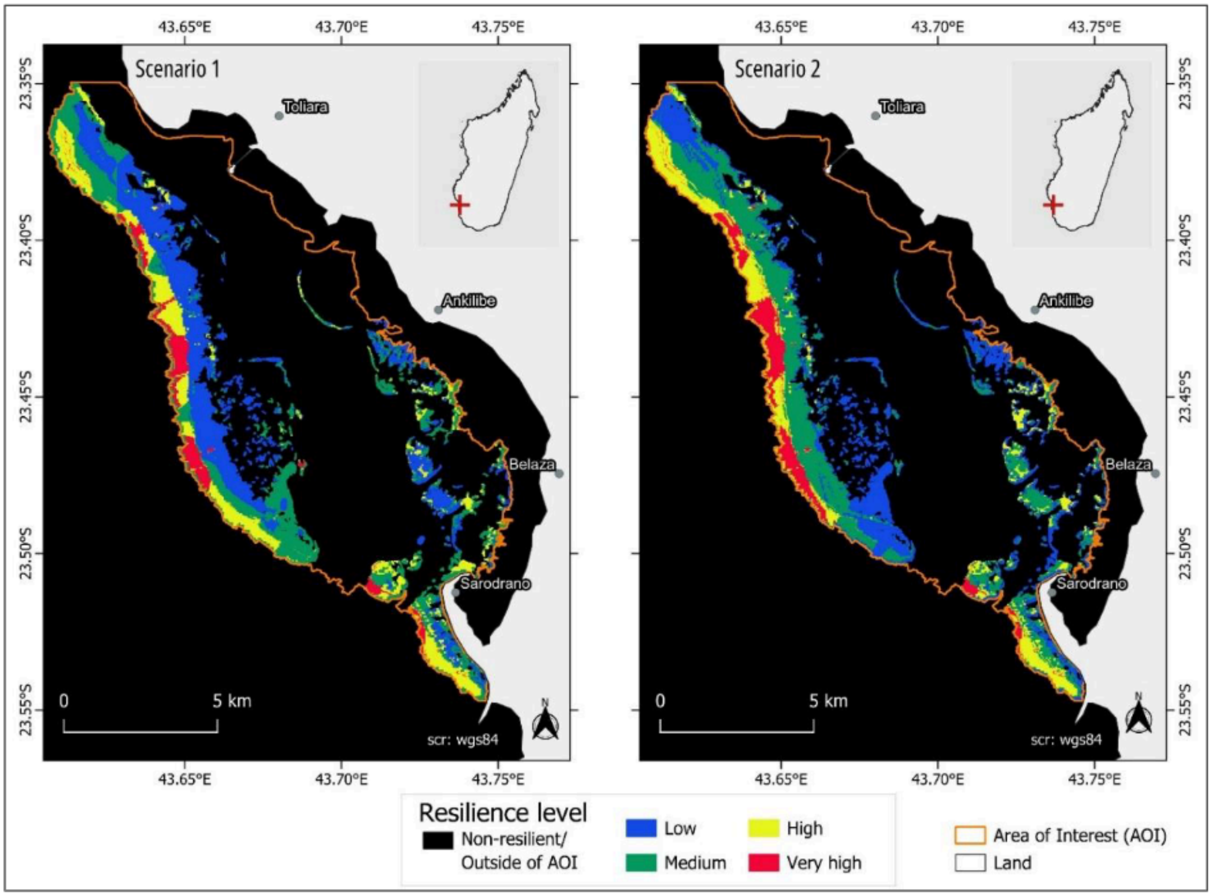

Fig.V. 3. Biodiversity-focused scenarios. Scenario 1: Prioritization of "Coral Abundance" and "HAA" with "Fishing Pressure" as least important. Scenario 2: Prioritization of "Coral Abundance" and "Framework" with "Thermal stress" as least important

4.3.2.2. Local Effect Scenarios

These scenarios emphasize factors influenced by local conditions: Fishing Pressure (human fishing activity) and Depth (local habitat variation). Scenario 3 (Annexe 6.3) prioritizes Coral Abundance and Depth, with Thermal stress as least important. This scenario links local habitat (Depth) with biodiversity (Coral Abundance), suggesting resilience hinges on coral thriving at specific depths (*e.g.,* deeper waters). Thermal stress is deprioritized, implying local conditions outweigh global warming effects. These reefs might be in areas with depth gradients offering refugia from surface stressors. Scenario 4 (Annexe 6.4) prioritizes "Fishing Pressure" and "Depth" with "Turbidity" as Least Important, indicating that resilience here depends more on managing overfishing and leveraging depth variations (e.g., deeper zones less fished). The local-effect scenarios also highlight areas of high to very high resilience along the outer reef slope of the GRT, as well as around Nosy Tafara and the Sarodrano fringing reef, particularly when locally driven factors such as "Fishing Pressure" and "Depth" were given higher weight (Figure V.4). In Scenario 4, "Fishing Pressure" and "Depth" were assigned the highest weights, leading to high and very high resilience values in deeper zones and in areas with lower fishing pressure, particularly along the outer reef slope of the GRT and the outer reef slope of Nosy Tafara and those of Sarodrano's fringing reef. Since "Turbidity" received the lowest weight, its influence on the analysis was minimal. As a result, other factors such as "Coral Abundance" (0.15), HAA (0.15), and "Framework" (0.09), as shown in Tableau V.2, played a more prominent role, contributing to the expansion of medium resilience areas, especially around Sarodrano, Belaza, and across the reef flat of the GRT (Figure V.4).

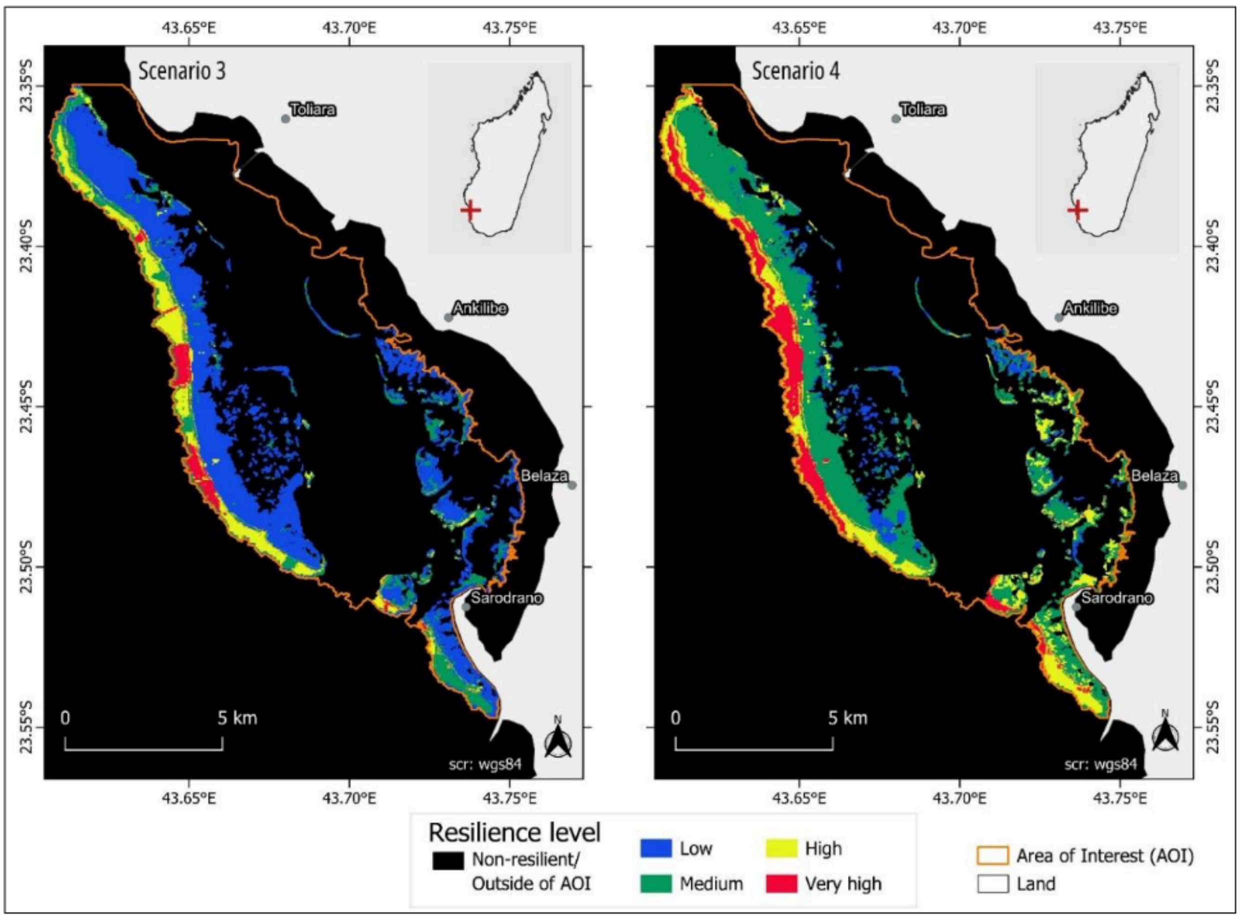

Fig.V. 4. Local effect scenarios. Scenario 3: Prioritization of "Coral abundance" and "Depth" with "Thermal stress" as least important. Scenario 4: Prioritization of Fishing Pressure and Depth with Turbidity as least important.

4.3.2.3. Global Effect Scenarios

These scenarios prioritize factors driven by broader environmental changes: “Thermal stress” (climate change) and Turbidity (runoff). Scenario 5 prioritizes Fishing Pressure and Thermal stress, with Framework as least important (Annexe 6.5). This mixes local (Fishing Pressure) and global (Thermal stress) effects, suggesting reefs scenarios where warming and overfishing are major threats. In this example, Framework is considered as least important, suggesting physical structure matters less than surviving heat stress and human pressure. These reefs might be in warming regions with fishing pressure, needing climate adaptation and local management. Since “Framework” received the lowest weight, its influence on the analysis was minimal. As a result, other factors such as “Coral Abundance” (0.16), “HAA” (0.09), as shown in Tableau 10, played a more prominent role, contributing to the expansion of high resilience areas, especially around Sarodrano, Nosy Tafara, and across northern part and southern part of the reef flat of the GRT (Figure V.5). Scenario 6 (Annexe 6.6) prioritizes “Thermal stress” and “Turbidity” with “Framework” as Least Important. Fully global-focused, this emphasizes “Thermal stress” and “Turbidity”, reflecting resilience tied to surviving climate change and high turbidity. The global-effect scenarios also highlight areas of high to very high resilience along the outer reef slope of the GRT, as well as around Nosy Tafara and the Sarodrano fringing reef, particularly when factors such as “Thermal stress”, and “Turbidity” were given higher weight. As a result, this contributes to the expansion of high resilience areas, especially around Sarodrano, Nosy Tafara, and across northern part and southern part of the reef flat of the GRT (Figure V.5).

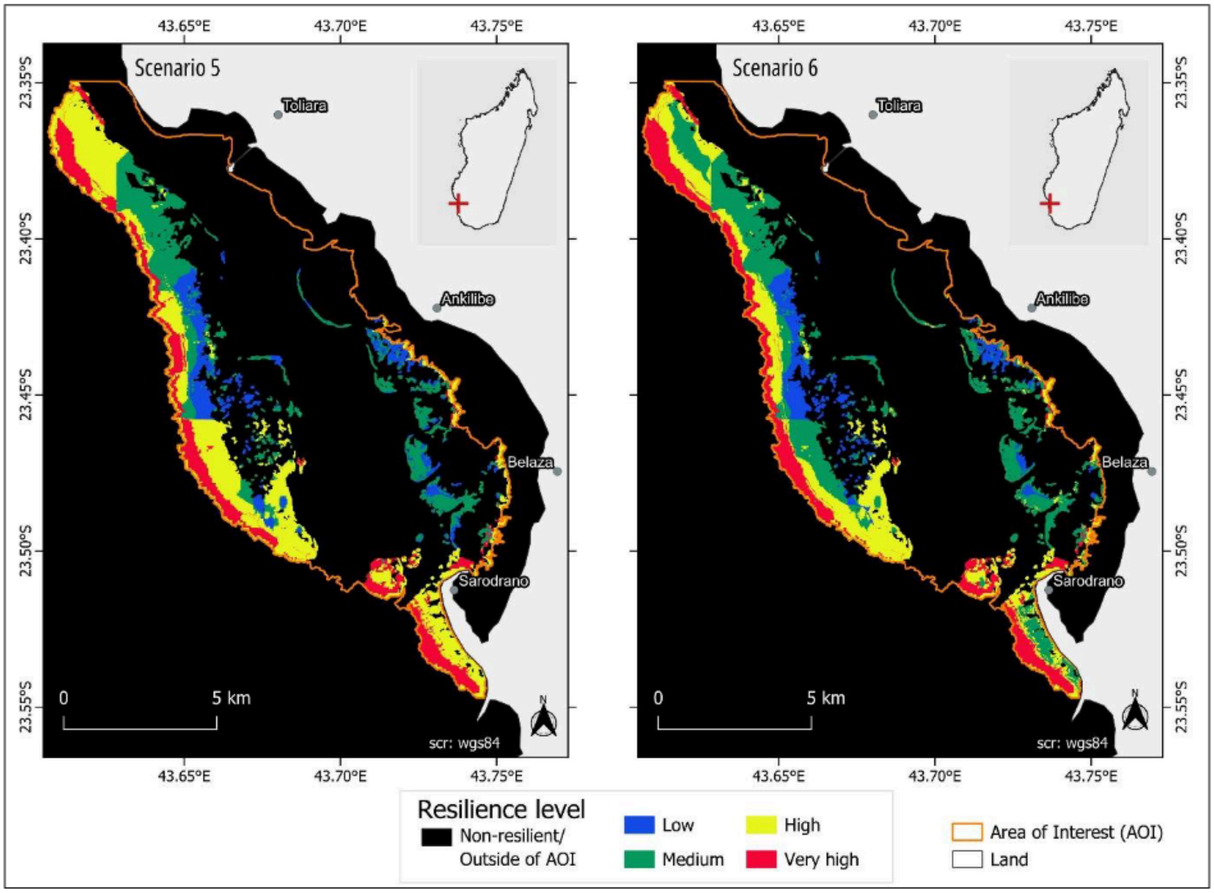

Fig.V. 5.Global effect scenarios. Scenario 5: Prioritization of Fishing Pressure and Thermal Stress with Framework as least important. Scenario 6: Prioritization of "Thermal stress" and "Turbidity" with "Framework" as least important

4.4. Discussion

4.4.1. Impact of Factor Weights on Coral Reef Resilience Across Scenarios

Our study's use of AHP and Weighted Linear Combination (WLC) to integrate ecological, local, and global factors into spatially explicit resilience maps. Previous studies have varied widely in the number of factors considered for resilience assessments. Randrianarivo et al. (2024) used eight factors to assess coral reef resilience, Obura et al. (2009) focused on 11 factors, Maynard et al. (2017) identified 17 factors, (McClanahan et al., 2012) considered 31 factors, and Lam (2017) recorded a total of 126 factors for coral reef resilience assessments. While these studies provide comprehensive frameworks, our study advances this by incorporating multiple scenario surface-based analysis with a focused set of seven key factors ("Coral Abundance", "Framework", "HAA", "Depth", "Fishing Pressure", "Temperature Stress", and "Turbidity"). Identifying sites with varying resilience potential is key for effective ecological assessments. Maynard et al. (2015) notes the challenge managers face in allocating resources: prioritizing high- or low-resilience sites. High-resilience sites, better at resisting and recovering from climate disturbances, sustain ecosystem goods and services (Maynard et al. 2017). They argue that resilience-based approaches, like the one in our study, can guide the allocation of conservation resources by prioritizing high and very high-resilience areas for protection while targeting medium-resilience areas for restoration, ensuring that management actions maximize long-term ecological benefits under climate change.

Biodiversity-focused Scenarios 1 and 2, which prioritize "Coral Abundance", "HAA", and "Framework", show a large extent of resilient areas ranging from Medium to Very high. Scenario 2 stands out with a structural emphasis, covering 2770 ha of Medium, High and Very High resilience areas (Tableau V.3), compared to Scenario 1's 2390 ha, highlighting the benefit of focusing on reef structure alongside coral health. Local-focused Scenarios 3 and 4, emphasizing "Fishing Pressure" and "Depth", demonstrate the value of managing fishing impacts and leveraging depth for resilience, particularly when "Thermal Stress" and "Turbidity" are less concerning, such as in the outer reef slopes of the GRT, Nosy Tafara and those of Sarodrano's fringing reefs. Global-focused Scenarios 5 (780 ha Very High) and 6 (820 ha Very High) show that climate-focused strategies can boost resilience, especially when "Fishing Pressure" and "Turbidity" are controlled, even if "Framework" is downplayed. During high coral bleaching events, managing "Fishing Pressure" can reduce low-resilience areas, while targeting restoration in low-turbidity zones can improve the success of coral transplantation and restoration efforts. Wooldridge (2009) supports this by mentioning the role for water clarity in lowering the thermal tolerance of corals, noting that while temperature is the primary driver of bleaching, water quality can reduce bleaching probability (e.g., Wooldridge, 2009).

Tab.V. 3. Surface area (Hectares) of resilience levels across scenarios

Resilience	Scn1	Scn2	Scn3	Scn4	Scn5	Scn6
Low	1430	1055	2300	250	390	355
Medium	1330	1570	760	2120	960	1400
High	780	800	560	895	1710	1200
Very High	280	400	190	560	780	820

Despite of the practicality of generating different resilient maps across different scenarios and their implication for decision-making, the varying priorities across scenarios reveal trade-offs in conservation strategies. Biodiversity-focused scenarios (1, 2) enhance ecological health but may overlook local stressors like Fishing Pressure, as seen in Scenario 1's large low-resilience area (1430 ha). Focusing on Framework (Scenario 2) improves resilience (2770 ha Medium to Very High) but might divert resources from addressing climate impacts, potentially leaving reefs vulnerable during bleaching events. To balance these trade-offs, a hybrid approach could integrate biodiversity, local, and global priorities, such as combining Scenario 2's ecological focus with Scenario 4's fishing management. This would maximize resilience while addressing both immediate community needs and long-term climate challenges. The spatially explicit resilience maps generated in this study align with the principles of integrated conservation planning, as demonstrated by Rowlands et al. (2012) and Knudby et al. (2014) who also used remote sensing approach and systematic conservation planning to design coral reef conservation zones that balance multiple objectives, including live "coral abundance", "framework abundance", "water depth variability", "fishing effort", and "temperature stress".

4.4.2. Potential Enhancements and New Research Avenues

The current study uses fixed weights for factors like Thermal Stress and Fishing Pressure, which may not reflect seasonal or annual variations. By integrating real-time data, such as climate forecasts or regular monitoring of small scale fishing using GPS tracking systems (Behivoke et al., 2021), weights could be adjusted dynamically. This would allow the model to adapt to changing conditions, such as sudden bleaching events or shifts in fishing pressure, providing more timely and relevant resilience maps. For instance, during a heatwave, increasing the weight of Temperature Stress could highlight vulnerable areas for immediate intervention, enhancing the model's utility for adaptive management. Another avenue for improvement is validating the resilience maps with long-term monitoring data to ensure their ecological accuracy. While the maps are based on standardized factors and validated with ground-truth data, their predictive power could be improved by comparing them against long-term time series datasets, such as coral cover trends or fish population surveys over decades. Besides, adding community-based observations from small-scale fishers could provide local insights, refining the maps' relevance.

For example, if Scenario 2's high-resilience areas (2770 ha of Medium, High and Very High) align with long-term recovery trends, this would confirm the model's reliability, while discrepancies could guide adjustments in factor weighting or selection. Expanding the scope of the study by including emerging stressors and engaging stakeholders offers a promising research direction. The current model focuses on seven factors, but emerging threats like ocean acidification, cyclones, or invasive species could significantly impact resilience. Adding these factors would provide a more comprehensive assessment, especially for global scenarios (e.g., Scenario 6), where climate stressors are prioritized. The absence of high-resolution bathymetric data is also one of the main limitations of this study. The analysis relied mainly on Lyzenga's depth-invariant index as a proxy for depth. Incorporating detailed bathymetric information could significantly improve the accuracy and depth of the analysis. Moreover, this study was restricted to areas shallower than 20 meters, yet deeper zones also host ecologically significant coral communities. For instance, Terrana et al. (2020) identified the presence of black corals the North channel of the GRT at depths between 30-50 meters, with about 20 species recorded. This highlights the importance of including deeper habitats in future assessments. Finally, establishing regular fish monitoring programs across the reef system would reduce reliance on proxies such Herbivorous Attractive Areas (HAA) and provide a more direct measure of ecosystem health for future resilience assessments. Moreover, turbidity and sedimentation are critical factors influencing coral resilience. While turbidity can serve as a useful indicator, future assessments would benefit from the installation of sediment traps throughout the reef system to directly measure sedimentation rates and their spatial variability. When building conservation scenarios, it is also crucial to consider logistical constraints and site accessibility, which can affect the feasibility of implementing decisions on the ground. This research led to the development of six scenarios: two biodiversity-focused, two addressing local pressures, and two reflecting global-scale influences. However, it is important to emphasize that the number of possible scenarios is not limited. Multiple parameters can be added, and the weight of each factor can be adjusted to reflect different priorities. The objective of this study is not to propose a definitive or exhaustive conservation strategy. Rather, it aims to serve as a foundation for participatory dialogue, bringing together scientists, decision-makers, NGOs, and local communities to collaboratively determine which factors should be prioritized and where conservation actions should be implemented. Engaging local stakeholders in the scenario development process can help ensure that the outputs are both contextually relevant and widely supported. For example, co-creating scenarios with fishers may result in a more nuanced consideration of fishing pressure, aligning resilience maps with local practices and promoting community-led conservation that is both effective and sustainable.

Conclusion

This study assesses coral reef resilience using a Multi-Criteria Evaluation (MCE) framework, integrating the Analytical Hierarchy Process (AHP) and Weighted Linear Combination (WLC) to map resilience across a reef system. Seven factors (Coral Abundance, Framework, HAA, Depth, Fishing Pressure, Temperature Stress, and Turbidity) were evaluated through six scenarios reflecting biodiversity (Scenarios 1–2), local (Scenarios 3–4), and global (Scenarios 5–6) priorities. Using satellites and field data, resilience maps were generated, categorizing areas as Low, Medium, High, and Very High, with hectare-based surface areas quantifying each level. Results show biodiversity-focused Scenario 2 (prioritizing Coral Abundance and Framework) achieved the largest resilient area (2770 ha of Medium to Very High), while local Scenario 4 (Fishing Pressure and Depth) minimized low-resilience areas (250 ha). Global Scenario 6 (Temperature Stress and Turbidity) showed strong very high resilience (820 ha). High-resilience zones were consistently along the reef front and external slope. This research advances coral reef management by providing a spatially explicit, scenario-based tool that integrates ecological, local, and global factors. It enables small-scale fishing communities and conservationists to prioritize protection in high-resilience areas and restoration in vulnerable zones. The methodology's flexibility, combining AHP with geospatial tools, sets a precedent for scalable resilience assessments, applicable beyond the study area. This study provides tools to foster dialogue among stakeholders (researchers, private and public sectors, civil society, and village communities) to collectively define not only the measures to prioritize but also to incorporate a spatial dimension into these measures: where the resilient areas are likely to be the highest and where to prioritize these conservation actions. An effective resilience based management depends on this collaboration and the geographic prioritization of the planned actions.

Chapitre 6

Discussion générale et conclusion

Chapitre 6 : Discussion générale et conclusion

6.1. Importance d'une approche combinée pour la recherche et la conservation des récifs coralliens

L'intégration de la télédétection et des données de terrain montre une avancée importante dans l'étude et la gestion des écosystèmes des récifs coralliens, en particulier dans des régions comme Toliara, Madagascar, où les pressions environnementales et anthropiques sont intenses. La télédétection, notamment via l'utilisation d'images satellitaires Sentinel-2A mises à disposition par l'Agence Spatiale Européenne (ESA) depuis 2015 permet une cartographie des zones géomorphologiques et des communautés benthiques, essentielle pour des régions comme le Grand Récif de Toliara (GRT). Cette capacité à couvrir de vastes étendues géographiques surpasse les limites des méthodes traditionnelles telles que les transects par interception linéaire (LIT) ou les quadrats, qui, bien que précises localement, manquent de représentativité à grande échelle (Bajjouk et al., 2019). Cependant, la télédétection seule présente des limites, notamment en termes de capacité à distinguer des classes benthiques spécifiques dans des environnements complexes. Le chapitre 2 met en évidence les défis rencontrés par certains algorithmes de classification, comme le Support Vector Machine (SVM), qui a montré une faible précision pour identifier les algues et les herbiers marins, contrairement au k-NN qui atteint une précision globale de 83 %. Ces variations soulignent la nécessité d'une calibration rigoureuse, souvent dépendante de données de terrain pour valider et affiner les résultats (Hedley et al., 2018). La synergie entre la télédétection et les données de terrain offre une évaluation holistique en combinant les forces de chaque méthode : l'échelle et la répétabilité de la télédétection avec la précision et la spécificité des observations *in situ*. Ainsi, bien que la télédétection fournisse une vue macroscopique, elle doit être complétée par des observations in situ pour garantir une interprétation fiable des données. Le Chapitre 4 utilise un modèle de Cellular Automata (CA) dans le plugin MOLUSCE pour projeter la couverture benthique jusqu'en 2034, prévoyant une perte continue de coraux et d'herbiers si les stress environnementaux persistent. Ces prédictions reposent sur des données historiques de Sentinel-2A validées par des relevés de terrain, illustrant comment la combinaison des deux sources permet de passer d'une analyse rétrospective à une prospective actionnable. L'utilisation de CNN pour la classification (81 % de précision en 2024) et de CA pour les projections met en lumière les transitions écologiques, comme la conversion de corail en débris (26,3 % entre 2015-

2024). Cette approche temporelle est cruciale pour suivre la dégradation historique du GRT, documentée depuis les années 1960 (Pichon, 1978), et anticiper les impacts futurs. Cependant, il faut noter que les variations interannuelles du recouvrement benthique dans les récifs de Toliara ne sont pas très significatives (Chapitre 4). Les changements notables ne deviennent apparents qu'à l'échelle d'une série temporelle d'environ dix ans. Cela suggère qu'il n'est peut-être pas nécessaire de mettre à jour les données chaque année. Le Chapitre 5 illustre la complémentarité entre ces deux approches à travers l'évaluation de la résilience des récifs coralliens à Toliara, où les données de terrain sur l'abondance corallienne, les poissons herbivores et la pression de pêche ont été intégrées dans un cadre d'évaluation multicritère (MCE). Cette approche a permis de générer des cartes de résilience spatialement explicites, identifiant des zones à haute résilience (1200 ha dans le scénario 2) pour la protection et celles nécessitant une intervention (760 ha de résilience moyenne résilience dans le scénario 3). Cette analyse contextuelle est importante à Madagascar, où les récifs soutiennent les communautés de pêcheurs face à des stress locaux (sédimentation, pression de pêche) et globaux (réchauffement) (Bruggemann et al., 2012). Dans l'avènement des nouvelles technologies, il est important de se rappeler que la technologie n'est pas le but final, mais un outil permettant aux scientifiques de collecter des informations de manière plus sûre, plus rapide et avec en grande quantité. Ainsi, l'introduction de nouvelles technologies dans la science des récifs coralliens, bien que nécessaire pour continuer à améliorer notre compréhension de la dynamique des récifs coralliens, ne doit pas interférer avec les méthodologies actuelles de collecte de données, mais plutôt améliorer ou compléter les méthodes actuelles (Obura, 2019).

6.2. Evolution des systèmes récifaux à Toliara depuis 1960 jusqu'en 2030

L'analyse spatio-temporelle des systèmes récifaux à Toliara montre une dégradation en cours. Dans les années 1960, les platiers récifaux du Grand Récif de Toliara (GRT) présentaient une couverture corallienne importante, dominée par des coraux branchus tels qu'*Acropora muricata* et *Isopora palifera*, ainsi qu'une diversité d'autres genres comme *Porites*, *Montipora*, *Lobophyllia* ou *Stylophora* (Pichon, 1978). Entre 1962 et 2011 (Figure VI.1), une évolution importante des communautés coralliennes a été mise en évidence à Toliara à partir de séries d'images aériennes et satellites. Les bandes transversales caractéristiques visibles au niveau du platier récifale dans les années 1960 ont progressivement laissé place, dès 2007, à des zones principalement composées de débris coralliens, de blocs isolés, et de coraux vivants couvrant moins de 5 % de la surface, souvent colonisés par des algues calcaires et macroalgues foliacées telles qu'*Ulva*, *Padina*, *Sargassum* et *Turbinaria* (Andréfouët et al., 2013). Une perte continue d'habitats coralliens sur les platiers externes du GRT a été documentée sur cette période, avec une perte moyenne estimée à 65 %, et une fourchette allant de 37 à 79 % (Andréfouët et al., 2013). Depuis 2024 (Figure VI.1.2), la couverture des platiers est majoritairement constituée de débris. Entre 2015 et 2024, les habitats coralliens ont perdu près de 7 km^2 et les herbiers marins près de 4km^2. Les modèles de prédiction indiquent que, si cette tendance se maintient, les pertes pourraient atteindre -1 km^2 (soit -2%) pour les coraux et -1.5 km^2 (soit -4%) pour les herbiers d'ici 2030. Bien que la dégradation des systèmes récifaux à Toliara soit bien documentée et susceptible de s'aggraver, des mesures de conservation stratégiques pourraient limiter ce déclin et préserver cet écosystème.

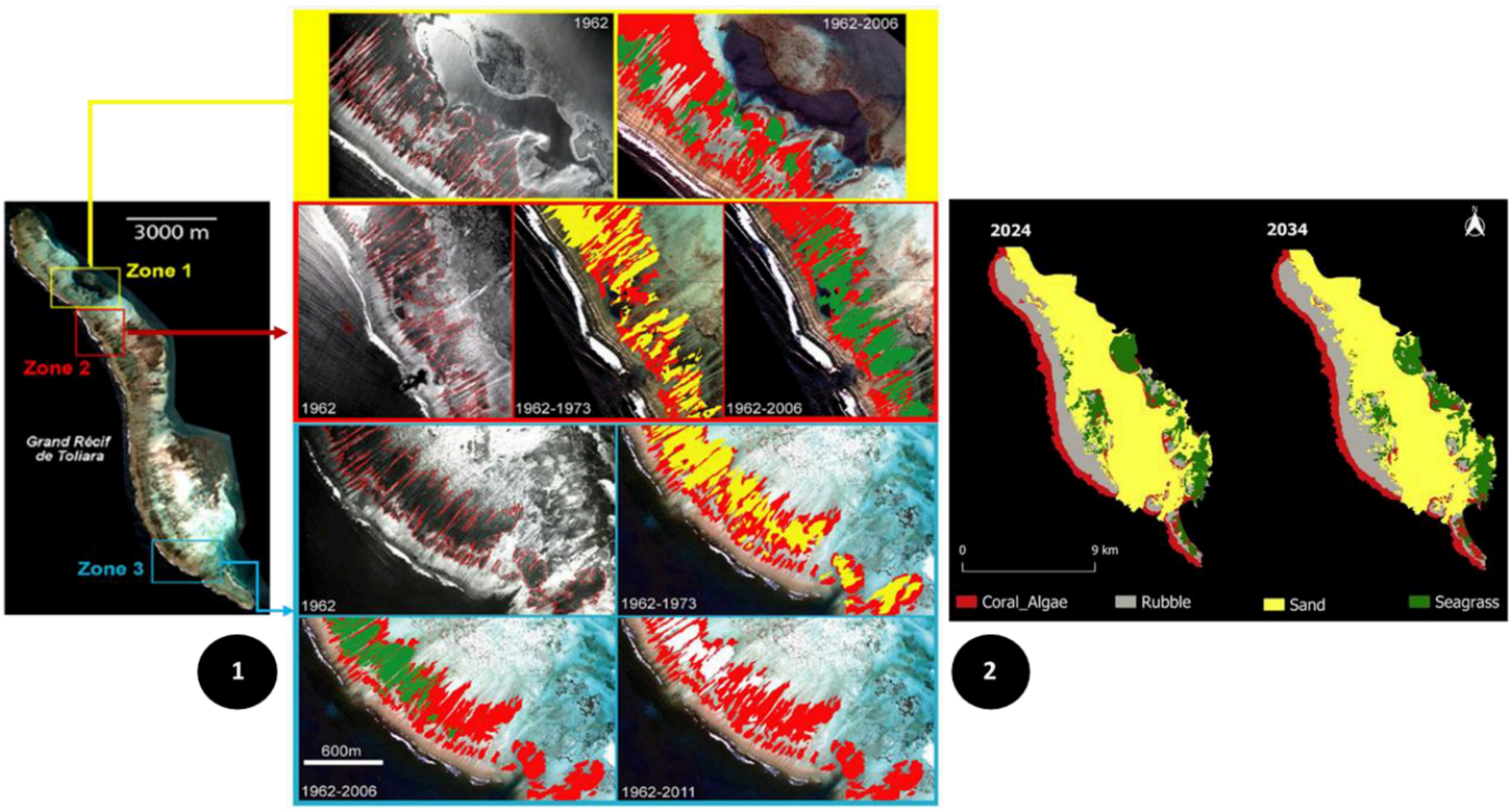

Fig.VI. 1. Evolution du GRT entre 1962 et 2034. Comparaison des photographies aériennes collectées en 1962 et en 1972 à des imageries satellitaires WorldView-2 collectés en 2006 et en 2011. Les couleurs rouges (Figure VI.1.1) indiquent la présence des coraux en 1962. Les couleurs jaunes indiquent les changements en 1972, les couleurs vertes indiquent les changements en 2006 et les couleurs blanches indiquent les changements qui ont eu lieu en 2011. Source : Andréfouet et al. 2013 (Modifiée). Fig.VI.1.2. Evolution du GRT entre 2024-2034 (traitement d'imageries Sentinel-2A), Chapitre 4 de cette thèse.

6.3. Gestion basée sur la résilience et scénarios de conservation

Le Cadre mondial de la biodiversité de Kunming à Montréal (Global Biodiversity Framework ou GBF) 30x30, adopté lors de la 15ème réunion des parties à la Convention sur la diversité biologique (CDB), vise à protéger 30 % des terres et des océans d'ici 2030 pour enrayer la perte de biodiversité. Les chapitres 3, 4 et 5 de cette thèse apportent des contributions à cet objectif mondial en fournissant des outils, des données et des approches transférables pour la conservation des écosystèmes marins, notamment les récifs coralliens, qui abritent une biodiversité exceptionnelle mais sont gravement menacés (Foo & Asner, 2019). Le Chapitre 4, avec son analyse des changements benthiques de 2015 à 2024 et ses prédictions jusqu'en 2034 via CNN et CA, contribue au GBF en fournissant un cadre pour surveiller l'état des récifs. Cette approche temporelle, utilisant des images accessibles comme Sentinel-2A, permet de suivre les tendances dans d'autres régions coralliennes, évaluant si les Aires Marines Protégés ou les habitats marins atteignent les objectifs de conservation du GBF. Le Chapitre 5 propose six scénarios de conservation pour offrir une dimension spatiale à l'évaluation de la résilience des écosystèmes récifaux. La résilience d'un récif corallien est définie par sa capacité à résister ou à revenir à son état initial après perturbation (Randrianarivo, 2023). Le concept de gestion basée sur la résilience (Resilience Based Management, RBM) a pris de l'importance récemment dans la gestion des écosystèmes de récifaux. Le RBM consiste à exploiter les connaissances sur les facteurs actuels et futures influençant les fonctions écosystémiques pour prioriser, mettre en œuvre et adapter les mesures de gestion qui préservent les écosystèmes et le bien-être humain (Mcleod et al., 2019). La quantification constitue un élément central dans l'application du RBM, et plusieurs travaux se sont attachés à identifier des métriques de résilience adaptées (Lam, 2017). Diverses études ont donc proposé des ensembles de métriques pour cette évaluation. (Randrianarivo et al., 2024) retiennent 8 métriques, incluant la richesse générique des coraux, la densité corallienne, la densité des juvéniles, la couverture corallienne, la couverture des coraux tolérants au stress, la couverture algale, la biomasse des poissons herbivores et les anomalies de température de surface (SST). Knudby et al. (2013) recensent 8 facteurs, tels que les taxons tolérants au stress, la diversité corallienne et la biomasse des herbivores. Rowlands et al. (2012) se basent sur 6 facteurs, notamment l'abondance des coraux vivants, l'abondance du substrat, la profondeur de l'eau, le stress thermique et le développement urbain. Ramahatratra (2014) se limite à un seul facteur : la biomasse de poissons herbivores. Obura et al. (2009) se sont focalisés sur 11 facteurs, Maynard et al. (2017) considèrent 17 facteurs, McClanahan et al. (2012) en identifient 31 facteurs, et Lam (2017) en évalue 126 pour les analyses de résilience des récifs coralliens. Dans cette étude, 7 facteurs ont été retenus pour leur pertinence dans l'évaluation et dans la zone d'étude, en s'inspirant de Rowlands (2011) et Knudby (2015), en proposant 6 scénarios. Ces scénarios sont classés selon qu'ils privilégient la biodiversité, les contextes locaux et globaux. Leur mise en œuvre reste complexe, car elle dépend non seulement du contexte environnemental, mais aussi des réalités sociales et économiques. Behivoke (2022) souligne la difficulté de l'application de la règlementation sur les engins non sélectifs étant donné que la petite pêche récifale est une pêche surtout de subsistance et de revenue pour les ménages locaux. Les zones où la pression de pêche est la plus forte sont désormais identifiées grâce au suivi de la trajectoire des pirogues à Toliara (Behivoke, 2022). Une solution envisagée pourrait donc consister à établir des réserves temporaires ou à installer des dispositifs de concentration de poissons (DCP) dans des zones moins fréquentées. Bien que ces mesures puissent être efficace, elles impliquent de modifier les pratiques et les habitudes de pêche, ce qui n'est pas sans conséquences pour les communautés. La limitation de l'accès libre compromettra le rôle de la petite pêche en tant que source de sécurité économique et/ou alimentaire, notamment pour les plus pauvres et les moins favorisés (Kolding and Van Zwieten, 2011). Au Kenya et en Tanzanie, dans le cadre du programme GMES and Africa, des données de télédétection détectent des zones de pêche potentielles et les communiquent en temps réel aux petits pêcheurs, accompagnées de prévisions météorologiques, d'équipements de sécurité et de soutien logistique pour naviguer au large, ainsi que d'un suivi régulier (Mutia and Sailale, 2021). Une autre piste d'intervention consiste à promouvoir l'aquaculture villageoise comme activité génératrice de revenus pour les petits pêcheurs tels l'holothuriculture, et de l'algoculture (Todinanahary et al., 2016). Rodine et al., (2024) recommandent également le développement de l'aquaculture de souches locales d'algues, notamment *H. musciformis, U. reticulata, H. opuntia, T. decurrens, P. pavonica, Gracilaria corticata, and U. lactuca*. Par ailleurs, plusieurs études ont proposé l'installation de récifs artificiels comme solution de restauration des habitats marins. Ces dispositifs ont montré des résultats prometteurs en moins de deux ans Todinanahary (2016) et Behivoke et al. (2018). La mise en place des Aires Marines Gérées Localement (LMMAs) représente également un levier important pour la conservation marine et le bien-être des populations côtières. De plus, l'intégration d'activités écotouristiques dans les stratégies de restauration et de conservation des écosystèmes marins émerge comme une mesure complémentaire, susceptible de générer des bénéfices économiques tout en valorisant le patrimoine naturel marin (Todinanahary et al., 2024) .

La dégradation des systèmes récifaux, tant à l'échelle locale que globale, incite à explorer diverses solutions pour freiner ou inverser cette tendance : régulation des engins et des zones de pêche, installation de récifs artificiels, promotion d'activités génératrices de revenus, ou encore reboisement en amont pour limiter la sédimentation liée aux apports fluviaux etc. Il ne suffit pas de se concentrer uniquement sur les effets globaux en ignorant les impacts locaux sur les systèmes récifaux, ni de privilégier les mesures de conservation locales au détriment des effets globaux. Face à la complexité de la dégradation des récifs, des solutions tout aussi complexes sont nécessaires. Toutes les mesures de gestion déjà mises en place ont leur pertinence et méritent d'être poursuivies. Toutefois, la difficulté réside dans leur application à grande échelle. C'est dans cette optique que le chapitre 5 de cette thèse a été élaboré. Résoudre un problème aussi complexe que la dégradation des systèmes récifaux de Toliara exige une approche adaptée.

Les zones récifales identifiées comme potentiellement résilientes, et nécessitant des actions de conservation, couvrent une superficie totale de 28 km² (résilience moyenne à très élevée) selon le scénario 2 (Tableau V.2). À cinq ans de l'échéance de l'objectif 2030 fixé par le Cadre mondial pour la biodiversité (GBF), atteindre la cible 30x30 implique pour les récifs de Toliara la protection de 30 % de ces 28 km², soit une surface de 8,4 km². En se basant sur le scénario 2 (Chapitre 5), axé sur la biodiversité, en privilégiant les facteurs « Abondance des coraux » et la « Abondance de substrats durs », et en réduisant l'effet du facteur « Stress thermique », on identifie des zones à très haute résilience totalisant 4 km². Celles-ci sont principalement situées sur la pente externe du Grand Récif de Toliara (GRT), autour de Nosy Tafara au sud, ainsi qu'au niveau de certaines portions du récif frangeant de Sarodrano (Figure V.1). La mise en protection de la partie nord de la pente externe du GRT représente une option stratégique, notamment en raison d'un effort de pêche relativement faible dans cette zone (Figure V.2- f), et une difficulté d'accès. Cette zone couvre environ 2 km². Par ailleurs, les zones résilientes au niveau des récifs de Norikazo, Beloza, Nosy Tafara, Mareana, ainsi que les récifs frangeants de Sarodrano, situés à proximité immédiate des villages côtiers, constituent des candidats pertinents pour des programmes de restauration, en particulier en raison de contraintes logistiques réduites. Ces zones couvrent ensemble une surface de 7 km². En combinant ces deux mesures de gestion, la mise en réserve de zones à faible pression halieutique et la restauration de récifs proches des communautés, il serait possible de protéger dès à présent environ 9 km² d'habitats récifaux à Toliara, contribuant ainsi de manière significative à l'atteinte de l'objectif 30x30 du GBF.

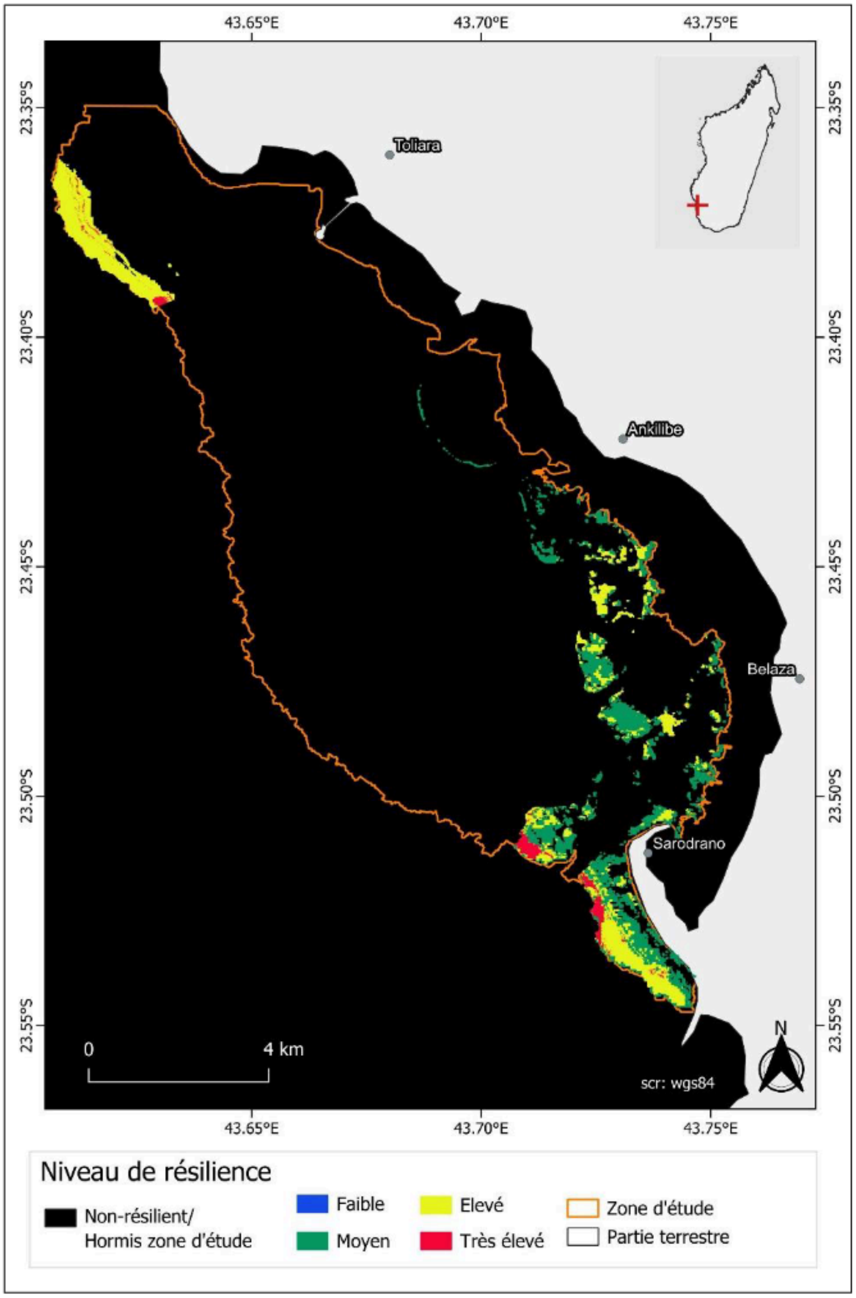

Fig.VI. 2.Contribution des zones récifales de Toliara à l'objectif GBF 30x30

Cette thèse va donc au-delà de la simple cartographie des habitats marins : il s’agit de fournir des outils pour encourager le dialogue entre les parties prenantes (chercheurs, secteur privé et publics, société civile, et communautés villageoises) afin de définir ensemble non seulement les mesures à privilégier mais surtout en intégrant une dimension spatiale à ces mesures : où prioriser ces actions de conservation. La Figure V.1 montre un diagramme factuel illustrant le rôle central des données scientifiques et de l'engagement des acteurs dans l'élaboration de scénarios de conservation des récifs coralliens pour optimiser les mesures de gestion. Convergeant vers la décision finale prise par une autorité (par exemple, un ministère), il intègre des scénarios de conservation, la politique générale, et les priorités globales/locales. Les données scientifiques, issues des données satellitaires (couverture corallienne, température, turbidité, etc.) et des relevés de terrain (biodiversité, photo transects, données de suivis écologiques, Paramètres physico-chimiques, etc.), apportent une dimension spatiale essentielle, permettant une délimitation des zones à protéger ou restaurer. Cette dimension spatiale accroît l'efficacité des scénarios. L’engagement des acteurs (société civile (ONG), pêcheurs villageois (connaissances locales), et secteur public/privé) repose sur une concertation multi-acteurs, où des interdépendances (collaboration, partenariats) renforcent la cohérence des propositions. Les mesures de gestion, incluant réserves marines, aquaculture villageoise, mise en place de récifs artificiels, régulation de la pêche, écotourisme, etc, traduisent ces informations en scénarios concrets. Les données scientifiques alimentent à la fois l’engagement et les mesures, tandis que la concertation propose des scénarios inclusifs à l’autorité décisionnelle. Ce processus met en lumière l’importance de la concertation pour des décisions éclairées et l’atout des données spatiales pour des scénarios efficaces. En intégrant science, concertation, et priorités stratégiques, le diagramme montre comment une approche collaborative et basée sur des données spatiales améliore la gestion des récifs coralliens, favorisant des décisions robustes et adaptées aux enjeux locaux et globaux. L’atteinte de l’objectif 30x30 repose sur cette approche intégrant science, concertation et priorisation géographique des actions envisagées.

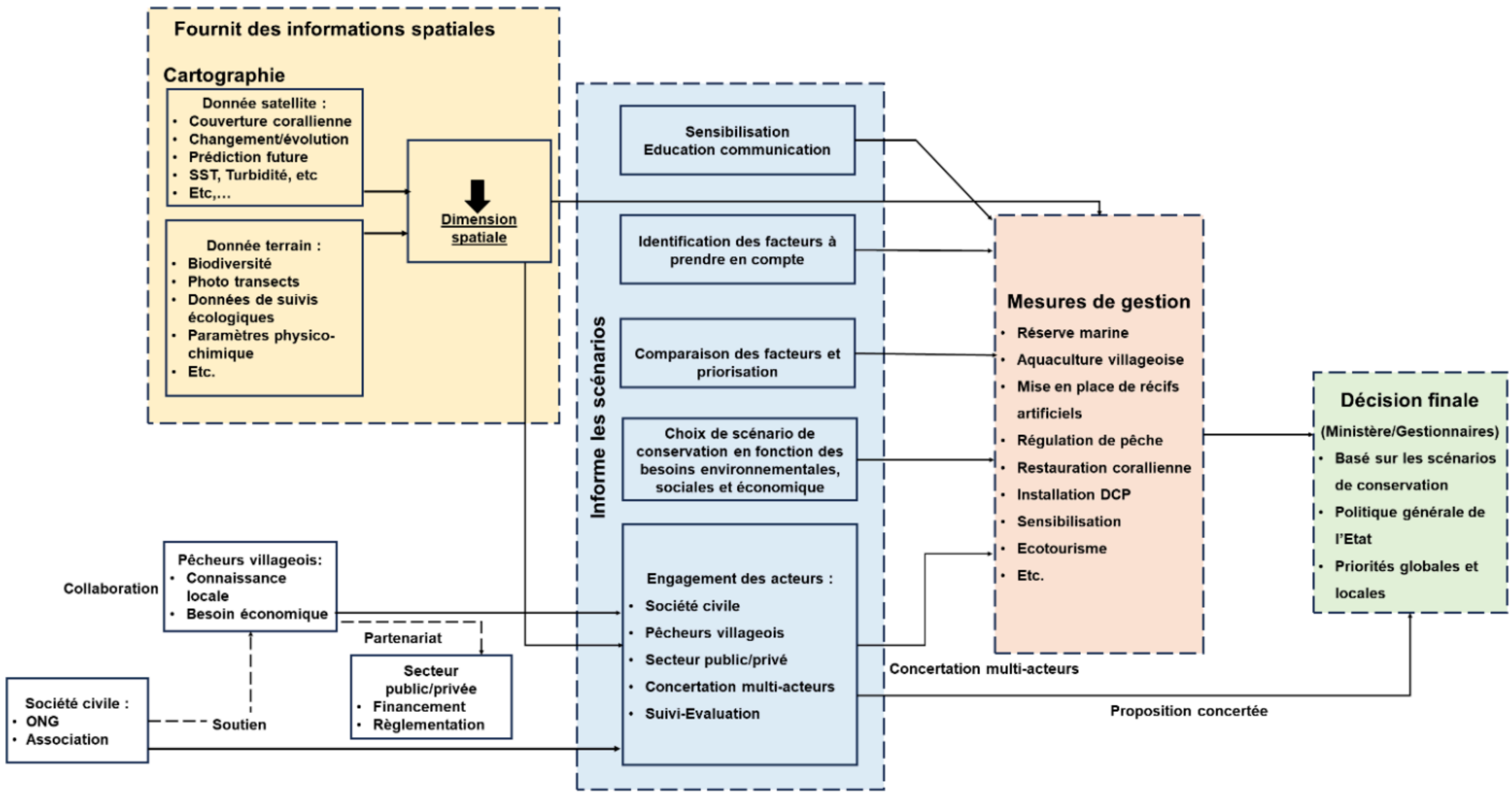

Fig.VI. 3. Diagramme factuel illustrant le rôle central des données scientifiques et de l'engagement des acteurs dans l'élaboration de scénarios

6.4. Améliorations potentielles et nouvelles pistes de recherche

Les chapitres 3, 4 et 5, centrés sur les récifs coralliens de Toliara à Madagascar, apportent des contributions significatives à la compréhension et à la gestion de ces écosystèmes grâce à l'intégration de la télédétection et des données de terrain. Cette thèse établit une base cartographique robuste en quantifiant les habitats benthiques de Toliara, surpassant les bases de données globales comme l'Allen Coral Atlas (d'une précision globale de 50 % contre 83 % dans cette thèse). Elle constitue ainsi un modèle de référence pour la cartographie des habitats marins à l'échelle de Madagascar. Parmi les perspectives envisagées, l'intégration de technologies émergentes, telles que les drones ou les caméras remorquées (permettant de collecter des données dans des zones trop profondes ou difficiles d'accès pour la plongée sous-marine), pourrait enrichir les données in situ. De plus, la résolution spatiale de 10 mètres, bien qu'adéquate pour une vue d'ensemble, limite la détection de détails fins, comme les petites colonies coralliennes ou les transitions subtiles entre habitats (Hedley et al., 2018). Cela peut sous-estimer la couverture réelle, notamment dans des zones hétérogènes comme les récifs frangeants de Sarodrano. La variabilité des algorithmes de classification pose également problème : le SVM affiche une faible précision (42 %) pour les algues et herbiers, tandis que le k-NN (83 %) domine, soulignant une dépendance au choix algorithmique et à la calibration locale (Nomenisoa et al., 2024). Une standardisation des protocoles de classification, comme suggéré dans le Chapitre 3, réduirait la variabilité algorithmique en établissant des lignes directrices pour le choix et l'optimisation des modèles (par exemple, k-NN vs SVM) en fonction des contextes locaux. Le chapitre 4 se concentre sur des facteurs comme la température, la turbidité et la pression de pêche, mais des menaces émergentes, telles que l'acidification des océans, les cyclones et les espèces invasives, restent sous-évaluées. L'évaluation de la résilience via une approche MCE avec sept facteurs, présente aussi des limites. Le choix de seulement sept facteurs exclut des stress émergents comme l'acidification ou la sédimentation ce qui peut sous-estimer la vulnérabilité réelle des récifs. L'incorporation d'informations bathymétriques détaillées pourrait améliorer significativement la précision et la profondeur de l'analyse. Cette étude s'est limitée aux zones de moins de 20 mètres de profondeur, alors que les zones plus profondes abritent également des communautés coralliennes écologiquement significatives. Enfin, la mise en place de programmes réguliers de suivi des poissons à travers le système récifal réduirait la dépendance aux indicateurs indirects comme les zones attractives pour les herbivores (HAA) et fournirait une mesure plus directe de la santé de l'écosystème pour les futures évaluations de résilience. De plus, la turbidité et la sédimentation sont des facteurs critiques influençant la résilience des coraux. Bien que la turbidité puisse servir d'indicateur utile, les futures évaluations bénéficieraient de l'installation de pièges à sédiments à travers le système récifal pour mesurer directement les taux de sédimentation et leur variabilité spatiale. Lors de l'élaboration de scénarios de conservation, il est également crucial de prendre en compte les contraintes logistiques et l'accessibilité des sites, qui peuvent affecter la faisabilité de la mise en œuvre des décisions sur le terrain. Il serait aussi pertinent d'explorer la création de nouveaux scénarios en intégrant des facteurs supplémentaires, en tenant compte des dynamiques environnementales, sociales et économiques, pour une approche plus holistique et adaptée.

Références

Ahmad, W., Neil, D.T., 1994. An evaluation of Landsat Thematic Mapper (TM) digital data for discriminating coral reef zonation: Heron Reef (GBR). Int. J. Remote Sens. 15, 2583–2597. https://doi.org/10.1080/01431169408954268

Allen Coral Atlas, 2020. Imagery, maps and monitoring of the world's tropical coral reefs. https://doi.org/10.5281/zenodo.3833242

Alzubaidi, L., Zhang, J., Humaidi, A.J., Al-Dujaili, A., Duan, Y., Al-Shamma, O., Santamaría, J., Fadhel, M.A., Al-Amidie, M., Farhan, L., 2021. Review of deep learning: concepts, CNN architectures, challenges, applications, future directions. J. Big Data 8, 53. https://doi.org/10.1186/s40537-021-00444-8

Ampou, E.E., Ouillon, S., Iovan, C., Andréfouët, S., 2018. Change detection of Bunaken Island coral reefs using 15 years of very high resolution satellite images: A kaleidoscope of habitat trajectories. Mar. Pollut. Bull. 131, 83–95. https://doi.org/10.1016/j.marpolbul.2017.10.067

Andréfouët, S., 2008. Coral reef habitat mapping using remote sensing: A user vs producer perspective. implications for research, management and capacity building. J. Spat. Sci. 53, 113–129. https://doi.org/10.1080/14498596.2008.9635140

Andréfouët, S., Chagnaud, N., Kranenburg, C., 2009. EEZ Madagascar, in: Atlas of Western Indian Ocean Coral Reefs. New Caledonia: Centre IRD de Nouméa.

Andréfouët, S., Guillaume, M.M.M., Delval, A., Rasoamanendrika, F.M.A., Blanchot, J., Bruggemann, J.H., 2013. Fifty years of changes in reef flat habitats of the Grand Récif of Toliara (SW Madagascar) and the impact of gleaning. Coral Reefs 32, 757–768. https://doi.org/10.1007/s00338-013-1026-0

Andréfouët, S., Muller-Karger, F., Robinson, J.A., Kranenburg, C., Torres-Pulliza, D., Spraggins, SA., Murch, B., 2006. Global assessment of modern coral reef extent and diversity for regional science and management applications: a view from space. Proc. 10th Int. Coral Reef Symp. 1732–1745.

Andréfouët, Serge, Muller-Karger, F., Robinson, J.A., Kranenburg, CJ., Torres-Pulliza, D., Spraggins, SA., Murch, B., 2006. Global assessment of modern coral reef extent and diversity for regional science and management applications: a view from space. Proc. 10th Int. Coral Reef Symp. 1732–1745.

Arnold, C., Biedebach, L., Küpfer, A., Neunhoeffer, M., 2024. The role of hyperparameters in machine learning models and how to tune them. Polit. Sci. Res. Methods 12, 841–848. https://doi.org/10.1017/psrm.2023.61

B. Lyons, M., M. Roelfsema, C., V. Kennedy, E., M. Kovacs, E., Borrego-Acevedo, R., Markey, K., Roe, M., M. Yuwono, D., L. Harris, D., R. Phinn, S., Asner, G.P., Li, J., E. Knapp, D., S. Fabina, N., Larsen, K., Traganos, D., J. Murray, N., 2020. Mapping the world's coral reefs using a global multiscale earth observation framework. Remote Sens. Ecol. Conserv. 6, 557–568. https://doi.org/10.1002/rse2.157

Bajjouk, T., Mouquet, P., Ropert, M., Quod, J.-P., Hoarau, L., Bigot, L., Le Dantec, N., Delacourt, C., Populus, J., 2019. Detection of changes in shallow coral reefs status: Towards a spatial approach using hyperspectral and multispectral data. Ecol. Indic. 96, 174–191. https://doi.org/10.1016/j.ecolind.2018.08.052

Baker, A.C., Glynn, P.W., Riegl, B., 2008. Climate change and coral reef bleaching: An ecological assessment of long-term impacts, recovery trends and future outlook. Estuar. Coast. Shelf Sci. 80, 435–471. https://doi.org/10.1016/j.ecss.2008.09.003

Battistini, R., Bourrouilh, F., Chevalier, J.-P., Coudray, J., Denizot, M., Faure, G., Ficher, J.-C., Guilcher, A., Harmelin-Vivien, M., Jaubert, J., Laborel, J., Montaggioni, L., Masse, J.-P., Mauge, L.-A., Peyrot-Clausade, M., Pichon, M., Plante, R., Plaziat, J.-C., Plessis, Y.B., Richard, G., Salvat, B., Thomassin, B.A., Vasseur, P., Weydert, P., 1975. Éléments de terminologie récifale indopacifique. Téthys 7, 1–111.

Behivoke, F., 2022. Caractérisation spatio-temporelle de la pêche aux poissons récifo-lagonaires par trajectométrie dans la baie de Toliara (sud-ouest de Madagascar) (Thèse de Doctorat). Université de Toliara, Option: Gestion des ressources marines.

Behivoke, F., Etienne, M.-P., Guitton, J., Randriatsara, R.M., Ranaivoson, E., Léopold, M., 2021. Estimating fishing effort in small-scale fisheries using GPS tracking data and random forests. Ecol. Indic. 123, 107321. https://doi.org/10.1016/j.ecolind.2020.107321

Behivoke, F., Randrianandrasana, J., Razakandrainy, A., Todinanahary, G., 2018. Adaptation au changement climatique au niveau de l'écosystème corallien: valorisation de débris de coraux morts pour la création d'habitats artificiels. Acte Colloq. Int. 10p.

Behivoke, F., Todinanahary, G., Randrianandrasana, J., Razakandrainy, A., Ravelojaona, D., 2022. Fishes Banking ecotechnology: new concept for coral reef restoration. WIOMSA symposium, Environmental and Climate Vulnerability, Resilience & Adaptation.

Bellwood, D.R., Hughes, T.P., Folke, C., Nyström, M., 2004. Confronting the coral reef crisis. Nature 429, 827–833. https://doi.org/10.1038/nature02691

Boston, T., Van Dijk, A., Thackway, R., 2023. Convolutional Neural Network Shows Greater Spatial and Temporal Stability in Multi-Annual Land Cover Mapping Than Pixel-Based Methods. Remote Sens. 15, 2132. https://doi.org/10.3390/rs15082132

Botosoamananto, R.L., Todinanahary, G., Razakandrainy, A., Randrianarivo, M., Penin, L., Adjeroud, M., 2021. Spatial Patterns of Coral Community Structure in the Toliara Region of Southwest Madagascar and Implications for Conservation and Management. Diversity 13, 486. https://doi.org/10.3390/d13100486

Bruggemann, J.H., Rodier, M., Guillaume, M.M.M., Andréfouët, S., Arfi, R., Cinner, J.E., Pichon, M., Ramahatratra, F., Rasoamanendrika, F., Zinke, J., McClanahan, T.R., 2012. Wicked Social-Ecological Problems Forcing Unprecedented Change on the Latitudinal Margins of Coral Reefs: the Case of Southwest Madagascar. Ecol. Soc. 17, art47. https://doi.org/10.5751/ES-05300-170447

Burns, C., Bollard, B., Narayanan, A., 2022. Machine-Learning for Mapping and Monitoring Shallow Coral Reef Habitats. Remote Sens. 14, 2666. https://doi.org/10.3390/rs14112666

Carver, S.J., 1991. Integrating multi-criteria evaluation with geographical information systems. Int. J. Geogr. Inf. Syst. 5, 321–339. https://doi.org/10.1080/02693799108927858

Chirayath, V., Instrella, R., 2019. Fluid lensing and machine learning for centimeter-resolution airborne assessment of coral reefs in American Samoa. Remote Sens. Environ. 235, 111475. https://doi.org/10.1016/j.rse.2019.111475

Clark Center for Geospatial Analytics-ClarkCGA, 2024. TerrSet liberaGIS v20.0.1. Clark University, 921 Main Street, Worcester MA 01610-1477 USA.

Congalton, R.G., Green, K., . A, 2008. Assessing the Accuracy of Remotely Sensed Data: Principles and Practices. Mapping Science. CRC Press, Boca Rotan FL., Second Edition. ed. CRC Press, Boca Rotan FL.

Cooke, A., 2012. Madagascar - A guide to marine biodiversity. MYE Andohalo, Antananarivo, Madagascar.

D. Elvidge, C., B. Dietz, J., Berkelmans, R., Andréfouët, S., Skirving, W., E. Strong, A., T. Tuttle, B., 2004. Satellite observation of Keppel Islands (Great Barrier Reef) 2002 coral bleaching using IKONOS data. Coral Reefs 23, 123–132. https://doi.org/10.1007/s00338-003-0364-8

Delwart, S., 2015. Sentinel-2 User Handbook, ESA Standard Document. ed.

Dietterich, T.G., 2000. An Experimental Comparison of Three Methods for Constructing Ensembles of Decision Trees: Bagging, Boosting, and Randomization. Mach. Learn. 40, 139–157.

Eakin, C.M., Nim, C.J., Brainard, R., Aubrecht, C., Elvidge, C., Gledhill, D.K., Muller-Karger, F., Mumby, P.J., Skirving, W., Strong, A.E., Wang, M., Weeks, S., Wentz, F., Ziskin, D., 2010. Monitoring coral reefs from space. Oceanography 23.

Erez, J., Reynaud, S., Silverman, J., Schneider, K., Allemand, D., 2011. Coral Calcification Under Ocean Acidification and Global Change, in: Dubinsky, Z., Stambler, N. (Eds.), Coral Reefs: An Ecosystem in Transition. Springer Netherlands, Dordrecht, pp. 151–176. https://doi.org/10.1007/978-94-007-0114-4_10

ESA's Sentinel-2 team, 2015. The story of Sentinel-2. Eur. Space Agency 161, 4–9.

Fang, B., Pan, L., Kou, R., 2019. Dual Learning-Based Siamese Framework for Change Detection Using Bi-Temporal VHR Optical Remote Sensing Images. Remote Sens. 11, 1292. https://doi.org/10.3390/rs11111292

Foo, S.A., Asner, G.P., 2019. Scaling Up Coral Reef Restoration Using Remote Sensing Technology. Front. Mar. Sci. 6. https://doi.org/10.3389/fmars.2019.00079

Green, E.P., Mumby, P.J., Edwards, A.J., Christopher, D.C., 2000. Remote sensing handbook for tropical coastal management, UNESCO. ed, Coastal Management Sourcebooks. Paris.

Hamylton, S.M., 2017. Mapping coral reef environments: A review of historical methods, recent advances and future opportunities. Prog. Phys. Geogr. Earth Environ. 41, 803–833. https://doi.org/10.1177/0309133317744998

Hedley, J., Roelfsema, C., Koetz, B., Phinn, S., 2012. Capability of the Sentinel 2 mission for tropical coral reef mapping and coral bleaching detection. Remote Sens. Environ. 120, 145–155. https://doi.org/10.1016/j.rse.2011.06.028

Hedley, J.D., Roelfsema, C., Brando, V., Giardino, C., Kutser, T., Phinn, S., Mumby, P.J., Barrilero, O., Laporte, J., Koetz, B., 2018. Coral reef applications of Sentinel-2: Coverage, characteristics, bathymetry and benthic mapping with comparison to Landsat 8. Remote Sens. Environ. 216, 598–614. https://doi.org/10.1016/j.rse.2018.07.014

Hedley, J.D., Roelfsema, C.M., Chollet, I., Harborne, A.R., Heron, S.F., Weeks, S., Skirving, W., Strong, A.E., Eakin, C.M., Christensen, T.R.L., Ticzon, V., Bejarano, S., Mumby, P.J., 2016. Remote Sensing of Coral Reefs for Monitoring and Management: A Review. Remote Sens. 8.

Hochberg, E.J., 2011. Remote Sensing of Coral Reef Processes, in: Coral Reefs: An Ecosystem in Transition. Springer, Netherlands, pp. 25–35.

Hughes, T.P., Graham, N.A.J., Jackson, J.B.C., Mumby, P.J., Steneck, R.S., 2010. Rising to the challenge of sustaining coral reef resilience. Trends Ecol. Evol. 25, 633–642. https://doi.org/10.1016/j.tree.2010.07.011

Hughes, T.P., Kerry, J.T., Álvarez-Noriega, M., Álvarez-Romero, J.G., Anderson, K.D., Baird, A.H., Babcock, R.C., Beger, M., Bellwood, D.R., Berkelmans, R., Bridge, T.C., Butler, I.R., Byrne, M., Cantin, N.E., Comeau, S., Connolly, S.R., Cumming, G.S., Dalton, S.J., Diaz-Pulido, G., Eakin, C.M., Figueira, W.F., Gilmour, J.P., Harrison, H.B., Heron, S.F., Hoey, A.S., Hobbs, J.-P.A., Hoogenboom, M.O., Kennedy, E.V., Kuo, C., Lough, J.M., Lowe, R.J., Liu, G., McCulloch, M.T., Malcolm, H.A., McWilliam, M.J., Pandolfi, J.M., Pears, R.J., Pratchett, M.S., Schoepf, V., Simpson, T., Skirving, W.J., Sommer, B., Torda, G., Wachenfeld, D.R., Willis, B.L., Wilson, S.K., 2017. Global warming and recurrent mass bleaching of corals. Nature 543, 373–377. https://doi.org/10.1038/nature21707

Joyce, K.E., Phinn, S.R., Roelfsema, C.M., Neil, D.T., Dennison, W.C., 2004. Combining Landsat ETM+ and Reef Check classifications for mapping coral reefs: a critical assessment from the southern Great Barrier Reef, Australia. Coral Reefs 21–25.

Kabiri, K., Pradhan, B., Samimi-Namin, K., Moradi, M., 2013. Detecting coral bleaching, using QuickBird multi-temporal data: A feasibility study at Kish Island, the Persian Gulf. Estuar. Coast. Shelf Sci. 117, 273–281. https://doi.org/10.1016/j.ecss.2012.12.006

Kahraman, C., Cebeci, U., Ulukan, Z., 2003. Multi-criteria supplier selection using fuzzy AHP. Logist. Inf. Manag. 16, 382–394. https://doi.org/10.1108/09576050310503367

Kennedy, E.V., Roelfsema, C.M., Lyons, M.B., Kovacs, E.M., Borrego-Acevedo, R., Roe, M., Phinn, S.R., Larsen, K., Murray, N.J., Yuwono, D., Wolff, J., Tudman, P., 2021. Reef Cover, a coral reef classification for global habitat mapping from remote sensing. Sci. Data 8, 196. https://doi.org/10.1038/s41597-021-00958-z

Knudby, A., Jupiter, S., Roelfsema, C., Lyons, M., Phinn, S., 2013. Mapping Coral Reef Resilience Indicators Using Field and Remotely Sensed Data. Remote Sens. 5, 1311–1334. https://doi.org/10.3390/rs5031311

Knudby, A., Pittman, S.J., Maina, J., Rowlands, G., 2014. Remote Sensing and Modeling of Coral Reef Resilience, in: Finkl, C.W., Makowski, C. (Eds.), Remote Sensing and Modeling, Coastal Research Library. Springer International Publishing, Cham, pp. 103–134. https://doi.org/10.1007/978-3-319-06326-3_5

Kolding, J., Van Zwieten, P.A.M., 2011. The Tragedy of Our Legacy: How do Global Management Discourses Affect Small Scale Fisheries in the South? Forum Dev. Stud. 38, 267–297. https://doi.org/10.1080/08039410.2011.577798

Kuchler, D.A., 1986. Geomorphological nomenclature: reef cover and zonation on the Great Barrier Reef. Great Barrier Reef Marine Park Authority, Townsville, Qld.

Lam, V.Y.Y., 2017. The Dynamics and Resilience of Coral Reefs (Thèse de Doctorat). University of Queensland, Brisbane, Queensland, AUSTRALIA, 4072.

Lesser, M.P., Slattery, M., Mobley, C.D., 2018. Biodiversity and Functional Ecology of Mesophotic Coral Reefs. Annu. Rev. Ecol. Evol. Syst. 49, 49–71. https://doi.org/10.1146/annurev-ecolsys-110617-062423

Lewis, D.D., 1998. Naive (Bayes) at forty: The independence assumption in information retrieval, in: Nédellec, C., Rouveirol, C. (Eds.), Machine Learning: ECML-98, Lecture Notes in Computer Science. Springer Berlin Heidelberg, Berlin, Heidelberg, pp. 4–15. https://doi.org/10.1007/BFb0026666

Li, J., Knapp, D.E., Fabina, N.S., Kennedy, E.V., Larsen, K., Lyons, M.B., Murray, N.J., Phinn, S.R., Roelfsema, C.M., Asner, G.P., 2020. A global coral reef probability map generated using convolutional neural networks. Coral Reefs 39, 1805–1815. https://doi.org/10.1007/s00338-020-02005-6

Liu, G., Heron, S., Eakin, C., Muller-Karger, F., Vega-Rodriguez, M., Guild, L., De La Cour, J., Geiger, E., Skirving, W., Burgess, T., Strong, A., Harris, A., Maturi, E., Ignatov, A., Sapper, J., Li, J., Lynds, S., 2014. Reef-Scale Thermal Stress Monitoring of Coral Ecosystems: New 5-km Global Products from NOAA Coral Reef Watch. Remote Sens. 6, 11579–11606. https://doi.org/10.3390/rs61111579

Louis, J., Debaecker, V., Pflug, B., Main-Knorn, M., Bieniarz, J., Mueller-Wilm, U., Cadau, E., Gascon, F., 2016. Sentinel-2 Sen2Cor: L2A processor for users, in: Proceedings of the Living Planet Symposium 2016. ESA SP-740, Prague, Czech Republic.

Lyons, M.B., Murray, N.J., Kennedy, E.V., Kovacs, E.M., Castro-Sanguino, C., Phinn, S.R., Acevedo, R.B., Alvarez, A.O., Say, C., Tudman, P., Markey, K., Roe, M., Canto, R.F., Fox, H.E., Bambic, B., Lieb, Z., Asner, G.P., Martin, P.M., Knapp, D.E., Li, J., Skone, M., Goldenberg, E., Larsen, K., Roelfsema, C.M., 2024. New global area estimates for coral reefs from high-resolution mapping. Cell Rep. Sustain. 100015. https://doi.org/10.1016/j.crsus.2024.100015

Lyzenga, D.R., 1981. Remote sensing of bottom reflectance and water attenuation parameters in shallow water using aircraft and Landsat data. Int. J. Remote Sens. 2, 71–82. https://doi.org/10.1080/01431168108948342

Lyzenga, D.R., 1978. Passive remote sensing techniques for mapping water depth and bottom features. Appl Opt 17, 379–383.

Maynard, J.A., Marshall, P.A., Parker, B., Mcleod, E., Ahmadia, G., van Hooidonk, R., Planes, S., Williams, G.J., Raymundo, L., Beeden, R., Tamelander, J., 2017. A Guide to Assessing coral reef resilience for decision support, United Nations Environment Programme. ed. UN Environment, Nairobi, Kenya.

Maynard, J.A., McKagan, S., Raymundo, L., Johnson, S., Ahmadia, G.N., Johnston, L., Houk, P., Williams, G.J., Kendall, M., Heron, S.F., van Hooidonk, R., Mcleod, E., Tracey, D., Planes, S., 2015. Assessing relative resilience potential of coral reefs to inform management. Biol. Conserv. 192, 109–119. https://doi.org/10.1016/j.biocon.2015.09.001

McClanahan, T., Donner, S., Maynard, J., MacNeil, A., Graham, N., Maina, J., Baker, A., Alemu, J., Beger, M., Campbell, S., 2012. Prioritizing key resilience indicators to support coral reef management in a changing climate. PLoS ONE.

Mcleod, E., Anthony, K.R.N., Mumby, P.J., Maynard, J., Beeden, R., Graham, N.A.J., Heron, S.F., Hoegh-Guldberg, O., Jupiter, S., MacGowan, P., Mangubhai, S., Marshall, N., Marshall, P.A., McClanahan, T.R., Mcleod, K., Nyström, M., Obura, D., Parker, B., Possingham, H.P., Salm, R.V., Tamelander, J., 2019. The future of resilience-based management in coral reef ecosystems. J. Environ. Manage. 233, 291–301. https://doi.org/10.1016/j.jenvman.2018.11.034

Mosadeghi, R., Warnken, J., Tomlinson, R., Mirfenderesk, H., 2015. Comparison of Fuzzy-AHP and AHP in a spatial multi-criteria decision making model for urban land-use planning. Comput. Environ. Urban Syst. 49, 54–65. https://doi.org/10.1016/j.compenvurbsys.2014.10.001

Mountrakis, G., Im, J., Ogole, C., 2011. Support vector machines in remote sensing: A review. ISPRS J. Photogramm. Remote Sens. 66, 247–259. https://doi.org/10.1016/j.isprsjprs.2010.11.001

Mumby, P.J., Dahlgren, C.P., Harborne, A.R., Kappel, C.V., Micheli, F., Brumbaugh, D.R., Holmes, K.E., Mendes, J.M., Broad, K., Sanchirico, J.N., Buch, K., Box, S., Stoffle, R.W., Gill, A.B., 2006. Fishing, Trophic Cascades, and the Process of Grazing on Coral Reefs. Science 311, 98–101. https://doi.org/10.1126/science.1121129

Mumby, P.J., Skirving, W., Strong, A.E., Hardy, J.T., LeDrew, E.F., Hochberg, E.J., Stumpf, R.P., David, L.T., 2004. Remote sensing of coral reefs and their physical environment. Mar. Pollut. Bull. 48, 219–228. https://doi.org/10.1016/j.marpolbul.2003.10.031

Mutia, D., Sailale, I., 2021. Application of Remote Sensing and GIS to Identifying Marine Fisheries off the Coasts of Kenya and Tanzania. Oceanography 46–47. https://doi.org/10.5670/oceanog.2021.supplement.02-18

Nguyen, T., Liquet, B., Mengersen, K., Sous, D., 2021. Mapping of Coral Reefs with Multispectral Satellites: A Review of Recent Papers. Remote Sens. 13, 4470. https://doi.org/10.3390/rs13214470

Nicet, J.-B., Porcher, M., Pennober, G., Mouquet, P., Alloncle, N., Denis, Y., Gabrié, C., Nicolas, A., Pribat, B., Tollis, S., 2016. Aide pour la réalisation et la commande de cartes d'habitats normalisées par télédétection en milieu récifal sur les territoires français.: Guide de mise en œuvre à l'attention des gestionnaires. IFRECOR.

Nomenisoa, A.L.D., Todinanahary, G., Edwin, H.Z., Razakarisoa, T., Israel, J.B., Raseta, S., Jaonalison, H., Mahafina, J., Eeckhaut, I., 2024. Remote sensing of coral reef habitats in Madagascar using Sentinel-2 satellite images. West. Indian Ocean J. Mar. Sci. 23, 41–56. https://doi.org/10.4314/wiojms.v23i2.4

Nurlidiasari, M., 2004. The application of QuickBird and Multi-temporal Landsat TM data for coral reef habitat mapping - Case study: Derawan Island, East Kalimantan, Indonesia (Master of Science in Geo-Information Science and Earth Observation specialisation Coastal zones studies). insternational Institute for Geo-Information Science and Earth Observation, Enschede, The Netherlands.

Obura, D., Grimsditch, G., Marshall, P., Setiasih, N., Aeby, G., McLeod, L., Green, A., Bellwood, D., Choat, H., Machano, H., Abdulla, A., Steneck, R., Tamelander, J., 2009. Resilience assessment of coral reefs: assessment protocol for coral reefs, focusing on coral bleaching and thermal stress, International Union for Conservation of Nature and Natural Resources. ed. IUCN, Gland, Switzerland.

Özkan, A., 2013. Evaluation of healthcare waste treatment/disposal alternatives by using multi-criteria decision-making techniques. Waste Manag. Res. J. Sustain. Circ. Econ. 31, 141–149. https://doi.org/10.1177/0734242X12471578

Palandro, D., Andréfouët, S., Dustan, P., Muller-Karger, F.E., 2003. Change detection in coral reef communities using Ikonos satellite sensor imagery and historic aerial photographs. Int. J. Remote Sens. 24, 873–878. https://doi.org/10.1080/0143116021000009895

Payet, E., Dumas, P., Pennober, G., 2011. Modélisation de l'érosion hydrique des sols sur un bassin versant du sud-ouest de Madagascar, le Fiherenana. VertigO 11–3. https://doi.org/10.4000/vertigo.12591

Pelletier, C., Webb, G., Petitjean, F., 2019. Temporal Convolutional Neural Network for the Classification of Satellite Image Time Series. Remote Sens. 11, 523. https://doi.org/10.3390/rs11050523

Phinn, S.R., Roelfsema, C.M., Mumby, P.J., 2012a. Multi-scale, object-based image analysis for mapping geomorphic and ecological zones on coral reefs. Int. J. Remote Sens. 33, 3768–3797. https://doi.org/10.1080/01431161.2011.633122

Phinn, S.R., Roelfsema, C.M., Mumby, P.J., 2012b. Multi-scale, object-based image analysis for mapping geomorphic and ecological zones on coral reefs. Int. J. Remote Sens. 33, 3768–3797.

Pichon, M., 1978. Recherches sur les peuplements a dominance d'anthozoaives dans les vecifs covalliens de Tulear (Madagascar), Atoll Research Bulletin. ed. THE SMITHSONIAN INSTITUTION Washington, D.C., U.S.A.

Pichon, M., 1972. Les peuplements à base de sléractiniaires dans les récifs coralliens de la Baie de Toliara (Sud-Ouest de Madagsacar), Station Marine d'Endoume. ed. Marseille, France.

Poursanidis, D., Traganos, D., Teixeira, L., Shapiro, A., Muaves, L., 2020. Cloud-native seascape mapping of Mozambique's Quirimbas National Park with Sentinel-2. Remote Sens. Ecol. Conserv. 7, 275–291. https://doi.org/10.1002/rse2.187

Purkis, S.J., Gleason, A.C.R., Purkis, C.R., Dempsey, A.C., Renaud, P.G., Faisal, M., Saul, S., Kerr, J.M., 2019. High-resolution habitat and bathymetry maps for 65,000 sq. km of Earth's remotest coral reefs. Coral Reefs 38, 467–488. https://doi.org/10.1007/s00338-019-01802-y

Rakotondralambo, A., 2008. Origine et connaissance de l'érosion des sols des bassins versants de Madagascar : Conséquences sur les habitats des écosystèmes continentaux et marins côtiers-Protocole de suivi des flux et application au fleuve Onilahy. (Thèse de doctorat). Institut Halieutique et des Sciences Marines, Université de Toliara.

Ramahatratra, F., 2014. Etude de la capacité de résilience du Grand Récif de Toliara et de sa gestion durable (Thèse de Doctorat). Université de Toliara, Institut Halieutique et des Sciences Marines, Toliara, Madagascar.

Ranaivomanana, L., 2006. Identification des conditions d'appropriation de la gestion durable des ressources naturelles et des écosystèmes : « cas du Grand Récif de Toliara » (Thèse de Doctorat). Université de Toliara, Institut Halieutique et des Sciences Marines (IH.SM), Thèse en co-tutelle, Ecole Nationale d'Agrocampus Rennes (France), et Université de Toliara (Madagascar).

Randrianandrasana, J., 2019. El-Niño 2015-2016 : Conséquences sur les récifs coralliens de Sud-Ouest de Madagascar (Master en Sciences Marines et Halieutiques). Institut Halieutique et des Sciences Marines, Université de Toliara.

Randrianarivo, M., Gasimandova, L.M., Tsilavonarivo, J., Razakandrainy, A., Philippe, J., Guilhaumon, F., Botosoamananto, R.L., Penin, L., Todinanahary, G., Adjeroud, M., 2024. Assessing recovery potential of coral reefs in Madagascar and the effects of marine protected areas. Reg. Stud. Mar. Sci. 77, 103710. https://doi.org/10.1016/j.rsma.2024.103710

Raphael, A., Dubinsky, Z., Iluz, D., Netanyahu, N.S., 2020. Neural Network Recognition of Marine Benthos and Corals. Diversity 12, 29. https://doi.org/10.3390/d12010029

Razakandrainy, A., 2018. Mécanismes de maintien des populations de coraux dans la région de Toliara, sud-ouest de Madagascar (Mémoire DEA en Océanographie Appliquée). Université de Toliara, Institut Halieutique et des Sciences Marines (IH.SM), Toliara, Madagascar.

Rodine, C., Jaonalison, H., Kira, J.M., Rakotoarimanana, A., Ranivoarivelo, L., Rakotomahazo, C., Todinanahary, G., Tsiresy, G., Nomenisoa, A.L.D., Rakotonjanahary, F., Eeckhaut, I., Remanevy, M.E., Spencer, J., Rasolofonirina, R., Lavitra, T., 2024. Spatio-temporal variation of macroalgal assemblages in southwestern Madagascar. WIO J. Mar. Sci. 23, 135–150.

Roelfsema, C.M., Markey, K., Kennedy, E.V., Kovacs, E.M., Borrego-Acevedo, R., Fox, H.E., Bambic, B., Free, B., Rice, K., Phinn, S.R., 2019. Protocol for Georeferenced Benthic Photoquadrat Surveys, Remote Sensing and Research Centre, School of Earth and Environmental Sciences. ed. University of Queensland, Brisbane, Australia.

Rogers, C., 1990. Responses of coral reefs and reef organisms to sedimentation. Mar. Ecol. Prog. Ser. 62, 185–202.

Rowlands, G., Purkis, S., Riegl, B., Metsamaa, L., Bruckner, A., Renaud, P., 2012. Satellite imaging coral reef resilience at regional scale. A case-study from Saudi Arabia. Mar. Pollut. Bull. 64, 1222–1237. https://doi.org/10.1016/j.marpolbul.2012.03.003

Saaty, T.L., 1977. A scaling method for priorities in hierarchical structures. J. Math. Psychol. 15, 234–281. https://doi.org/10.1016/0022-2496(77)90033-5

Sefrin, O., Riese, F.M., Keller, S., 2020. Deep Learning for Land Cover Change Detection. Remote Sens. 13, 78. https://doi.org/10.3390/rs13010078

Sentinel Hub, 2025a. Normalized difference vegetation index. https://custom-scripts.sentinel-hub.com/custom-scripts/sentinel-2/ndvi/.

Sentinel Hub, 2025b. EVI (Enhanced Vegetation Index). https://custom-scripts.sentinel-hub.com/custom-scripts/sentinel-2/evi/.

Taherdoost, H., 2017. Decision Making Using the Analytic Hierarchy Process (AHP); A Step by Step Approach. Int. J. Econ. Manag. Syst. 2. https://hal.science/hal-02557320v1

Teichert, C., 1995. Photointerpretation of coral reefs in Australia during World War II. Carbonates Evaporites 10, 102–104. https://doi.org/10.1007/BF03175245

Terrana, L., Bo, M., Opresko, D.M., Eeckhaut, I., 2020. Shallow-water black corals (Cnidaria: Anthozoa: Hexacorallia: Antipatharia) from SW Madagascar. Zootaxa 4826. https://doi.org/10.11646/zootaxa.4826.1.1

Thamarai, M., Aruna, S.P., 2023. Stressed Coral Reef Identification Using Deep Learning CNN Techniques. J. Electron. Inf. Syst. 5, 1–9. https://doi.org/10.30564/jeis.v5i2.5808

Todinanahary, G.G.B., 2016. Evaluation du potentiel biologique, économique et social de la coralliculture dans le sud-ouest de Madagascar (Thèse de Doctorat). Université de Mons (Belgique), Faculté des Sciences, Biologie des Organismes Marins et Biomimétisme.

Todinanahary, G.G.B., Behivoke, F., Nomenisoa, A.L.D., Ravelojaona, D.K., Rakotoson, T., Tatangirafeno, S., Rakotonjanahary, F., Tsiresy, G., Mara, E., Eeckhaut, I., Lavitra, T., 2016. Inventaire et étude de faisabilité de sites propices à l'algoculture, l'holothuriculture, la gestion de l'exploitation de poulpes et de crabes dans la Région Atsimo Andrefana, Contrat n° 166/C/PIC2/2016. ed.

Todinanahary, G.G.B., Randriamanantsoa, B., Randrianandrasana, J., Maharavo, J., Zerambay, S., Falinirina, A.M., Botosoamananto, R.L., Behivoke, F., Tsilavina, J.L., Rabemanantsoa, S.A., Tsimbazafihery, J.P., Bunyan, I.J., Masoava, J.A., David, J.M., Randrianarivo, M., Nomenisoa, A.L.D., 2024. État De Santé Des Récifs Coralliens A Madagascar, De 2016 A 2021.

Trimble Germany GmbH, 2022. eCognition Developer.

UNEP-WCMC, 2010. Global distribution of coral reefs, compiled from multiple sources including the Millennium Coral Reef Mapping Project. Version 1.3. Includes contributions from IMaRS-USF and IRD (2005), IMaRSUSF (2005) and Spalding et al. (2001).

UNEP-WCMC, WorldFish Centre, WRI, TNC, 2021. Global distribution of coral reefs, compiled from multiple sources including the Millennium Coral Reef Mapping Project. Version 4.1, updated by UNEP-WCMC. Includes contributions from IMaRS-USF and IRD (2005), IMaRS-USF (2005) and Spalding et al. (2001). Camb. UK UN Environ. Programme World Conserv. Monit. Cent. https://doi.org/10.34892/t2wk-5t34

Van Hooidonk, R., Maynard, J., Tamelander, J., Gove, J., Ahmadia, G., Raymundo, L., Williams, G., Heron, S.F., Planes, S., 2016. Local-scale projections of coral reef futures and implications of the Paris Agreement. Sci. Rep. 6, 1–8. https://doi.org/10.1038/srep39666

Velloth, S., Mupparthy, R.S., Raghavan, B.R., Nayak, S., 2014. Coupled correction and classification of hyperspectral imagery for mapping coral reefs of Agatti and Flat Islands, India. Int. J. Remote Sens. 35, 5544–5561. https://doi.org/10.1080/01431161.2014.926410

Veron, J., 2000. Corals of the World. Townsville: Australian Institute of Marine Science.

Voogd, H., 1983. Multicriteria evaluation for urban and regional planning, Pion Limited. ed. Pion Limited, 207 Brondesbury Park, London NW2 5JN.

Wicaksono, P., 2016. Improving the accuracy of Multispectral-based benthic habitats mapping using image rotations: the application of Principle Component Analysis and Independent Component Analysis. Eur. J. Remote Sens. 49, 433–463. https://doi.org/10.5721/EuJRS20164924

Wilkinson, C., 2008. Status of Coral reefs of the World, Global Coral Reef Monitoring Network (GCRMN). ed. PO Box 772, Townsville, 4810 Australia.

Wilson, S.K., Graham, N. a. J., Pratchett, M.S., Jones, G.P., Polunin, N.V.C., 2006. Multiple disturbances and the global degradation of coral reefs: are reef fishes at risk or resilient? Glob. Change Biol. 12, 2220–2234. https://doi.org/10.1111/j.1365-2486.2006.01252.x

Wooldridge, S.A., 2009. Water quality and coral bleaching thresholds: Formalising the linkage for the inshore reefs of the Great Barrier Reef, Australia. Mar. Pollut. Bull. 58, 745–751. https://doi.org/10.1016/j.marpolbul.2008.12.013

Wouthuyzen, S., Abrar, M., Corvianawatie, C., Salatalohi, A., Kusumo, S., Yanuar, Y., Darmawan, Samsuardi, Yennafri, Arrafat, M.Y., 2019. The potency of Sentinel-2 satellite for monitoring during and after coral bleaching events of 2016 in the some islands of Marine Recreation Park (TWP) of Pieh, West Sumatra. IOP Conf. Ser. Earth Environ. Sci. 284, 012028. https://doi.org/10.1088/1755-1315/284/1/012028

Xie, G., Niculescu, S., 2021. Mapping and Monitoring of Land Cover/Land Use (LCLU) Changes in the Crozon Peninsula (Brittany, France) from 2007 to 2018 by Machine Learning Algorithms (Support Vector Machine, Random Forest, and Convolutional Neural Network) and by Post-classification Comparison (PCC). Remote Sens. 13, 3899. https://doi.org/10.3390/rs13193899

Xu, J., Zhao, D., 2014. Review of coral reef ecosystem remote sensing. Acta Ecol. Sin. 34, 19–25. https://doi.org/10.1016/j.chnaes.2013.11.003

Xu, J., Zhao, J., Wang, F., Chen, Y., Lee, Z., 2021. Detection of Coral Reef Bleaching Based on Sentinel-2 Multi-Temporal Imagery: Simulation and Case Study. Front. Mar. Sci. 8, 584263. https://doi.org/10.3389/fmars.2021.584263

Yamano, H., 2013. Multispectral Applications, in: Goodman, J.A., Purkis, S.J., Phinn, S.R. (Eds.), Coral Reef Remote Sensing. Springer Netherlands, Dordrecht, pp. 51–78. https://doi.org/10.1007/978-90-481-9292-2_3

Yunus, A.P., Jie, D., Song, X., Avtar, R., 2019. High Resolution Sentinel-2 Images for Improved Bathymetric Mapping of Coastal and Lake Environments (preprint). EARTH SCIENCES. https://doi.org/10.20944/preprints201902.0270.v1

Zarin, R., Azmat, M., Naqvi, S.R., Saddique, Q., Ullah, S., 2021. Landfill site selection by integrating fuzzy logic, AHP, and WLC method based on multi-criteria decision analysis. Environ. Sci. Pollut. Res. 28, 19726–19741. https://doi.org/10.1007/s11356-020-11975-7

Zeleny, M., 1975. Multiple Criteria Decision Making, Kyoto 1975, M. Beckmann and H. P. Könzi. ed. 22d international meeting of TIMS, Kyoto, Japan.

Zhou, Z., Ma, L., Fu, T., Zhang, G., Yao, M., Li, M., 2018. Change Detection in Coral Reef Environment Using High-Resolution Images: Comparison of Object-Based and Pixel-Based Paradigms. ISPRS Int. J. Geo-Inf. 7, 441. https://doi.org/10.3390/ijgi7110441

Zhu, Z., Wulder, M.A., Roy, D.P., Woodcock, C.E., Hansen, M.C., Radeloff, V.C., Healey, S.P., Schaaf, C., Hostert, P., Strobl, P., Pekel, J.-F., Lymburner, L., Pahlevan, N., Scambos, T.A., 2019.

Benefits of the free and open Landsat data policy. Remote Sens. Environ. 224, 382–385. https://doi.org/10.1016/j.rse.2019.02.016

Zoffoli, M.L., Gernez, P., Rosa, P., Le Bris, A., Brando, V.E., Barillé, A.-L., Harin, N., Peters, S., Poser, K., Spaias, L., Peralta, G., Barillé, L., 2020. Sentinel-2 remote sensing of Zostera noltei-dominated intertidal seagrass meadows. Remote Sens. Environ. 251, 112020. https://doi.org/10.1016/j.rse.2020.112020

Annexes

Annexe 1: Exemple de fichiers de sorties d'une analyse d'image au CPCe

11170 fichiers similaires à ceux présentés ci-dessous ont été obtenu à partir des annotations au CPCe des phototransects à Toliara et à Salary. Ces données peuvent servir de données de validation terrain et d'entrainement de modèles d'apprentissage automatique.

RESULTS SUMMARY CHART	# Points	%	SW Index	Simpson (1-D)
CORAL (C)	31	63.27	1.76	0.75
SOFT CORAL (SC)	0	0.00	0.00	1.00
SPONGE (SP)	0	0.00	0.00	1.00
ZOANTHINIDAE (Z)	0	0.00	0.00	1.00
MACROALGAE (MA)	16	32.65	0.00	0.00
OTHER LIVE (OL)	0	0.00	0.00	1.00
CORALINE ALGAE (CA)	0	0.00	0.00	1.00
DEAD CORAL (DC)	2	4.08	0.00	0.00
SEAGRASS (SG)	0	0.00	0.00	1.00
SAND, PAVEMENT, RUBBLE (SPR)	0	0.00	0.00	1.00
UNKNOWNS (U)	0	0.00	0.00	1.00
TAPE, WAND, SHADOW (TWS)	0	0.00		
TOTALS	**49**	**100.00**		
NOTES (% of transect)				
Aspergillus (ASP)	0	0.00		
Black Band Disease (BBD)	0	0.00		
Bleached coral point (BL)	0	0.00		
Fluorescent bleaching (FLUOR)	0	0.00		
Other disease (OD)	0	0.00		
Plague, Type II (White Plague, Type II) (PLA)	0	0.00		
Recently dead coral with algae (RD)	0	0.00		
White Band Disease (WBD)	0	0.00		
Yellow Blotch Disease (YBD)	0	0.00		
NOTES (% of coral)				
Aspergillus (ASP)	0	0.00		
Black Band Disease (BBD)	0	0.00		
Bleached coral point (BL)	0	0.00		
Fluorescent bleaching (FLUOR)	0	0.00		
Other disease (OD)	0	0.00		
Plague, Type II (White Plague, Type II) (PLA)	0	0.00		
Recently dead coral with algae (RD)	0	0.00		
White Band Disease (WBD)	0	0.00		
Yellow Blotch Disease (YBD)	0	0.00		

CATEGORIES	# Points	%	SW Index	Simpson (1-D)
Coral				
Acanthastrea (Acan)	0	0.00	0.00	0.00
Acropora (Acr)	2	4.08	0.18	0.00
Acropora (branching) (Acr_Br)	1	2.04	0.11	0.00
Acropora (corymbose) (Acr_C)	0	0.00	0.00	0.00
Acropora (digitate) (Acr_D)	0	0.00	0.00	0.00
Acropora (encrusting) (Acr_E)	0	0.00	0.00	0.00
Acropora (submassive) (Acr_SM)	0	0.00	0.00	0.00
Acropora (tabulate) (Acr_T)	0	0.00	0.00	0.00
Alveopora (Alv)	0	0.00	0.00	0.00
Anomastraea (Anom)	0	0.00	0.00	0.00
Astreopora (Ast)	0	0.00	0.00	0.00
Blastomussa (Bla)	0	0.00	0.00	0.00
Cantharellus (Can)	0	0.00	0.00	0.00
Catalaphyllia (Catal)	0	0.00	0.00	0.00
Caulastrea (Cau)	0	0.00	0.00	0.00
Coeloseris (Coe)	0	0.00	0.00	0.00
Coral (branching) (HcB)	0	0.00	0.00	0.00
Coral (corymbose) (HcC)	0	0.00	0.00	0.00
Coral (digitate) (HcD)	0	0.00	0.00	0.00
Coral (encrusting) (HcE)	0	0.00	0.00	0.00
Coral (foliose) (HcF)	0	0.00	0.00	0.00
Coral (massive) (HcM)	0	0.00	0.00	0.00
Coral (solitary) (HcSo)	0	0.00	0.00	0.00
Coral (submassive) (HcSM)	0	0.00	0.00	0.00
Coral (tabulate) (HcT)	0	0.00	0.00	0.00
Coscinaraea (Cos)	0	0.00	0.00	0.00
Ctenactis (Cten)	0	0.00	0.00	0.00
Ctenella (Ctn)	0	0.00	0.00	0.00
Cycloseris (Cyc)	0	0.00	0.00	0.00
Cynarina (Cyn)	0	0.00	0.00	0.00
Cyphastrea (Cyp)	0	0.00	0.00	0.00
Diaseris (Dia)	0	0.00	0.00	0.00
Diploastrea (Dip)	0	0.00	0.00	0.00
Echinophyllia (Ecy)	0	0.00	0.00	0.00
Echinopora (Ech)	0	0.00	0.00	0.00
Euphyllia (Eup)	0	0.00	0.00	0.00
Favia (Fav)	0	0.00	0.00	0.00
Favites (Fts)	1	2.04	0.11	0.00
Fungia (Fun)	0	0.00	0.00	0.00
Galaxea (Gal)	2	4.08	0.18	0.00
Gardineroseris (Gar)	0	0.00	0.00	0.00
Goniastrea (Gon)	3	6.12	0.23	0.01
Goniopora (Gnp)	0	0.00	0.00	0.00
Gyrosmilia (Gyr)	0	0.00	0.00	0.00
Halomitra (Hal)	0	0.00	0.00	0.00
Heliopora (Hel)	0	0.00	0.00	0.00
Herpolitha (Her)	0	0.00	0.00	0.00
Heterocyathus (Htc)	0	0.00	0.00	0.00
Heteropsammia (Htp)	0	0.00	0.00	0.00
Horastrea (Hst)	0	0.00	0.00	0.00
Hydnophora (Hyd)	0	0.00	0.00	0.00
Isopora (Iso)	0	0.00	0.00	0.00
Leptastrea (Lptas)	0	0.00	0.00	0.00

Leptoria (Lptor)	0	0.00	0.00	0.00
Leptoseris (Lep)	0	0.00	0.00	0.00
Lithophyllon (Lyth)	0	0.00	0.00	0.00
Lobophyllia (Lob)	0	0.00	0.00	0.00
Merulina (Mer)	0	0.00	0.00	0.00
Micromussa (Mic)	0	0.00	0.00	0.00
Millepora (Mil)	0	0.00	0.00	0.00
Montastrea (Mta)	0	0.00	0.00	0.00
Montipora (Mtp)	3	6.12	0.23	0.01
Mycedium (Myc)	0	0.00	0.00	0.00
Oulophyllia (Oul)	0	0.00	0.00	0.00
Oxypora (Oxy)	0	0.00	0.00	0.00
Pachyseris (Pach)	0	0.00	0.00	0.00
Pavona (Pav)	0	0.00	0.00	0.00
Pectinia (Pct)	0	0.00	0.00	0.00
Physogyra (Phy)	0	0.00	0.00	0.00
Platygyra (Ptyg)	0	0.00	0.00	0.00
Plerogyra (Ple)	0	0.00	0.00	0.00
Plesiastrea (Ples)	0	0.00	0.00	0.00
Pocillopora (Poc)	4	8.16	0.26	0.02
Podobacia (Pod)	0	0.00	0.00	0.00
Polyphillia (Pol)	0	0.00	0.00	0.00
Porites (Por)	0	0.00	0.00	0.00
Porites (branching) (PorBr)	0	0.00	0.00	0.00
Porites (massive) (PorM)	0	0.00	0.00	0.00
Porites (submassive) (PorSM)	0	0.00	0.00	0.00
Poritopora (Prt)	0	0.00	0.00	0.00
Psammocora (Psa)	0	0.00	0.00	0.00
Pseudosiderastrea (Psd)	0	0.00	0.00	0.00
Scolymia (Scl)	0	0.00	0.00	0.00
Seriatopora (Ser)	14	28.57	0.36	0.20
Siderastrea (Sid)	0	0.00	0.00	0.00
Stylaraea (Str)	0	0.00	0.00	0.00
Stylocoeniella (Stc)	0	0.00	0.00	0.00
Stylophora (Stp)	0	0.00	0.00	0.00
Symphyllia (Sym)	0	0.00	0.00	0.00
Trachyphyllia (Trc)	0	0.00	0.00	0.00
Tubastrea (Tub)	0	0.00	0.00	0.00
Turbinaria (Tur)	1	2.04	0.11	0.00
Soft Coral				
Soft Coral (SCor)	0	0.00	0.00	0.00
Sponge				
Sponge (Sp)	0	0.00	0.00	0.00
Zoanthinidae				
Zoanthid (Zoa)	0	0.00	0.00	0.00
Macroalgae				
Articulated Calcareous (ArtC)	0	0.00	0.00	0.00
Blue-Green Algae (cyanophyta) (BGa)	0	0.00	0.00	0.00
Caulerpa (Clpa)	0	0.00	0.00	0.00
Chlorodesmis (Chlr)	0	0.00	0.00	0.00
Corticated Macrophyte (CortM)	0	0.00	0.00	0.00
Dictyosphaeria (Dsph)	0	0.00	0.00	0.00
Dictyota (Dict)	0	0.00	0.00	0.00
Filamentous (Fil)	0	0.00	0.00	0.00
Foliose algae (Fol)	0	0.00	0.00	0.00
Gracilaria (Grac)	0	0.00	0.00	0.00
Halimeda (Hhali)	0	0.00	0.00	0.00
Hydroclathrus (Hydr)	0	0.00	0.00	0.00
Leathery Macrophyte (LeaM)	0	0.00	0.00	0.00
Liagora (Liagor)	0	0.00	0.00	0.00
Lobophora (Lobo)	0	0.00	0.00	0.00
Macroalgae (ALGAE)	16	32.65	0.00	1.00
Padina (Pad)	0	0.00	0.00	0.00
Sargassum (Sarg)	0	0.00	0.00	0.00
Stypopodium (Sty)	0	0.00	0.00	0.00
Thick Turf (TTurf)	0	0.00	0.00	0.00
Turbinaria (Turb)	0	0.00	0.00	0.00
Turf (Turf)	0	0.00	0.00	0.00
Other live				
Anemone (Anem)	0	0.00	0.00	0.00
Gorgonian (Gorg)	0	0.00	0.00	0.00
Mollusc (Mol)	0	0.00	0.00	0.00
Coraline Algae				
crustose coralline algae (CCA)	0	0.00	0.00	0.00
upright coralline algae (CAup)	0	0.00	0.00	0.00
Dead Coral				
Recently dead coral (RDC)	2	4.08	0.00	1.00
Seagrass				
Cymodocea rotundata (C_rot)	0	0.00	0.00	0.00
Cymodocea serrulata (C_ser)	0	0.00	0.00	0.00
Enhalus acoroides (E_aco)	0	0.00	0.00	0.00
Halodule uninervis (H_uni)	0	0.00	0.00	0.00
Halodule wrightii (H_wri)	0	0.00	0.00	0.00

					Halodule wrightii (H_wri)	0	0.00	0.00	0.00
					Halophila ovalis (H_oval)	0	0.00	0.00	0.00
					Halophila stipulacea (H_stip)	0	0.00	0.00	0.00
					Seagrass (SG)	0	0.00	0.00	0.00
					Syringodium isoetifolium (S_iso)	0	0.00	0.00	0.00
					Thalassia hemprichii (T_hemp)	0	0.00	0.00	0.00
					Thalassondendron ciliatum (T_cil)	0	0.00	0.00	0.00
					Sand, pavement, rubble				
					Pavement (P)	0	0.00	0.00	0.00
					Rubble (R)	0	0.00	0.00	0.00
					Sand (S)	0	0.00	0.00	0.00
					Silt (Slt)	0	0.00	0.00	0.00
					Unknowns				
					Unknown (UNK)	0	0.00	0.00	0.00
					Tape, wand, shadow				
					Shadow (SHAD)	0	0.00		0.00
					Tape (TAPE)	0	0.00		0.00
					Wand (WAND)	0	0.00		0.00
					Total pts. minus (tape+wand+shadow):	49.00	100.00		

Annexe 2 : Caractéristiques des bandes multispectrales du satellite Sentinel-2A. Les bandes choisies dans cette étude sont les bandes 2, 3, 4, et 8

Numéro de bande	**Bandes spectrales (ou canaux spectrales)**	**Intervalle de longueur d'ondes**	**Longueur d'onde centrale (nm)**	**Résolution spatiale (m)**
1	Aerosol	433 – 453	442.7	60
2	Bleu	457.5 – 522.5	492.7	10
3	Vert	542.5 – 577.5	559.8	10
4	Rouge	650 – 680	664.6	10
5	Bord rouge 1	697.5 – 712.5	704.1	20
6	Bord rouge 2	732.5 – 747.5	740.5	20
7	Bord rouge 3	773 – 793	782.8	20
8	Proche Infrarouge	784.5 – 899.5	832.8	10
8A	Proche Infrarouge étroit	855 – 875	864.7	20
9	Vapeur d'eau	935 – 955	945.1	60
10	Infra rouge à ondes courtes-Cirrus	1360 – 1390	1373.5	60
11	Infra rouge à ondes courtes1	1565 – 1655	1613.7	20
12	Infra rouge à ondes courtes2	2100 – 2280	2202.4	20

Annexe 3: Equipement de base pour la collecte de photos géoréférencées

Annexe 4: Les paramètres choisies pour alimenter le modèle CNN

Parameters	Value domain	Chosen values
Sample patch size	8	
	16	
	32	32
	64	
	128	
	256	
Sample multiplier	10	10
	25	
	50	
	75	
	100	
	150	
	200	
Number of hidden layers	1	
	2	
	3	3
Kernel size	3x3	
	5x5	5x5
	7x7	7x7
	9x9	
	11x11	11x11
Number of feature maps	8	
	12	12
	16	
	32	
	64	
	128	
	256	
Max pooling	yes	yes
	no	no
Learning rate	10^-3	10^-3
	10^-4	
	10^-5	
Batch size	16	
	32	
	64	
	128	128
Training steps	(sample size/batch size) x number of epochs	20000

Annexe 5 : Exemples des capacités d'imagerie et de résolution de différentes techniques de télédétection des récifs coralliens au récif de l'île Lizard, dans le nord de la Grande Barrière de Corail. a Imagerie satellitaire (imagerie Sentinel-2A. Résolution spatiale = 10 m), b véhicules aériens non occupés et drones (UAV) (résolution spatiale ~ 10 cm, mais couverture d'étendues plus vastes), c drones grand public (résolution spatiale ~ 2 cm, emprise spatiale beaucoup plus petites), d et e photographie sous-marine à haute résolution (résolution spatiale ~ 5 mm). Source : Lutzenkirchen et al, 2024

Annexe 6 : **Pairwise comparison matrices used in the Analytic Hierarchy Process (AHP) for each scenarios**

Annexe 6.1: Prioritization of “Coral Abundance” and “HAA” with “Fishing Pressure” as least important (Scn1)

Factor	Fishing Pressure	Thermal stress	Turbidity	Coral Abundance	Depth	Framework	HAA
Fishing Pressure	1	1/5	1/5	1/9	1/3	1/2	1/9
Thermal stress	5	1	1	1/2	2	3	1/2
Turbidity	5	1	1	1/2	2	3	1/2
Coral Abundance	9	2	2	1	3	5	1
Depth	3	1/2	1/2	1/3	1	2	1/3
Framework	2	1/3	1/3	1/5	1/2	1	1/5
HAA	9	2	2	1	3	5	1

Annexe 6.2: Prioritization of “Coral Abundance” and “Framework” with “Thermal stress” as least important (Scn.2)

Factor	Fishing Pressure	Thermal stress	Turbidity	Coral Abundanc e	Depth	Framework	HAA
Fishing Pressure	1	3	2	1/3	1/2	1/3	1/2
Thermal stress	1/3	1	1/2	1/7	1/5	1/7	1/5
Turbidity	1/2	2	1	1/5	1/3	1/5	1/3
Coral Abundance	3	7	5	1	3	1	2
Depth	2	5	3	1/3	1	1/3	1
Framework	3	7	5	1	3	1	2
HAA	2	5	3	1/2	1	1/2	1

Annexe 6.3: Prioritization of "Coral abundance" and "Depth" with "Thermal stress" as least important (Scn.3)

Factor	Fishing Pressure	Thermal stress	Turbidity	Coral Abundance	Depth	Framework	HAA
Fishing Pressure	1	5	1	1/3	1/3	3	2
Thermal stress	1/5	1	1/4	1/9	1/9	1/2	1/3
Turbidity	1	4	1	1/4	1/4	2	1
Coral Abundance	3	9	4	1	1	7	5
Depth	3	9	4	1	1	7	5
Framework	1/3	2	1/2	1/7	1/7	1	1/2
HAA	1/2	3	1	1/5	1/5	2	1

Annexe 6.4: Prioritization of Fishing Pressure and Depth with Turbidity as least important (Scn.4)

Factor	Fishing Pressure	Thermal stress	Turbidity	Coral Abundance	Depth	Framework	HAA
Fishing Pressure	1	3	7	2	1	3	2
Thermal stress	1/3	1	5	1/2	1/3	1	1/2
Turbidity	1/7	1/5	1	1/5	1/7	1/3	1/5
Coral Abundance	1/2	2	5	1	1/2	2	1
Depth	1	3	7	2	1	3	2
Framework	1/3	1	3	1/2	1/3	1	1/2
HAA	1/2	2	5	1	1/2	2	1

Annexe 6.5: Prioritization of Fishing Pressure and Thermal Stress with Framework as least important (Scn.5)

Factor	Fishing Pressure	Thermal stress	Turbidity	Coral Abundance	Depth	Framework	HAA
Fishing Pressure	1	1	3	2	6	9	4
Thermal stress	1	1	3	2	6	9	4
Turbidity	1/3	1/3	1	1/2	2	5	1
Coral Abundance	1/2	1/2	3	1	3	7	2
Depth	1/6	1/6	1/2	1/3	1	3	1/2
Framework	1/9	1/9	1/5	1/7	1/3	1	1/4
HAA	1/4	1/4	1	1/2	2	4	1

Annexe 6.6: Prioritization of "Thermal stress" and "Turbidity" with "Framework" as least important (Scen6)

Factor	Fishing Pressure	Thermal stress	Turbidity	Coral Abundance	Depth	Framework	HAA
Fishing Pressure	1	1/3	1/3	2	2	5	1
Thermal stress	3	1	1	5	3	7	3
Turbidity	3	1	1	5	3	7	3
Coral Abundance	1/2	1/5	1/5	1	1/2	3	1/2
Depth	1/2	1/3	1/3	2	1	5	1
Framework	1/5	1/7	1/7	1/3	1/5	1	1/3
HAA	1	1/3	1/3	2	1	3	1

Annexe 7 : Communications scientifiques

Articles scientifiques avec comité de lecture publiés

1. Henitsoa Jaonalison, Marilaure Grégoire, Jamal Mahafina, James Mwaluma, Helga Berjulie Ravelohasina, **Aina Le Don Nomenisoa**, Toky Justino Mory, Lantoasinoro Ranivoarivelo, Dominique Ponton, Bruno Frédérich. Drivers of fish diversity and size spectra across lagoonal habitats of the Toliara Reef system (SW Madagascar) 2025. Marine Environmental Research, 210. 1-14 [doi.org/10.1016/j.marenvres.2025.107330]
2. **Nomenisoa A.L.,** Todinanahary G, Edwin HZ, Razakarisoa T, Israel JB, Raseta S, Jaonalison H, Mahafina J, Eeckhaut I, 2024 - Remote sensing of coral reef habitats in Madagascar using Sentinel-2 satellite images. Western Indian Ocean Journal of Marine Science 23(2): 41-56 [http://doi.org/doi:10.4314/wiojms.v23i2.4]
3. Claudia Rodine, Henitsoa Jaonalison, Jean M. Kira, André Rakotoarimanana, Lantoasinoro N. Ranivoarivelo, Cicelin Rakotomahazo, Gaëtan Tsiresy, Gildas B. G. Todinanahary, **Aina Le Don Nomenisoa**, Fidèle Rakotonjanahary, Igor Eeckhaut, Mara E. Remanevy, Spencer Jamie, Richard Rasolofonirina, Thierry LavitraW. 2024 - Spatio-temporal variation of macroalgal assemblages in southwestern Madagascar. IO Journal of Marine Science 23 (2) 2024 135-150 [http://doi.org/10.4314/wiojms.v23i2.11]
4. C Rodine, A Rakotoarimanana, AB Ramamonjisoa, LN Ranivoarivelo, C Rakotomahazo, GBG Todinanahary, G Tsiresy, H Jaonalison, **AL Nomenisoa**, I Eeckhaut, ME Remanevy, JS Obe, R Rasolofonirina, T Lavitra. Local knowledge, utilisation and consumption of seaweed in coastal communities of southwestern Madagascar (2024) - African Journal of Marine Science, 46:3, 177-190, [http://doi.org/10.2989/1814232X.2024.2371526]
5. Thierry Lavitra, Franciana Moridy, Mihary Rabearison, Claudia Rodine, Cicelin Rakotomahazo, **Aina Le Don Nomenisoa**, Lantoasinoro Nirinarisoa Ranivoarivelo, Richard Rasolofonirina, Andre Rakotoarimanana, Christopher Franberg, Max Troell, Igor Eeckhaut, and Gildas Boleslas Georges Todinanahary. 2024 - Local perceptions of the socioeconomic and environmental impacts of sea cucumber farming in southwestern Madagascar. SPC Beche-de-mer Information Bulletin #44
6. Golden CD, Hartmann AC, Gibbons E, Todinanahary G, Troell MF, Ampalaza G, Behivoke F, David JM, Durand J-D, Falinirina AM, Frånberg C, Declèrque F, Hook K, Kelahan H, Kirby M, Koenen K, Lamy T, Lavitra T, Moridy F, Léopold M, Little MJ,

Mahefa JC, Mbony J, Nicholas K, **Nomenisoa ALD**, Ponton D, Rabarijaona RR, Rabearison M, Rabemanantsoa SA, Ralijaona M, Ranaivomanana HS, Randriamady HJ, Randrianandrasana J, Randriatsara HO, Randriatsara RM, Rasoanirina M, Ratsizafy MR, Razafiely KF, Razafindrasoa N, Romario, Solofoarimanana MY, Stroud II RE, Tsiresimiary M, Volanandiana AJ, Volasoa NV, Vowell B, and Zamborain-Mason J. 2024 - HIARA study protocol: impacts of artificial coral reef development on fisheries, human livelihoods and health in southwestern Madagascar. Front. Public Health. 12:1366110. [http://doi.org/10.3389/fpubh.2024.1366110]

Articles scientifiques en cours de publication

1. **Aina Le Don Nomenisoa**, Gildas Todinanahary, Eylem Elma, Edwin Hubert Zafimampiravo, Mandimbilaza Tsiresimiary, Mitondrasoa Yves Amoros, Michel Ratsizafy, Toky Razakarisoa, Henitsoa Jaonalison, Jamal Mahafina, Igor Eeckhaut. Change Detection of Benthic Coral Cover in Toliara, Madagascar: Past, Present, and Future Trends. *Journal of Marine Conservation.*
2. **Aina Le Don Nomenisoa**, Gildas Todinanahary, Edwin Hubert Zafimampiravo, Mandimbilaza Tsiresimiary, Mitondrasoa Yves Amoros, Michel Ratsizafy, Toky Razakarisoa, Henitsoa Jaonalison, Jamal Mahafina, Igor Eeckhaut. Assessing Coral Reef Resilience through Remote Sensing and field based approach for Decision Support in Small-Scale Fishing Communities. *Perspectives in Ocean, Marine and Coastal Governance: Coastal resilience, access and livelihoods*

Présentation Orale

1. **NOMENISOA Aina Le Don**, Gwilym Rowlands, Ranivoarivelo L. N. (2025). Cartographie et surveillance des herbiers marins. LASMMI- Large Scale Seagrass Mapping and Management Initiative. Présentation orale. Seagrass monitoring workshop. 24-28 March 2025. UK International Development, JNCC, Madagascar National Parks. Palm Beach, Nosy Be (Madagascar)

2. **NOMENISOA Aina Le Don** (2024). The Madagascar Oceanographic Data Center: Past, Present and Future perspectives. Présentation orale. IOC-UNESCO. United Nation Decade for Ocean Sciences. Barcelone (Espagne) 10-12 Avril 2024.
3. **NOMENISOA Aina Le Don** (2024). Protéger les récifs coralliens à Madagascar : Une décennie de changements des récifs coralliens révélée par les imageries satellitaires et l'intelligence artificielle. Présentation orale. Colloque international sur : « les enjeux pertinents de la maritimisation. 2nd Edition.18-20 Septembre 2024. Toamasina (Madagascar). Akademia Malagasy
4. **NOMENISOA Aina Le Don** (2023). Sea level rise station marine facilities in Madagascar. Présentation orale. Global Ocean Summit (GOS). Qindao (China). Laoshan Laboratory. Qindao Marine Science and Technology Center. 25-27September 2023
5. **NOMENISOA Aina Le Don** (2023). Optimisation de la collecte de données benthique à grande échelle à l'aide d'imageries satellitaires gratuites. Présentation orale. Atelier sur le traitement d'images sous-marines et aériennes (drones), cartographie avec l'intelligence artificielle et la photogrammétrie. [https://doi.org/10.5281/zenodo.7928814]. INTERREG-G2OI, IFREMER, IH.SM. Toliara, Madagascar
6. **NOMENISOA Aina Le Don** (2022). Remote Sensing and Mapping of Blue Carbon Ecosystems. Training workshop on Research and sustainable management of Blue Carbon Ecosystems in the Indian Ocean. Indian Ocean Rim Association (IORA) 27 November - 2 December 2022, Toliara, Madagascar
7. **NOMENISOA Aina Le Don,** Alessa Dinoi, Gildas Todinanahary (2021). Western Indian Ocean Marine Ecosystem Services valuation: a systematic review of current output, gaps and future direction. Présentation Orale. Western Indian Ocean Governance Network (WIOGEN). 27-29 October 2021

Présentation Poster

1. **Nomenisoa A.L.**, G. Rowlands, Razakarisoa T. Rakotondratsimba F.P., Mandimbilaza T., Razanamalala B.R., Ratsizafy M., Andrianjatovo P.Y., Mitondrasoa Y.A., Ranivoarivelo L.N. (2024). Cartographie et Gestion des Herbiers Marins : Une Initiative Collaborative pour l'Océan Indien Occidental. Symposium sur la Biodiversité Marine. Thème : Quel modèle de gestion durable de la biodiversité marine et du développement durable des

activités économiques dans les aires marines de Madagascar 2 et 3 décembre 2024 à l'Hôtel Le Vahiné, Toliara. FAPBM, WIOMSA, IH.SM

2. **Nomenisoa, A.L.**; Edwin, Z.; Israel, J.; Razakarisoa, T.; Raseta, S.; Mahafina, J.; Jaonalison, H.; Eeckhaut,I.; Todinanahary, G. - Benthic habitats mapping of coral reefs in Madagascar based on Sentinel-2A free satellite image. Présentation Poster. 12th WIOMSA Scientific Symposium 10th – 15th October 2022 The Boardwalk Convention Centre, Nelson Mandela Bay, South Africa THEME II: Coral Ecosystems: Community Structures and Associated Organisms.
3. Razafimanantsoa, M. M.; Mahasanjo, S. O.; **Nomenisoa, A. L.** - Risk of hypersedimentation of the Great Reef of Toliara from the Onilahy watershed. Présentation Poster. 12th WIOMSA Scientific Symposium 10th – 15th October 2022 The Boardwalk Convention Centre, Nelson Mandela Bay, South Africa. THEME III: Multiple Impacts on Coral Reefs and Management Strategies
4. Edwin, Z.; **Nomenisoa A.L.**; Razakarisoa, T.; Israel, J.; Raseta, S.; Henitsoa, J.; Mahafina, J.; Eeckhaut, I.; Todinanahary, G. - Remote sensing and field-based approach to support coral reef resilience management in Madagascar. Présentation Poster. 12th WIOMSA Scientific Symposium 10th – 15th October 2022 The Boardwalk Convention Centre, Nelson Mandela Bay, South Africa . THEME X: Governance of Coastal and Marine Environment
5. Felana, N.; **Nomenisoa, A.L.**; Behivoke, F.; Todinanahary, G. - Determining the gleaning fishing index in the bay of Toliara, southwestern Madagascar. Présentation Poster. 12th WIOMSA Scientific Symposium 10th – 15th October 2022 The Boardwalk Convention Centre, Nelson Mandela Bay, South Africa THEME XIV: Fisheries: Ecology, Gears Impacts and Stock Status
6. Rembert, R.; **Nomenisoa, A.L.**; Todinanahary, G. - Geological and geomorphological formation in the marine and coastal waters of Madagascar. Présentation Poster. 12th WIOMSA Scientific Symposium 10th – 15th October 2022 The Boardwalk Convention Centre, Nelson Mandela Bay, South Africa THEME XVIII: Physical and Geological Processes
7. Andrianjatovo, P. Y, N.; Rakotoson, I. J.; **Nomenisoa, A.L.**- Satellite remote sensing assessment of the coastal changes occurring in Ambotsibotsiky and Andaboy, Southwest

Madagascar. Présentation Poster. 12th WIOMSA Scientific Symposium 10th – 15th October 2022 The Boardwalk Convention Centre, Nelson Mandela Bay, South Africa THEME XVIII: Physical and Geological Processes

8. Israel, J.; **Nomenisoa, A.L.**; Edwin, Z.; Razakarisoa, T.; Eeckhaut, I.; Todinanahary, G. - Benthic Mapping and Spatial Distribution of Fish Biomass in Soariake MPA, Southwestern Madagascar. Présentation Poster. 12th WIOMSA Scientific Symposium 10th – 15th October 2022 The Boardwalk Convention Centre, Nelson Mandela Bay, South Africa THEME XX: Fish Ecology and Biodiversity
9. Andriambola, T.; **Nomenisoa, A.L.**; Rasolofonirina, R.; Ranivoarivelo, L. - Evaluation of carbon stock in Mangrove Ecosystem: Studied case of Mangrove in the National Park of Sahamalaza (North Western Region of Madagascar). Présentation Poster. 12th WIOMSA Scientific Symposium 10th – 15th October 2022 The Boardwalk Convention Centre, Nelson Mandela Bay, South Africa THEME XXIII: Mangroves Ecosystems
10. Razakarisoa, T.; Rakotonjanahary, F.; **Nomenisoa, A.L.**; Todinanahary, G.; Zafimampiravo, H.; Isreal, J.; Mahafina, J.; Henitsoa, J.; Lavitra, T.; Ranivoarivelo, L.; - Seagrass species diversity and geographical distribution in Ranobe Bay (south-western Madagascar). Présentation Poster. 12th WIOMSA Scientific Symposium 10th – 15th October 2022 The Boardwalk Convention Centre, Nelson Mandela Bay, South Africa THEME XXIV: Coastal Ecosystems and Associated Organisms
11. Yhasy, E.; Todinanahary, G.; **Nomenisoa, A.L.**; Lavitra, T.; Ranivoarivelo, L. - Distribution and quality of carrageenophyte algae (*Kappaphycus sp, Kappaphycus striatus, Euchema sp and Euchema odontophorum*) in the South-west region of Madagascar. Présentation Poster. 12th WIOMSA Scientific Symposium 10th – 15th October 2022 The Boardwalk Convention Centre, Nelson Mandela Bay, South Africa. THEME XXIV: Coastal Ecosystems and Associated Organisms

Rapport techniques

1. Jean Marie Rakotovao, **Aina Le Don Nomenisoa**, José Randrianandrasana, Gédice Fernand Tiandrainy, Gildas Todinanahary (2024). La Biodiversité Marine de Madagascar : Quel modèle de gestion durable de la biodiversité marine et le développement durable des activités économiques dans les aires marines de Madagascar ? FAPBM, WIOMSA, IH.SM. 33 pages.
2. Claire Ward, Edwin Mwashinga, Frank Mirobo, Lilian Omolo, Riaan Cedras, David Ailars, Gloria Ajani, Anthony Akpan, Joseph Ansong, Frédéric Bonou, Alessia Dinoi, Abdulrahman Dirie, Isa Olalekan Elegbede, Juliet K. Igbo, Ogunrai Jumoke, Deepeeka Kaullysing, Anim Mabel, **Aina Le Don Nomenisoa**, Isaac Nyameke, Ngozi Oguguah, Titus Ogunseye, Idowu Olayemi, Funmilola Oluwafemi, Derrick Omollo, Frank Owusu, Alberta Ama Sagoe, Mouneshwar Soondur, Ramah Sundy, Rachel Thoms. Mika Odido (2023). United Nations Ocean Decade for Africa: The Science we Need for the Ocean we Want in Africa. *Published by* the Western Indian Ocean Marine Science Association (WIOMSA) in partnership with the Intergovernmental Oceanographic Commission's Sub Commission for Africa and the Adjacent Island States (IOC-AFRICA), UNESCO Regional Office for Eastern Africa. 55 pages
3. **Aina Le Don Nomenisoa**, Jaonalison Henitsoa, Yasmine Soilihi, Soa Cynthia Nomeny Iariniaina, Rabemanantsoa Sarah, Lavitra Thierry, Mara Edouard Remanevy, Christian Ralijaona, Naly Rakotoarivony, Herizo Emmanuel Ravelomanana, Mahafina Jamal. 2023. Symposium régional sur la pêche industrielle illégale, non déclarée et non réglementée. MPEB, Ambassade des Etats-Unis, IH.SM et Blue Ventures. IBIS, Antananarivo (101), Madagascar. 33 pages
4. Samoelina A. Ramantsialonina, Andrew Cooke, **Aina Le Don Nomenisoa**, Gaëtan Tsiresy, Rija Ranaivoarison, Gildas Todinanahary (2022). Atlas et diagnostic maritime de la région Menabe. USAID, MATSF, MPEB, MEDD. 51 pages
5. Gildas GB Todinanahary, Bemahafaly Randriamanantsoa, José Randrianandrasana, Jean Maharavo, Sarah Zerambay, Aroniaina Falinirina, Radonirina Botosoamananto, Faustinato Behivoke, Vaonirina Jeanne L'Or Tsilavina, Anita Sarah Rabemanantsoa, Jules Pierro Tsimbazafihery, Israel John Bunyan, Joël Arnaud Masoava, Jean Marie David, Mahery

Hambinintsoa Randrianarivo, **Aina Le Don Nomenisoa**. (2024). État De Santé Des Récifs Coralliens A Madagascar, De 2016 A 2021. 107 pages

Données publiées

1. Sylvain Poulain, **Aina Le Don Nomenisoa**, Herinomena Andriamasinoro, Julien Barde. (2023). Orthophoto & DEM (MNE) issues d'images drone à Madagascar : Nosy Ve, Anakao, Sakatia, Sarodrano, Ankilibe, GRT, Massif des roses, Toliara
[doi : https://zenodo.org/records/10079913]
[doi : https://zenodo.org/records/10079939]
[doi : https://zenodo.org/records/10079922]
[doi : https://zenodo.org/records/10079898]
[doi : https://zenodo.org/records/10079951]
[doi : https://zenodo.org/records/10079942]
[doi : https://zenodo.org/records/10182432]
[doi : https://zenodo.org/records/10079914]
[doi : https://zenodo.org/records/10079947]

2. **Nomenisoa A.L.**, Mitondrasoa Y.A., Todinanahary G, Edwin HZ, Razakarisoa T, Israel JB, Raseta S, Ratsizafy M., Mandimbilaza T., Jaonalison H., Mahafina J., Eeckhaut I, (2025). 11 170 Phototransects sous-marins géoréférencés et annotés collectés dans la Baie de Toliara et à Salary Nord (Madagascar) en 2021 et en 2024. [doi : En cours]

Annexe 8 : Remote sensing of coral reef habitats in Madagascar using Sentinel-2 satellite images

Original Article

Remote sensing of coral reef habitats in Madagascar using Sentinel-2 satellite images

Aina L. Nomenisoa[1,2], Gildas Todinanahary[1], Hubert Z. Edwin[1], Toky Razakarisoa[1], John Bunyan Israel[1], Saverio Raseta[1], Henitsoa Jaonalison[1], Jamal Mahafina[1], Igor Eeckhaut[2]

[1] Institut Halieutique et des Sciences Marines (IH.SM), University of Toliara, PO Box 141, Toliara, Madagascar

[2] Laboratoire de Biologie des Organismes Marins et Biomimétisme, University of Mons, PO Box 7000, Mons, Belgium

Western Indian Ocean JOURNAL OF Marine Science

Open access

Citation:
Nomenisoa ALD, Todinanahary G, Edwin HZ, Razakarisoa T, Israel JB, Raseta S, Jaonalison H, Mahafina J, Eeckhaut I (2024) Remote sensing of coral reef habitats in Madagascar using Sentinel-2 satellite images. Western Indian Ocean Journal of Marine Science 23(2): 41-56 [doi: 10.4314/wiojms.v23i2.4]

Received:
September 2, 2023

Accepted:
June 26, 2024

Published:
October 18, 2024

* **Corresponding author:**
ainaledon294@gmail.com

Abstract

Publicly available Sentinel-2 satellite imagery was used to map the coral reef systems of Toliara in Madagascar, to standardize methods for monitoring reef health and guiding management decisions. Fieldwork conducted between March and December 2021 used georeferenced photoquadrats to assess benthic structure. The satellite image classification was based on the Object-Based Image Analysis (OBIA) and machine learning algorithms, with k-NN achieving the highest overall accuracy at 83 %, followed by the Bayes classifier (79 %), DT (68 %), RT (67 %) and SVM (42 %). The analysis identified distinct surface areas occupied by seagrass (21 km²), sand (73 km²), rubble (21 km²), coral (10 km²) and algae (6 km²). Comparative assessment with the Allen Coral Atlas underscored the importance of aligning satellite image analysis with *in-situ* data. The study emphasized the role of selecting appropriate classifier algorithms for precise mapping and stressed the importance of local data collection for accurate habitat mapping. It also showcased the successful application of OBIA with satellite imagery and field data for coral reef mapping, providing insights into habitat health and spatial changes essential for effective conservation.

Keywords: remote sensing, coral reef, Madagascar, Sentinel-2, OBIA, Machine learning algorithms

Introduction

Coral reefs protect shorelines against storms, serve as fish nurseries, and provide socio-economic benefits when associated with tourism and recreation, shoreline protection, fisheries, and biodiversity services (Eakin *et al.*, 2010). However, these ecosystems face significant threats on both global and local scales, primarily due to climate change and anthropogenic pressures (Xu and Zhao, 2014). Nearly half of the world coral reefs have been destroyed or badly damaged in the last 30 years (Wilkinson, 2008). Current trends suggest that between 70 % to 90 % of global coral reefs are at risk of extinction within the foreseeable future (Foo and Asner, 2019), a fate that extends to the reefs of Madagascar as well (van Hooidonk *et al.*, 2016). Effective management and conservation efforts requires comprehensive monitoring strategies that encompass both spatial and temporal dimensions, focusing on the distribution of species on the benthos as well as their associated substrates (Nurlidiasari and Budiman, 2010). Such measures require a reliable method that can efficiently process continuous data into manageable spatial units (Kennedy *et al.*, 2021). The European Space Agency (ESA) has made Sentinel-2 images freely available since 2015 (ESA's Sentinel-2 team, 2015) offering a 10 m spatial resolution (pixel size), which significantly enhances the utility of these images for coral reef mapping. Remote sensed mapping of coral reefs is particularly important for developing countries, where 80 % of the world's coral reefs occur (UNEP-WCMC, WorldFish Centre, WRI, TNC, 2021). Therefore, it is critical to determine the efficacy of mapping using freely available satellite images from Sentinel-2 (Hedley *et al.*, 2012, 2018; Wouthuyzen *et al.*, 2019; Yunus *et al.*, 2019).

To achieve comprehensive mapping of coral reefs, it is crucial to derive maps of geomorphic zones and benthic communities at various scales (Phinn, *et al.*, 2012). Numerous initiatives have been undertaken globally to map coral reefs and understand their distribution, including coral reefs from Madagascar. However, existing datasets, such as those from the United Nations Environment Program-World Conservation Monitoring Centre (UNEP-WCMC) and the Allen Coral Reef Atlas, have limitations such as irregular updates, and unstable accuracy, hindering their applicability in dynamic monitoring. Although efforts to study coral reefs from Madagascar have provided valuable insights, further studies are necessary to fully comprehend these ecosystems and their changing habitats.

Efficient and cost-effective methods using remote sensing data are needed to delineate comprehensive reef coverage, geomorphic zoning, and benthic composition in Madagascar. Despite numerous studies on mapping coral reefs, variations in processing schemes, data characterization, and classification methods pose challenges, emphasizing the necessity for a tailored methodology. Therefore, there is a need for a comprehensive methodology tailored to coral reefs from Madagascar, encompassing standardized fieldwork data collection and image processing workflows. This study focuses on the barrier reef in Toliara, commonly known as the 'Grand Récif de Toliara' (GRT), and the reefs of Ankilibe and Sarodrano, where local coral reef geomorphology has been conducted

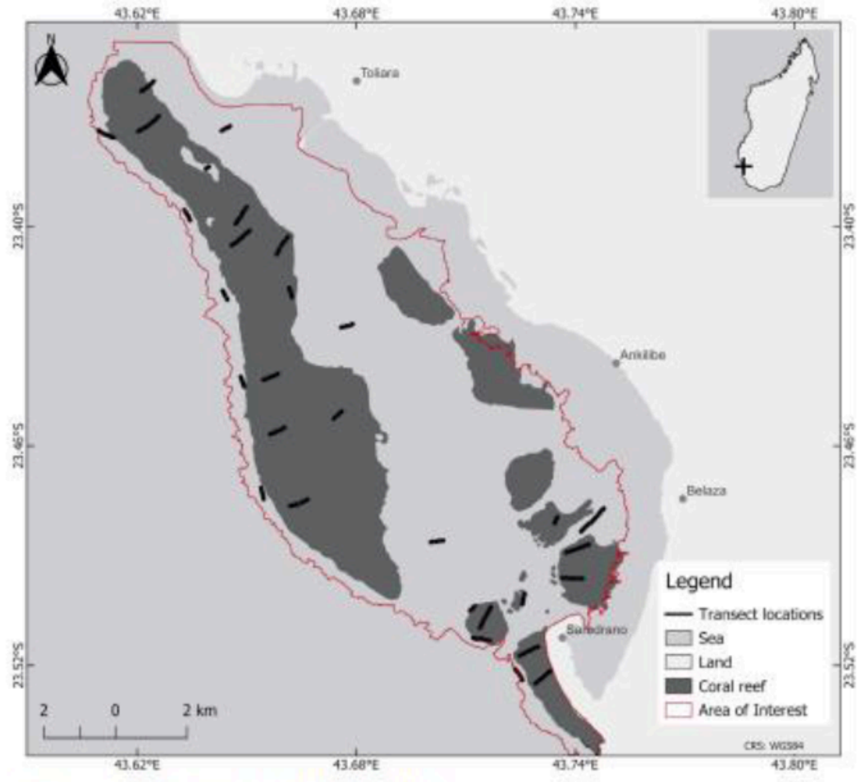

Figure 1. Study area with the placement of the transect lines.

(Pichon, 1972; Battistini *et al.*, 1975; Andréfouët *et al.*, 2013), and several studies focusing on the bio-ecology of coral reefs have been realized (Todinanahary, 2016; Razakandrainy, 2018; Botosoamananto *et al.*, 2021). Undertaking a comprehensive study at the scale of the Toliara region is essential for coral reefs of Madagascar, necessitating standardized methodologies for future data collection and processing. The primary aim of this research was to develop a methodology for coral reef mapping in Madagascar, using freely accessible satellite imagery and advanced remote sensing techniques. Specifically, the study aimed to assess geomorphic zonation and benthic coverage along the barrier reef and fringing reefs of Toliara, using Object-Based Image Analysis (OBIA) applied to Sentinel-2 satellite data, alongside fieldwork data acquisition. This study seeks to establish a foundational understanding of nearshore benthic communities in Madagascar, serving as a vital resource for marine scientists to effectively track ecosystem changes. Furthermore, it aims to furnish policymakers with essential data for monitoring the health of these reefs and formulating sustainable management strategies over the long term.

Materials and methods

Study area, field data collection and processing

The study was carried out within the Bay of Toliara, and was focused on the fringing reef of Sarodrano, the fringing reef of Ankilibe, and the barrier reef of Toliara (Fig. 1). The selection of these sites was based on several factors: (1) accessibility, (2) ecological variability, encompassing both degraded and healthy areas to facilitate the discernment of local stressors, and (3) ecological complexity, given the co-existence of a barrier reef, a fringing reef, and patch reefs within the same coral reef system. Fieldwork was conducted between March and December 2021, during low spring tides to optimize the time available for in-water surveying. It consisted of collecting georeferenced photoquadrats (in-water images) along transect lines (Fig. 1). Due to the limitation of GPS signal penetration underwater, the GPS device was secured in a floating airtight bag at the surface. This device was programmed to record new geographic positions every second. Specifically, one diver captured benthic images every 3-5 meters, guided by a compass to maintain course, while a second diver at the surface maneuvered the GPS-containing bag, moving in synchronization with the diver below (Fig. 2). Each dive averaged 30 minutes, covering approximately 500 meters of transect where current conditions allowed; however, in instances of stronger currents, transects were shortened accordingly. Initial and final GPS coordinates of each transect were logged on a diving slate to facilitate subsequent GPS data integration. Approximately 250 photos were collected per transect, totaling 4187 photos across the 30 transects. Ground-truthing data collection was confined to depths shallower than 20 meters. Subsequently, the photos were linked to GPS data to assign specific geographic positions to each photoquadrat using the software GPS Photo Manager (Roelfsema *et al.*,

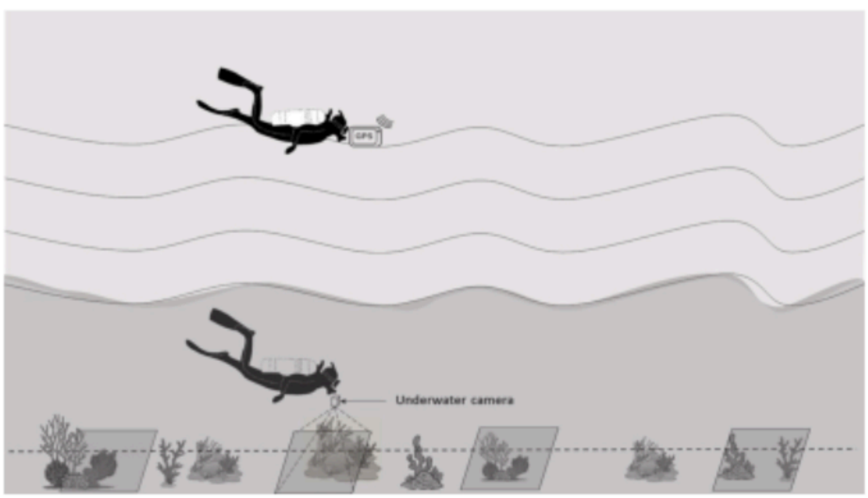

Figure 2. Method of photoquadrat data collection.

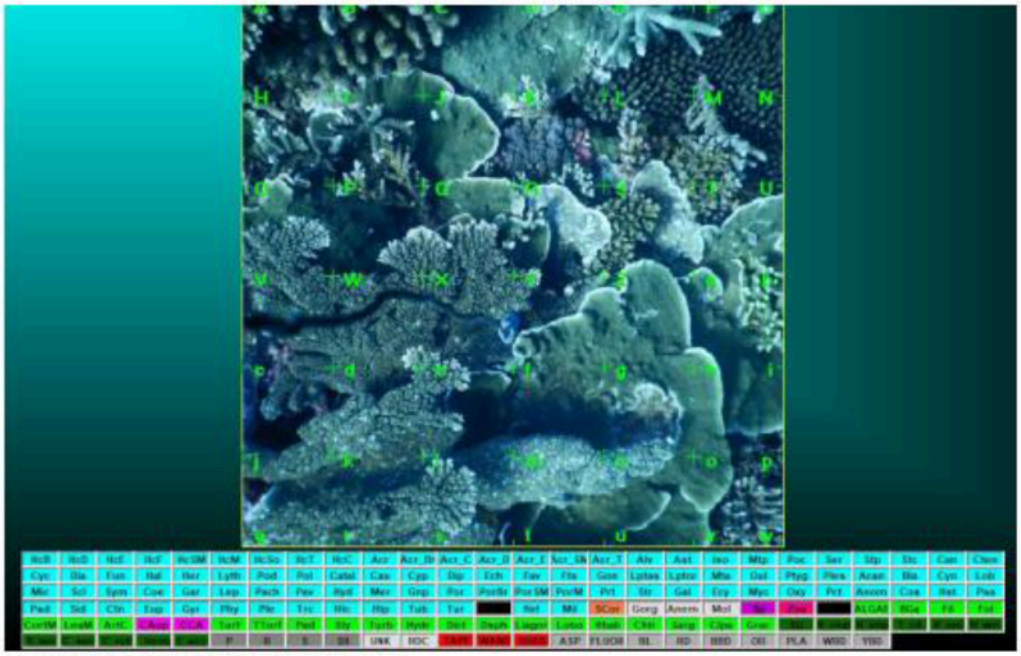

Figure 3. 49 stratified points (7 points per lines) on CPCE.

2019). This integration facilitated the visualization of photos and associated benthic attributes within a Geographic Information System (GIS) interface. All the GIS operations in this study were performed using the QGIS software, version 3.34.

Assessment of benthic cover from geotagged photos

Benthic cover within the transect lines was obtained from each geotagged photo by analyzing photoquadrats using the Coral Point Count with Excel extension (CPCe) software (Kohler and Gill, 2006). A total of 49 stratified points were distributed on each photo and the substrates corresponding to these points were identified using a predefined code name "CPCe benthic codes 41 Madagascar" provided with the software (Fig. 3). Based on their knowledge and the 41 CPCe benthic codes, the users attributed specific classes to each of the 49 stratified points. This number of stratified points per photoquadrat was sufficient to identify down to the level of benthic habitat classes. The benthic cover of the photoquadrat was then automatically estimated by the software as a function of the number of points occupied by each category of substrate. Once the analysis was finished, the software exported the data in an Excel file.

Conversion of the CPCE data into calibration and validation sample points

The data points produced by the CPCe software spans a 1x1 meter area, whereas the pixel size of a Sentinel-2 image measures 10 meters by 10 meters. To ensure comparability between CPCe data points and Sentinel pixels, the 41 benthic CPCe codes were refined into five classes: Coral (i.e., live corals), Algae, Rubbles, Sand, and Seagrass. These data points were then overlaid onto the Sentinel-2 image layer. A new sample was then manually created and assigned a pixel category based on the predominant benthic cover depicted in the CPCe data pie chart (Fig. 4). From the 4187 photos, 1243 control points were derived, where 75 % were used for calibrating the machine learning algorithms to classify the satellite image, while the remaining 25 % served as validation points to assess their accuracy.

Satellite image processing

Pre-processing

Sentinel-2A data were accessed from the Copernicus server (https://scihub.copernicus.eu/dhus/#/home). The Sentinel-2A image collected on 21-08-2021 was used in this study (Table 1). The Sentinel-2 satellite was launched in 2015 and offers 10 m spatial resolution for the visible and the Near Infra-Red (NIR)

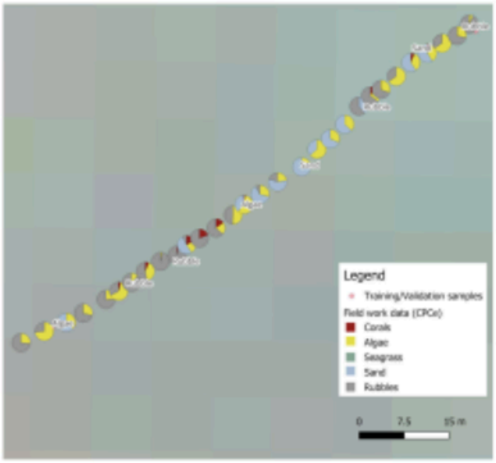

Figure 4. Calibration and validation sample points.

bands (ESA's Sentinel-2 team, 2015). The most appropriate images for coral reef habitat mapping are those that contain the least cloud cover and sun glint and are acquired during the spring low tide period. This last requirement is crucial in the analyses as the characterization of the benthos is complicated especially when they are submerged in the water column. The raw downloaded Sentinel-2 image was first corrected for the effect of the atmosphere. For this correction, the sen2cor atmospheric Correction Processor algorithm was used from the SNAP software or Sentinel Application Platform (Louis *et al.*, 2016). This approach consisted of transforming the Level-1C image (surface reflectance measured at the top of the atmosphere) into Level-2A (bottom-of-atmosphere reflectance). Next, as the benthos was submerged underwater, the water column effect needed to be corrected. The water column correction algorithm of Lyzenga (1981) was used for this purpose. This was processed using the sen2coral module of the SNAP software. As a result, three bands of the depth invariant index (DII) were generated, each composed of different combinations of spectral bands (Table 1): blue and green (DII_B2B3), blue and red (DII_B2B4), and green and red (DII_B3B4). Additionally, the Normalized Difference Vegetation Index (NDVI) was computed (Zoffoli *et al.*, 2020). These newly generated layers were added to the atmospheric corrected image for the geomorphic and benthic image classification.

Image classification

Coral reef habitat classification serves as an important tool for surveying and understanding these marine ecosystems. The process involves leveraging raw input data—such as videos or images—captured from coral sites (Nguyen *et al.*, 2021). Through this data, distinctive features of the seabed, referred to as classes, are extracted and categorized, including corals, sands, rubbles, seagrass, etc. To undertake this mapping,

Table 1. Sentinel-2 image specification used in this study.

Name		**Sentinel-2A**		
Correction level		Level 1A		
Date of acquisition		21-08-2021		
Radiometric resolution		12 bit/pixel		
Swath width		290 km at nadir		
	Band number	**Spectral Bands**	**Central wavelength (nm)**	**Spatial resolution (m)**
	1	Coastal Aerosol	442.7	60
	2	Blue	492.7	10
	3	Green	559.8	10
	4	Red	664.6	10
	5	Vegetation Red Edge	704.1	20
Multispectral Bands	6	Vegetation Red-Edge	740.5	20
	7	Vegetation Red-Edge	782.8	20
	8	Near Infra-Red (NIR)	832.8	10
	8A	Narrow NIR	864.7	20
	9	Water vapor	945.1	60
	10	Short Wave Infra-Red (SWIR)-Cirrus	1373.5	60
	11	Short Wave Infra-Red (SWIR)	1613.7	20
	12	Short Wave Infra-Red (SWIR)	2202.4	20

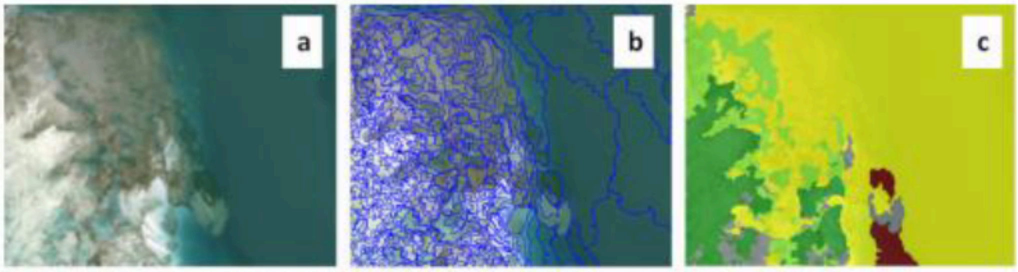

Figure 5. Object based image analysis (OBIA)process. a) Acquired image, b) Image segmentation, c) Image classification.

there are two approaches used: manual extraction of features, which offers high accuracy but is laborious and time-intensive, or the use of machine-learning algorithms for rapid processing and replicability, albeit with a potential risk of misclassification. While manual methods ensure precision, the advent of machine learning presents an efficient alternative, albeit with a need for careful validation and refinement to minimize errors in classification. For this, the OBIA method (Object-Based Image Analysis) was applied using eCognition Developer Software version 10.3 (Trimble Germany GmbH, 2022). This approach consists of grouping similar pixels (form, colour, texture, etc.) into segments (Fig.5), and then attributing classes to those segments (Hedley *et al.*, 2016).

Geomorphic zonation

The concept of geomorphic zonation in coral reefs involves identifying features that are relatively stable over time. In this study, the extraction of several key geomorphic features was focused on, including Internal Reefs, Lagoon, Reef Flat, Enclosed Basins, Reef Crest, Reef Front, and Reef Slope, following the definitions provided by Battistini *et al.* (1975). A lagoon is a naturally occurring depression with varying depths and sizes, typically found either behind a barrier reef or completely enclosed by reef structures. Enclosed basins, on the other hand, are smaller, shallower depressions or pools nestled within the reef structure on the reef flat. The reef slope constitutes the submerged front portion of a reef, sloping seaward with differing inclinations. It comprises coral formations and sedimentary deposits primarily of biogenic origin. The reef front delineates the outer edge of the reef flat at low tide, particularly during spring tides. Meanwhile, the reef flat is a horizontally oriented platform atop a reef structure, often reaching or surpassing sea level. It may exhibit material accumulations and surface incisions. The reef crest is primarily composed of coarse elements and is situated on the anterior part of the reef flat, manifesting in various shapes such as domes, ramparts, or scattered accumulations. Internal reefs are positioned within a lagoon, frequently separated from the open ocean by a barrier reef. They exhibit diverse sizes and shapes and are typically surrounded by shallow lagoon waters. These internal reefs consist of lagoonal coral patches, some of which extend to the surface and larger lagoon reefs, which are substantial coral formations within the lagoon, either partially exposed or submerged. These larger formations often display distinctive zoning patterns akin to those observed on reef flats.

After the image segmentation, these features were extracted by the visual photo-interpretation method using the built-in manual classification tools within the Ecognition Developer software.

Benthic image classification

For this purpose, the processed satellite image comprised: (i) the 10-meter resolution spectral bands from Sentinel-2 images (Table 1) which were atmospherically corrected, (ii) the calculated depth invariant bottom indexes (DII_B2B3, DII_B2B4, DII_B3B4), and (iii) the NDVI layer. Several satellite imageries, classification techniques, typologies and machine learning algorithms have been globally adopted to gather data on benthic coverage of coral reefs (Burns *et al.*, 2022). However, determining the most effective approach presents challenges due to inconsistencies in various factors, including the spectral and spatial resolutions of satellite images, methodologies for *in situ* reference data collection, the diversity and quantity of benthic classes mapped, and protocols for accuracy assessment. In this study, five prominent machine learning classifiers commonly employed in mapping coral reef benthic habitats were assessed with the goal of identifying the best performer tailored to environmental conditions, fieldwork data characteristics, and the particular benthic classes under study. These findings

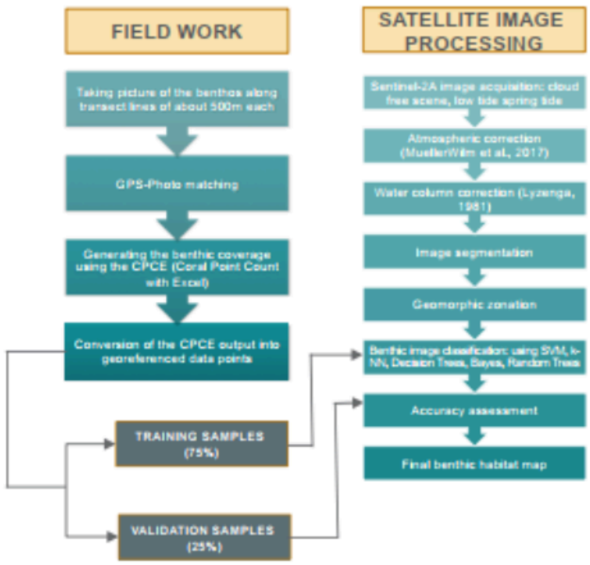

Figure 6. Image processing workflow.

will inform future investigations, guiding parameter choices, and streamlining classification processes, minimizing trial-and-error efforts. The five machine learning classifiers were:

Support Vector Machine (SVM). This assigns class labels to segmented objects by determining an optimal hyperplane, guided by feature vectors extracted from objects' attributes such as spectral values, texture, and spatial relationships. This hyperplane maximizes the margin between classes while minimizing misclassifications, with a focus on support vectors to define the boundary effectively (Mountrakis *et al.*, 2011).

Decision Tree (DT). The DT algorithm recursively partitions the dataset into subsets based on feature conditions, constructing a tree where each internal node represents a feature test and each leaf node denotes a class label. It employs a divide-and-conquer approach to classify instances, following a path from the root to a leaf node determined by feature conditions (Dietterich, 2000).

Random Trees (RT). This is a combination of multiple tree-based classifiers to produce a single classification, an ensemble of decision trees, where each single tree contributes a vote for the assignment of the most popular class to the input data (Xie and Niculescu, 2021).

k-Nearest Neighbour (k-NN). The k-NN algorithm classifies segmented objects based on the class most represented by their k nearest neighbours. K is a user-defined parameter that is the number of nearest neighbouring objects that are included in the majority voting process (Burns *et al.*, 2022) Bayes.

The Bayesian algorithm assigns classes to segmented objects by calculating the probability of each class given the object's features. It uses Bayes' theorem to compute the conditional probability of each class, incorporating prior knowledge and assuming feature independence to make informed decisions (Lewis, 1998). The flow chart of the image processing is provided in Fig. 6.

Benthic class description

The coral class (Fig. 7a) refers to a category with a hard underlying framework that is typically composed of coral-derived limestone, although non-carbonate materials can also be present. This class includes living corals. The rubble class (Fig. 7b) pertains to any area featuring loose, cylindrical to irregularly shaped fragments of bedrock or clasts of corals, bivalves, and coralline algae. This category encompasses limestone reef matrix and underlying areas of coral sand cemented together. The macroalgae class (Fig. 7c) is composed of large, multicellular marine plants that typically thrive in shallow waters surrounding coral reefs. Macroalgae are often observed on top of dead

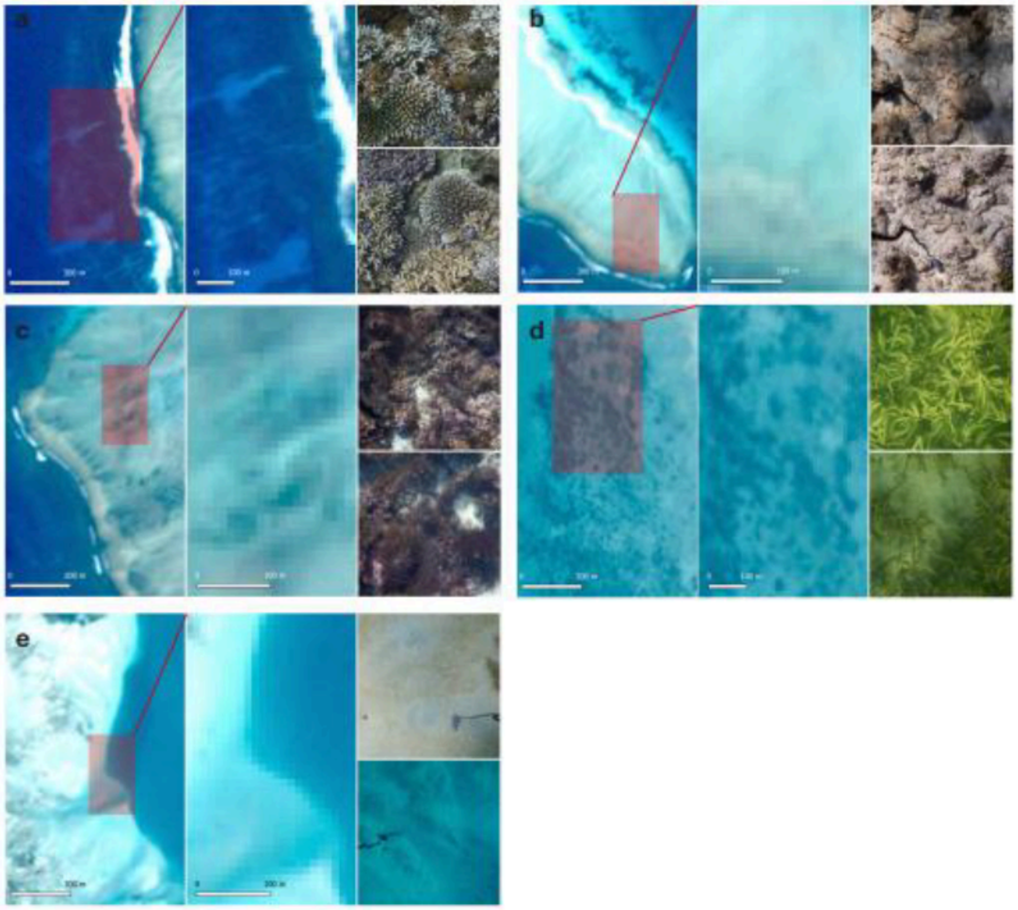

Figure 7. Benthic Classes Across Multiple Scales: 300 m (Sentinel-2 image), 100 m (Sentinel-2 image), and 1 m scale (photoquadrat). (a) Coral, (b) Rubbles, (c) Algae, (d) Seagrass, (e) Sand.

corals, in areas with clear water and abundant sunlight. The seagrass class (Fig. 7d) pertains to a soft-bottomed environment that is mainly characterized by the prevalence of a single or a combination of different species of seagrass. This classification also encompasses sparser or spatially confined seagrass as long as it forms the dominant benthic class. The sand class (Fig. 7e) pertains to soft-bottomed reef regions where fine unconsolidated granular material prevails. This granular material is finer than coral rubble but coarser than mud and thickly overlays any underlying bedrock. Sparse algae, scattered rocks, or small, isolated coral heads may also occur in the sand class. This class also encapsulates areas that are covered by a layer of fine-grained sediment that is mostly composed of organic matter and inorganic particles.

Accuracy assessment of the benthic habitat mapping

The validity, or usefulness, of any interpretation or classification map may be determined with an accuracy assessment that compares the created map with the field work data (Yamano, 2013). Accuracy assessment is commonly derived using an error matrix (also called confusion matrix), which tabulates the level of agreement between the thematic class at a location in the image-based map and the same location in the reference data (Yamano, 2013). The accuracy of each mapping category is described by the individual class accuracies, or according to the user's accuracy (UA) and producer's accuracies (PA) and Overall accuracy (OA), which are all derived from the error matrix. This is generated by using the built-in accuracy assessment tool in the eCognition Developer software. These metrics adhere to the definitions provided by Congalton and Green (2008). OA focuses on assessing the general performance of a classification algorithm across all classes in a dataset. It provides a holistic measure of the classifier's accuracy by considering all classes simultaneously. PA represents the proportion of correctly classified pixels or features for a specific class in relation to the total number of pixels or features that belong to that class on the ground. It focuses on how accurately the algorithm identifies and maps the pixels or features that truly belong to a specific class on the ground. UA represents the proportion of correctly classified pixels or features for a specific class in relation to the total number of pixels or features classified as that class by the classifier. It focuses on how accurately the algorithm assigns pixels or features to a particular class, regardless of whether they truly belong to that class or not. Five classifier algorithms (SVM, DT, RT, Bayes, k-NN) were executed on the image and their accuracy evaluated. Using the classifier algorithm that demonstrated the highest overall accuracy, the benthic classification outcome was refined by merging similar classes and eliminating small misclassified objects, thus improving the clarity and coherence of the final result.

Accuracy assessment of the Allen Coral Atlas

To assess the effectiveness of the benthic cover results for the reefs surrounding Toliara, a comparison with vector data from the Allen Coral Reef Atlas (ACA) (https://allencoralatlas.org) was conducted, acquired in August 2021. This data was cropped to match the scale of the current study, enabling meaningful comparisons. The ACA has the great advantage that it covers reefs around the world, so it is easy to refer to this atlas for a first approximation of benthic coverage of coastal and reef habitats (ACA, 2020).

Andréfouët (2008) mentioned the necessity of alignment of the extent of the ground truth data with the spatial resolution of the sensors. For a meaningful multi-sensor comparison accompanied by objective accuracy assessment, it is imperative that ground truth observations and typology align with the spatial resolution of the sensors. Given this, the raw CPCe data from this study, derived from 1 m x 1 m photoquadrat (with new pictures captured every 3-5 meters), offers a suitable basis for evaluating the accuracy of the ACA data rather than the readapted training and validation data (Fig. 4) that was used to match with the pixel size of the Sentinel-2 image. The ACA data is sourced from Planet Dove satellite images, a commercial satellite that provides a spatial resolution of 3-5meters (Safyan, 2020).

The benthic cover of the reefs of the ACA was composed by 6 categories: "Coral/Algae", "Microalgal Mats", "Rock", "Rubble", "Sand", and "Seagrass". To facilitate this comparison, the field work dataset was reorganized to mirror the typology of the ACA for the accuracy assessment. Specifically, classes such as "Coral" were changed to "Coral/Algae" and "Algae" to "Coral/Algae" in order to align with the ACA data. Classes such as "Rock" and "Microalgal mats" were also removed, as they were absent in the typology of raw data from the current study. However, classes like "Seagrass", "Sand", and "Rubbles" remained unaltered to maintain consistency across datasets.

Results

Accuracy of the image classifications

The overall accuracies of the classifier algorithms used for classifying benthic habitats of coral reefs in Toliara are depicted in Figure 8. The k-NN algorithm showed the highest Overall Accuracy (OA) at 83 %, followed by the Bayes classifier, DT, RT, and SVM, with OA values of 79 %, 68 %, 67 %, and 42 % respectively. Table 2 provides an in-depth analysis of classifier performance in categorizing various benthic habitat samples. It highlights the challenges faced by the Support Vector Machine (SVM) algorithm in accurately classifying Algae and Seagrass samples, with low values of Producer's Accuracy (PA) and User's Accuracy (UA). Other classifiers, such as Naive Bayes, DT, k-NN, RT, showed more robust performance. Naive Bayes and DT achieved high PA values for Rubble

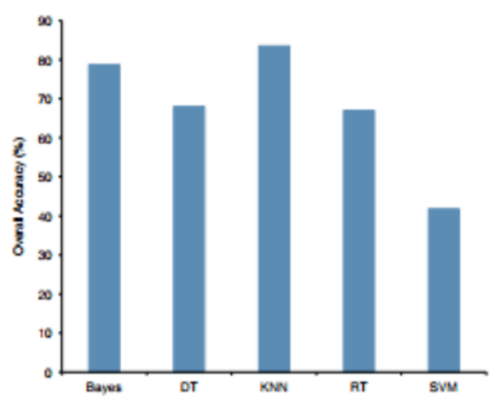

Figure 8. Overall accuracies of the classifiers algorithms used for benthic image classification.

Table 2. Confusion matrix of the five classifiers algorithms.

Classifier Algorithm	User Class \ Sample	Algae	Coral	Rubble	Sand	Seagrass
Bayes OA = 79%	Algae	9	0	0	0	0
	Coral	0	6	0	0	0
	Rubble	2	0	23	5	3
	Sand	1	0	1	20	2
	Seagrass	0	0	2	6	23
	PA	0,75	1	0,885	0,645	0,821
	UA	1	1	0,697	0,833	0,742
DT OA = 68%	User Class \ Sample	Algae	Coral	Rubble	Sand	Seagrass
	Algae	9	0	2	1	5
	Coral	0	6	0	0	0
	Rubble	0	0	22	7	9
	Sand	3	0	1	23	4
	Seagrass	0	0	1	0	10
	PA	0,75	1	0,846	0,742	0,357
	UA	0,529	1	0,579	0,742	0,909
k-NN OA = 83%	User Class \ Sample	Algae	Coral	Rubble	Sand	Seagrass
	Algae	11	0	2	2	2
	Coral	0	6	0	0	0
	Rubble	0	0	19	1	1
	Sand	1	0	4	28	3
	Seagrass	0	0	1	0	22
	PA	0,917	1	0,731	0,903	0,786
	UA	0,647	1	0,905	0,778	0,957
RT OA = 67%	User Class \ Sample	Algae	Coral	Rubble	Sand	Seagrass
	Algae	10	0	3	2	3
	Coral	0	6	0	0	0
	Rubble	0	0	16	6	6
	Sand	2	0	4	23	5
	Seagrass	0	0	3	0	14
	PA	0,833	1	0,615	0,742	0,5
	UA	0,556	1	0,571	0,676	0,824
SVM OA = 42%	User Class \ Sample	Algae	Coral	Rubble	Sand	Seagrass
	Algae	0	0	0	0	0
	Coral	3	6	0	2	0
	Rubble	4	0	12	1	0
	Sand	4	0	2	9	12
	Seagrass	1	0	12	19	16
	PA	0	1	0,462	0,290	0,571
	UA	undefined	0,545	0,706	0,333	0,333

and Seagrass, respectively, while k-NN demonstrated effectiveness in identifying Coral and Algae habitats. RF performed well in classifying Algae and Sand but struggled with Seagrass. In contrast, SVM struggled with Algae and Seagrass classification, with notably low PA values across multiple classes and variable UA values. Compared to other classifiers evaluated in this study, SVM exhibited lower OA, UA and PA for most habitat classes, indicating its potentially unsuitability for benthic habitat mapping applications under the given data calibration types and benthic environment. Figure 9 depicts various outputs of benthic habitat classification, highlighting the variability in results despite employing identical calibration data and image pre-processing techniques. This shows the importance of selecting the appropriate classifier algorithm, as it profoundly impacts the outcomes of benthic coverage assessment and the precise evaluation of each benthic habitat's surface area.

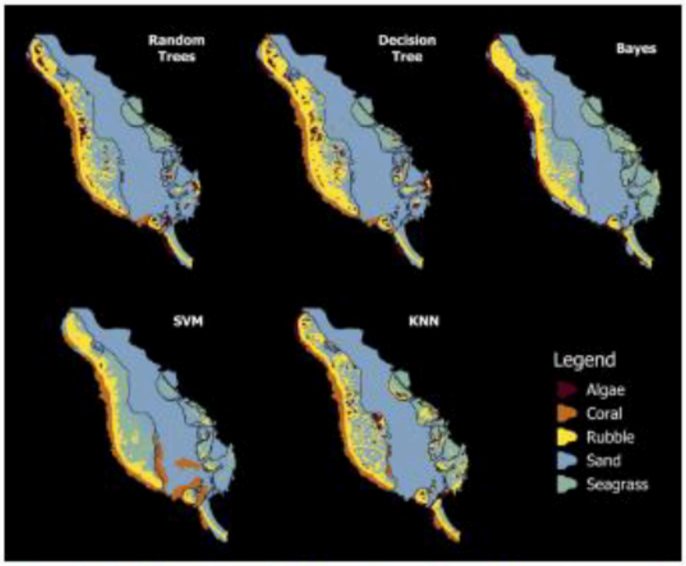

Figure 9. Outputs of different machine learning algorithms to map the benthic coverage of Toliara's coral reefs.

In reference to ACA, Table 3 presents the outcome of the accuracy assessment for its benthic coverage data. Compared with the 4187 CPCe data, the ACA achieves an overall accuracy of 50 %, failing to meet the 60 % minimum standard outlined in Yamano (2013). Additionally, a very low overall accuracy (OA) and user accuracy (UA) was noticed across all classes, particularly for rubbles and seagrass habitats.

Benthic coverage extent of the reefs of Toliara

The benthic coverage of the Toliara reefs was evaluated by using the k-NN classifier, which demonstrated the highest accuracy compared to the four other algorithms. Each habitat type is categorized based on its location within the reef system (Fig. 10). The internal reefs, along with their associated habitats, primarily span the area between Ankilibe and Sarodrano, as illustrated in Fig. 12c. The surface area measurements are presented for five benthic classes: Rubble (21 km²), Coral (10 km²), Algae (6 km²), Seagrass (22 km²), and Sand (73 km²). Internal reefs exhibit substantial surface area coverage, particularly for Seagrass (8 km²) and Rubble (4 km²). Coral and Algae also contribute significantly to the internal reef ecosystem, with surface areas of 0.4 km² and 1.46 km² respectively. The Lagoon habitat features smaller surface areas compared to internal reefs. Notably, Sand is the predominant substrate in the lagoon, covering a substantial area of 57 km². Unlike Rubble (0.4 km²), Coral (0.3 km²) and Algae (0.5 km²) that represent less significant surface coverage, Seagrass emerges as the next dominant feature in this habitat type, spanning an area of 5 km² indicating its importance as a habitat within the lagoon environment. Reef flat habitats showcase considerable surface area coverage, particularly for Seagrass (8 km²) and Rubble (11 km²) and Sand (12 km²).

Table 3. Confusion matrix of the benthic coverage of the Allen Coral Atlas data.

OA= 50%	Coral/Algae	Rubble	Sand	Seagrass
Coral/Algae	596	35	155	54
Rubble	181	617	408	281
Sand	2	53	180	15
Seagrass	206	140	103	241
User accuracy (%)	0.6	0.7	0.2	0.4
Producer accuracy (%)	0.7	0.4	0.7	0.3

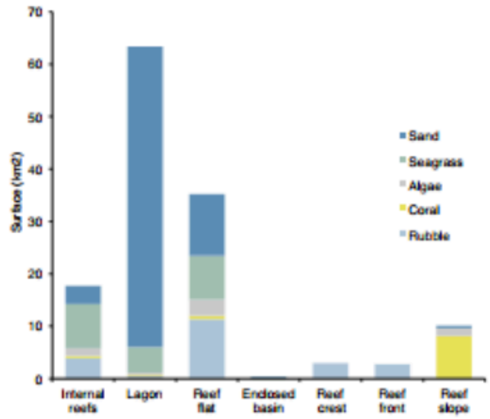

Figure 10. Surface of coral benthic cover per reef geomorphology.

Enclosed basin habitats exhibit relatively smaller surface area coverage compared to other habitat types. Sand dominates this habitat type, covering 0.2 km², while Coral (0.04 km²), Algae (0.004 km²) and Seagrass (0.006 km²) habitats exhibit minor surface area coverage. Both Reef Crest and Reef Front habitats exhibit minimal surface area coverage for all habitat classes, indicating their relatively limited extent within the reef system. These habitats are predominantly composed of Rubble which both represents about 3 km².

Reef slope habitats demonstrate unique characteristics with significant surface area coverage for Coral (8 km²). Algae (1 km²) and Sand (0.5 km²) classes also exhibit notable coverage, while Seagrass (0.017 km²) and Rubble classes are present in smaller amounts.

Discussion

Evaluating global coral reef mapping initiatives

Recent initiatives aimed at enhancing global coral reef mapping, such as the Allen Coral Atlas (Allen Coral Atlas, 2020) and the Global Distribution of Coral Reefs (UNEP-WCMC, WorldFish Centre, WRI, TNC, 2021), provide publicly accessible datasets facilitating easy access to information on coral reef geomorphology and benthic coverage. However, caution is warranted when using such data for national coral reef management strategies, restoration programmes, or economic valuations of these ecosystems. A comparison of the coral reef data generated by the UNEP-WCMC, the ACA geomorphology and the present study is provided in Figure 12. A total surface of 162 km² for the total extent of coral reef systems surrounding Toliara was calculated in the present study, while ACA provides a total of 126.8 km² and the UNEP-WCMC coral reef data totaled 61.1 km². It is also worth noting that this later dataset misses the fringing reef of Sarodrano (Fig. 12.a) which is present in both Figure 12.b and Figure 12.c. Figure 12.b also shows that the enclosed basin, locally

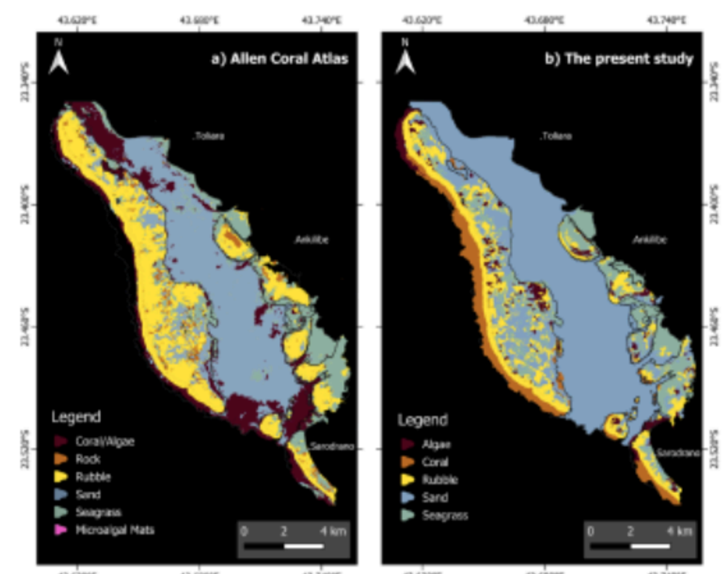

Figure 11. Comparison of benthic coverage provided by the ACA data and the present study.

known as "*Grande Vasque*" is erroneously interpreted as reef slope. This figure also showcases several hard reef structures within the lagoon which are misrepresented as reef slopes where it is clearly just a deep lagoon. Furthermore, concerning the benthic coverage of the coral reef system in Toliara, the current analysis reveals surface areas occupied by seagrass, sand, rubble, coral, and algae, amounting to 21 km², 73 km², 21 km², 10 km², and 6 km² respectively. Had marine scientists or policymakers used the ACA dataset, their calculations would have shown 22 km² for seagrass, and 48 km² for sand, 21 km² for Coral/Algae, and 28 km² for Rubble. The findings from the present study align with those reported by Botosoamananto *et al.* (2021), who conducted localized surveys within this coral reef system. The outer reef slope is predominantly characterized by robust hard corals, as highlighted, with the highest concentration of macroalgae observed in its northern section. Additionally, the authors noted substantial hard coral coverage within the reef patches of Sarodrano and the southern segment of the inner slope of the "*Grand Récif de Toliara*" (GRT). They also observed a significant presence of rubble on the reef flats as illustrated in Figure 11, a phenomenon documented by Bruggemann *et al.* (2012) and Andréfouët *et al.* (2013). These studies describe this particular section of the barrier reef, marked by an accumulation of dead coral and rubble on the reef flat.

Insight and considerations to enhance coral reef mapping

Assessment of benthic cover of coral reefs requires special attention, as variations in methodology can lead to inconsistencies in coral reef mapping and classification. The total surface area of coral reefs in Madagascar has been reported differently across studies, with UNEP-WCMC, WorldFish Centre, WRI, TNC (2021) reporting a total surface area of about 3,100 km² and the Allen Coral Atlas (Allen Coral Atlas, 2020) showing a total of 5,076 km² for the coral reefs of Madagascar. These variations do not indicate changes in coral reef extent but rather the different methodologies used to assess them. Coral reefs are complex and diverse ecosystems, with different species, morphology, and spatial arrangement depending on local environmental conditions. Inaccurate coral reef mapping and classification can have serious consequences for conservation efforts, leading to misinformed policy and management decisions. Overestimating coral cover can lead to inappropriate land-use decisions such as coastal development or tourism which can result in coral reef degradation and loss. Conversely, underestimating coral cover can result in inadequate protection or management measures, putting these important ecosystems at risk. Therefore, when using remote sensing techniques, a consistent and standardized methodology for assessing marine habitats is essential for accurate and effective conservation

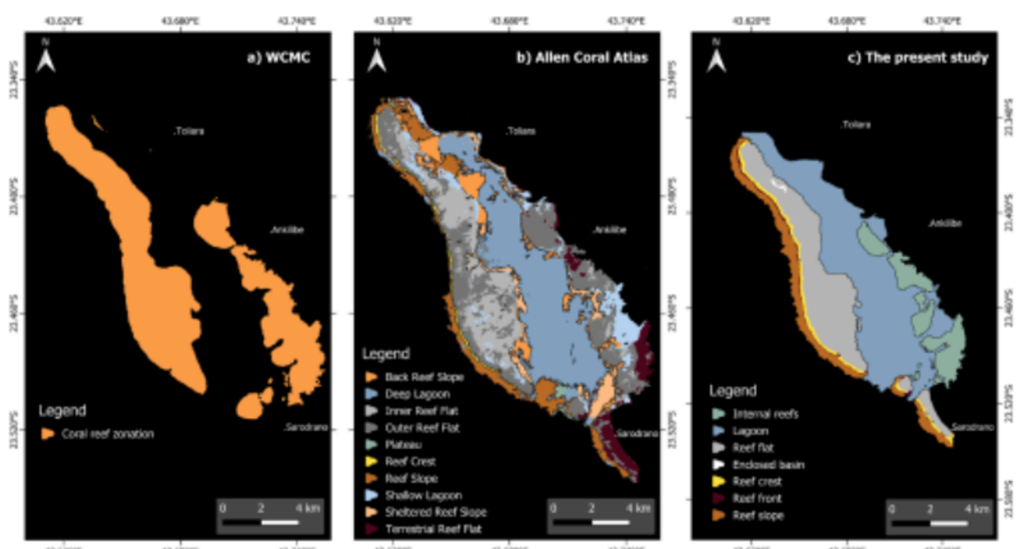

Figure 12. Comparison between the available data of coral reef geomorphology in Toliara.

and management. Validation and calibration of these techniques using *in-situ* data are necessary to ensure their accuracy and reliability. Overall, remote sensing can be a powerful tool for marine habitat assessment but it must be used with caution and care to avoid the negative consequences of methodology diversity. This study of the Toliara coral reef system underscores the significance of integrating multiple fieldwork datasets into the model training process, resulting in a notably enhanced mapping accuracy. This emphasizes the crucial role of *in situ* data collection in refining remote sensing techniques for more precise benthic habitat mapping. Across the globe, various classification algorithms are used for coral reef classification, with their effectiveness contingent upon regional characteristics, available field data, and the spectral and temporal resolution of satellite imagery. While SVM, k-NN, and RT algorithms are prevalent in object-based coral reef benthic mapping publications (Burns *et al.*, 2022), studies such as those by Mountrakis *et al.*, (2011) indicate that SVM often yields higher accuracy values compared to other techniques. However, the current research reveals that in this specific context, the k-NN algorithm outperforms SVM in terms of accuracy. This highlights the importance of selecting the most suitable algorithm tailored to local conditions when mapping coral habitats. Moreover, the performance of classification algorithms is subject to variations in image quality and resolution, training data set size, class types, and algorithm-specific parameter tuning. Hence, it is imperative to identify the most effective approach for this region based on these factors.

Conclusion

This study highlights the successful application of the OBIA method in conjunction with *in-situ* data to map coral reefs at local scales, using freely available high-resolution satellite images from Sentinel-2. This approach provides a replicable methodology for coral reef mapping projects using the same types of image and field data and lays the foundation to assess long-term changes in coral reef habitats, spatial observations of coral reef resilience, evaluation of seagrass distribution, and assessment of habitat health for herbivorous fishes. The use of georeferenced photographs not only establishes a formal linkage between the image and field data but also presents a valuable opportunity for informing stakeholders, managers, and other interested parties on the capabilities of satellite imaging for mapping and measuring reef features. Over 4,000 georeferenced photographs were used as reference data to produce a highly accurate map of the 18 km-long barrier reef of Toliara and the nearby reef systems. The efficacy of this mapping approach relies on both the quantity and quality of fieldwork data used to train the classifier algorithms for identifying features within satellite images. The greater the availability of comprehensive field data, the higher the accuracy of the resultant map. This explains why the ACA does not perform optimally in areas with limited field data. While global data may offer an initial reference for evaluating the extent or likelihood of coral reef occurrence, solely depending on such information for decision-making concerning coral reef management or restoration programmes entails considerable risks. Therefore, nations should prioritize local data collection and national-level satellite image processing to ensure precise assessments. This study illustrates that, even with freely available satellite imagery such as Sentinel-2 and basic logistical resources for field work data collection, sufficient accuracy can be attained to produce maps of coral reef geomorphology and benthic habitats.

Acknowledgements

We are sincerely grateful for the invaluable support extended by multiple institutions, whose contributions were instrumental in the success of this study. We extend our heartfelt appreciation to the Académie de Recherche et d'Enseignement Supérieur – Coopération Belge (ARES-CCD), the Western Indian Ocean Marine Sciences Association (WIOMSA), the Foundation for Future Generation (AETHER Fund), and the Station Marine de Belaza for their unwavering assistance in facilitating this research.

References

Allen Coral Atlas (2020) Imagery, maps and monitoring of the world's tropical coral reefs [doi: 10.5281/zenodo.3833242]

Andréfouët S (2008) Coral reef habitat mapping using remote sensing: A user vs producer perspective, implications for research, management and capacity building. Journal of Spatial Science 53: 113-129 [doi: 10.1080/14498596.2008.9635140]

Andréfouët S, Guillaume MMM, Delval A, Rasoamanendrika FMA, Blanchot J, Bruggemann, JH (2013) Fifty years of changes in reef flat habitats of the Grand Récif of Toliara (SW Madagascar) and the impact of gleaning. Coral Reefs 32: 757-768 [doi: 10.1007/s00338-013-1026-0]

Battistini R, Bourrouilh F, Chevalier JP, Coudray J, Denizot M, Faure G, Ficher JC, Guilcher, A, Harmelin-Vivien M, Jaubert J, Laborel J, Montaggioni L, Masse JP, Mauge LA, Peyrot-Clausade M, Pichon M, Plante R, Plaziat JC, Plessis YB, Richard G, Salvat B, Thomassin BA, Vasseur P, Weydert P (1975) Éléments de terminologie récifale indopacifique. Téthys 7: 1-111

Botosoamananto RL, Todinanahary G, Razakandrainy A, Randrianarivo M, Penin L, Adjeroud M, (2021) Spatial patterns of coral community structure in the Toliara region of southwest Madagascar and implications for conservation and management. Diversity 13: 486 [doi:10.3390/d13100486]

Bruggemann, JH, Rodier M, Guillaume MMM, Andréfouët S, Arfi R, Cinner JE, Pichon M, Ramahatratra F, Rasoamanendrika F, Zinke J, McClanahan TR (2012) Wicked social–ecological problems forcing unprecedented change on the latitudinal margins of coral reefs: the case of southwest Madagascar. Ecological Society 17: 4-21 [doi:10.5751/ES-05300-170447].

Burns C, Bollard B, Narayanan A (2022) Machine-learning for mapping and monitoring shallow coral reef habitats. Remote Sensing 14: 2666 [doi:10.3390/rs14112666]

Congalton RG, Green K (2008) Assessing the accuracy of remotely sensed data: Principles and practices. Mapping Science. CRC Press, Boca Rotan FL., Second Edition. 183 pp

Dietterich TG (2000) An experimental comparison of three methods for constructing ensembles of decision trees: Bagging, boosting, and randomization. Machine Learning 40: 139-157

Eakin CM, Nim CJ, Brainard R, Aubrecht C, Elvidge C, Gledhill DK, Muller-Karger F, Mumby PJ, Skirving W, Strong AE, Wang M, Weeks S, Wentz F, Ziskin D (2010) Monitoring coral reefs from space. Oceanography 23:119-133

ESA's Sentinel-2 team (2015) The story of Sentinel-2. European Space Agency 161: 4-9

Foo SA, Asner GP (2019) Scaling up coral reef restoration using remote sensing technology. Frontiers in Marine Science 6: 1-8 [doi:10.3389/fmars.2019.00079]

Hedley JD, Roelfsema CM, Phinn SR, Mumby PJ (2012) Environmental and sensor limitations in optical remote sensing of coral reefs: Implications for monitoring and sensor design. Remote Sensing 4: 271-302 [doi: doi:10.3390/rs4010271]

Hedley JD, Roelfsema CM, Chollet I, Harborne AR, Heron SF, Weeks S, Skirving W, Strong AE, Eakin CM, Christensen TRL, Ticzon V, Bejarano S, Mumby PJ (2016) Remote sensing of coral reefs for monitoring and management: A review. Remote Sensing 8: 1-40

Hedley JD, Roelfsema C, Brando V, Giardino C, Kutser T, Phinn S, Mumby PJ, Barrilero O, Laporte J, Koetz B (2018) Coral reef applications of Sentinel-2: Coverage, characteristics, bathymetry and benthic mapping with comparison to Landsat 8. Remote Sensing of the Environment 216: 598-614 [doi:10.1016/j.rse.2018.07.014]

Kennedy EV, Roelfsema CM, Lyons MB, Kovacs EM, Borrego-Acevedo R, Roe M, Phinn SR, Larsen K, Murray NJ, Yuwono D, Wolff J, Tudman P (2021) Reef Cover, a coral reef classification for global habitat mapping from remote sensing. Scientific Data 8: 1-20 [doi:10.1038/s41597-021-00958-z]

Kohler KE, Gill SM (2006) Coral point count with Excel extensions (CPCe): A Visual Basic programme for the determination of coral and substrate coverage using random point count methodology. Computers & Geosciences 32: 1259-1269 [doi:10.1016/j.cageo.2005.11.009]

Lewis DD (1998) Naive (Bayes) at forty: The independence assumption in information retrieval, In: Nédellec C, Rouveirol C (eds) Machine Learning: ECML-98, Lecture Notes in Computer Science. Springer Berlin, Heidelberg pp 4–15 [doi:10.1007/BFb0026666]

Louis J, Debaecker V, Pflug B, Main-Knorn M, Bieniarz J, Mueller-Wilm U, Cadau E, Gascon, F (2016) Sentinel-2 Sen2Cor: L2A processor for users. In: Proceedings of the Living Planet Symposium 2016. ESA SP-740, Prague, Czech Republic. 8 pp

Lyzenga DR (1981) Remote sensing of bottom reflectance and water attenuation parameters in shallow water using aircraft and Landsat data. International Journal of Remote Sensing 2: 71-82 [doi:10.1080/01431168108948342]

Mountrakis G, Im J, Ogole C (2011) Support vector machines in remote sensing: A review. ISPRS Journal of Photogrammetry and Remote Sensing 66: 247-259 [doi:10.1016/j.isprsjprs.2010.11.001]

Nguyen T, Liquet B, Mengersen K, Sous D (2021) Mapping of coral reefs with multispectral satellites: A review of recent papers. Remote Sensing 13: 4470 [doi:10.3390/rs13214470]

Nurlidiasari M, Budiman S (2010) Mapping coral reef habitat with and without water column correction using Quickbird image. International Journal of Remote Sensing and Earth Sciences 2:45-56 [doi:10.30536/j.ijreses.2005.v2.a1357]

Phinn SR, Roelfsema CM, Mumby PJ (2012) Multi-scale, object-based image analysis for mapping geomorphic and ecological zones on coral reefs. International Journal of Remote Sensing 33: 3768-3797 [doi:10.1080/01431161.2011.633122]

Pichon M (1972) Les peuplements à base de scléractiniaires dans les récifs coralliens de la Baie de Tuléar

(Sud-Ouest de Madagsacar), Station Marine d'Endoume. ed. Marseille, France. pp 135-154

Razakandrainy A (2018) Mécanismes de maintien des populations de coraux dans la région de Toliara, sud-ouest de Madagascar (Mémoire DEA en Océanographie Appliquée). Université de Toliara, Institut Halieutique et des Sciences Marines (IH.SM), Toliara, Madagascar. 54 pp

Roelfsema CM, Markey K, Kennedy EV, Kovacs EM, Borrego-Acevedo R, Fox HE, Bambic B, Free B, Rice K, Phinn SR (2019) Protocol for georeferenced benthic psotoquadrat surveys. Remote Sensing and Research Centre, School of Earth and Environmental Sciences. University of Queensland, Brisbane, Australia. 17 pp

Safyan M (2020) Planet's Dove Satellite Constellation. In: Pelton, JN (ed) Handbook of small satellites. Springer International Publishing, Cham. pp 1-17 [doi:10.1007/978-3-030-20707-6_64-1]

Todinanahary GGB (2016) Evaluation du potentiel biologique, économique et social de la coralliculture dans le sud-ouest de Madagascar (Thèse de Doctorat). Université de Mons (Belgique), Faculté des Sciences, Biologie des Organismes Marins et Biomimétisme.

Trimble Germany GmbH (2022) eCognition Developer.

UNEP-WCMC, WorldFish Centre, WRI, TNC (2021) Global distribution of coral reefs, compiled from multiple sources including the Millennium Coral Reef Mapping Project. Version 4.1, updated by UNEP-WCMC. Includes contributions from IMaRS-USF and IRD (2005), IMaRS-USF (2005) and Spalding *et al.* (2001). UN Environment Programme-World Conservation Monitoring Centre, Cambridge, UK [doi: 10.34892/t2wk-5t34]

van Hooidonk R, Maynard J, Tamelander J, Gove J, Ahmadia G, Raymundo L, Williams G, Heron, SF, Planes S (2016) Local-scale projections of coral reef futures and implications of the Paris Agreement. Scientific Reports 6:1-8 [doi:10.1038/srep39666]

Wilkinson C (2008) Status of coral reefs of the world. Global Coral Reef Monitoring Network (GCRMN). Townsville, Australia. 294 pp

Wouthuyzen S, Abrar M, Corvianawatie C, Salatalohi A, Kusumo S, Yanuar Y, Darmawan, Samsuardi Y, Arrafat MY (2019) The potency of Sentinel-2 satellite for monitoring during and after coral bleaching events of 2016 in the some islands of Marine Recreation Park (TWP) of Pieh, West Sumatra. Earth and Environmental Science 284: 012028 [doi: 10.1088/1755-1315/284/1/012028]

Xie G, Niculescu S (2021) Mapping and monitoring of land cover/land use (LCLU) changes in the Crozon Peninsula (Brittany, France) from 2007 to 2018 by machine learning algorithms (Support Vector Machine, Random Forest, and Convolutional Neural Network) and by Post-classification Comparison (PCC). Remote Sensing 13: 3899 [doi:10.3390/rs13193899]

Xu J, Zhao D (2014) Review of coral reef ecosystem remote sensing. Acta Ecologica Sinica 34: 19-25 [doi:10.1016/j.chnaes.2013.11.003]

Yamano H (2013) Chapter 3: Multispectral applications. In: Coral reef remote sensing: A guide for mapping, monitoring and management. Springer, Dordrecht, Netherlands. pp 51-78

Yunus AP, Jie D, Song X, Avtar R (2019) High resolution Sentinel-2 images for improved bathymetric mapping of coastal and lake environments (preprint). Earth Sciences [doi:10.20944/preprints201902.0270.v1]

Zoffoli ML, Gernez P, Rosa P, Le Bris A, Brando VE, Barillé A-L, Harin N, Peters S, Poser K, Spaias L, Peralta G, Barillé L (2020) Sentinel-2 remote sensing of *Zostera noltei*-dominated intertidal seagrass meadows. Remote Sensing of Environment 251: 112020 [doi:10.1016/j.rse.2020.112020]